Department of
Architecture and
Built Environment



University of
Nottingham
UK | CHINA | MALAYSIA

The feasibility of Passive Downdraught Evaporative Cooling (PDEC) of multi-storey office buildings in Cairo - A Modelling Study

Omar Ibraheem
BSc, MSc

Thesis submitted to the University of Nottingham
for the degree of Doctor of Philosophy
September 2018

Abstract

Climatic stress on buildings in hot-dry climates has long been negotiated by means of evaporative cooling, the origins of which could be traced back to Egypt and the Middle East. However, this millennia-old strategy needs to undergo much scrutiny in its design and implementation to meet the requirements of contemporary comfort standards for offices. The task is even more onerous if multi-storey buildings are considered. Acknowledging Cairo to be one of the most densely populated cities in the world and in light of the growing demand on high-quality office space in recent years, it is anticipated that extending the application of evaporative cooling to medium and high-rise office buildings is imperative if this strategy is to be widely adopted as an alternative to conventional air-conditioning in Cairo given that existing research and applications are limited to low-rise buildings.

This work proposes a four-stage plan to achieve that. The first stage entails the development of a generic prototype of the Passive Downdraught Evaporatively Cooled (PDEC) multi-storey office building that allows three distinct airflow patterns and two modes of operation to take place. The second stage makes use of analytic models for the initial sizing of the airflow components. The third stage assesses the performance of a base case model of the generic PDEC building in terms of bulk airflow rates, airflow distribution across the floors, internal thermal conditions, and relevant environmental costs using EnergyPlus, the whole building dynamic thermal simulation program with integrated airflow network modelling. The fourth and final stage is that of optimisation wherein the effects of varying a number of parameters on performance are established.

The study shows that in comparison to free-running naturally-ventilated buildings, and depending on the thermal comfort model adopted, PDEC can potentially deliver comfort conditions for all occupied hours of the cooling season in Cairo. Buoyancy ‘stack’ forces alone generated by temperature differences can drive sufficient airflow rates without wind assistance, a scenario that is likely to occur in dense urban contexts. The study demonstrates the effectiveness’ of dividing multi-storey buildings into isolated segments in terms of airflow (segmentation) and the benefits of extending PDEC operation beyond occupied hours. Changes in wind direction and speed were also considered and have shown to be of less significance if air inlets and outlets are properly located. Fine tuning of the building management system and adopting a more relaxed overheating criterion are key factors in limiting the increase in daily water consumption due to PDEC in light of the diminishing availability of sustainable water resources in the region. This study is the first to provide an understanding of how multi-storey office buildings in hot-dry climates can be designed and operated to incorporate PDEC as a viable alternative to AC. The novelty here lies not in the methodology which uses available models, but in the detailed investigation of flow rates, flow patterns, indoor temperatures, and water consumption.

Acknowledgments

All thanks and praise to God for granting me the opportunity and patience to complete this work. This work would not have seen the light had it not been for the continuous support and encouragement of my Mother; the love, dedication, and patience of my wife Kadria; and the joy, affection, and above all, hope that my daughter Layla brings.

My deepest gratitude goes to Professor Brian Ford for his supervision, invaluable support, constructive suggestions and encouraging words, Dr David Etheridge for his supervision and invaluable feedback, and Dr Jonathan Hale for his understanding and assistance. Special thanks and profound gratitude to Professor John Chilton; had it not been for his understanding, encouragement and moral support, it would have been very difficult to complete this work.

This has unquestionably been the most strenuous endeavour I have ever had to pursue, one that was continuously interrupted by unfortunate events. Throughout the course of this work, my family and I have been blessed with the presence of some wonderful people in our lives without which the journey would have been unbearable; Dalia Said and her family for making this place a home away from home, Linda Brooks for her guidance, dedication, and love, and for always being there for us, Allison Barnett for her affectionate and endless support, and Sally McEwan, for her understanding and generosity.

Table of Contents

Abstract ..... **I**

Acknowledgments ..... **II**

Table of Contents ..... **III**

List of Figures ..... **VIII**

List of Tables ..... **XV**

List of Acronyms ..... **XVI**

Nomenclature ..... **XVIII**

Chapter 1: Introduction **1**

1.1 Background 1

1.2 Research Problem 3

1.3 Research Aim and Objectives 5

1.4 Research Methodology 6

1.5 Scope and Beneficiaries 9

1.6 Thesis Outline 10

Chapter 2: PDEC: Background and Previous Work **15**

2.1 Chapter Overview 15

2.2 Basics of natural ventilation in buildings 15

2.2.1 Natural Ventilation and Building Configuration 16

2.2.2 Objectives and Indices of Natural ventilation 19

2.2.2.1 The purpose of natural ventilation 20

2.2.2.2 Indices of performance 21

2.2.3 Driving Forces 22

2.2.4 Ventilation Strategies 23

2.2.4.1 Isolated Spaces 23

2.2.4.2 Connected spaces 27

2.2.5 Ventilation Principle 28

2.2.6 Flow Direction 30

2.2.6.1 Edge in – Centre out (E-C) 31

2.2.6.2 Edge in – Edge out (E-E) 32

2.2.6.3 Centre in – Edge out (C-E) 33

2.2.6.4 Centre in – Centre out (C-C) 33
2.2.7 Flow Path 34
2.2.7.1 Local supply and exhaust paths 35
2.2.7.2 Central supply and exhaust paths 35
2.2.8 Modes of Operation 37
2.2.9 Control 41
2.2.10 Conclusions: Describing the ventilation concept of a building 43
2.3 Passive Downdraught Evaporative Cooling 44
2.3.1 Origins and historical applications of PDEC 44
2.3.2 Contemporary applications 45
2.3.2.1 Cool towers 46
2.3.2.2 Shower towers 46
2.3.2.3 Porous ceramics 46
2.3.2.4 Misting Towers 47
2.3.3 Psychrometrics of Evaporative Cooling 47
2.4 Review of research on PDEC 49
2.5 Summary 55

Chapter 3: Context and Comfort 56
3.1 Chapter Overview 56
3.2 Overview of Egypt's Climate 56
3.2.1 Cairo's Climate 57
3.2.2 Wind in Egypt 60
3.2.3 Cairo's wind potential 61
3.3 Thermal Comfort 65
3.3.1 Existing thermal comfort studies related to PDEC buildings 65
3.3.1.1 Givoni's Building Bioclimatic Charts 65
3.3.1.2 Lomas et al. comfort envelopes for PDEC Buildings 67
3.3.1.3 Fiala's Dynamic Thermal Sensation (DTS) Model 68
3.3.1.4 Schiano-Phan's Post Occupancy Evaluation of PDEC buildings 71
3.3.2 Fanger's Heat Balance Model 72
3.3.3 The Adaptive Comfort Model (ACM) 75

3.3.3.1 The ACM in ASHRAE standard 55 76
3.3.3.2 The ACM in EN 15251 76
3.3.3.1 Farghal's Neutral temperature 77
3.3.4 Discussion 78
3.4 Climate Suitability of PDEC in Cairo 79
3.4.1 Method 1: Givoni's Building Bio-Climatic Charts 80
3.4.2 Method 2: Climate Suitability Analysis Method (CSAM) 80
3.4.3 Results 84
3.5 Overview of office building design and energy use in Cairo 86
3.6 The case for Tall Buildings in Cairo 88
3.6.1 Driving Forces Worldwide 88
3.6.2 The Case for and against 91
3.6.3 The Case for High-Rise Buildings in Cairo 92
3.6.3.1 Geography and Demography of Cairo 93
3.6.3.2 Driving Forces for High-Rise Buildings in Cairo 94
3.7 Summary 96

Chapter 4: Plan for the design of PDEC multi-storey office buildings 98

4.1 Chapter Overview 98
4.2 Conceptual Design: Ventilation Strategies and Modes of Operation 99
4.2.1 Precedents and Case Studies 101
4.2.1.1 PDEC Buildings 102
4.2.1.2 Naturally Ventilated (NV) Tall Buildings 123
4.2.2 Application of PDEC to office buildings 142
4.2.2.1 Ventilation Concept 142
4.2.2.2 Spatial Configuration 144
4.2.2.3 Critical design considerations 146
4.2.3 Application of Natural Ventialtion to high-rise office buildings 147
4.2.3.1 Spatial Configuration 147
4.2.3.2 Ventilation Concept 148
4.2.3.3 Characteristic Design Feature 149
4.2.4 Developing the PDEC multi-storey office building prototype 151
4.3 Modelling techniques of Natural Ventilation and PDEC in buildings 157

4.4 Initial Sizing of the PDEC Components using EFM 161
4.5 Modelling PDEC using the AFN integrated DTM program EnergyPlus .. 165
4.6 Summary 169

Chapter 5: Simulation of the Base Case Model 170
5.1 Chapter Overview 170
5.2 Pilot Model 170
5.2.1 Modelling assumptions 171
5.2.1.1 Construction Profiles and Shading 172
5.2.1.2 Occupancy and internal heat gains 173
5.2.1.3 AFN Control-logic 173
5.2.1.4 Sizing of PDEC Components 177
5.2.2 Preliminary run 177
5.2.2.1 Flow reversal 178
5.2.2.2 Temperature Fluctuation 181
5.3 Model Refinement: The Base Case Model 183
5.3.1 Addition of a second outlet to the DSF 183
5.3.2 Resizing of the PDEC Components 184
5.3.3 Aperture Modulation and Control Logic 185
5.3.3.1 The Global control logic 186
5.3.3.2 The Local control logic 192
5.4 Results and Discussion 196
5.4.1 Overall Performance 199
5.4.2 Overheating and Comfort 202
5.4.3 Airflow rates 207
5.5 Summary 221

Chapter 6: Parametrisation and Optimisation of the BCM 225
6.1 Chapter Overview 225
6.2 Segmentation 226
6.2.1 Modelling assumptions 227
6.2.2 Airflow 229
6.2.2.1 Monthly average bulk volume airflow rates 229
6.2.2.2 Dispersion of airflow rates between floors 232

6.2.2.3 Flow Reversal 234
6.2.3 Comfort and Overheating 238
6.2.4 Water Consumption 245
6.3 Duration of PDEC operation 247
6.3.1 Modelling assumptions 247
6.3.2 Overheating and water consumption 250
6.4 Wind forces, C_p values and Orientation 254
6.4.1 Modelling assumptions 255
6.4.2 Airflow 262
6.4.1 Comfort and Water consumption 265
6.5 Comfort model and overheating criterion 267
6.5.1 Modelling assumptions 268
6.5.2 Results 271
6.6 Summary 277

Chapter 7: Summary and Conclusions 284
7.1 Summary 284
7.2 Conclusions 287
7.3 Contribution to Knowledge 296
7.4 Future Work 297

References 300
Appendix A 312
Appendix B 327

List of Figures

Figure 1-1 a) Sandra Day O'Connor United States Courthouse (Schiano-Phan, 2012), b) Malta Stock Exchange (Ford & Diaz, 2003), c) Torrent Research Centre (Ford, Patel, Zaveri, & Hewitt, 1998) 3
Figure 1-2 Thesis Outline 14
Figure 2-1 Maximum depth of spaces in isolated ventilation strategies. Source (Liddament, 1996) 26
Figure 2-2 Buoyancy driven stack ventilation. Source (Liddament, 1996) 28
Figure 2-3 a) Air movement in a mixing ventilation system. b) Typical increase in concentration with distance for a mixing ventilation system. c) Flow produced by floor displacement ventilation. d) Typical increase in concentration with distance for floor displacement ventilation. Source (Davey, 2006) 30
Figure 2-4 Schematic diagrams of the different flow directions. Source (Lomas, 2007) 31
Figure 2-5 E-C flow direction in the Queens Building at De Montfort University (EEBPP, 1997) 32
Figure 2-6 E-E flow direction in the BRE Building (Delsante & Vik, 2000) 32
Figure 2-7 C-E flow direction in the SSEES building (Lomas, Short, et al., 2004) 33
Figure 2-8 C-C and C-E flow directions in the Frederick Lanchester Library (Cook et al., 1999a) 34
Figure 2-9 Mixed-mode ventilation systems 42
Figure 2-10 Description of a building's ventilation concept 43
Figure 2-11 Ground floor plans of a) Casa de Pilatos (Ernest & Ford, 2012) and b) Suhaimi House (Almaiyah, Elkadi, & Cook, 2010) 45
Figure 2-12 Psychrometric process of direct evaporative cooling 49
Figure 3-1 World Map of Köppen-Geiger Climate classification (Kottek et al., 2006) 57
Figure 3-2 Monthly dry bulb temperature range 59
Figure 3-3 Monthly average diurnal temperature 59

Figure 3-4 Hourly average dry bulb temperature and relative humidity for each month..... 60
Figure 3-5 Cairo's annual wind rose..... 62
Figure 3-6 Monthly wind roses for Cairo..... 64
Figure 3-7 Boundaries of climatic conditions under which direct evaporative cooling is applicable. After (Givoni, 1992)..... 66
Figure 3-8 Predicted comfort envelopes for PDEC. Source (Martínez et al., 2000) 70
Figure 3-9 Comfort zones for the PMV-PPD model in ASHRAE Standard 55. Adapted from (ASHRAE, 2013b) 73
Figure 3-10 Air speed to offset temperatures above warm temperature boundaries of Figure 3-9. Source (ASHRAE, 2013a) 74
Figure 3-11 Percentage of hours during the cooling season for which PDEC yields thermal comfort conditions in Cairo 84
Figure 4-1 The Torrent Research Centre. Source (Ford et al., 1998)..... 104
Figure 4-2: Ventilation concept of the TRC (left) and the Central open concourse (right) Source (Ford et al., 1998) 105
Figure 4-3 Summer day and night modes of operation in the TRC. Source (Ford et al., 1998)..... 107
Figure 4-4 Inspector General of Police Complex. Source (Prajapati, 2007) ... 108
Figure 4-5 Ten enclosed shafts within the plan are used to cool the IGP. Source (Prajapati, 2007) 109
Figure 4-6: Detail of the shower tower. Source (Prajapati, 2007) 110
Figure 4-7 The SSEES Building. Source (www.shortandassociates.co.uk).... 111
Figure 4-8 Typical floor plan configured as a core zone, an open plan area, and a perimeter zone. Source (Lomas, Short, et al., 2004) 112
Figure 4-9 a) BMS controlled openings b) winter mode c) mid-season mode d) summer mode. Source (Lomas, Short, et al., 2004) 115
Figure 4-10 Office building in Seville. Source (Ford, 2001) 116
Figure 4-11 Typical plan (top) and cross section (bottom) of the Seville office building. Source (Ford, 2001) 117
Figure 4-12 Summer day ventilation Concept. Source (Ford, 2001) 119

Figure 4-13 1:50 Scale model of the PDEC Catania office building. Source (Francis, 2000) 120
Figure 4-14 The Deutsche Post Tower. Source (www.jahn-us.com) 124
Figure 4-15 Cross section showing the segmentation (left) and typical floor plan (right). Source (Jahn, 2003) 125
Figure 4-16 a) Ventilation concept in section b) Ventilation concept in plan (Wood & Salib, 2013b) c) Exhaust of air from the offices to the atrium via raised floor grilles (Jahn, 2003) d) Automatically controlled vents at the top of the atrium (Salib, 2008) 127
Figure 4-17 Extreme summer and winter modes of operation. Source (Salib, 2008) 128
Figure 4-18 The Commerzbank Headquarters Building. Source (www.fosterandpartners.com) 129
Figure 4-19: Plan and section of the Commerzbank. Source (Buchanan, 1998) 130
Figure 4-20: Ventilation on the level of the sky-gardens and atrium. Source (Buchanan, 1998) 132
Figure 4-21: Modes of operation in offices and sky-gardens a) office ventilation in natural mode b) office ventilation in mechanical mode c) sky-garden ventilation in summer d) sky-garden ventilation in winter. Source (Davey, 1997) 133
Figure 4-22 The Liberty Tower of Meiji University. Source (Chikamoto et al., 1999) 135
Figure 4-23: a) Ventilation concept in section b) Ventilation concept in plan c) Perimeter counter units. Source (Chikamoto et al., 1999) 136
Figure 4-24: a) CFD simulation of the wind floor b) Wind fences. Source (Chikamoto et al., 1999) 137
Figure 4-25 The New European Central Bank Headquarters (ECB). Source (www.coop-himmelblau.at) 138
Figure 4-26: a) A double skin façade is wrapped around the two buildings to create a linear atrium between them b) ventilation concept of offices c) the double skin acts as a thermal stack that extracts air from the offices. Source (Cody, 2008) 140

Figure 4-27: The form of the building is designed to create areas of high and low pressures at the inlets and outlets respectively. Source (Cody, 2008) 141
Figure 4-28: The two different types of PDEC/PHDC buildings 144
Figure 4-29: The four reviewed buildings have a similar configuration 148
Figure 4-30: Flow Directions in the high-rise towers 149
Figure 4-31: Design considerations in High-rise buildings 151
Figure 4-32: PDEC high-rise model 152
Figure 4-33: Top-down and Bottom-Up modes of operation 154
Figure 4-34: Alternative configuration for PDEC model 155
Figure 4-35 Top-Up mode of operation 156
Figure 4-36 Five-cell representation of a three-storey model of the PDEC building during a) the T-D flow pattern, b) the B-U flow pattern, and c) the T-U flow pattern 162
Figure 5-1 Pilot Model 172
Figure 5-2 Dry bulb temperature profile for middle floor throughout extreme summer week (from 13/8 to 18/8) 178
Figure 5-3 Dry bulb temperature and Volume flow rate profiles on the 14th of August for the Pilot model 180
Figure 5-4 Alternating flow patterns during PDEC operation in the early working hours for the Pilot model 181
Figure 5-5 Dry-bulb temperature and Airflow rate profiles for the middle floor of the Pilot model on the 17th of August 182
Figure 5-6 Flow Patterns for the Base Case model during PDEC operation in the early working hours 184
Figure 5-7 Dry-bulb temperature and Airflow rate profiles for the middle floor of the Base Case Model on the 17th of August 197
Figure 5-8 Number of hours in which t_{db} exceeds 27°C during occupied hours of the cooling season for the segment's middle floor 198
Figure 5-9 Number and magnitude of temperature fluctuations occurring during occupied hours of the whole year due to changes in the aperture size at the atrium/office interface of the segment's middle floor 199

Figure 5-10 Monthly, seasonal, and whole-year proportion of time in which the segment operates in each mode (flow pattern) during occupied hours 202
Figure 5-11 Distribution of the proportion of occupants voting ‘warm’ or ‘hot’ on the ASHRAE scale (*P*) during occupied hours of the cooling season 205
Figure 5-12 Percentile profiles for hourly aggregated values of the proportion of subjects voting ‘warm’ or ‘hot’ on the ASHRAE (*P*) scale for the three floors of the segment 206
Figure 5-13 Monthly average volume flow rates (a) and monthly average *OF* values (b) during occupied hours of the cooling sea..... 209
Figure 5-14 Monthly average airflow rates during occupied hours for a) B-U flow pattern, b) T-U flow pattern, and c) T-D flow pattern 210
Figure 5-15 Average airflow rates at equal *OF* values during occupied hours for of the cooling season for a) B-U flow pattern, b) T-U flow pattern, and c) T-D flow pattern 211
Figure 5-16 Timestep-averaged airflow rates and proportion of time operating modes/flow patterns occupy during the working hours of August .. 213
Figure 5-17 Variation of the ratio of airflow rates in the middle (Q_2) and upper (Q_3) floors of the segment to the lower floor with $R_{\Delta t}$ and R_A during the B-U and T-D flow patters 218
Figure 5-18 Variation of the ratio of airflow rates in the Middle (Q_2) and Upper (Q_3) floors of the segment to the airflow rate in the lower floor (Q_1) with R_A for $R_{\Delta T}$ = 0.25, 0.5, 0.75, and 1.0 219
Figure 5-19 Variation of the percentage ratio of airflow rates in the middle (Q_2) and upper (Q_3) floors of the segment to the airflow rate in the lower floor (Q_1) with R_A during the T-U flow pattern 220
Figure 5-20 Variation of scaled dimensionless airflow rates with vent area ratio R_A 221
Figure 6-1 Monthly average airflow rates of the three-storey, six-storey, and 12-storey segmented 12-storey building during May and August for a) the B-U flow pattern, b) the T-U flow pattern, and c) the T-D flow pattern 231

Figure 6-2 Monthly standard deviation of flow rates under different flow patterns 233
Figure 6-3 Proportion of occupied time of the cooling season during which reverse flows occur on each floor of the three models 236
Figure 6-4 Reverse flow occurrence by flow pattern during occupied hours of the cooling season a) by total number of hours and b) as a proportion of the duration of the flow pattern 237
Figure 6-5 Cumulative frequency of P during occupied hours of the cooling season aggregated over all floors for instances when $T_{op} > T_{cmf_ASH}$ ($\Delta t_{ASH} > 0$) 240
Figure 6-6 Cumulative frequency of P during occupied hours of the cooling season when the T-U flow pattern was in operation, aggregated over all floors for instances when $t_{op} > t_{cmf_ASH}$ ($\Delta t_{ASH} > 0$) 241
Figure 6-7 Cumulative frequency of the proportion of people voting hot or warm on the ASHRAE seven-point scale P during occupied hours of August 242
Figure 6-8 Frequency distribution of volume flow rates during occupied hours of August 243
Figure 6-9 Operative temperature and Volume flow rate profiles on August 24th 245
Figure 6-10 Water consumption per unit area 246
Figure 6-11 Water Consumption and Overheating Risk Index during the cooling season 251
Figure 6-12 Cumulative frequency of the proportion of people voting hot or warm on the ASHRAE seven-point scale P during occupied hours of August 252
Figure 6-13 Mean radiant temperature on the 23rd and 24th of August for the base case and variants -12 and 14 254
Figure 6-14 Surface-averaged Wall Pressure Coefficients for Tall Buildings (Atkins et al., 1979) 257
Figure 6-15 Local pressure coefficients (C_p x 100) for a tall building sited in urban terrain with wind direction varying at an increment of 30°

(Davenport & Hui, 1982) with the two locations of averaged C_p values overlaid 260
Figure 6-16 Mean wind pressure coefficients on a high-rise building with wind direction varying at an increment of 30° (TPU, 2013) with the two locations of averaged C_p values overlaid 261
Figure 6-17 Average volume airflow rates across the floors during occupied hours of the cooling season for the 12-storey segment model at different orientations with and without wind effects 263
Figure 6-18 Average volume airflow rates across the floors during occupied hours of the cooling season for the 12-storey segment model in the B-U flow pattern at different orientations with and without wind effects 264
Figure 6-19 Proportion of time during which each flow pattern operates for the wind and no-wind variants of the 12-storey segment model 265
Figure 6-20 Annual water consumption per unit area for the wind and no-wind variants 266
Figure 6-21 Average *P* values during occupied hours of the cooling season for the wind and no-wind variants oriented towards the four cardinal directions when a) operating in a B-U flow pattern b) in a T-U flow pattern c) in a T-D flow pattern d) overall average 267
Figure 6-22 Cumulative frequency of exceedance of *P* for ORI and EXI variants 272
Figure 6-23 Averge *P* values of NV, EX, OR, and MAX variants 273
Figure 6-24 PDEC water consumption in EX and OR variants 274
Figure 6-25 Exceedance of NV and EX variants based on their respective Adaptive comfort model 275
Figure 6-26 Exceedance of NV and EX variants based on the PMV-PPD model with still air conditions(PMV), the PMV-PPD model with internal airspeeds of up to 0.8m/s (PMV_0.8), and the Fiala model with air speeds of up to 0.6m/s (Fiala) 276

List of Tables

Table 3-1 Applicability categories of EN 15251 and associated acceptable temperature ranges 77
Table 4-1 Summary of review of modelling techniques of NV and PDEC 160
Table 5-1 Annual cooling energy for the BCM_AC 200
Table 5-2 Summary of whole-year results for the BCM during occupied hours only 201
Table 5-3 Summary of whole-year results for airflow rates in the BCM 207
Table 6-1 Vent sizes calculated by EFM 229
Table 6-2 Terrain-Dependent Coefficients (ASHRAE, 2013a)..... 256
Table 6-3 Average Cp Values at the top and bottom openings 261

List of Acronyms

AC	Air-Conditioning / Air-Conditioning mode
ACH	Air changes per hour
ACM	Adaptive Comfort Model
AFN	Air Flow Network
AIJ	Architecture Institute of Japan
ANV	Advanced Naturally Ventilated Building
ASHRAE	American Society of Heating, Refrigerating and Air-Conditioning Engineers
BBCC	Building Bio-Climatic Charts
BCM	Base Case Model
BCO	British Council for Offices
BMS	Building Management System
BEMS	Building Energy Management System
B-U	Bottom-Up flow pattern
C-E	Centre-in Edge-out flow direction
CAPMAS	Central Agency for Public Mobilisation and Statistics (Egypt)
CFD	Computational Fluid Dynamics
CIBSE	Chartered Institute of Buildings Services Engineers (UK)
CSAM	Climate Suitability Analysis Method
DEC	Direct Evaporative Cooling
DSF	Double Skin Façade
DSP	Dynamic Simulation Program
DTM	Dynamic Thermal Modelling
DTS	Dynamic Thermal Sensation
E-C	Edge-in Centre-out flow direction
EFM	Envelope Flow Models
EMS	Energy Management System
ETMY	Egyptian Typical Meteorological Year
EX	Exceedance
EXI	Exceedance Index
HBRC	Housing and Building Research Centre (Egypt)
IAQ	Indoor Air Quality
IBEC	Institute for Building Environment and Energy Conservation
ICC	International Energy Conservation Code
IGP	Inspector General of Police (India)
IDEC	Indirect Evaporative Cooling
IPCC	International Panel on Climate Change
JICA	Japan International Cooperation Agency

MM	Mixed Mode
MOEE	Ministry of Electricity and Energy (Egypt)
MOHUUD	Ministry of Housing, Utilities, and Urban Development (Egypt)
NC	Night Cooling
NM	Neutral Mode
NV	Natural Ventilation / Natural Ventilation Mode
OF	Opening Factor
OR	Overheating Risk
ORI	Overheating Risk Index
PDEC	Passive Downdraught Evaporative Cooling
PF	Projection factor
PHDC	Passive and Hybrid Downdraught Cooling
PM	Pilot Model
PMV	Predicted Mean Vote
PPD	Percentage People Dissatisfied
RH	Relative Humidity
SCAT	Smart Controls and Thermal Comfort
SHGC	Solar heat gain coefficient
SSEES	School of Slavonic and Eastern European Studies (UK)
T-D	Top-Down flow pattern
T-U	Top-Up flow pattern
TPU	Tokyo Polytechnic University (Japan)
UCLA	University of California Los Angeles
UTCI	Universal Thermal Climate Index
WBT	Wet-bulb Temperature
WWR	Window to wall ratio

Nomenclature

A^*_j	combined effective area of openings at the atrium/office and office/DSF interfaces on the jth floor
A^*_s	combined effective area of the segment's inlet/outlet openings
A'_{jA}	effective area of openings at the Atrium/office interface on the jth floor
A'_{jDSF}	effective area of openings at the office/DSF interface on the jth floor
A_A	area of opening at atrium/office interface
A_{AMAX}	maximum area of opening at atrium/office interface
A_i	area of opening *i*
B	sensible heat gain
C_d	discharge coefficient
c_p	specific heat capacity of air
C_p	wind surface pressure coefficient
g	acceleration due to gravity
h	floor height
H	total height of building
H_{met}	height of the standard meteorological wind speed measurement
j	floor level
n	number of floors in the segment
n_m	number of micronisers
OF	opening factor
P	proportion of people voting 'warm' or 'hot' on the ASHRAE comfort scale
P_{E0}	external hydrostatic pressure
P_{I0}	internal hydrostatic pressure
P_w	wind surface pressure relative to static pressure in undisturbed flow
P_{wi}	wind pressure at opening *i*
q_i	volume flow rate of air at opening *i*
Q_j	volume flow rate on the jth floor
Q_{tot}	total volume flow rate for the whole segment
R_A	vent area ratio
RH	relative humidity
RH_{PDEC}	post evaporation relative humidity
$R_{\Delta t}$	ratio of difference in air temperatures between the Atrium and DSF to the difference between the Atrium and external air temperature
t_A	dry-bulb temperature in the Atrium
t_{AC}	setpoint for mechanical air conditioning
t_{cmf_ASH}	ASHRAE's adaptive comfort temperature
t_{cmf_EN}	EN15251's adaptive comfort temperature

t_{db}	internal dry-bulb temperature
t_{DSF}	dry-bulb temperature in the DSF
t_{isp}	initiation setpoint temperature
t_{lb_ASH}	temperature at the lower boundary of the 90% acceptability range of the adaptive comfort model as defined by ASHRAE Standard
t_{mr}	mean radiant temperature
t_{op}	operative temperature
t_{PDEC}	post evaporation dry-bulb temperature
t_{PDEC_ACM}	post evaporation dry-bulb temperature recalculated at upper humidity level imposed on the ACM
t_{PDEC_PP}	post evaporation dry-bulb temperature recalculated at upper humidity level imposed on the PMV-PPD model
t_s	supply air temperature
t_{s_max}	upper limit for supply temperature
t_{ub_ASH}	temperature at the upper boundary of the 90% acceptability range of the adaptive comfort model as defined by ASHRAE Standard
t_{wb}	wet-bulb temperature
t_x	external dry-bulb temperature
t_{x_prv}	external dry-bulb temperature at previous timestep
U_H	reference wind speed at local height
U_{met}	wind speed at meteorological station
V_a	volume of air
V_m	water delivery rate
V_w	volume of water
W	humidity ratio/moisture content
W_{PDEC}	post evaporation humidity ratio/moisture content
z_i	height of opening i
α	terrain-dependent exponent at site
α_{met}	terrain-dependent exponent at meteorological station
δ	boundary layer thickness coefficients for the given terrain type at site
δ_{met}	boundary layer thickness coefficient for the given terrain type at meteorological station
Δp_i	pressure difference across opening i
Δt_A	difference between the Atrium and external air temperature
Δt_s	difference in air temperatures between the Atrium and DSF
ρ_a	density of air
ρ_w	density of water

Chapter 1: Introduction

1.1 Background

According to the Egyptian Ministry of Electricity and Energy, around 70% of the total energy produced in Egypt is consumed in buildings, 9% and 13% of which is consumed in commercial and governmental office buildings respectively (MOEE, 2016). It is estimated that mechanical ventilation and air-conditioning account for around 56% of the total energy used in these buildings (Khalil, 2008). Such high rates of energy consumption and the associated increase in greenhouse gas emissions are likely to have adverse impacts on the environment by contributing to global climate change. If existing trends are to persist, it is very likely that a viscous circle is created with the growing demand on air-conditioning systems.

The reliance on mechanical means however, is not restricted to office buildings located in hot climates but is also commonplace in the moderately mild climates of the Northern Hemisphere where it is often needed to avoid overheating resulting from high internal gains. In an effort to mitigate the negative impacts of mechanical cooling, an increasing number of buildings in Europe have recently been designed to incorporate innovative natural ventilation (NV) strategies. In addition to their financial and environmental benefits, NV buildings have long been recognised to have health benefits as fresh air intake dilutes or removes airborne pollutants within the occupied spaces, a causative factor of sick building syndrome (Wilson & Hedge, 1987).

In hot climates however, daytime ambient temperatures during the cooling season usually exceed internal temperatures. In such cases, NV is unlikely to achieve acceptable internal conditions unless incoming air is pre-cooled. In dry climates, this may be achieved by passive means using evaporative cooling. When water evaporates within a stream of ambient air, the temperature of the air is lowered, and its moisture content is elevated, while its wet-bulb temperature remains constant. The cooling of the air is also reflected in an increase in density, sufficient to drive a downdraught of air through a building (Ford, 2001). This technique termed Passive Downdraught Evaporative Cooling (PDEC) (Bowman et al., 1997), has two main advantages over HVAC systems. Energy required to cool the supply air by evaporation is negligible compared to that consumed in HVAC. Additionally, PDEC has the potential to drive air through the building saving around 30-40% of the electrical energy otherwise consumed by fan power (Ford, Schiano-Phan, & Francis, 2010). Finally, in terms of spatial efficiency, incorporating PDEC would potentially eliminate the need for ductwork and suspended ceilings which could lead to a 15% reduction in floor height.

PDEC is believed to be viable in rural as well as in city centre locations. This is due to it largely being a wind neutral passive strategy, i.e. one that does not depend on wind forces to drive air through the building. Air is also introduced to the building at high levels, where the concentration of pollutants is significantly lower than that at street level allowing for the building facades to be buffered from the noise and pollution characteristic of city centre locations. Furthermore, PDEC has the potential of being applied to almost any city located in a hot dry climate and has in fact been incorporated in a number of buildings around the world such

as the Sandra Day O'Connor United States Courthouse in Phoenix, USA, the Malta Stock Exchange in Malta and the Torrent Research Centre in Ahmedabad, India (Ford et al., 2010). It is noteworthy however, that it is the availability of a sustainable water resource that could impose limitations on the application of PDEC.



a b c

Figure 1-1 a) Sandra Day O'Connor United States Courthouse (Schiano-Phan, 2012), b) Malta Stock Exchange (Ford & Diaz, 2003), c) Torrent Research Centre (Ford, Patel, Zaveri, & Hewitt, 1998)

1.2 Research Problem

A review on the current body of knowledge on PDEC has indicated that research undertaken to understand and predict the thermal and airflow behaviour of buildings incorporating this strategy is limited to the study and design of low-rise buildings (Bowman, Eppel, Lomas, Robinson, & Cook, 2000; Cunningham, Mignon, & Thompson, 1987; Ford, 2001; Ford et al., 2010; Robinson, Lomas, Cook, & Eppel, 2004).

Acknowledging that Cairo is one of the most densely-populated cities in the world (Demographia, 2017), and given the pressing demand on high-quality office space in recent years, it is anticipated that extending the application of PDEC to

medium and high-rise deep-plan office buildings is imperative if PDEC is to be widely adopted as an alternative to conventional air-conditioning in Cairo.

However, it is anticipated that in achieving this, the following problems are likely to arise owing to the increase in building height as pointed out by (Etheridge & Ford, 2008):

1- The potential magnitudes of buoyancy forces become greater causing high pressure differences between the upper and lower floors which ultimately leads to marked discrepancies in airflow rates over the height of the building.

2- The potential magnitude of the wind forces acting on the building envelope also become greater due to lack of shelter at greater heights. This compromises the robustness of the ventilation strategy.

One way round the first problem would be to use internal resistances, i.e. small openings, at the lower floors. However, in tall buildings, the number of internal openings and their possible permutations would be large and could lead to less predictable behaviour. Alternatively, in NV tall buildings, this problem could be resolved by the use of segmentation, that is, to divide the building vertically into several segments that are isolated from one another in terms of airflow. Although the segmentation strategy has long been implemented in NV tall buildings such as the Commerzbank in Frankfurt (Davey, 1997) and the Deutsche Post Tower in Bonn (Wood & Salib, 2013a), it has yet to be tested prior to its application to PDEC tall buildings given that NV and PDEC buildings have different airflow patterns and modes of operation. Whilst vertical spaces in NV tall

buildings are used as exhausts for the hot air rising from the offices, they are likely to be used as air inlets and cool air reservoirs in PDEC buildings. This raises a few concerns, namely; the capacity of this strategy to deliver acceptable air change rates, the method to be implemented to extract displaced stale air, and the possibility of adopting several modes of operation to allow daytime and night-time ventilation alongside PDEC for example.

The previous observations and concerns in turn pose a number of questions; can PDEC be successfully applied to medium and high-rise buildings? What are the ventilation and cooling strategies involved and how can they be integrated into the building form? Finally, is there a PDEC tall building, a building whose configuration is derived from the downdraught cooling phenomenon?

1.3 Research Aim and Objectives

To answer the previous questions the main aim of this research is *to investigate the potential for Passive Downdraught Evaporative Cooling of medium and high-rise office buildings in Cairo.*

To achieve this aim, the following objectives need to be fulfilled:

1- To critically investigate the comfort requirements and overheating criteria involved in PDEC buildings and accordingly, the suitability of this passive strategy to the climate under consideration

2- To identify the airflow patterns and building configurations that give rise to such patterns

3- To develop a generic prototype of the PDEC high-rise multi-storey office building

4- To determine the appropriate sizes of the PDEC airflow components (inlet and outlet opening sizes)

5- To predict the performance of the PDEC generic prototype and establish the number of overheating hours and water consumption levels

6- Finally, to optimise the performance of the PDEC strategy in terms of water consumption whilst maintaining comfort conditions

1.4 Research Methodology

The research methodology provides an outline of the plan that must be carried out to achieve the research objectives. This implies that the research objectives are best used to inform on the most appropriate methodology to be adopted and thus guide the way data is gathered and analysed and conclusions are drawn. In light of the research objectives of this study, the research methodology could be outlined as follows:

A literature review on the current body of knowledge on PDEC was initially conducted, the outcome of which was the identification of the research problem and formulation of the research questions. The review included the Psychrometrics of evaporation as well as the means through which PDEC is incorporated in buildings.

Having established the research objectives, the first step was to conduct a literature review on thermal comfort requirements and overheating criteria in

office buildings. The Heat balance model (Fanger, 1970) and the adaptive thermal comfort model (de Dear & Brager, 2001) were both considered as well as the way both are incorporated in international standards such as ASHRAE Standard 55 (ASHRAE, 2010) and EN15251 (CEN, 2008). Recent developments in the topic of overheating criteria were also of particular interest to this study to provide an objective basis for evaluation (Nicol, Hacker, Spires, & Davies, 2009).

This was followed by a review on the available methods of assessing the climatic suitability of passive cooling strategies to determine the preliminary applicability of PDEC in Cairo. These include Givoni's Building Bioclimatic Charts (Givoni, 1992; Lomas, Fiala, Cook, & Cropper, 2004) and the Climate suitability analysis method (Axley & Emmerich, 2002).

To develop a generic prototype model of the PDEC high-rise office building, an a priori concept of the required morphology in fairly broad terms was required. An a priori is generally acquired either by choice of an existing solution or by drawing analogy between the current problem and previous solutions of a similar problem. Accordingly, an analysis of building precedents was carried out. This entails an understanding of the airflow and thermal behaviour of existing PDEC buildings and NV high-rise buildings and an identification of the characteristic elements that give rise to this behaviour. Relevant buildings identified for this study include, the Torrent Research building in Ahmedabad, India (Ford et al., 1998), the Inspector General of Police Complex in Gulbarga, India, the School of Slavonic and Eastern European Studies (SSEES) in London, UK (Short, Cook, & Woods, 2009), a speculative office building in Seville, Spain (Ford, 2001), The Deutsche Post Tower in Bonn, Germany (Helmut, Blaser, Werner, & Matthias,

2003), The Commerzbank in Frankfurt, Germany (Wood & Salib, 2013a), The Liberty Tower of Meiji University in Tokyo, Japan (Chikamoto, Kato, & Ikaga, 1999), and the New European Central Bank Headquarters (ECB) in Frankfurt, Germany (Cody, 2008).

Once the PDEC high-rise office building prototype model had been developed, the next and most critical step was to predict its performance. Again, a literature review on the available modelling techniques of NV and PDEC in buildings was required. Envelope flow models (EFM) (Etheridge, 2011b; Irving, Ford, & Etheridge, 2005) were selected for the initial sizing of the PDEC components (area of vent openings) and EnergyPlus (Crawley, Lawrie, Pedersen, & Winkelmann, 2000), a Dynamic thermal simulation program with an integrated airflow network model was selected to better understand the time-varying behaviour and assess the long-term performance of the model.

Having established the nature of the modelling tools to be used, two more aspects have to be defined in order to proceed with performance assessment; the physical characteristics of the model and the operational profile. To determine the physical characteristics of the model a survey on the current state of office building design and practice in Egypt is required. With the absence of any published data—to the best of the author's knowledge—on the current office building stock in Cairo, data was mainly obtained from the review carried out by Hamza N. (2004) on office buildings in Cairo. Existing construction profiles obtained are then compared with the requirements of Part II of the Egyptian Code for Improving Energy Efficiency in Buildings (HBRC, 2005) as well as a number

of international codes such as ASHRAE standard 90.1 (ASHRAE, 2004b) and the International Energy Conservation Code (ICC, 2012).

After establishing the performance of the base case model, a number of parametric studies are carried out to optimise the performance of the PDEC high-rise office building. These include the number of floors in a single segment, the duration of PDEC operation, wind forces and orientation, and finally thermal comfort model and overheating criterion

1.5 Scope and Beneficiaries

The study seeks to provide a platform for building confidence in proposed PDEC multi-storey office building designs by providing designers and their clients with sufficient data to proceed with passive, evaporatively cooled buildings. The anticipated outcomes are:

- A generic prototype of the PDEC multi-storey office building to aid architects in the conceptual and schematic design stages
- A methodology that enables building designers to easily assess the climatic suitability of PDEC to any given location
- Information about the appropriate range of sizes of the PDEC components such as the area of the inlet and outlet openings and the maximum number of floors within a single segment of the building
- Sets of quantitative data on the potential performance of PDEC office buildings in Cairo that pertain to the expected number of hours of overheating and the potential annual water consumption

1.6 Thesis Outline

Chapter Two provides a background on PDEC. PDEC is considered to be a form of natural ventilation (NV) insofar as the driving forces and governing thermodynamic properties are concerned. The chapter therefore begins in section 2.2 by providing an overview of the basics of natural ventilation, its objectives and indices, the driving forces, ventilation strategies and principles, flow paths, modes of operation, and control. A simple method to describe a building's ventilation concept is then presented. Section 2.3 provides a background on Evaporative cooling as a natural cooling strategy, presenting its origins, historical and contemporary applications, and psychrometric processes. The chapter concludes by presenting a literature review on previous work carried out on Evaporative cooling. In light of the intended objectives of the study, the review focuses on studies addressing forms of evaporative cooling in which buoyancy forces resulting from evaporation are used to generate a downdraught that naturally drives airflow through a single floor (room) or several floors of a building.

Chapter Three presents an overview of the climatic and urban contexts of Cairo as well as the thermal comfort requirements in PDEC buildings. In section 3.2, An analysis of Cairo's climate and wind potential is given. An understanding of the thermal comfort requirements in PDEC buildings is a necessary prerequisite for assessing the feasibility of the strategy and are therefore presented in section 3.3. A method based on the Climate Suitability Analysis Method (CSAM) to assess the preliminary applicability of PDEC to any location is elucidated in section 3.4 and results compared to Givoni's Building Bioclimatic

Charts (BBCC). Section 3.5 presents an overview of aspects of office building design in Cairo that are relevant to this study. Finally, section 3.6 presents the case for tall buildings in Cairo and in turn for extending the application of PDEC to medium and high-rise office buildings.

In Chapter Four, the proposed plan for the design of PDEC multi-storey office buildings is outlined. The plan proposes four stages. The first, henceforth referred to as the conceptual design stage, is where the ventilation strategy of the model is proposed and the generic prototype of the building that allows for such a strategy to work is developed. The second stage is that of design development and is where the initial sizes of the vents proposed in the generic prototype are calculated. The third and most important stage is that of performance assessment in which the airflow behaviour, resulting thermal conditions and environmental costs are established. The fourth and final stage of the design process is that of optimisation. Each stage requires different research tools and methods. The conceptual design stage entails knowledge of the ventilation strategies, flow patterns, and modes of operation involved. Knowledge of the building configuration that gives rise to such behaviour is however a prerequisite. Accordingly, analysis of precedents of PDEC buildings and NV tall buildings is presented in section 4.2 which then culminates in the development of the generic prototype of the PDEC multi-storey office building. The second and third design stages require knowledge of the modelling techniques and assessment tools available for PDEC and NV. A review of those tools is therefore presented in section 4.3. Each modelling technique is described, and examples of its application given. Suitability of each modelling technique for the various design

stages is highlighted together with its advantages and limitations. The review concludes with the selection of an analytic model (Envelope flow models EFM) for the initial sizing of the vents of the generic PDEC prototype (design development stage) and of an integrated dynamic thermal and airflow model (EnergyPlus) for the performance assessment stage. In section 4.4, description of Envelope Flow Models (EFM) and the procedure used to calculate the initial sizes of the generic prototype is presented. In section 4.5, a brief description of EnergyPlus is given and the procedure used to simulate PDEC is presented.

In Chapter Five, results of the integrated thermal and airflow simulations of the Base Case Model (BCM) of the proposed PDEC Multi-storey Office Building are presented. The BCM represents the foundation to which the model variants and the parametric investigations performed on them in the following chapters are compared. To assess the preliminary validity of the proposed model in EnergyPlus and accordingly allow for any necessary refinement, a pilot model was deemed necessary. Section 5.2 describes the Pilot Model (PM), its modelling assumptions, construction profiles, occupancy and Internal heat gains schedule, aperture control logic, and initial sizing of PDEC components (i.e. the size of openings throughout the model). Results of the preliminary investigation are also presented in this section. Based on the results of the PM, a process of refinement was performed to reach the BCM, details of which are presented in Section 5.3. Analysis of the results of the BCM is presented in Section 5.4 together with a discussion on the thermal and airflow behaviour of the model. In Section 0, conclusions on the overall performance of the BCM are drawn and issues raised

from the analysis of the results of the BCM are highlighted to be investigated in the following chapters.

In Chapter Six, parametric investigations are carried out to examine the effect of varying different input parameters on simulation outputs with the aim of optimising the PDEC strategy in the proposed generic configuration of the multi-storey office building in order to deliver acceptable internal conditions for occupants whilst minimising environmental costs. In Section 6.2, the effect of increasing the number of floors in a segment on the overall bulk airflow rates in the segment and the distribution of airflow rates across the floors was investigated together with the implications of that on internal conditions and water consumption. The effects of extending PDEC operation during unoccupied hours on reducing the mean radiant temperature the following day is discussed in Section 6.3 with the implications of that on water consumption. Section 6.4 discusses the inclusion of wind forces and their effects on airflow rates across the floors of the segment. The effects of varying the orientation of the building segment and the subsequent change in solar gains and wind forces on the thermal and airflow behaviour of the PDEC building model is also investigated. Choice of the thermal comfort model and overheating criteria has a significant bearing on the assessment of acceptability of internal conditions for human occupancy and is therefore the subject of Section 6.4 in which the effect of adopting different comfort models and overheating criteria is examined.

Chapter Seven presents the Summary and conclusions, contribution to knowledge, and suggested future work.

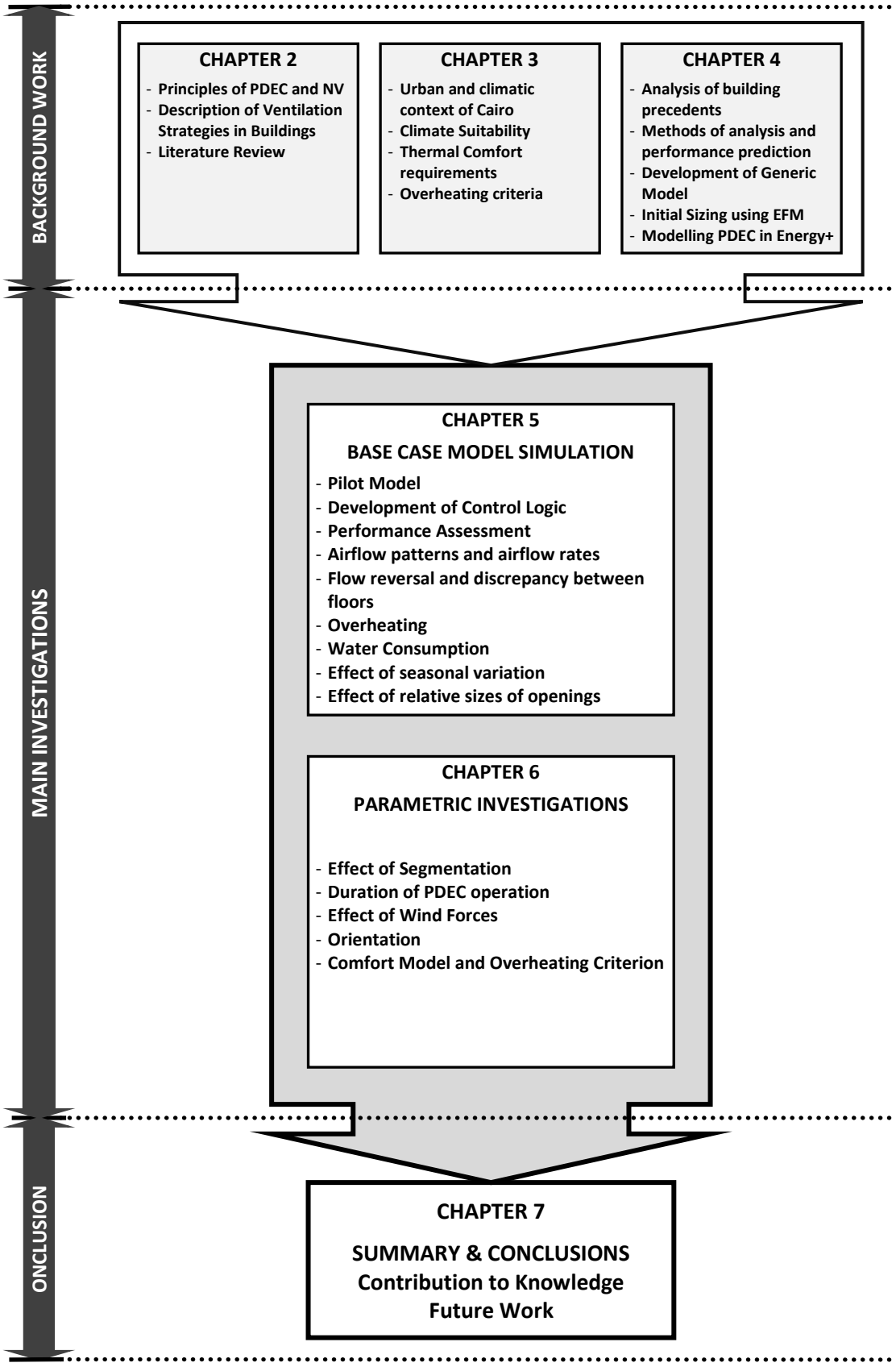

Figure 1-2 Thesis Outline

Chapter 2: PDEC: Background and Previous Work

2.1 Chapter Overview

This chapter provides a background on PDEC. PDEC can be considered a form of natural ventilation (NV) insofar as the driving forces and governing thermodynamic properties are concerned. The chapter therefore begins in section 2.2 by providing an overview of the basics of NV, its objectives and indices, driving forces, strategies and principles, flow paths, modes of operation, and control. A simple method to describe a building's ventilation concept is then presented. Section 2.3 provides a background on Evaporative cooling as a natural cooling strategy, presenting its origins, historical and contemporary applications, and psychrometric processes. The chapter concludes by presenting a literature review on previous work carried out on Evaporative cooling. In light of the intended objectives of the study, the review focuses on studies addressing forms of evaporative cooling in which buoyancy forces resulting from evaporation are used to generate a downdraught that naturally drives airflow through a single floor (room) or several floors of a building.

2.2 Basics of natural ventilation in buildings

As previously mentioned, PDEC can be considered to be a form of NV. As such, it is essential to begin by giving a brief description of the basic principles of building ventilation. The section starts by defining the notion of a building's *ventilation concept* and the different terms involved. A new framework is

proposed that links and describes these terms in relation to the spatial elements of a building. The terms are then reviewed and finally presented in a way that describes the different modes of operation of a building's ventilation system over the course of the year.

2.2.1 Natural Ventilation and Building Configuration

The following section briefly describes the basic principles and physical processes involved in the ventilation of buildings. It is imperative to appreciate that, consistent with Kleiven (2003), this study adopts the notion of a building's 'Ventilation Concept' as that which *'fully describes the building's overall ventilation system and the way it operates over the course of the year'*; i.e. a notion that encompasses the objectives, driving forces, ventilation strategies, and ventilation principles employed, as well as the flow direction and flow path in each mode of operation (summer/winter – day/night – natural/mechanical), together with the means through which the building switches between these modes. An explanation of the different terms and issues involved in this definition is given below preceded by a discussion on the objectives of natural ventilation in buildings and hence its relevance in contemporary architectural practice.

However, before proceeding, and with the aim of facilitating the description of a building's ventilation concept, this study proposes a new framework in which the building is divided into three distinct spatial zones of different functions in terms of airflow. This division would presumably provide a frame of reference that links the various terms involved in the building's ventilation concept to each other and more pertinently to the building's morphology which is central to the study at

hand. In other words, this framework allows for the various terms to be described with reference to and in terms of the building's three spatial zones. The three spatial zones are:

The Delivery Zone

This is the zone which is intended to be ventilated and cooled by the system and is usually comprised of a number of occupied spaces.

The Supply Zone

This is the zone through which incoming air passes before being admitted to the occupied spaces. There are two distinct functions in terms of airflow that take place in this zone; air inlet and air distribution. In most cases the two functions are performed in a single space of which typical examples are atria, wind towers and double skin façades. However, in some cases, the two functions take place in two separate spaces and so, it is relevant to further divide this zone into two sub-zones;

- **The Inlet zone**: is essentially where outdoor air first enters the building. It represents an intermediate zone that connects the distribution zone to the external environment. Typical examples of this zone are sky-gardens, air plena, and embedded air ducts.

- **The Distribution zone**: is the space where incoming air is distributed in the building before being delivered to the occupied spaces. Typical examples of this zone are lightwells and atria.

The building of the School of Slavonic and Eastern European Studies (SSEES) in London, represents a typical example where the inlet and distribution zones occupy two separate spaces (Short, Cook, & Woods, 2009). However, not all buildings necessarily have a supply zone. For example, in cases where the occupied spaces are directly connected to the outside via openings in the external façade, the supply zone is not contained inside the building but can, in this case, be taken to be the external environment itself.

The Exhaust Zone

This is the zone through which used air passes after leaving the delivery zone to the point where it is exhausted out of the building. Similar to the supply zone, one can differentiate between two functions that occur in the exhaust zone; air extraction and air outlet. In the majority of cases if not all, the two functions are contained in one single space. Nevertheless, in some rare cases, they take place in two separate spaces, hence the relevance of the following sub-division;

- **The Extract zone**: in contrast to the distribution zone, the extract zone is where the used air leaving the delivery zone is collected before being exhausted. Typical examples of this type are again atria, exhaust stacks/chimneys, and Double Skin Facades (DSF).
- **The Outlet Zone**: is not very common in naturally ventilated buildings but nevertheless has to be differentiated from the extract zone as it sometimes exists as an intermediate zone that connects the extract zone to the external environment. Typical examples of this zone are the wind floor in the Liberty Tower of Meiji University (Chikamoto et al., 1999) and the sky-gardens at the top of each segment in the Commerzbank (Buchanan, 1998).

Again, it has to be noted that not all naturally ventilated buildings have an exhaust zone. Similar to the example presented to describe a building with no supply zone, if used air is allowed to leave through openings in the external façade of the delivery zone, the exhaust zone is suppressed or can, in this case, be taken to be the external environment.

Furthermore, in naturally ventilated buildings that solely depend on openings in the external façade of the delivery zone for the supply and exhaust of fresh air, both supply and exhaust zones are suppressed and the whole building is considered a delivery zone. In this case the building is said to have a simple ventilation concept as opposed to an Advanced Naturally Ventilated building (ANV) (Lomas, 2007) which is stack ventilated as will be elucidated in section 2.2.4.2. ANV buildings usually have either a supply or exhaust zone or both.

2.2.2 Objectives and Indices of Natural ventilation

Following the energy crisis in 1973 (Merrill, 2007), research and practice of buildings, especially those located in temperate and cold climates have predominantly focused on thermal insulation, air-tightness and heat recovery as means of reducing the total heat loss or gain of buildings with the aim of decreasing the energy needed for their heating or cooling respectively (Delsante & Vik, 2000). Whilst awareness of issues related to energy efficiency had already begun to emerge, nevertheless buildings were still designed to be completely isolated from the external environment, exclusively depending on artificial lighting, mechanical ventilation, and active heating and cooling systems to control the indoor environment.

In recent years, there has been a surge of interest in the sustainable design of buildings by means of harnessing renewable resources abundantly available in nature. In this approach and in contrast to the previous, buildings are designed to interact with the external environment, utilising natural resources by applying passive design strategies (as opposed to active) to buildings in order to create a comfortable indoor environment whenever possible.

2.2.2.1 The purpose of natural ventilation

One of the most sustainable and energy-efficient passive design strategies that has drawn a great deal of interest in terms of research and practice is natural ventilation (Awbi, 2013; Etheridge & Sandberg, 1996; Ghiaus & Allard, 2016; Irving et al., 2005; Liddament, 1996). This is mainly due to the fact that the natural ventilation of buildings can fulfil two primary purposes:

- *An acceptable indoor air quality (IAQ)*: This is essentially based on the supply of fresh air and the removal or dilution of indoor pollution concentration.
- *Passive Cooling*: This is also essential in order to achieve thermal comfort by providing a heat transport mechanism between the external and internal environments.

However, in this study, emphasis will be given to the use of natural ventilation for cooling purposes which is a major concern in the hot-dry regions of the world. This emphasis is further supported by the fact that the design of natural ventilation systems for passive cooling will usually meet the requirements of the two (Irving et al., 2005), provided that a suitable

ventilation concept is adopted as will be discussed later. This is because the ventilation rates needed for cooling are normally well in excess of those needed to meet the IAQ requirements of occupants.

2.2.2.2 Indices of performance

Basically, there are two indices that measure the performance of a ventilation system; *Ventilation rate* and *Ventilation efficiency*.

Ventilation rate: also called airflow rate is a measure of the *quantity* of fresh air passing through an enclosure (e.g. room or entire building) in a specified time interval. This quantity can be measured in volume or mass per unit time (second or hour) and in some cases also per person or per unit area. The most commonly used unit for airflow rate is air changes per hour (ACH) which is the volume flow rate of an enclosure divided by its volume (Liddament, 1996).

Ventilation efficiency: describes the mixing behaviour of air and the distribution of pollutant within a space and is thus a measure of the *quality* of air inside an enclosure. Ventilation efficiency is based on an evaluation of the 'age' of air and on the concentration distribution of pollutant within the air. Some indices are based on room averaged values, while others refer to specific points or locations. This has important consequences because while room values provide some guidance to the overall performance of a ventilation system, point values indicate regions where localised poor ventilation might occur (Daniels, Stoll, Pultz, & Schneider, 1993).

2.2.3 Driving Forces

Natural ventilation in buildings occurs as a result of pressure differences generated across the openings in the building's envelope. The pressure differences are basically generated by two fundamental forces;

- *Wind*, which acts on the building's envelope creating areas of positive and negative pressures
- *Gravity*, which acts on density (temperature) differences between the internal and external air (buoyancy forces)

It is seldom to find a ventilation system that solely depends on one driving force. Therefore, a successful design will utilise a combination of both wind and buoyancy seeking ways to ensure that the effects of the two complement rather than oppose each other. Design practice is often to size the openings based on buoyancy forces alone, and to engineer the design so that any wind effect will enhance the driving forces. The magnitude and pattern of natural air movement through a building depends on the strength and direction of these natural driving forces and on the resistance of the flow path, that is, the building's geometry and internal configuration (Irving et al., 2005).

However, in the absence of sufficient natural driving forces that bring air into a building, as is the case when wind speeds are low or temperature differences between the inside and outside are small, a mechanical backup system has to be included in order to continuously deliver the required airflow rates. These mechanical systems can either be in the form of fans to deliver the required airflow rates, or in the form of active cooling to achieve thermal comfort. A

ventilation system that utilises both natural and mechanical driving forces is said to be a mixed-mode (MM) or hybrid ventilation system (de Gids & Jicha, 2010).

2.2.4 Ventilation Strategies

In order to successfully utilise the natural driving forces to generate airflow inside a building, or to be more specific, inside the occupied spaces (delivery zone), an appropriate ventilation strategy has to be adopted, the choice of which depends on the type of driving forces available on site, the climate, and the type of activity housed in the building. The ventilation strategy indicates how the exterior and interior airflows are linked, and hence how the natural driving forces are utilised to ventilate the occupied spaces. In other words, the ventilation strategy is an indication of how occupied spaces are configured in relation to the external environment and to the building as a whole. Accordingly, and consistent with CIBSE AM10, it is relevant to divide ventilation strategies from this perspective into two basic categories; ventilation strategies for isolated spaces and for connected spaces (Irving et al., 2005).

2.2.4.1 Isolated Spaces

Spaces are considered isolated in terms of airflow when the openings connecting them to other spaces of the building are small in relation to the openings connecting them to the external environment. Consequently, the ventilation of occupied spaces in this category is independent on their configuration in relation to the building and as such does not necessitate the existence of either a supply or exhaust zone within the building which can in

this case, be taken to be the external environment. Ventilation strategies for such spaces can be summarised as follows (Irving et al., 2005).

Single-sided ventilation

This is usually the simplest form of naturally ventilating a space whereby a simple opening is used to allow outdoor air to enter the building and room air to leave either from the same opening or from another opening situated on the same wall, i.e. the supply and exhaust zones are the same and are on the same side of the space. With a single ventilation opening in the room, the main driving force for natural ventilation is the time-varying pressure difference due to wind turbulence. As a rule of thumb, the limiting depth for effective ventilation in this case is about 2*h* from the opening itself, where *h* is the floor to ceiling height. Where multiple ventilation openings are provided at different heights within the façade, then the ventilation rate can be enhanced due to the stack effect. The stack induced flows increase with the vertical separation of the openings and with the inside to outside temperature difference. As well as enhancing the ventilation rate, the double opening increases the depth of penetration of the fresh air into the space to 2.5*h* (Figure 2-1). It is also possible to get buoyancy driven exchanges through a single opening provided the opening is reasonably large in the vertical dimension.

<u>Pros and cons of single-sided ventilation</u>

1- A very common and inexpensive strategy

2- Can be easily employed to serve individual offices

3- Driving forces are relatively small hence low ventilation rates are generated
4- Only effective over a distance of about 2.5*h* from the opening
5- Only suitable in moderate climates
6- Unreliable and highly variable and so, is not recommended as part of a controlled natural ventilation strategy

Cross Ventilation

Cross ventilation occurs via ventilation openings on opposite sides of the external envelope of an enclosed space. This means that the supply and exhaust zones are on two different sides of the space. The flow of air in this case is mainly due to wind forces which create differences in pressure between openings on the windward side and those on the leeward side, whereas buoyancy pressures become important only if there is a significant difference in height between the inflow and outflow openings. A significant difference in wind pressure between the inlet and outlet openings and a minimal internal resistance to flow are needed to ensure sufficient ventilation flow. As a rule of thumb, the building floorplan depth in the direction of the ventilation flow must be limited to a maximum length of 5*h* to effectively remove heat and pollutants from the space (Figure 2-1). This is usually achieved with a linear built form with an ‘open plan’ interior. In order to improve air distribution into deeper spaces, it is possible to use ducted or underfloor ventilation pathways. However, due to the low driving pressures with natural ventilation, it is important to design the supply duct for very low pressure drops.

Pros and Cons of cross ventilation

1- There is a limit on the depth of space that can be effectively cross-ventilated. This implies a narrow plan depth for the building.
2- The narrow plan depth associated with this approach has the added benefit of enhancing the potential for natural lighting.
3- Internal partitions and other obstructions can affect or disturb the air flow pattern in the room and the air penetration depth.
4- Unsuitable for cooling in hot climates where external temperatures are higher than internal ones. In this case any attempt to pre-cool incoming air will lead to very high pressure drops and hence very small airflow rates.

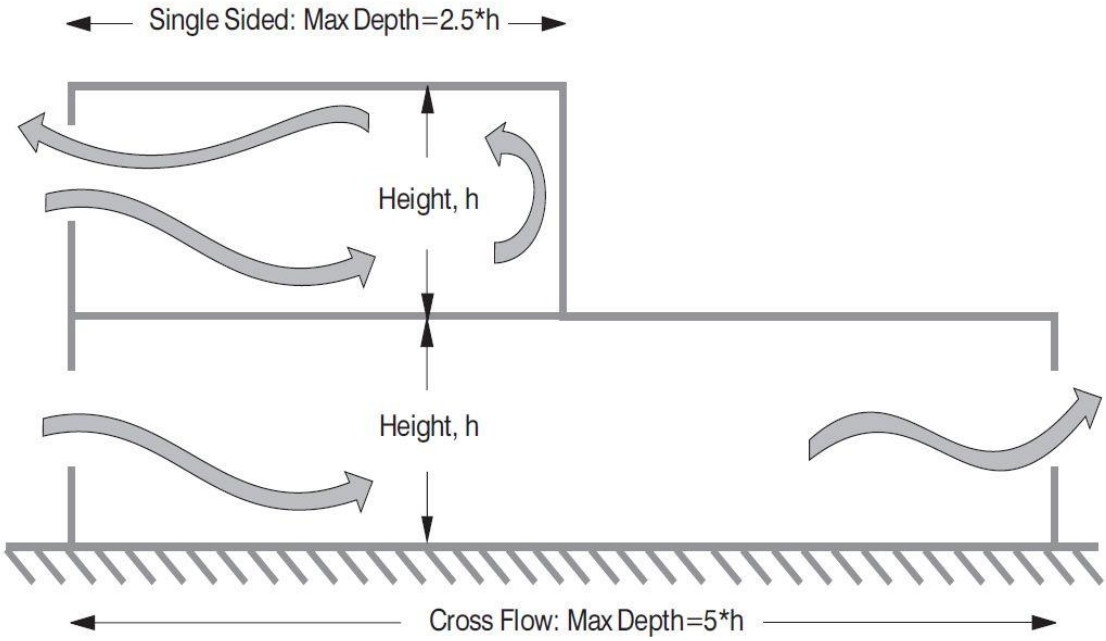

Figure 2-1 Maximum depth of spaces in isolated ventilation strategies.
Source (Liddament, 1996)

2.2.4.2 Connected spaces

On the other hand, spaces are considered connected in terms of airflow when they form a single cell. This necessitates the existence of either a supply or exhaust zone to connect the occupied spaces to the rest of the building and to the external environment. The flow of air in this case is mainly due to buoyancy pressures. The ventilation strategy in this case is summarised as follows:

Buoyancy driven stack ventilation

Buoyancy-driven stack ventilation relies on density differences to draw cool, outdoor air in at low ventilation openings and exhaust warm, indoor air at higher ventilation openings. The stack pressure is determined by the difference between the internal and external temperature and the height of stack, thus a vertical space is frequently used as the supply or exhaust zone to generate sufficient buoyancy forces to achieve the needed flow. In such a strategy, wind forces can also be important. Depending on the position of air inlet and outlet in the building, the wind pressure could assist the stack pressure, reduce its influence or indeed reverse the effect. Therefore, when stacks are incorporated in the building, careful design considerations are needed to avoid these adverse effects occurring. A successful design is one that will seek ways to make full advantage of both.

<u>Pros and Cons of buoyancy driven stack ventilation</u>

1- Can be used in areas where wind speeds are very low

2- More reliable in terms of the stability of airflow rates

3- Delivers smaller airflow rates if compared to wind-driven strategies, especially at instances of high wind speeds.

4- Since the building acts as a single space, the overall height is the determinant of the buoyancy force. Thus, the areas of inlet openings have to vary with the building's height which can, in some cases, be inconvenient.

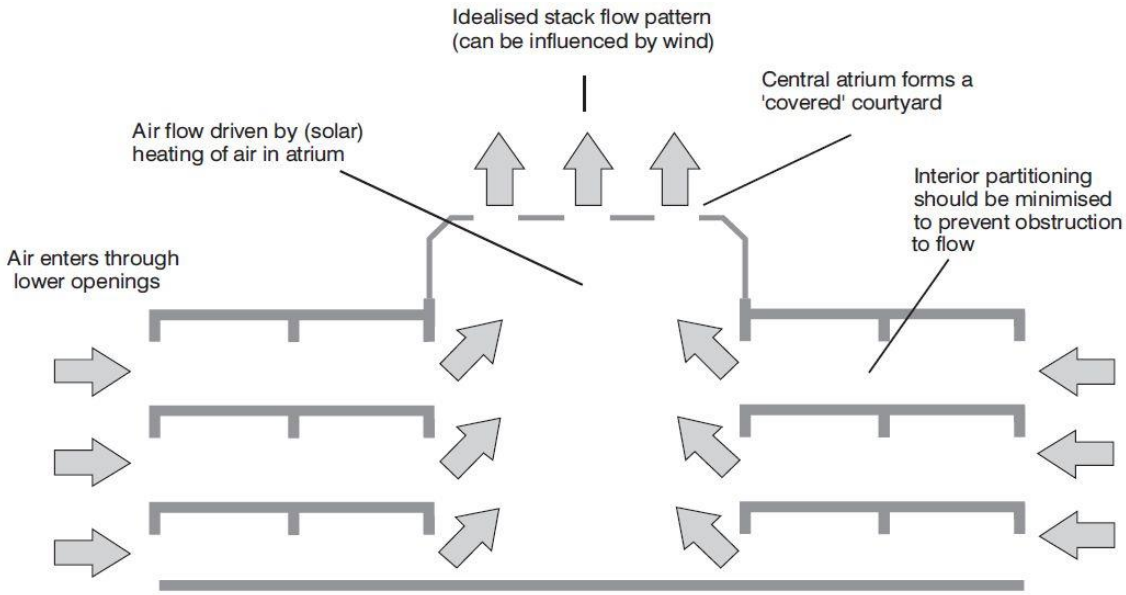

Figure 2-2 Buoyancy driven stack ventilation. Source (Liddament, 1996)

2.2.5 Ventilation Principle

A very important factor that controls the ventilation efficiency of a system is the ventilation principle employed which describes the way air flows within the delivery zone from entry to exit and hence, the method heat and contaminants are distributed and eventually dissipated. There are basically two ventilation principles; mixing and displacement (Figure 2-3).

Mixing ventilation: This method requires that the supply air and room air are well mixed by the actions of the supply jet momentum and buoyancy. This is still the most widely used method in ventilation and air-conditioning systems because, with proper design, it can be used for heating and cooling as well as ventilation and can also cope with much larger room loads than in displacement ventilation. The supply air is used to dilute the concentration of contaminants in the room but not to displace them as in the displacement method. However, unless the sources of pollution are evenly distributed throughout the space, high concentration levels are always found near these sources. Because the outdoor air is usually supplied at high level (i.e. above the occupied zone) the concentration levels above the occupied zone are generally lower than those existing within the zone. In addition, stagnant zones of high concentration levels and/or short-circuiting of supply air to the extract points can cause a sharp drop in the ventilation efficiency (Awbi, 2013).

Displacement Ventilation: This type relies on the displacement of room air by a fresh supply of air. Displacement ventilation is used in buildings with large occupancy and internal heat gains, where mainly cooling is required. There are upward and downward displacement ventilation systems. However, the upward system is more widely used than the downward system because it produces better indoor air quality for the occupants. In this system, outdoor air or a mixture of outdoor and recirculated air is delivered close to the floor of the room at a low velocity (0.25 - 0.35 m/s) which then rises through the room by a combination of momentum and buoyancy forces, the latter caused by the presence of people or warm surfaces such as IT equipment in offices. Temperature and concentration

stratification then develop with cool, clean air at low level and warm, contaminated air at a higher level above the occupants (Davey, 2006).

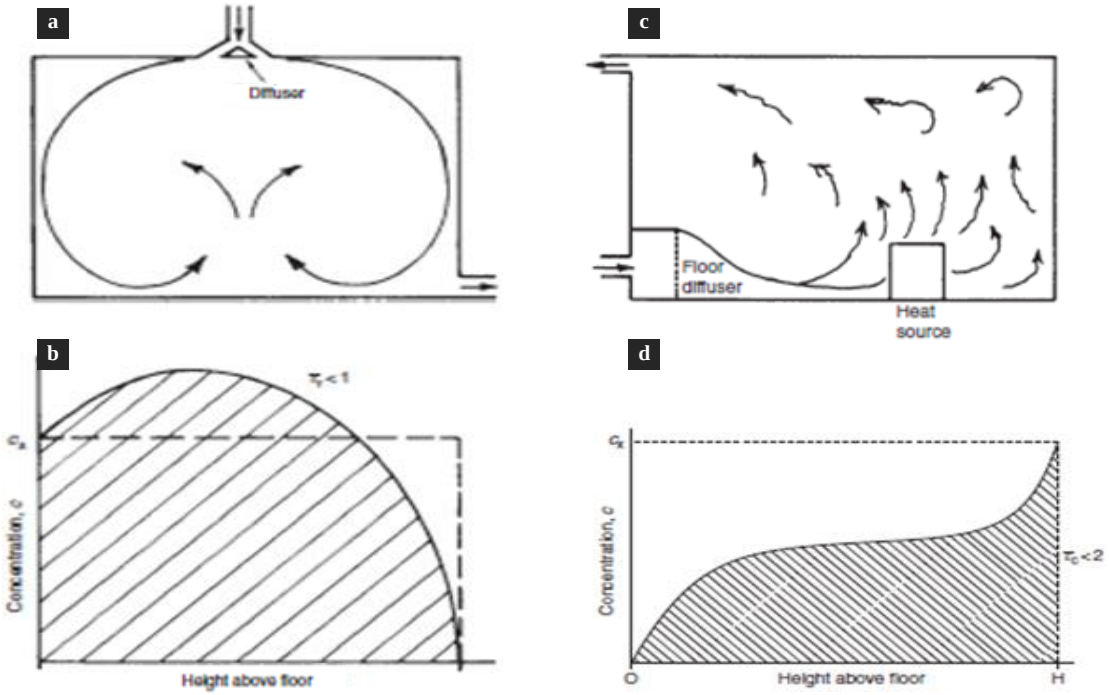

Figure 2-3 a) Air movement in a mixing ventilation system. b) Typical increase in concentration with distance for a mixing ventilation system. c) Flow produced by floor displacement ventilation. d) Typical increase in concentration with distance for floor displacement ventilation. Source (Davey, 2006)

2.2.6 Flow Direction

The flow direction describes the direction of airflow from the distribution to the extract zone in relation to the building's morphology. In other words, it describes the location of both the distribution and extract zones relative to the position of the delivery zone in the building. For example, if the delivery zone is located between the external envelope and the distribution zone, while the extract zone is located between the delivery zone and the external envelope, the flow direction is from centre to edge. This is consistent with the taxonomy of naturally

ventilated buildings proposed by Lomas & Cook (2005) which divides them into four main types or more precisely, four different flow directions (Figure 2-4**Error! Reference source not found.**) as follows (Lomas & Cook, 2005):

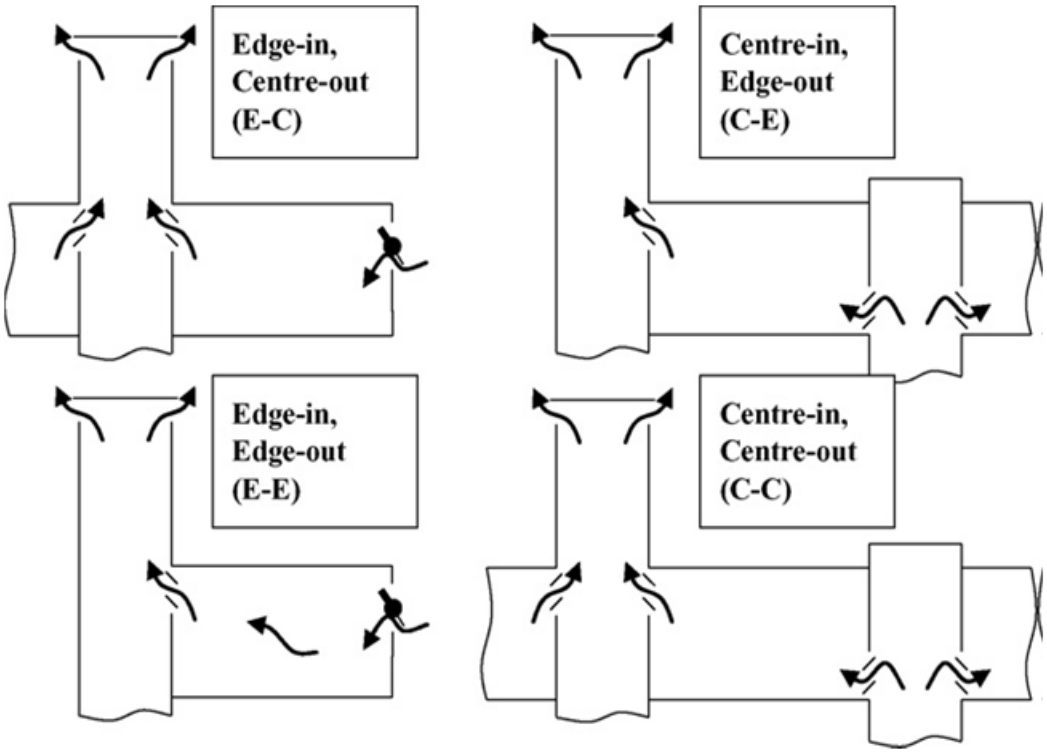

Figure 2-4 Schematic diagrams of the different flow directions. Source (Lomas, 2007)

2.2.6.1 Edge in – Centre out (E-C)

In this case the supply zone lies at the external perimeter of the delivery zone while the extract zone is surrounded by the delivery zone. This flow direction is employed in the Queens Building at De Montfort University, Leicester, UK (Asbridge & Cohen, 1996; EEBPP, 1997) as shown in Figure 2-5.

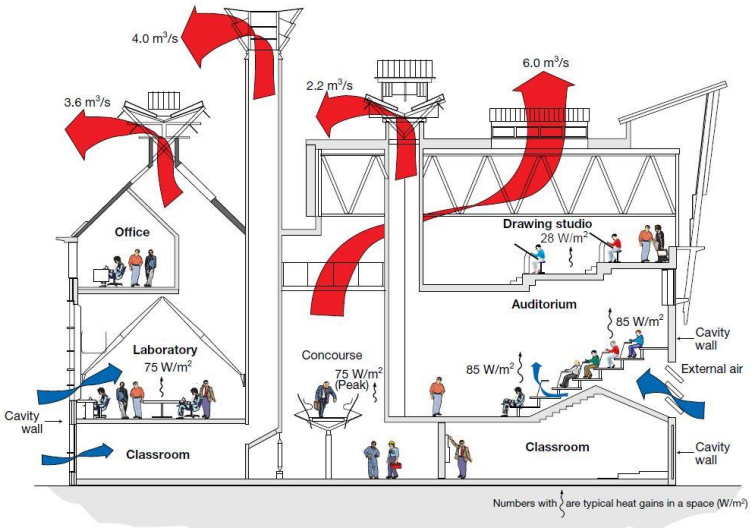

Figure 2-5 E-C flow direction in the Queens Building at De Montfort University (EEBPP, 1997)

2.2.6.2 Edge in – Edge out (E-E)

In this case both the supply and extract zone lie at the external perimeter of the delivery zone. This flow direction is employed in the UK Building Research Establishment's (BRE) Environmental (Delsante & Vik, 2000) as shown in Figure 2-6.

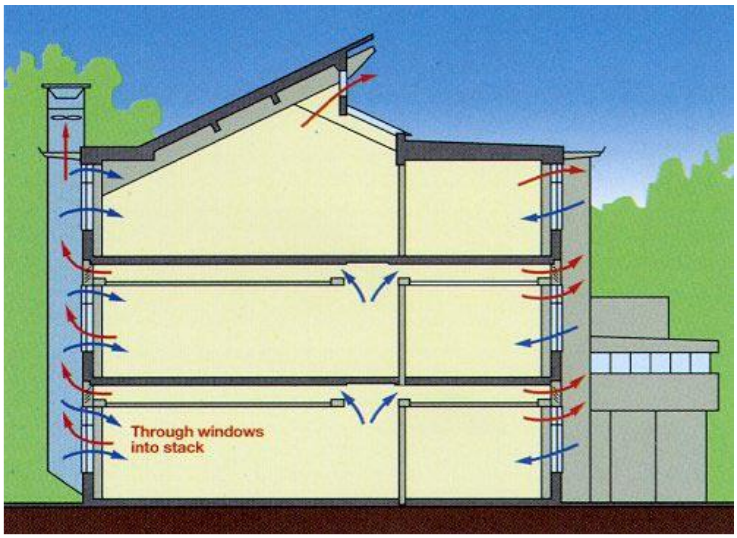

Figure 2-6 E-E flow direction in the BRE Building (Delsante & Vik, 2000)

2.2.6.3 Centre in – Edge out (C-E)

In this case the supply zone is surrounded by the delivery zone while the extract zone lies at the external perimeter of the delivery zone. This flow direction is employed in the SSEES building in London (Lomas, 2007; Lomas, Short, & Woods, 2004; Short, Cook, & Lomas, 2009) as shown in Figure 2-7.

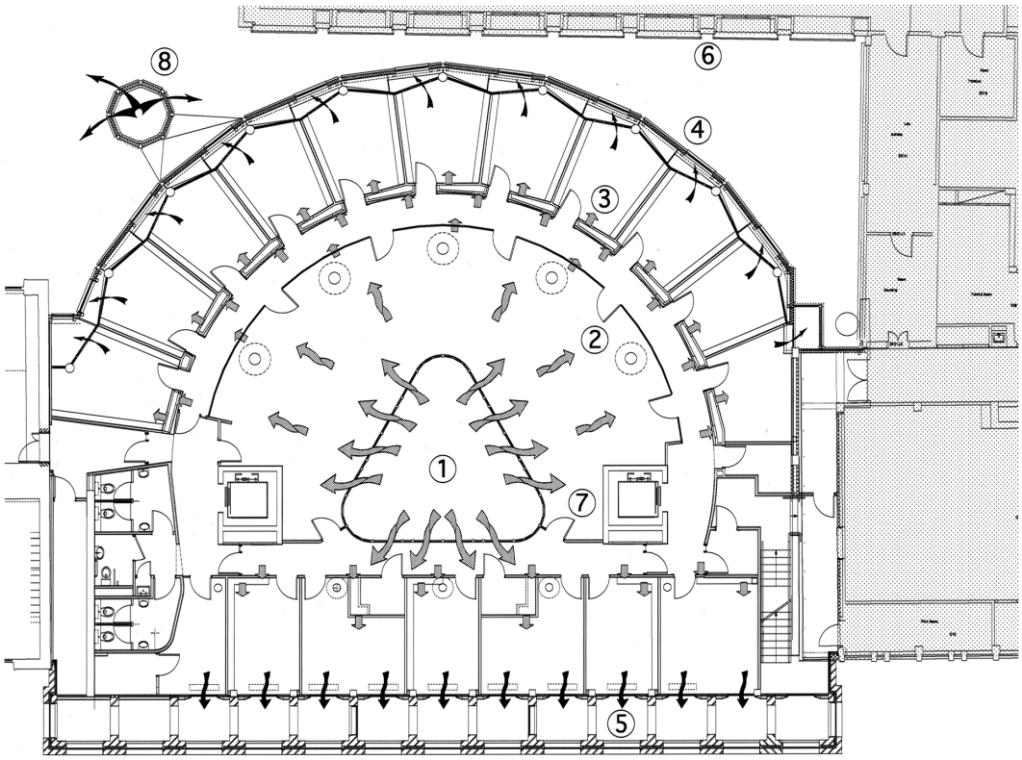

Figure 2-7 C-E flow direction in the SSEES building (Lomas, Short, et al., 2004)

2.2.6.4 Centre in – Centre out (C-C)

In this case both the supply and extract zone are surrounded by the delivery zone and have no direct connection to the external envelope. This flow direction is rarely employed alone but can nevertheless be used alongside

with other flow directions. One example of this is the Frederick Lanchester Library in Coventry, UK (Cook, Lomas, & Eppel, 1999a; Lomas, 2007; Lomas, Short, et al., 2004) which employs both the C-C and C-E flow directions as shown in Figure 2-8.

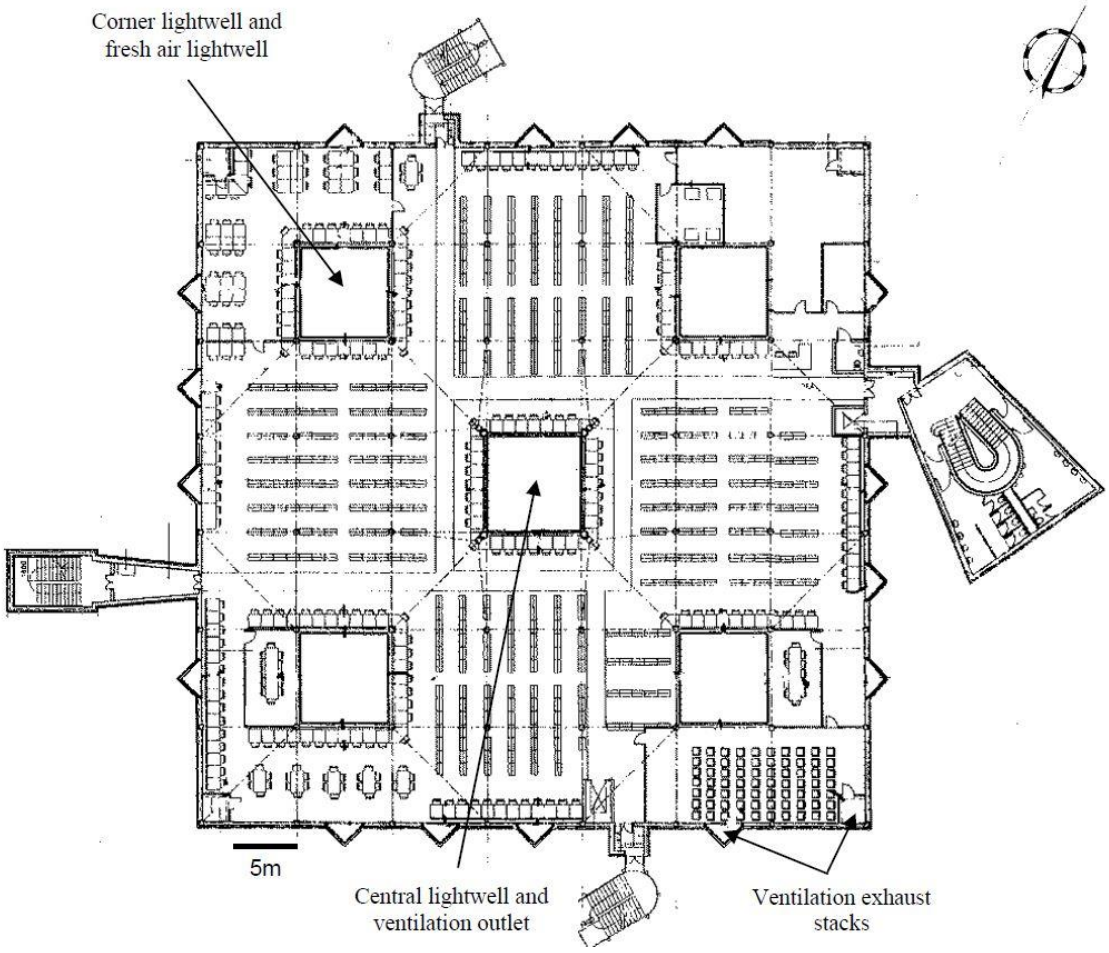

Figure 2-8 C-C and C-E flow directions in the Frederick Lanchester Library (Cook et al., 1999a)

2.2.7 Flow Path

As opposed to the ventilation principle, the flow path describes the route that the ventilating air follows between the outside and the delivery zone inside a

building and not the airflow path within the occupied zones. The supply and exhaust paths can be divided into two categories; local and central.

This distinction is important if treatment of the incoming air is needed as is the case when external temperatures exceed internal ones.

2.2.7.1 Local supply and exhaust paths

In this type each space in the delivery zone is independently linked to the outdoor environment. A local supply path therefore means that fresh air is directly introduced to the space, while a local exhaust path means that the used air is directly exhausted to the outside with no intermediate distribution or extract zone associated with them respectively. Single-sided and cross ventilation are the typical ventilation strategies associated with local supply and exhaust paths.

2.2.7.2 Central supply and exhaust paths

In a central supply path, two or more spaces in the delivery zone are serviced by one supply zone. This means that any treatment along the supply zone will benefit all the serviced spaces at the same time. This is extremely vital when the incoming airflow needs to be strengthened, for example by fans, to overcome any pressure drops; or treated, be it by cooling, heating, or filtering. In naturally ventilated buildings, typical examples of central supply paths are atria and wind catchers. On the other hand, a central exhaust path combines used air leaving two or more spaces into an exhaust zone that terminates at

a single opening in the building envelope. Typical examples of central exhaust paths are solar chimneys, atria, and DSFs.

A single occupied zone can have a combination of different types of supply and exhaust paths, that is, it can have a local supply path whereas its used air is exhausted to a central path and vice versa. Moreover, a single building can adopt different types of supply and exhaust paths in different zones of the building (i.e. spatially variant) or can switch between two co-existing paths in the same spatial zone depending on the time of day or year (i.e. time variant) as is the case with night ventilation.

Both local and central supply and exhaust paths have their advantages and drawbacks. For local supply and exhaust paths, the main advantage compared to central paths is that they offer more flexibility in terms of future changes in interior layout. Furthermore, in cases where no treatment of outdoor air is required (i.e. good outdoor air quality), the quality of air can be maintained with no risk of degradation that may otherwise occur in central supply paths due to the relatively longer distance air travels before reaching the serviced zones. On the other hand, one key advantage that central paths have over local ones is that one single treatment unit can service the entire supply airflow offering huge savings in space, energy, and initial and maintenance costs. Thus, preheating or precooling of incoming air, as is the case with PHDC, is greatly facilitated. However, in some cases fresh air can be supplied to a space through a central path while a local heater/cooler provides the required thermal conditioning of either the incoming air or the space. This is why it is useful to differentiate between the supply of fresh air

and the supply of heating/cooling to a space. Another advantage of central paths is that, in contrast to local paths where the serviced spaces are ventilated with fresh air from the perimeter of the building, central paths allow for deeper floor plates without compromising the area which can be effectively ventilated. Finally, when both supply and exhaust paths are central, heat recovery is possible.

2.2.8 Modes of Operation

As previously mentioned, in order to fully describe a building's ventilation concept, it is necessary to include a description of the time varying behaviour of the building, with respect to diurnal and seasonal changes, i.e. changes in external conditions. Buildings are designed to operate in different modes in order to maintain comfort conditions at all times. The mode of operation mainly depends on the time of year and day which could, in extreme climatic conditions, require the inclusion of a mechanical mode. As a result, over the past few years, a number of mixed-mode systems have developed. Although they all combine both natural and mechanical ventilation technologies, these systems differ in the means through which this combination occurs on the physical and operational level. Based on two distinct frameworks proposed by the CIBSE Application Manual 13 (CIBSE, 2000) and the IEA Annex 35 (van Heemst, 2001), Kleiven (2003) developed a framework that describes the various ways mixed-mode systems could potentially operate. This framework could also be extended to describe any building's ventilation system and operational modes. Following is a brief description of the new framework.

The framework describes a mixed-mode ventilation system on four different hierarchical levels (Figure 2-9):

1- Spatial Extension

On the topmost level of the framework, it is important to distinguish between the building's serviced zones and its ventilation system. The former describes how the serviced zones are ventilated in hybrid mode, while the latter describes the system itself that provides hybrid ventilation. Therefore, at this level, two distinct spatial extensions are identified; the *Building* and the *System*.

2- Physical Design

This level describes the physical design of both the *Building* and the *System*. On the level of the *Building*, the CIBSE AM13 identifies 3 different physical designs (CIBSE, 2000):

- *Contingency design*: is the case when a space is equipped so that a future change of ventilation system is facilitated, for example when altered user demands require mechanical ventilation with air conditioning instead of natural ventilation.
- *Zoned design*: simply means that different ventilation systems are applied in different parts of a building. An example of this is an office building with stack-ventilated office cells along the perimeter and with mechanically ventilated meeting rooms in the core area.
- *Complementary design*: is the case when a natural ventilation system is assisted by a mechanical ventilation system, or the other way around.

On the level of the *System*, two different physical designs can be identified:

- *Natural and mechanical ventilation*: which means two fully autonomous systems where the control strategy either switches between the two systems or uses one system for some tasks and the other system for other tasks. An example is spaces that are mechanically ventilated during the heating and cooling seasons and naturally ventilated in the intermediate seasons. The Liberty Tower of Meiji University in Tokyo (Chikamoto et al., 1999), is a typical example of this principle.
- *Combined*: this term applies when natural and mechanical ventilation technologies are combined within one single system, i.e. when a natural ventilation system is combined with an extract or supply fan or when a mechanical ventilation system makes optimal use of natural driving forces.

3- Operational strategy

This level describes the different strategies that are adopted to enable a building to operate in hybrid mode. Again, a distinction is made between the operational strategies adopted on the level of the *Building* and those adopted on the level of the *System*.

On the level of the *Building*, the CIBSE AM13 identifies two operational strategies for Complimentary designs (CIBSE, 2000):

- *Concurrent operation*: means that mechanical and natural ventilation systems operate in parallel. One example is a space that is served with a balanced mechanical ventilation system, where the windows can be opened in addition.

- *Changeover operation*: means that “natural and mechanical systems are available and used as alternatives according to need, but they do not necessarily operate at the same time”. Some examples of different changeover operation strategies as mentioned in the CIBSE AM13 are:
  - Seasonal changeover: e.g. when operable windows are shut and replaced by balanced mechanical ventilation in winter to avoid draft and facilitate heat recovery.
  - Daily changeover: e.g. night cooling.
  - Local changeover: e.g. when window detectors ensure that nearby air conditioning or other mechanical cooling devices are shut off when a window is opened.

On the level of the *System*, two operational strategies exist:

- *Switching the active component on/off*: this strategy provides the possibility to turn fans in the system off when natural driving forces are strong enough to provide the ventilation rate needed, and on again when they do not suffice, or to turn an active cooling component like chilled water pipes on when passive cooling of the incoming air is not possible.
- *Switching between alternative airflow paths*: at certain instances, a switch between alternative airflow paths can occur to cope with changes in internal and/or external conditions. Three different types of alternative airflow paths can be identified:
  - Switching between local and central airflow paths: e.g. from a local façade inlet to an embedded duct to reduce draft problems on cold days, to cool the air on hot days, or to dampen noise from outdoors.

- Night ventilation: special paths, e.g. voids in the floor slab, an embedded duct or special windows may be applied to boost cold night air through the building to cool the structure during the night.
- Bypass path: i.e. alternative air paths provided around air handling components that are not continuously in operation and that represent a significant pressure drop, e.g. heat exchangers and filters.

2.2.9 Control

This describes the means by which the changeover between the different operational modes occurs and how the mechanical system if present is initiated. This can be performed in two different ways;

- *Manually*: where occupants can have control over the internal environment by opening or closing openable windows and dampers depending on their thermal sensation.
- *Automatically*: using a Building Management System BMS which is comprised of a number of temperature and CO_2 sensors distributed throughout the occupied spaces to monitor indoor conditions. When internal temperatures rise above or fall below predefined ranges, or when CO_2 levels exceed set-values, the BMS automatically sends signals to attenuators which in turn control the opening and closing of windows and dampers to readjust the indoor conditions. Occupants can manually override the BMS by opening or closing windows. When this occurs, the system automatically turns off the active component supplying the space with cooling, heating or fresh air in order to save energy.

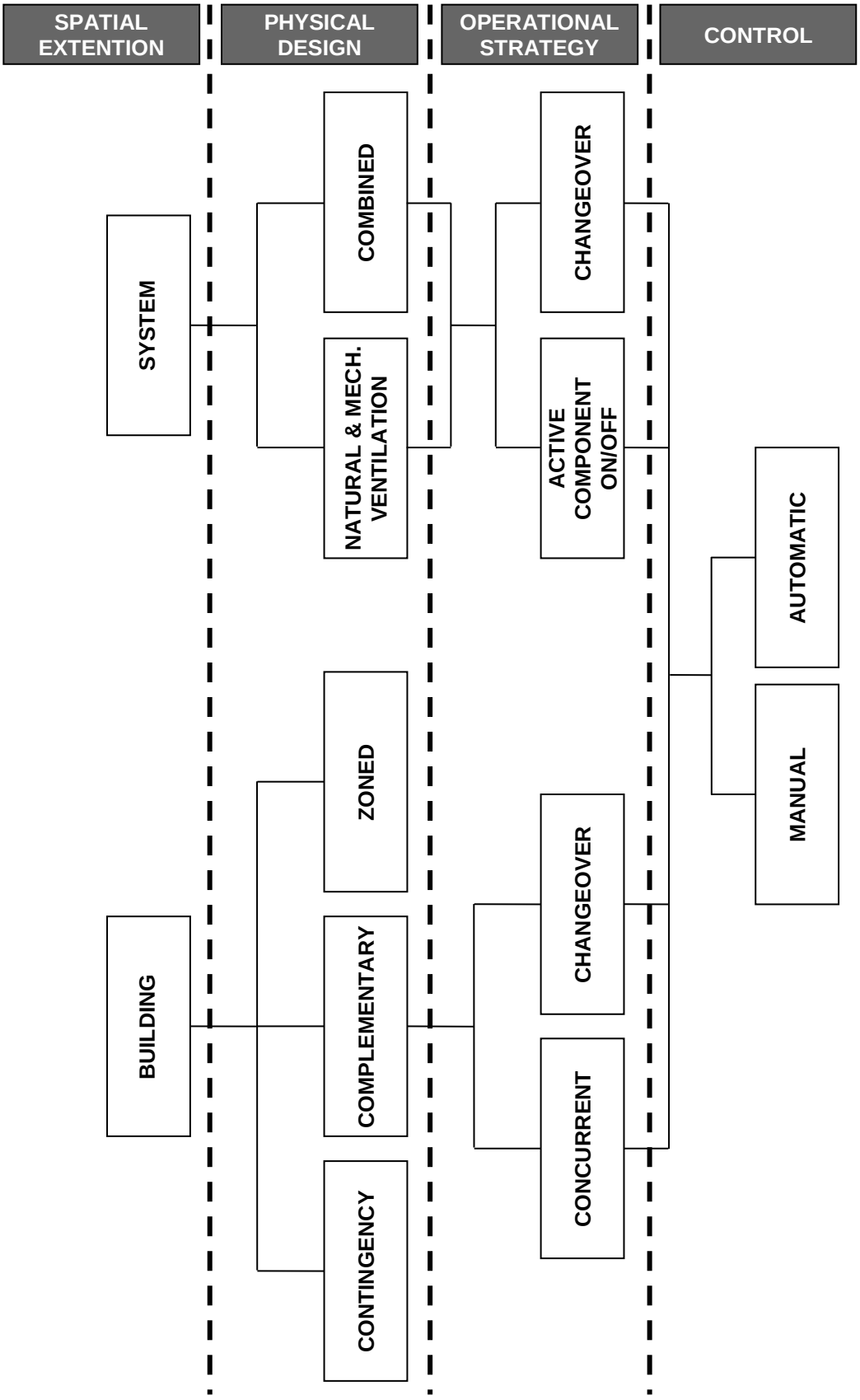

Figure 2-9 Mixed-mode ventilation systems

2.2.10 Conclusions: Describing the ventilation concept of a building

The ventilation concept of a building can be presented as a table as shown in Figure 2-10. The table could be used to label any naturally ventilated or mixed-mode building by providing an all-encompassing easy to read description.

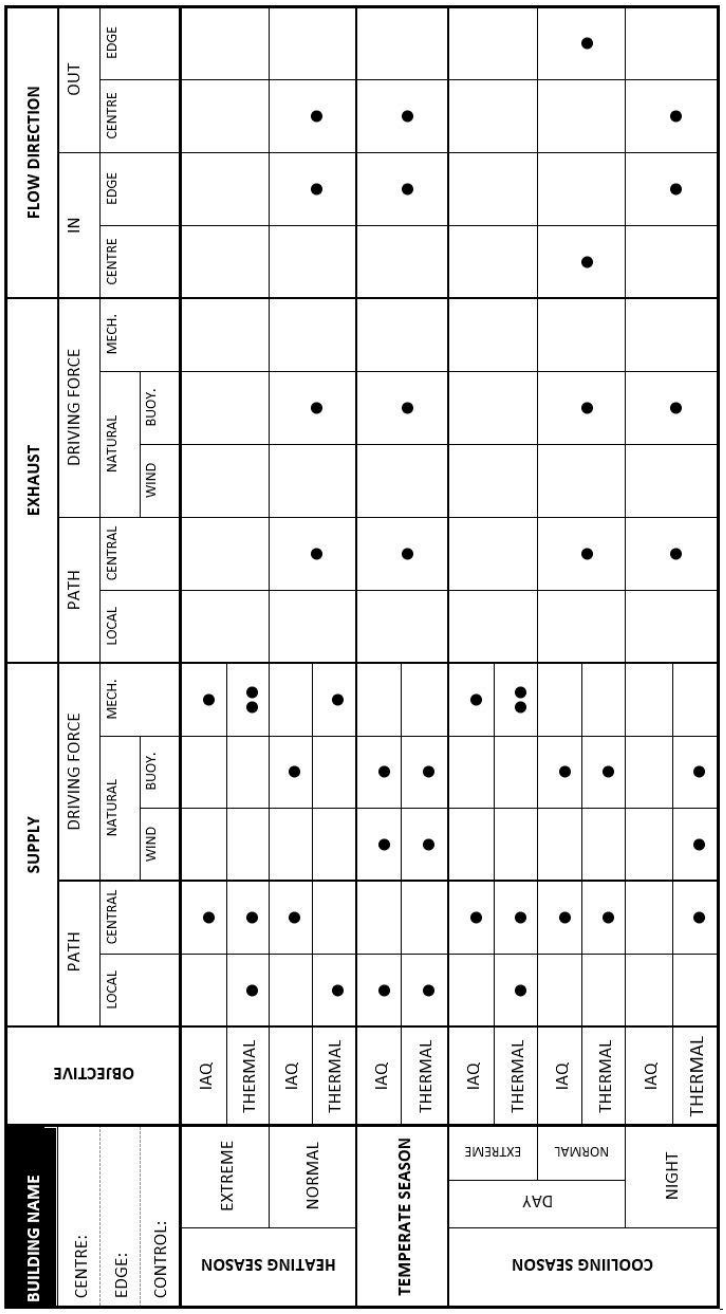

Figure 2-10 Description of a building's ventilation concept

2.3 Passive Downdraught Evaporative Cooling

Natural cooling of buildings is the process in which dissipation of heat from buildings to an environmental sink (like air, water, sky or ground) takes place via a heat transfer mode that requires the minimal consumption of carbon-based energy. Natural cooling is termed as *passive* whenever the processes involved do not require the expenditure of any non-renewable energy and as *low-energy* when only limited energy is required for pumps and/or fans (Ford et al., 2010).

In severe climates characterised by high dry bulb temperatures and low relative humidities, evaporative cooling could be employed to relieve climatic stress, the heat sink being air (the wet bulb depression) and the heat transfer mode evaporation. When water evaporates within a stream of ambient air, the temperature of the air is lowered, and its moisture content is elevated, while its wet-bulb temperature remains constant. The cooling of the air is also reflected in an increase in density, sufficient to drive a downdraught of air through a building (Ford, 2001), a natural cooling strategy referred to as Passive Downdraught Evaporative Cooling (PDEC).

2.3.1 Origins and historical applications of PDEC

The cooling potential of evaporating water has its origins in ancient Egypt. Success in modifying the micro-climate around buildings in this way subsequently spread eastwards through the Middle East and Iran to north India with the Moghul empire, and westwards across north Africa to southern Spain (Ford et al., 2010). This strategy has historically been exploited in different ways, including ‘evapo-transpiration’ by vegetation as can be seen in the Casa de Pilatos in Seville,

Spain and the Suhaimi House in Cairo, Egypt (Ernest & Ford, 2012); the use of water features like pools, fountains and falling water with fine examples found in the Moghul architecture of north India and Moorish architecture of southern Spain ; and direct evaporation within a column of air such as a wind catcher with porous water pots that have been used in the Middle East for centuries to encourage air movement and evaporative cooling both within and between buildings (Bahadori, 1994).

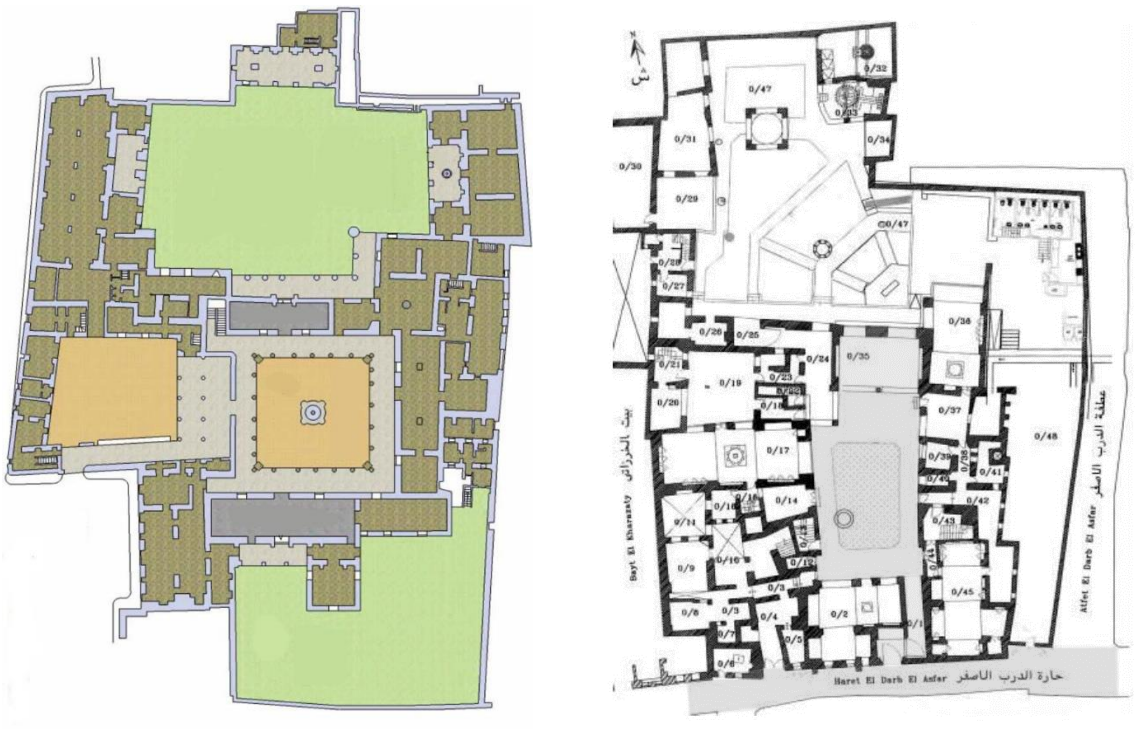

a b

Figure 2-11 Ground floor plans of a) Casa de Pilatos (Ernest & Ford, 2012) and b) Suhaimi House (Almaiyah, Elkadi, & Cook, 2010)

2.3.2 Contemporary applications

Of the four historical techniques, only the direct evaporation of water within a column of air has survived the scrutiny of contemporary building requirements due to its efficiency in delivering cooling to the point of need. Ford et al. (2010)

categorised existing applications of this technique in contemporary buildings into four different systems according to the method of evaporation;

2.3.2.1 Cool towers

In this system, wetted cellulose pads are placed in the air-stream flowing down the tower. This system has been used in the cool towers at Zion National Park Visitor's Centre in Utah, USA (Long, Torcellini, Pless, & Judkoff, 2005). The main limitations of this method are the significant resistance to airflow caused by the cellulose pads as well as the raised risk of mould growth and mosquito infestation due to the continuous wetting of the pads and the collection of excess water.

2.3.2.2 Shower towers

In this system large droplet shower heads are placed within the tower. This system avoids the disadvantages of the cool towers and has the added benefit of generating greater down flow due to the momentum transfer from the drops to the air. However, it is not as efficient as the misting towers system in terms of cooling and water consumption because the water droplets are not fully evaporated resulting in less reduction in supply air temperature and the need to recover and recirculate the excess water.

2.3.2.3 Porous ceramics

Porous ceramic jars have long been used to promote evaporative cooling. The advantages of using contemporary interpretations lie in their applicability in locations where water quality is poor or relatively high-tech solutions not feasible.

2.3.2.4 Misting Towers

In misting towers, large droplet shower heads are replaced by fine droplet misting nozzles (micronisers). The misting system is usually configured using rows of micronisers to produce an artificial fog. In this case the water droplets are totally evaporated before reaching the tower outlet. This system is considered to be the most efficient in terms of cooling outcome and water consumption.

2.3.3 Psychrometrics of Evaporative Cooling

When water is brought into contact with non-saturated hot air, a simultaneous heat and mass transfer process takes place. On one hand, the temperature difference between the air and the water gives rise to a net heat transfer between them. On the other hand, the concentration gradient of water vapour between the water surface and the non-saturated air provokes the evaporation of the water which requires certain energy for the phase change. In relation to the thermal level of the water, these two phenomena have an opposed effect. The heat transfer tends to increase the water temperature whereas the latent energy absorbed by the evaporated water cools the water. The result is an equilibrium temperature called wet bulb temperature.

Once the water has reached the wet bulb temperature, the latent heat of evaporation must come from the air and consequently its temperature decreases. The evaporative cooling occurs as a consequence of the latent heat of vaporisation, that is, the amount of energy that is required to convert unit mass of water from liquid to vapour (~2,260kJ/kg). This is appreciably greater than the

specific heat required to raise the temperature of unit mass of water (4.18kJ/kg). In evaporative cooling, the energy is supplied by ambient air whose heat content and capacity to hold vapour are indicated by its dry bulb temperature and relative humidity. The transfer of heat energy from ambient to water supports the phase change process and so reduces the temperature of the ambient air (Bowman et al., 2000).

For a given pressure, the wet bulb temperature depends on the air temperature and the humidity content of the air. The extent of reduction in supply air temperature (sensible cooling) due to direct evaporative cooling depends on the magnitude of the dry-bulb to wet-bulb depression and is usually equal to 70-80% of that depression. On a psychrometric chart (Figure 2-12), the evaporative cooling process can be depicted as ambient air of dry-bulb temperature t_{db} and wet-bulb temperature t_{wb} moves from point 1 to point 2 on a constant enthalpy line (that can be approximated to a constant wet-bulb temperature line). In this adiabatic process, sensible heat changes to latent heat.

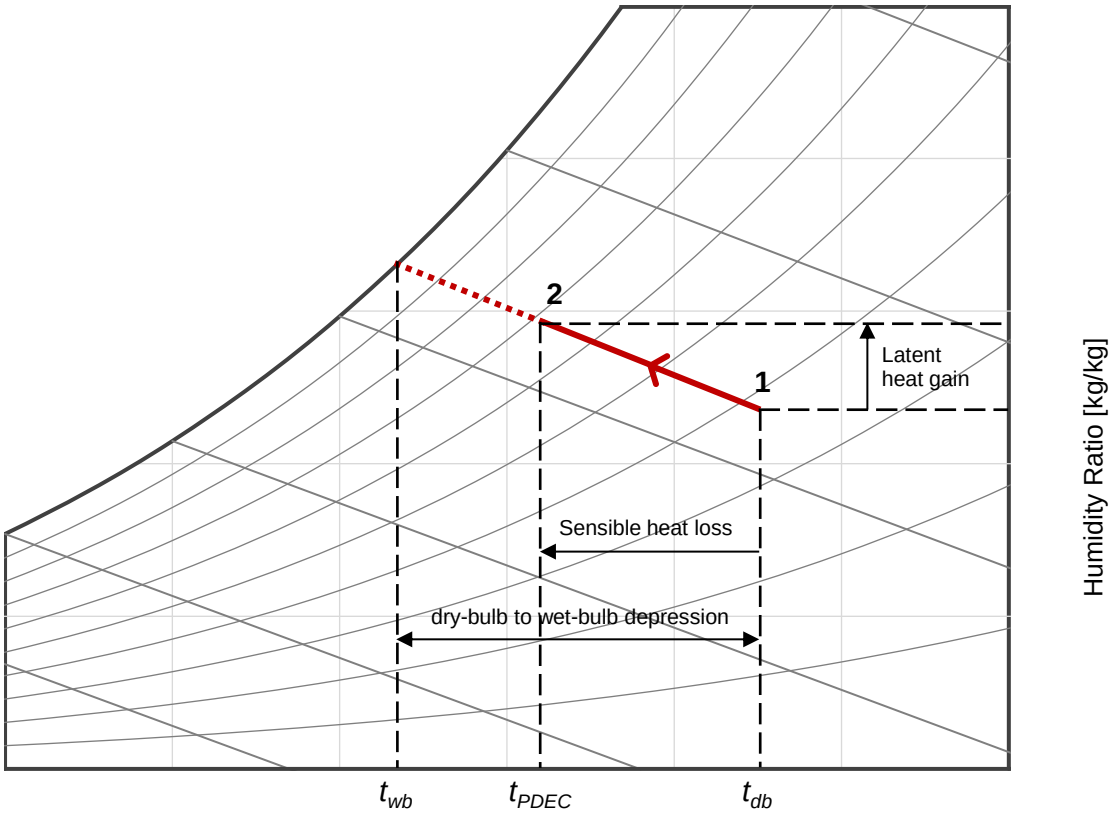

Figure 2-12 Psychrometric process of direct evaporative cooling

2.4 Review of research on PDEC

Many studies have addressed the topic of evaporative cooling at large, be it delivered in the form of fan-operated desert coolers (Bruno, 2011; El-Dessouky, Ettouney, & Bouhamra, 2000; Kant, Kumar, & Mullick, 2001; McKenzie, Pistochini, Loge, & Modera, 2013; Riangvilaikul & Kumar, 2010; Sodha, Singh, & Sawhney, 1995), evapo-transpiration (Ernest & Ford, 2012; Gage, 1997; Perini, Magliocco, & Giulini, 2016), or the use of porous ceramics (He & Hoyano, 2010, 2011; Ibrahim, Shao, & Riffat, 2003; Lanceta et al., 2007). However, in light of the intended objectives of this study, the following review will focus on the specific topic of evaporative cooling in which buoyancy forces resulting from evaporation

are used to generate a downdraught that naturally drives airflow through a single room or several floors of a building with particular emphasis on the latter.

A number of studies have been carried out that report on various aspects related to the application of PDEC to buildings both domestic and non-domestic. The majority of those studies focused on the modelling and performance appraisal of the evaporation of water within a column of air. In an experimental building in Tucson, Arizona, Cunningham, Mignon, & Thompson (1987) demonstrated the effectiveness of direct evaporative cooling in driving a substantial airflow through the building using a downdraught tower incorporating wetted cellulose pads.

Pearlmutter, Erell, Etzion, Meir, & Di (1996) investigated the performance of a down-draught evaporative cool tower integrated in a glazed courtyard in the arid Negev Highlands. Performance of a small-scale tower was monitored, and results indicated a potential for temperature reduction of 10 °C under summer daytime conditions, but insufficient cooling output when using a natural draft system. A wind capture mechanism for increasing inlet pressure and air flow to the space was proposed. A multi-stage down-draft evaporative cool tower was later developed as an improvement. The new tower incorporates a secondary air inlet to increase the cooling output and reduce water consumption. The secondary air, which may be drawn from the interior space being cooled, is cooled by evaporation in the lower section of the tower. Results showed that substantial airflow could be generated through the secondary air inlet, that additional features such as a deflector cone at the outlet of the tower could increase flow rate in certain conditions (Erell, Pearlmutter, & Etzion, 2008a), and

that the secondary air inlet potentially saves water (Erell, Pearlmutter, & Etzion, 2008b).

Badran (2003) investigated the capacity of traditional cool towers that use evaporative cooling and natural down-draught to achieve natural cooling under various climates in Jordan using analytic models and demonstrated that under those climates, the height of the tower necessary to create proper airflow is less than 9m and that a tower of 4m height and cross section dimensions of 0.57x0.57m can produce an airflow rate of 0.3m^3/s and cool it from a dry-bulb temperature of 36 to 25 °C.

da Silva (2005) developed a model to predict the temperature and relative humidity of a mono-zone building served by a solar chimney and an evaporative cooling tower. The model enables the dimensioning of the solar chimney provided that the outside climatic conditions, the geometry of the building and the internal heat gains.

Cláudia, Melo, & Guedes (2006) investigated the use of PDEC in an existing brick chimney in southern Portugal traditionally used for summer ventilation through chimney effect using field measurements, thermal modelling and computational fluid dynamics and demonstrated that PDEC can provide comfort conditions in some but not all summer conditions and that a hybrid system can extend the period during which downdraught cooling is applicable.

A novel design of wind towers was numerically investigated (CFD) by Saffari & Hosseinnia (2009). Their proposed design used wetted curtains hung in the tower column, which were modelled as surfaces that inject droplets of water with

very low speed. The effects of water droplet diameter, water droplet temperature, wind velocity, temperature, and relative humidity inlet on the thermal performance of the wind tower were investigated. Results showed that a height of 10m of wetted columns decreases ambient air temperature by 12K and raises relative humidity by 22%.

Kalantar (2009) developed a general mathematical model to simulate the performance of natural evaporative cooling tower system. The results showed that the cooling system was capable of decreasing air temperatures by 10-15 °C at the peak of its performance, depending on configuration and ambient conditions and that most 80% of the reduction in temperature was achieved within the top 2m of the tower, even when sprayers were spaced evenly throughout its height. The system produced a peak cooling output of just over 100 kW with a water consumption rate of approximately 0.025 l/s.

Phillip & Lau (2013) investigated the applicability of PDEC in residential buildings in this region by using a proposed PDEC system for a prototype house as a research vehicle. The thermal simulation was done using Bentley TAS and the results showed the proposed PDEC system fulfilled the cooling requirements for more than 75% of the required periods for both present-day and future climatic conditions using interpolated weather data.

Kang & Strand (2013) performed computational process modelling using a flow package FLUENT to investigate the characteristics of air distribution within the effective tower area of a PDEC component. They demonstrated that the design of bottom outlets and accordingly, the location of wind catcher of the tower

are likely to be strongly impacted by the wall-bounded airstream flows formed at the opposite side of the incoming air at external relative humidities above 40% due to the delayed evaporation of water. They later formulated two regression equations for predicting supply air temperature and velocity (Kang & Strand, 2016).

Grosso & Ahmadi (2016) analysed a model comprising a one-channel wind tower and a room attached to it. The performance of the model was assessed using a simulation software calculating the potential cooling energy reduction due to controlled natural ventilation. The effects of orientation, height, size and direction of inlet and outlet apertures were considered.

Spentzou, Cook, & Emmitt (2017) tested four retrofit strategies against the existing single-sided ventilation of an urban multi-storey apartment building in Greece, using computational fluid dynamics simulations. They demonstrated that during buoyancy driven flows, acceptable ventilation rates for comfort could be achieved with the implementation of a wind-catcher and a dynamic facade. Under wind-driven ventilation, these strategies delivered significant increases in ventilation rates (up to seven times) and contributed to reductions in indoor air temperatures of up to 2K relative to the existing strategy. Cooling by water evaporation enhanced the cooling performance of the wind-catcher providing up to 4K temperature reductions.

The studies presented above have mainly addressed the factors affecting the evaporation process in a cool tower and the likely conditions along the height of the tower and at its outlet in terms of air temperature, humidity, velocity, flow rate

and stream flow pattern. However, little or no information on the distribution of the outlet air over more than one floor has been provided. Perhaps the most detailed and relevant work addressing this was that carried out by the participants of a three-year multi-disciplinary research project, in the frame of the European Commission JOULE II programme (Bowman et al., 1997). The PDEC project as it was named investigated the application of Passive Downdraught Evaporative Cooling to non-domestic buildings in southern Europe. The project was divided into three broad subject areas: Architectural Design Studies; Building Performance Assessment; and Experimentation and Monitoring. Designs for two hypothetical office buildings were generated, one in Seville, Spain (Ford, Diaz, & Hewitt, 2000) and the other in Catania, Italy (Francis, 2000). Thermal modelling (Robinson et al., 2004) and CFD analysis (Cook, Robinson, Lomas, Bowman, & Eppel, 2000) were undertaken for the hypothetical buildings. For the climates and building types considered, a mixed-mode solution was found to be the most appropriate involving natural ventilation at night and PDEC during the day with mechanical cooling if temperatures were still uncomfortably high. It was also found that PDEC alone could not generate a sufficient temperature depression to achieve comfort in all ambient conditions. The best method of cooling buildings using PDEC was found to be the creation of a reservoir of cool air in the PDEC capture zone and that the magnitude and uniformity of the airflow and water consumption was very dependent upon the position, size and control of openings. The results also asserted the need to avoid the effects of wind when PDEC systems are operating. Energy savings of 66% were predicted for the office building in Seville, Spain and 27% for the building in Catania, Italy. (Bowman et al., 1998).

The literature review conducted above highlighted the issues that have been investigated in previous studies but in doing so, has also highlighted the fact that, to the best of the author's knowledge, no studies have addressed the issue of extending PDEC to medium and high-rise buildings and the consequent difficulties the arise from such an extension, a subject of great significance should this strategy be applicable to dense urban locations such as Cairo, Egypt.

2.5 Summary

PDEC is considered a form of natural ventilation (NV) insofar as the driving forces and governing thermodynamic properties are concerned and as such an overview of the basics of NV, its objectives and indices, driving forces, strategies and principles, flow paths, modes of operation, and control were presented. A method to label any naturally ventilated or mixed-mode building by providing an all-encompassing easy to read description was also given. An overview of Evaporative cooling as a natural cooling strategy was presented and its viability in relieving climatic stress in hot-dry climates demonstrated through historical and contemporary applications. Four types of Evaporative cooling systems were described. Advantages of misting towers over other forms were highlighted. These include requiring height for full evaporation of water, better control of humidity levels at outlet, less water consumption, no pressure losses. Finally, literature review conducted on PDEC research highlighted the fact that no studies have addressed the issue of extending PDEC to medium and high-rise buildings.

Chapter 3: Context and Comfort

3.1 Chapter Overview

This chapter presents an overview of the climatic and urban contexts of Cairo as well as the thermal comfort requirements in PDEC buildings. In section 3.2, An analysis of Cairo's climate and wind potential is given. An understanding of the thermal comfort requirements in PDEC buildings is a necessary prerequisite for assessing the feasibility of the strategy and are therefore presented in section 3.3. A method based on the Climate Suitability Analysis Method (CSAM) to assess the preliminary applicability of PDEC to any location is elucidated in section 3.4 and results compared to Givoni's Building Bioclimatic Charts (BBCC). Section 3.5 presents an overview of aspects of office building design in Cairo that are relevant to this study. Finally, section 3.6 presents the case for tall buildings in Cairo and in turn for extending the application of PDEC to medium and high-rise office buildings.

3.2 Overview of Egypt's Climate

According to the Köppen-Geiger Climate classification (Figure 3-1), Egypt is located within the arid desert hot climate zone (BWh), where deserts occupy more than 96% of its total area (Kottek, Grieser, Beck, Rudolf, & Rubel, 2006). Accordingly, the main characteristics of hot dry climates could be applied for the whole country with the exception of the coastal strip of land that maintains a hot humid environment. The northern coast expands relatively deeper inland than the eastern coast. The presence of the Nile has a gentle effect on the climate which is most evident in the delta.

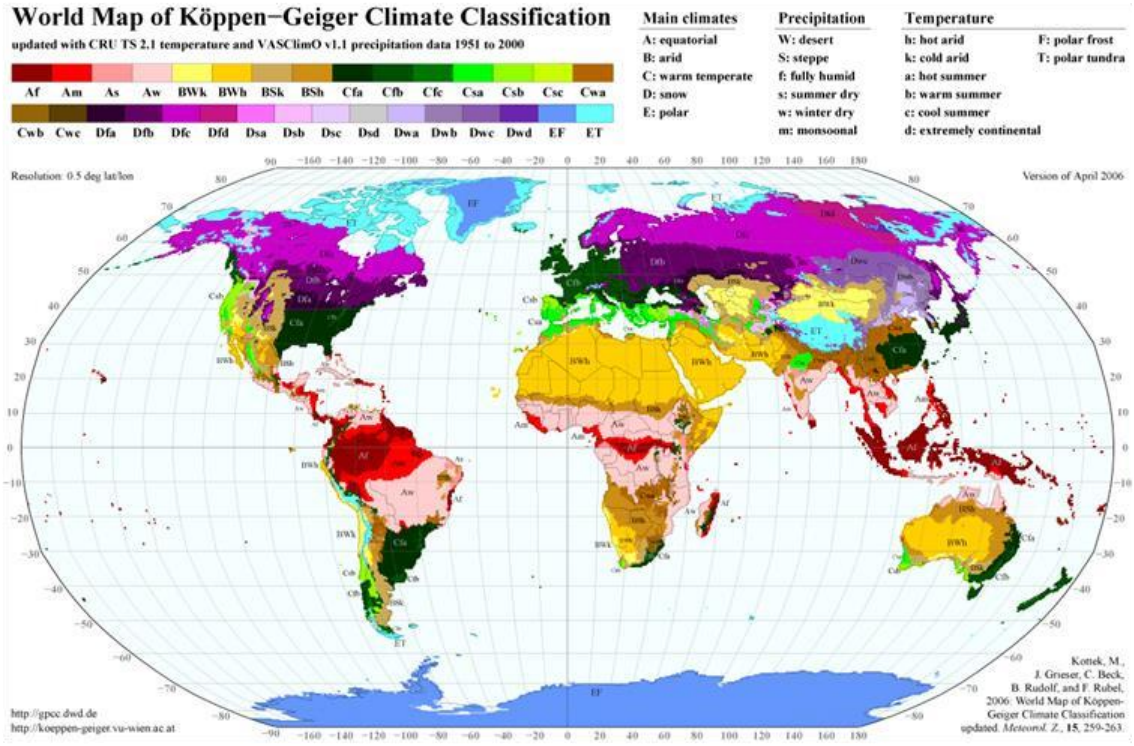

Figure 3-1 World Map of Köppen-Geiger Climate classification (Kottek et al., 2006)

This is consistent with the climatic classification developed by the Housing and Building Research Centre in which Egypt is classified into eight climatic zones (HBRC, 2006). The Delta and Cairo zone, wherein Cairo lies, is characterised by moderately elevated relative humidity levels ranging between 32% and 84%.

3.2.1 Cairo's Climate

The Cairo International Airport meteorological station, operated by the Egyptian Meteorological Authority (http://nwp.gov.eg/), is the nearest meteorological station to Cairo. The station lies approximately 11 miles to the east of the city centre. Climatic analysis, described in the following section, uses the Egyptian Typical Meteorological Year (ETMY) developed for standards

development and energy simulation by Joe Huang from data provided by the U.S. National Climatic Data Centre for periods of record from 12 to 21 years, all ending in 2003 (www.energyplus.net/weather/sources). The graphic representations of these readings are the output of Climate Consultant 6.0, a graphic-based computer program developed at UCLA (http://www.energy-design-tools.aud.ucla.edu).

Figure 3-2 shows the monthly dry bulb temperature data (range, mean, and design values) while Figure 3-3 shows both the monthly-averaged hourly dry-bulb temperature (upper red curve) and wet-bulb temperature (lower dark red curve) as well as the hourly range of dry-bulb temperatures. Typical of a city in the hot dry zone, the annual temperature range is very wide reaching up to 35K. The diurnal temperature ranges vary depending on the time of year where, unlike the moderate winter season, they noticeably increase in summer to reach their maximum of 14K in the months of July and August.

The cooling season extends from May to October, that is, over the whole period of summer and short periods of spring and autumn. The heating season, on the other hand, is only limited to the short period spanning from December to February whereby most of the heating requirements could be provided for using solar and internal gains. For the cooling season, the average daily maximum and minimum dry-bulb temperatures are 33.1°C and 21.5°C respectively with a peak dry-bulb temperature of 44°C. The average daily maximum and minimum wet-bulb temperatures (WBT) for the same period are 21.8°C and 18.4°C respectively.

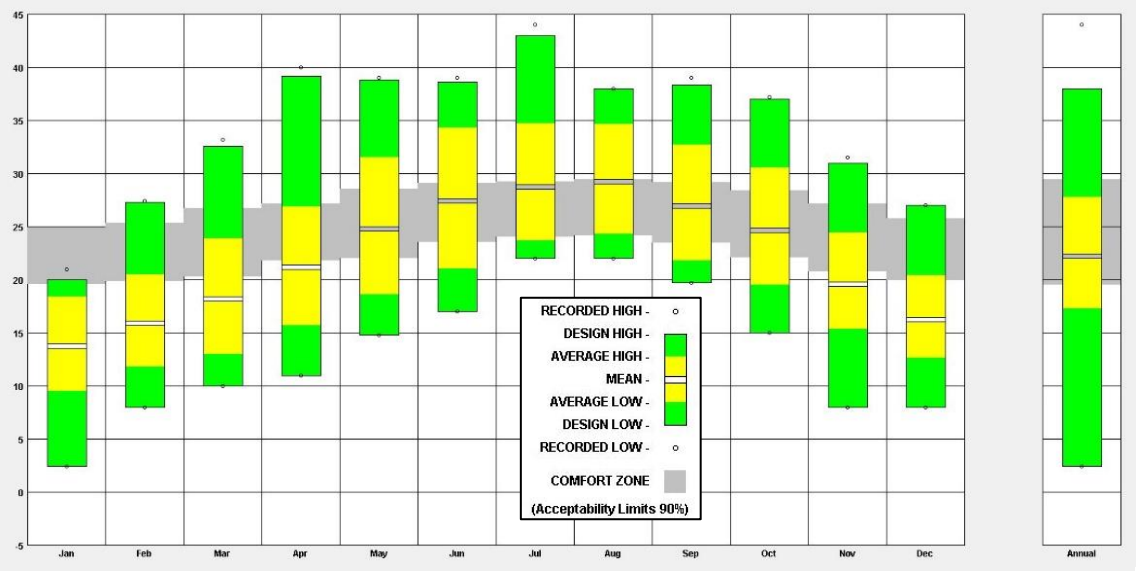

Figure 3-2 Monthly dry bulb temperature range

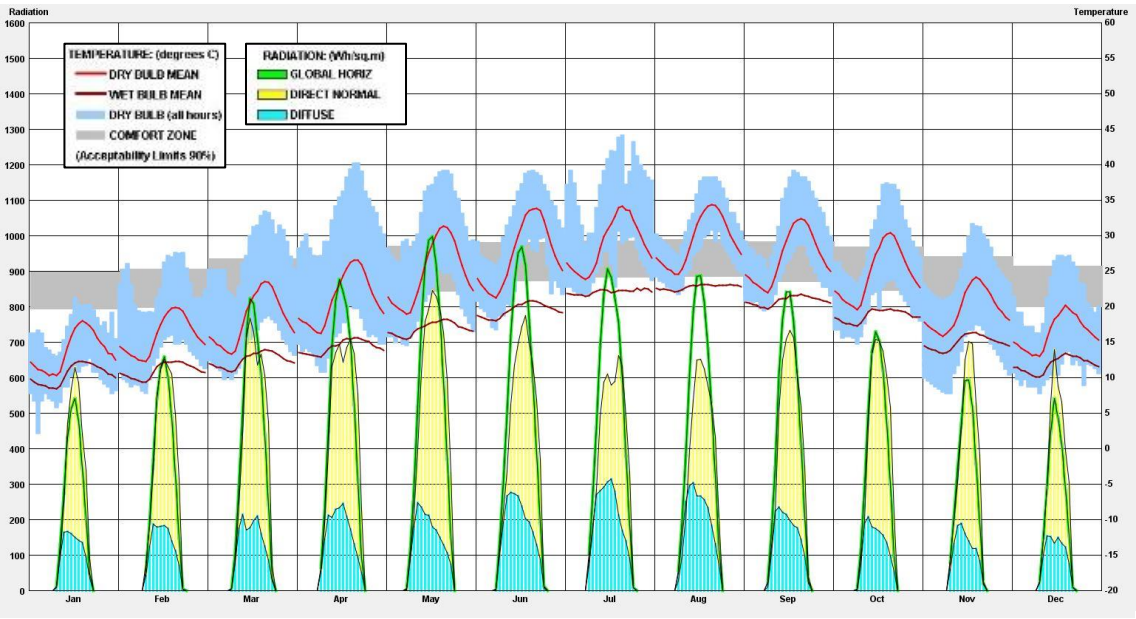

Figure 3-3 Monthly average diurnal temperature

Figure 3-4 shows the monthly-average hourly dry bulb temperatures plotted against the monthly-averaged hourly values of relative humidity generated for the 12 months of the year and demonstrate the potential effectiveness of adopting direct evaporative cooling in office buildings during the cooling season (May to

October) because elevated relative humidity levels mainly occur during the night and early morning when the buildings are unlikely to be occupied.

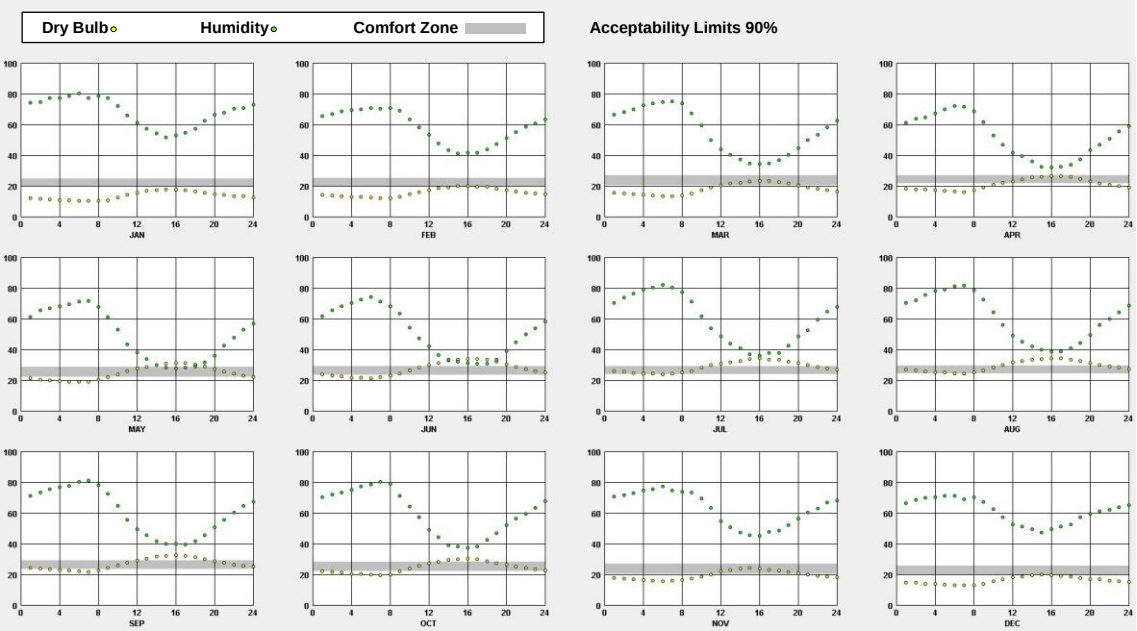

Figure 3-4 Hourly average dry bulb temperature and relative humidity for each month

3.2.2 Wind in Egypt

According to the Egyptian Organization for Energy Conservation and Planning (1998), wind speed and direction vary from time to time according to different climatic factors such as land and sea breezes and the earth's seasonal inclination. Northern wind directions prevail for the majority of Egyptian cities. In the North coast, Northern and North-western winds are dominant in equinoxes and winter respectively; they represent 46% of the total wind incidence per year. South of the Delta, Northern winds represent 32%, in addition to North-eastern winds that appear in both autumn and winter. Further south, in Central and Upper Egypt, there is a sort of equilibrium between calm conditions and Northern upcoming winds. Wind in Egypt fluctuates in strength from gentle breezes to

occasional storms and hurricanes. Mean wind velocities range between 7 km/h (light breeze) and 20 km/h (Moderate breeze) in normal cases in Egypt. '*Khamaseen*' winds, seasonal storms that occur between the end of March and the beginning of May (derived from the Arabic number of 50), are warm sandy storms originating from Southern and South-western orientations (Organization for Energy Conservation and Planning, 1998).

3.2.3 Cairo's wind potential

Prevailing wind directions in Cairo are mainly Northern (Figure 3-5). Wind speeds are relatively low averaging at 3 m/s. A more detailed analysis of the monthly wind roses (Figure 3-6) shows that north eastern directions are more prevalent in the equinoxes while north western winds are dominant in the hot summer periods. In the hottest months of the year, namely July, August and September, when cooled air is mostly needed, winds almost blow exclusively from northern orientations, while in the cold winters when winds are not favourable; they mainly blow from southern orientations. This consistency in wind direction can have its positive implications on the design solution. The wind roses of March, April and May show the seasonal winds of '*Khamaseen'* originating from the Saharan desert Southwest of Egypt (Organization for Energy Conservation and Planning, 1998).

The application of night time ventilation in summer coupled with high thermal mass inertia is highly recommended due to significant variations in diurnal temperatures. Evaporative cooling could also be used during the cooling season due to its very dry nature especially at peak hours of the day (16:00) where the

temperatures rise considerably, and relative humidity drops. Harnessing of the wind potential could also prove beneficial due to the consistency of wind direction provided that the air is cooled down before it is allowed to enter.

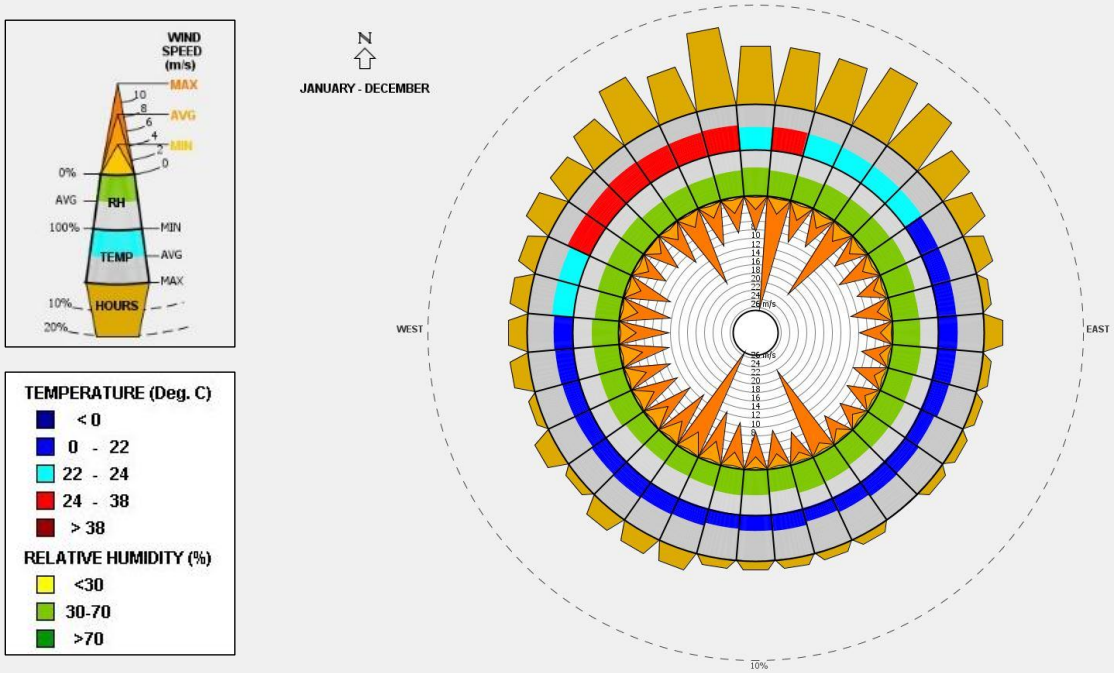

For each wind direction, the wind rose displays the wind velocity and frequency along with concurrent dry-bulb temperature and relative humidity. The outer ring shows the percentage of hours wherein the wind comes from each direction. On the next ring the height and colour of the bars shows the average temperature of the wind coming from that direction (light blue is in the comfort zone, blue is cool or cold, and red is warm or hot). The next smaller ring shows average humidity (light green is comfortable, yellow is dry, and green is humid). The innermost circle shows the wind velocities that come from each direction; the tallest brown triangle is the maximum velocity for that period, medium brown is the average velocity, and the smallest light brown triangle is the minimum velocity. Hours when there is zero wind speed do not appear on the chart. The graphic key to all this information is summarized in the icon in the lower right labelled Wind Speed, RH, Temp, and Hours

Figure 3-5 Cairo's annual wind rose

During the hot hours of the summer day, the movement of cool air stored from the previous night between internal spaces is strongly encouraged. This is due to the fact that external air temperatures are relatively high and consequently, any direct exchange would lead to an increase in heat gains. Solar gains have to be avoided during the cooling season but could render useful in winter. They could also play an important role in facilitating the internal movement of air

through temperature differences by utilising spaces such as trombe-walls and solar chimneys.

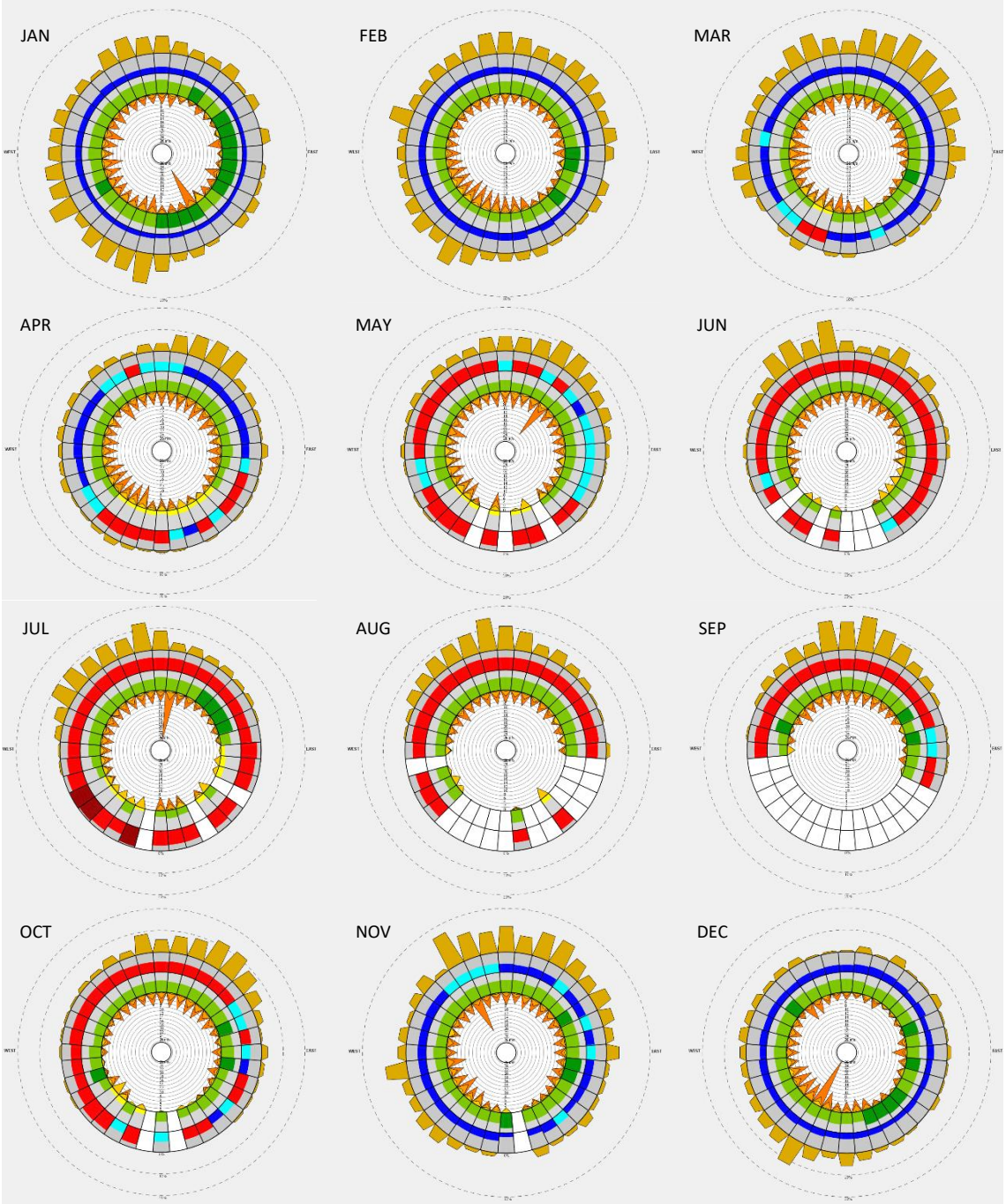

Figure 3-6 Monthly wind roses for Cairo

3.3 Thermal Comfort

The first step of ascertaining the feasibility of PDEC must be to establish what the required conditions would be, that is, the limits of thermal comfort. A widely used definition of thermal comfort is 'that condition of mind which expresses satisfaction with the thermal environment' (ASHRAE, 1966). Such a definition emphasises that comfort is a cognitive phenomenon, one that may involve—but is not solely dependent on—the physical environment and/or physiological state.

3.3.1 Existing thermal comfort studies related to PDEC buildings

Despite the extensive body of work on thermal comfort since the beginning of the 20th century (for a detailed review see Auliciems & Szokolay (2007) and Parsons (2014)), very few have purposely attempted to address the specific issue of thermal comfort in PDEC buildings in a systematic way and none have done so in the field with actual human subjects involved.

3.3.1.1 Givoni's Building Bioclimatic Charts

Perhaps one of the best known and earliest works to relate comfort conditions to direct evaporative cooling is that undertaken by Givoni (1992). His charts suggest *"boundaries of climatic conditions within which various building design strategies and natural cooling systems can provide indoor comfort"* (Givoni, 1992). These strategies include daytime ventilation, nocturnal ventilation and direct and indirect evaporative cooling (DEC & IDEC). In a hot-arid climate such as that of Cairo, only the boundaries for DEC are of interest.

The boundaries of Givoni's Building Bioclimatic charts (BBCC) were demarcated for two different contexts, namely developed and developing

countries. The original boundaries (for developed countries) were based on research conducted in the US, Europe, and Palestine. He defined the acceptable conditions (i.e. comfort zone) for still air (i.e. assumed to be less than 0.25 m/s) in summer as ranging between 20-27 °C. The upper summertime temperature limits start to decrease above 50% RH to reach an upper humidity level of 0.015 kg/kg humidity ratio and 80% RH. However, based on Givoni's personal evaluation and taking into account data obtained from Humphreys (1978), Milne and Givoni (1979), Tanabe (1988) and Webb (1959), Givoni proposed elevations of about 2K in the upper temperature limit and 0.002 kg/kg in the upper vapour content limit whilst maintaining the 80% RH limits. These extensions in the comfort zone are also applied to the boundaries defining DEC where the upper limits of the developed countries are increased from 42 °C to 44 °C and from 22 °C to 24 °C for the dry bulb and wet bulb temperatures respectively (Figure 3-7).

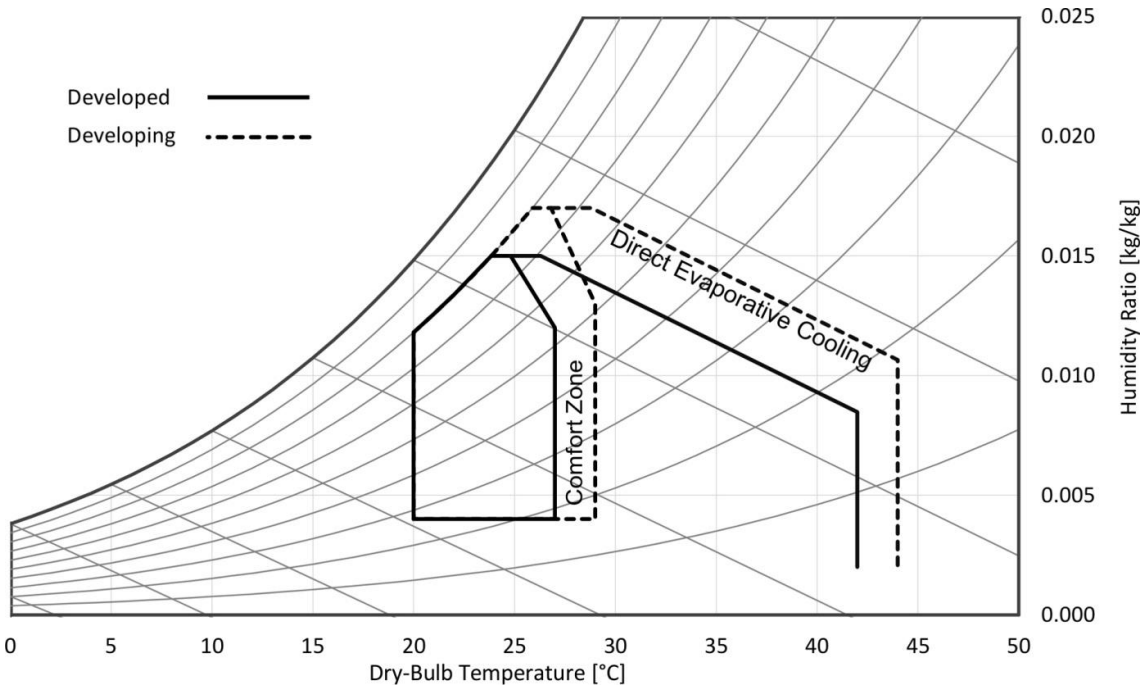

Figure 3-7 Boundaries of climatic conditions under which direct evaporative cooling is applicable. After (Givoni, 1992)

3.3.1.2 Lomas et al. comfort envelopes for PDEC Buildings

Givoni's boundaries for developing countries were based on the assumption that people living in these parts of the world are highly acclimatised to the hot and sometimes humid conditions which they experience in their everyday life. This might be true for the vast majority of Cairenes who live, work, and commute in free running buildings and unconditioned means of transport. However, caution need be taken in extending such expectations to speculative tenants of high-rise office buildings who likely live and commute in fully air-conditioned environments, a point also highlighted by Schiano-Phan (2012).

Moreover, even if the DEC boundaries for developed countries were adopted for office buildings in Cairo, a number of issues as raised by Lomas, Fiala, Cook, & Cropper (2004) regarding the application of Givoni's BBCC—which were developed based on experiments conducted on a limited number of residential buildings—to non-domestic PDEC buildings need to be discussed due to the inherent differences between the two building types as follows:

- Non-domestic buildings have a much deeper plan than residential buildings and as such, spaces further away from the PDEC source may well not enjoy the cooling benefits
- Non-domestic buildings tend to be heavily glazed which may create perimeter zones exposed to high amounts of solar radiation altering the thermal sensations of the occupants.
- The internal heat gains of non-domestic buildings are likely to be much higher than in residential buildings due to the fact that they are densely occupied and heavily equipped.

- Finally, night ventilation cooling may also be less effective as the exposed thermal mass relative to the occupied volume is lower than in residential buildings and could be more heavily charged with heat during the daytime.

Accordingly, Lomas et al. (2004) proposed the development of another set of DEC boundaries for office buildings, but ones that are based on detailed dynamic thermal modelling of a prototypical office building located in a specific location. However, the greatest limitation to their proposed BBCC as they have argued is its restriction to one climatic data set and one building type provided that the building modelled is typical of the type for which the chart is being defined. Their study made no attempt as well to explore the validity of Givoni's comfort envelopes. Therefore, it seems unlikely that their BBCC for PDEC buildings is applicable to this study.

3.3.1.3 Fiala's Dynamic Thermal Sensation (DTS) Model

Fiala, Lomas, & Stohrer (1999, 2001, 2003) developed a model of thermal comfort that predicts the dynamic thermal sensation (DTS) of subjects on the 7-point ASHRAE scale from physiological states using a multi-node, dynamic model of human thermoregulation. The new comfort model was validated and was used to explore the effect of temporally changing environmental and personal conditions. The DTS model showed good general agreement with experimental data for a range of steady boundary conditions (air temperature between 13°C and 48°C; metabolic rates between 1 met and 10 met), and various types of transient conditions including step changes, gradual changes, and

periodic changes in environmental conditions (Fiala et al., 2003). The model was further validated (Bröde, Krüger, Rossi, & Fiala, 2012; Kampmann, Bröde, & Fiala, 2012; Psikuta et al., 2012), and then adapted and extended to predict human responses specifically to outdoor climate conditions to form the basis of the Universal Thermal Climate Index (UTCI) (Fiala, Havenith, Bröde, Kampmann, & Jendritzky, 2012).

Fiala, Lomas, Martinez, & Cook (1999) used the DTS model to study responses of occupants exposed to PDEC controlled environments. The subjects were assumed to be wearing typical summer clothing (0.55 clo) and be engaged in typical office activities (1.2 met). Zones of comfort were accordingly defined for PDEC office buildings considering two levels of air velocity (0.3 m/s and 0.8m/s). The impact of varying solar radiation on subjects' responses (0 W/m^2 and 25 W/m^2) were also assessed. The study showed that relative humidities as high as 80% were predicted to be thermally acceptable for the PDEC-building occupants. The comfort envelopes developed thus established a new upper limit for relative humidity which allows PDEC systems to operate above the 60% limit of ASHRAE Standard 55-1992 (ASHRAE, 1992) and the 0.012 kg/kg moisture content limit of all the subsequent revisions (ASHRAE, 2004a, 2010, 2013b).

The comfort envelopes were then extended in a later study by the same authors (Martínez, Fiala, Cook, & Lomas, 2000) to include the effects of adaptive opportunities offered by wearing lighter clothing, increasing local air speed and controlling solar radiation. The upper and lower limits of the new extended comfort envelopes were obtained from the former study (relative humidity of 80% and a moisture content of 0.0045 kg/kg respectively). The right and left

boundaries of the new comfort zones were defined by the operative temperature and relative humidity at which 90% of the people will be thermally comfortable. Figure 3-8 shows the comfort envelopes plotted onto a psychrometric chart.

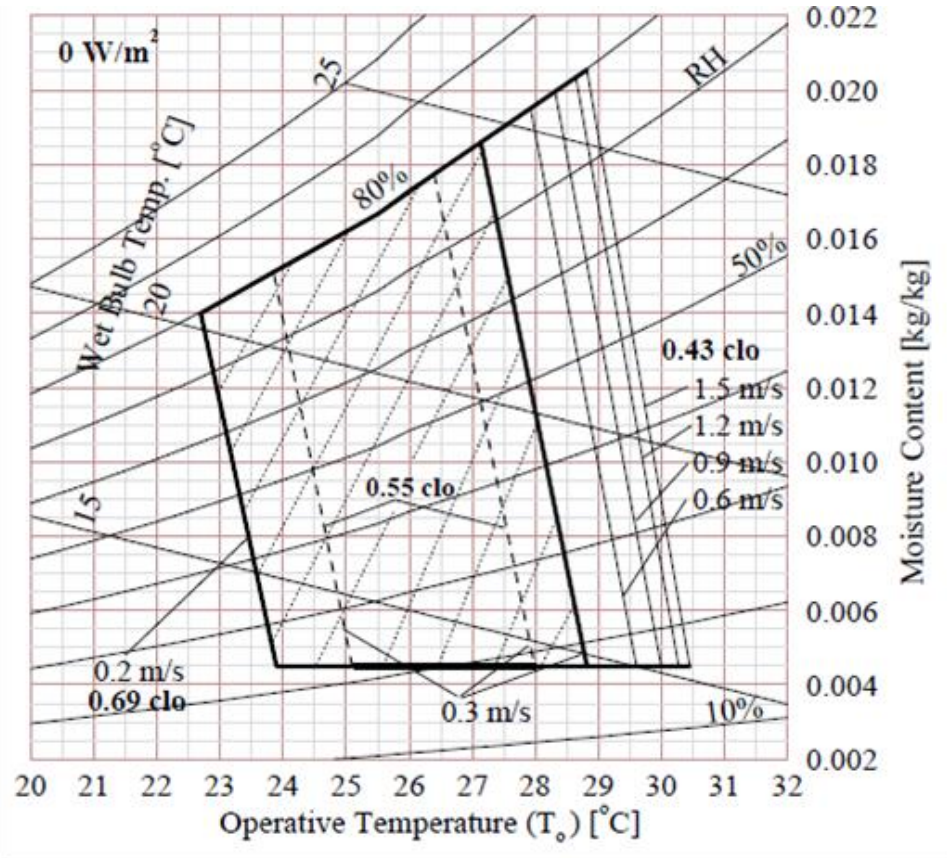

Figure 3-8 Predicted comfort envelopes for PDEC. Source (Martínez et al., 2000)

The new comfort envelopes extend from 22.7°C at 80 % RH to 28.8°C at approximately 17% RH in absence of solar radiation which is about 2K wider than that obtained in the former study. In the presence of diffuse solar radiation of 50 W/m^2, the comfort envelopes shift towards cooler air temperatures by about 2K. A further extension of about 0.7K towards warmer temperatures was achieved by increasing the air speed from 0.3 m/s to 0.6 m/s. However, this effect becomes less efficient as the air speed continues to rise. It was also found that increasing

air speed is more effective in the presence of solar radiation. It must be noted that validation of the Fiala model does not necessarily extend to include the comfort envelopes in PDEC buildings as development of those envelopes preceded the completion of the model and the subsequent validation. Furthermore, independent validation of the comfort envelopes with field data from real PDEC buildings was not carried out. Accordingly, despite being perhaps the only comfort envelopes developed specifically for PDEC buildings, caution need be taken in using them.

3.3.1.4 Schiano-Phan's Post Occupancy Evaluation of PDEC buildings

The only other study investigating occupant responses in PDEC buildings is the POE surveys of four case study buildings using PDEC in the United States undertaken by Schiano-Phan (2012). The surveys were carried out using a two-page workplace questionnaire developed by the Building Use Studies, UK (The Usable Buildings Trust, 2006). The survey included questions on thermal comfort (summer and winter), air quality, lighting, noise, design, need, perceived health and productivity and image to visitors with special emphasis on the summer performance and aspects such as perceived thermal comfort, air quality and control.

The study argued that the 'success' of a PDEC system is often related to the ability of the designers to anticipate the implications for the users of their buildings (i.e. building integration) and to the robustness of the overall passive design strategy. The study also showed that the occupants' perception of such buildings is influenced by their expectations (pre-conditioning) and by their ability to control

their surrounding environment. However, due to the absence of simultaneous measurements of environmental and personal factors (temperature, humidity, air speed, clothing …etc.), it was not possible to quantifiably infer any generalisable information pertaining to conditions of thermal comfort in PDEC buildings.

The previous review demonstrates that there is a general lack of information on comfort conditions in PDEC buildings. Accordingly, focus was shifted to the two widely accepted models of thermal comfort; the heat balance model (Fanger, 1970) and the adaptive comfort model (de Dear & Brager, 2001; Nicol & Humphreys, 2010).

3.3.2 Fanger's Heat Balance Model

The heat balance model is probably the most detailed analysis of the human body's thermal relationship with its proximal environment (Auliciems & Szokolay, 2007). The model predicts what is called the Predicted Mean Vote (PMV) which is the mean vote of a population on the ASHRAE 7-point comfort scale, and the corresponding percentage of people dissatisfied (PPD) using environmental properties (Air temperature, Radiant temperature, Humidity, and Air speed) and personal factors (Metabolic rate and Clothing insulation) as inputs in the heat balance equation (Fanger, 1970).

The model assumes that comfort occurs at PMV=0 when there is no thermal load on the body. Large datasets collected from climate chamber questionnaires show that even under this condition, 5% of the population would be dissatisfied. With departure from a PMV of zero, PPD rapidly increases.

Th heat balance model and its PMV-PPD index form the basis of ASHRAE Standard 55 (ASHRAE, 2013b) and ISO 7730 (ISO, 2005). Figure 3-9 shows the acceptable range of operative temperature and humidity for ASHRAE Standard 55. The range is for 80% occupant acceptability. This is based on a 10% dissatisfaction criterion for general (whole body) thermal comfort based on the PMV-PPD index (-0.5 ≤ PMV ≤ +0.5), plus an additional 10% dissatisfaction that may occur on average from local (partial body) thermal discomfort. The range applies to spaces where the occupants have activity levels that result in metabolic rates between 1.0 met and 1.3 met, where clothing is worn that provides between 0.5 clo and 1.0 clo of thermal insulation, and where air speeds are not greater than 0.2 m/s.

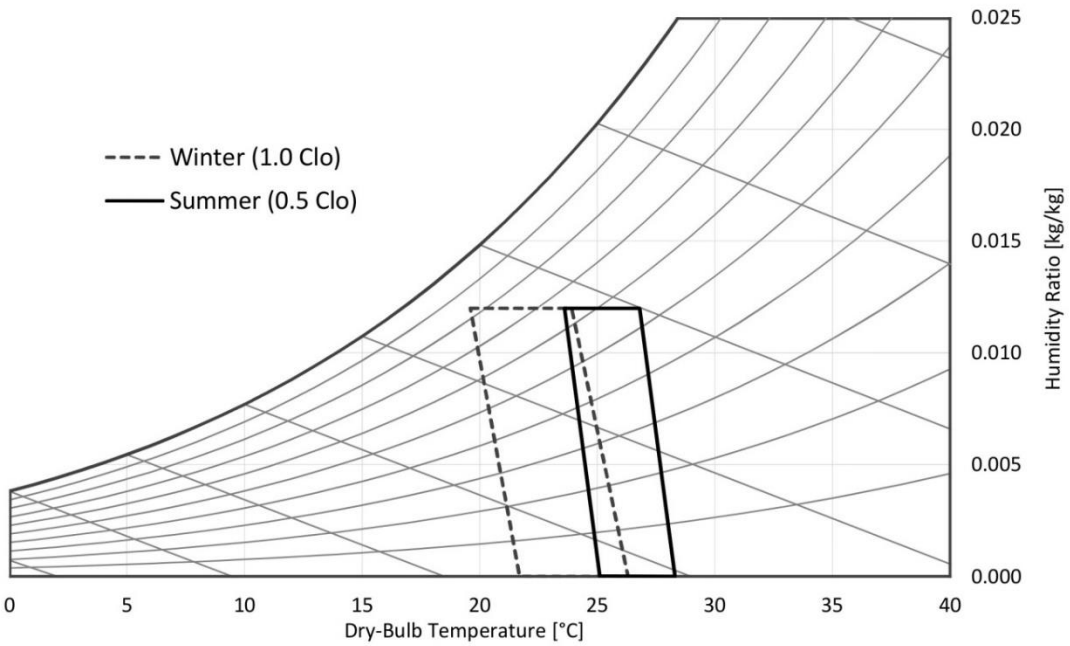

Figure 3-9 Comfort zones for the PMV-PPD model in ASHRAE Standard 55. Adapted from (ASHRAE, 2013b)

The standard allows elevated air speed to be used to increase the maximum temperature for acceptability. The amount that the temperature may be increased is shown in Figure 3-10. The combinations of air speed and temperature defined by the lines in this figure result in the same heat loss from the skin. The reference point for these curves is the upper temperature limit of the comfort zone (PMV = +0.5) and 0.2 m/s of air speed.

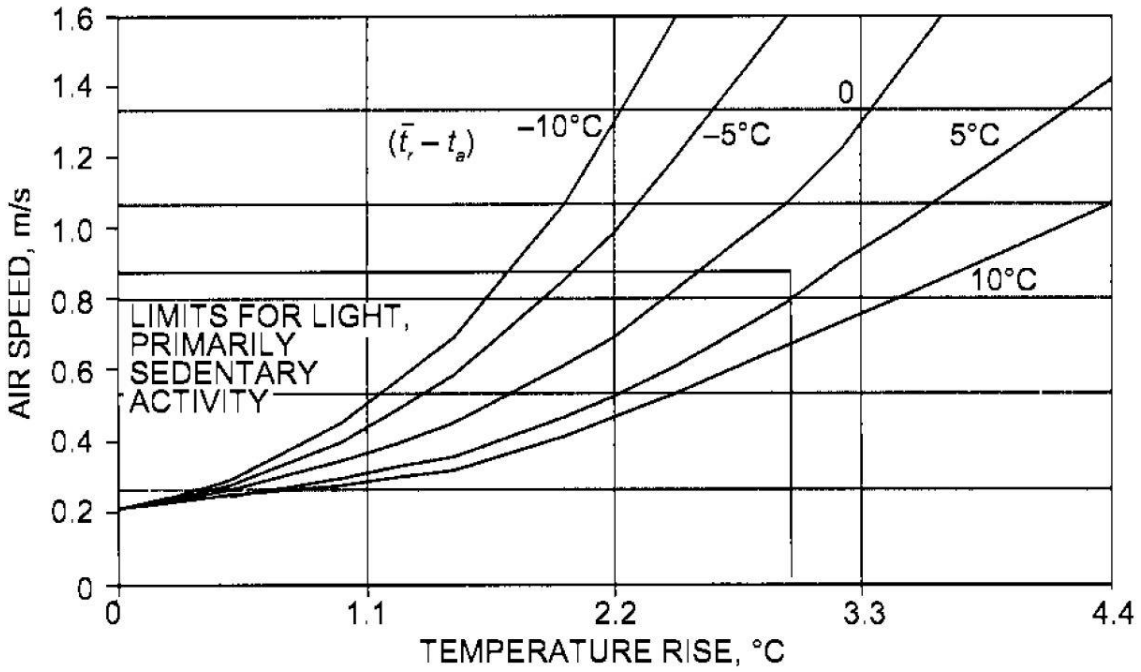

Figure 3-10 Air speed to offset temperatures above warm temperature boundaries of Figure 3-9. Source (ASHRAE, 2013a)

The 2010 and subsequent 2013 version of ASHRAE standard 55 allow elevated air speed to be used to increase the maximum operative temperature for acceptability under certain conditions using the Standard Effective Temperature (SET) model (ASHRAE, 2010, 2013b). The SET model uses a thermophysiological simulation of the human body to reduce any combination of environmental and personal variables into the temperature of an imaginary

standard environment in which the occupant's skin heat loss is equal to that of the person in the actual environment. This model enables air velocity effects on thermal comfort to be related across a wide range of air temperatures, radiant temperatures, and humidity ratios.

The heat balance model is based on extensive and rigorous laboratory experiments, albeit in the artificial, closely controlled environment of climate chambers. Field studies in actual buildings have nonetheless shown that it is remarkably successful at predicting comfort temperatures in those that are HVAC-controlled (de Dear & Brager, 2002b). Attempts to provide explanations for this and for its inability on the other hand, to accurately predict comfort temperatures in free-running buildings have paved the way for the development of the adaptive comfort model as described below.

3.3.3 The Adaptive Comfort Model (ACM)

Over the last three decades a number of studies have demonstrated the inability of the PMV-PPD model to accurately describe thermal comfort conditions in naturally ventilated buildings (Auliciems, 1981; de Dear & Brager, 2001; Humphreys, 1975; Humphreys & Nicol, 1996). Accordingly, an adaptive model of thermal comfort was developed and has gained strong credibility for determining acceptable thermal conditions in naturally conditioned spaces. The adaptive comfort model (ACM) asserts the strong statistical dependence of thermal neutralities (i.e. temperatures at which minimal stress was reported on verbal scales) on some measure of recent external temperatures. This correlation varies depending on the source of information.

3.3.3.1 The ACM in ASHRAE standard 55

The adaptive comfort model (ACM) included as an option for naturally conditioned spaces in ASHRAE Standard 55 (ASHRAE, 2013b) since the 2004 revision was derived from the analysis of 21,000 sets of raw data compiled from 160 buildings located on four continents in varied climatic zones (de Dear & Brager, 2002b). The ACM expresses the external temperature as the mean monthly outdoor temperature. The correlation used is (Brager & de Dear, 2001):

$$t_{cmf_ASH} = 0.31 t_m + 17.8 \qquad \text{Equation 3-1}$$

where t_{cmf_ASH} is the indoor operative temperature corresponding to a neutral sensation [°C] and t_m is the mean monthly outdoor air temperature [°C]. The range of temperatures corresponding with 90% and 80% thermal acceptability can then be expressed as a mean comfort zone band of 5K and 7K centred on t_{cmf_ASH}. The ACM is only applicable for outdoor temperatures between 10°C and 33.5°C and cannot be extrapolated beyond this range, otherwise this option may not be used, and no specific guidance for naturally conditioned spaces is included in the standard.

3.3.3.2 The ACM in EN 15251

An independent database of thermal comfort responses in offices comes from the Smart Controls and Thermal Comfort (SCATs) project, and is the basis of the adaptive relation included in European Standard EN 15251 (CEN, 2008). The SCATs Project was a year-round study of the indoor environment in European offices, with particular emphasis on the thermal environment. The project consisted of a study of selected office buildings in France, Greece,

Portugal, Sweden and the UK (Nicol & Humphreys, 2007). The adaptive approach assumes the neutral temperature is related to a person's thermal history with more recent experiences being more influential. The correlation used is (Nicol & Humphreys, 2010):

$$t_{cmf_EN} = 0.33t_{rm} + 18.8 \qquad \text{Equation 3-2}$$

where t_{cmf_EN} is the indoor operative temperature corresponding to a neutral sensation [°C] and t_{rm} is the running mean of outdoor temperatures weighted according to their distance in the past [°C]. The ACM in EN15251 is only applicable for t_{rm} values between 15°C and 30°C. The range of temperatures considered thermally acceptable is then dependant on the category to which the building belongs (Table 3-1).

Table 3-1 Applicability categories of EN 15251 and associated acceptable temperature ranges

Category	Explanation	Range
Category I	High level of expectation only used for spaces occupied by very sensitive and fragile persons	±2
Category II	Normal expectation for new buildings and renovations	±3
Category III	A moderate expectation (used for existing buildings)	±4
Category IV	Values outside the criteria for the above categories (only acceptable for a limited periods)	>4

3.3.3.1 Farghal's Neutral temperature

Based on a class three thermal comfort study in three educational buildings in the Greater Cairo Region, Farghal & Wagner (2010) developed a correlation between the neutral temperature and the mean monthly outdoor temperature as:

$$t_{cmf_FAR} = 0.859t_m + 0.59 \qquad \text{Equation 3-3}$$

where t_{cmf_FAR} is the indoor operative temperature corresponding to a neutral sensation [°C] and t_m is the mean monthly outdoor air temperature [°C]. The model assumes the same acceptability ranges of indoor operative temperatures and applicability ranges of outdoor mean monthly temperatures and as the ACM in ASHRAE standard 55 (ASHRAE, 2013b). This correlation offers a much wider range of acceptable internal conditions than both previous standards.

3.3.4 Discussion

Comfort conditions in PDEC buildings do not strictly conform to the applicability criteria of the Adaptive Comfort Model. However, given that it is not within the scope of this study—tempting as it is—to investigate those comfort conditions, it is argued that they could be considered to be equally in conformity with the predictions of the ACM as those in naturally ventilated and mixed-mode buildings for the reasons given below.

Internal and external conditions in PDEC buildings are closely linked to each other—as opposed to being decoupled in sealed mechanically conditioned buildings—just as much as they are in NV and MM buildings. Moreover, the fact that the forces driving airflow through such buildings are purely passive in that they predominantly depend on buoyancy generated by temperature differences which are in turn closely coupled to external conditions, makes it all the more reasonable to assume that PDEC is more a form of natural ventilation than it is a form of mechanical cooling. This argument resonates with that put forward by Nicol and Humphreys (2007) in their formulation of the now widely used equation for comfort temperatures in free-running buildings as a function of the running

mean outdoor temperature (Nicol & Humphreys, 2007). In their analysis of the data available from the SCATs project (McCartney & Nicol, 2002), they departed from the procedure adopted by de Dear and Brager (de Dear & Brager, 2002a) by making a distinction between free-running and heated/cooled modes of operation rather than between naturally ventilated and air-conditioned buildings. For them, the key factor is whether the temperature in the building fluctuates with the weather or not, irrespective of the method of ventilation employed. They explain that in buildings operating in a heated/cooled mode, the indoor temperature is largely decoupled from the outdoor temperature whilst in free-running buildings, the indoor temperature tracks the outdoor temperature through the agency of the building design, construction and use (Nicol & Humphreys, 2007).

It is evident from the description above that PDEC buildings are more likely to fall within the category of free-running buildings rather than heated/cooled buildings simply because the supply air temperature in such buildings, that is the temperature of the air resulting from the evaporation process, is a function of both the outdoor dry-bulb and wet-bulb temperatures.

3.4 Climate Suitability of PDEC in Cairo

To test whether PDEC might deliver summer time thermal comfort in office buildings under Cairo's climatic conditions, two different methods have been utilised in this study. The first is Givoni's Building Bioclimatic Charts (BBCC) (Givoni, 1992), whilst the second makes use of the Climate Suitability Analysis Method (CSAM) first described by (Axley, 2001), and recently developed to

include an adaptive comfort option (Emmerich, Polidoro, & Axley, 2011). However, some minor modifications were made to extend its application to PDEC.

3.4.1 Method 1: Givoni's Building Bio-Climatic Charts

Bioclimatic analysis methods offer a quick and simple way to assess the climatic suitability of several passive design strategies to a specific location at the early design stages. As previously mentioned, one of the best-known works on BBCCs is that undertaken by Givoni (see §3.3.1.1). However, due to the issues highlighted by Lomas, Fiala, Cook, & Cropper, (2004) (see §3.3.1.2) Givoni's BBCCs are only used in this study to provide a first stab at the suitability of PDEC and as a backdrop for the results of the CSAM.

3.4.2 Method 2: Climate Suitability Analysis Method (CSAM)

The CSAM was initially developed to evaluate the potential of a given location for both direct and night-time ventilative cooling (Axley, 2001). It is based on a general single-zone thermal model of a building configured to make optimal use of direct and/or night-time ventilative cooling. It therefore represents a useful analytical tool during the early design stages. The method uses a simple steady-state expression of the thermal response of a building to determine periods when direct and night-time ventilative cooling may be applied and to estimate the ventilation rates needed to maintain thermal comfort during these periods as defined by the PMV-PPD model of comfort incorporated in ASHRAE Standard 55 (ASHRAE, 2013b). The CSAM was recently developed to make use of the adaptive thermal comfort model included as an option in ASHRAE Standard 55

(Emmerich et al., 2011). Further details about the theory behind the CSAM can be found in (Axley, 2001; Axley & Emmerich, 2002; Emmerich et al., 2011).

As mentioned earlier, CSAM was initially developed to evaluate the potential of a given location for both direct and night-time ventilative cooling. In this study, only calculations for the direct ventilative cooling potential are of interest. However, for this to work with PDEC three modifications were considered; namely, the upper humidity limit in the comfort models used with CSAM, the period over which the analysis was performed, and the relevant indicator of the supply air temperature. These are discussed below.

For reasons unrelated to occupant thermal comfort, Emmerich et al., (2011) proposed an upper dew point temperature of 17°C corresponding to an humidity ratio limit of 12g/kg. In this study however, the humidity ratio limit was replaced by an upper relative humidity limit of 80%. This is consistent with the upper limits proposed by (Givoni, 1992) and the comfort envelopes for office buildings with PDEC developed by (Martínez et al., 2000). This value is also in agreement with ASHRAE's recommendations for the upper limit of relative humidity inside buildings to avoid the risk of surface condensation and mould growth (ASHRAE, 2013a).

The second modification relates to the period over which the analysis is performed. For the original method, the whole year was considered (8760 hours). In this study the period of interest is limited to occupied hours during the cooling season, that is, between 08:00 and 18:00 from May to October, giving a total of 1320 hours.

The third modification to be considered was to use the predicted hourly post-evaporation air temperature in lieu of the hourly values of external dry-bulb temperature used in the original method as an indicator of the supply temperature for direct ventilative cooling. It is estimated that a well-designed PDEC system would yield air temperatures as low as 80% of the dry-bulb to wet-bulb temperature depression (Cunningham et al., 1987; Ford et al., 2010; Givoni, 1992; Robinson et al., 2004). Accordingly, a simple approximation was used to emulate the performance of the PDEC system. For every occupied hour during the cooling season, a temperature t_{PDEC} was calculated as follows:

$$t_{PDEC} = t_x - 0.7(t_x - t_{wb}) \qquad \text{Equation 3-4}$$

where t_{PDEC} is the post-evaporation air temperature, and t_x and t_{wb} are the external dry-bulb and wet-bulb temperatures respectively.

For each hour, using the value of t_{PDEC} together with its coincident external wet-bulb temperature, the corresponding post-evaporation humidity ratio W_{PDEC} and relative humidity RH_{PDEC} were calculated. It was found that for a substantial number of hours, the calculated values of W_{PDEC} and RH_{PDEC} exceeded the upper humidity limit suggested by the PMV-PPD model and that imposed on the ACM in ASHRAE standard 55 (ASHRAE, 2013b) respectively. This meant that unnecessary excess humidification occurred which would eventually lead to an overestimation of the percentage of hours lying outside the comfort boundaries. In effect, t_{PDEC} was recalculated in two different ways to differentiate between the post evaporation temperature used with the PMV-PPD model and the ACM. For the PMV-PPD method, for each hour coinciding with a calculated W_{PDEC} greater

than 12g/kg, W_{PDEC} was taken to be 12g/kg and t_{PDEC} was recalculated as t_{PDEC_PP}. Similarly, for the ACM, for each hour coinciding with a calculated RH_{PDEC} greater than 80%, RH_{PDEC} was taken to be 80% and t_{PDEC} was recalculated as t_{PDEC_ACM}. On a psychrometric chart, t_{PDEC_PP} would represent the dry-bulb temperature value at the intercept between the two lines representing 12g/kg humidity ratio and the external wet-bulb temperature whereas t_{PDEC_ACM} would represent the dry-bulb temperature value at the intercept between the two lines representing 80% relative humidity and the external wet-bulb temperature. These were determined using an iterative calculation based on the psychrometric equations described in (ASHRAE, 2009). It has to be noted that, assuming internal moisture production has negligible impact on humidity levels (due to the high airflow rates likely to exist in PDEC buildings), and taking into consideration the way t_{PDEC_PP} and t_{PDEC_ACM} were calculated, it can be inferred that the upper humidity limits would only filter out those hours coinciding with an external humidity ratio above 12g/kg for the PMV-PPD model or an external relative humidity above 80% for the ACM.

Having established hourly values for t_{PDEC_PP} and t_{PDEC_ACM}, the calculation procedure for the CSAM described in (Emmerich et al., 2011) together with the suggested modifications were then used to determine periods when PDEC may be applied and to estimate the ventilation rates needed to maintain thermal comfort during these periods.

3.4.3 Results

Annual hourly climate data of the Egyptian Typical Meteorological Year (ETMY) made available by the US Department of Energy were used in the analyses. Figure 3-11 shows the results of the two methods used to assess the climatic suitability of PDEC in office buildings in Cairo.

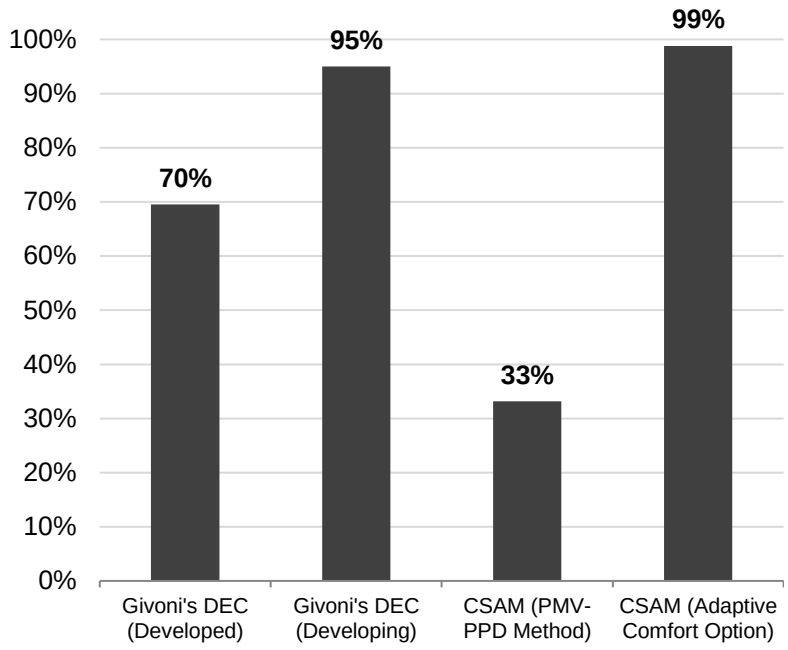

Figure 3-11 Percentage of hours during the cooling season for which PDEC yields thermal comfort conditions in Cairo

To estimate the ventilation rates needed to maintain thermal comfort during the periods when PDEC may be applied in the CSAM, three values of internal gains were considered; 10W/m^2, 30W/m^2, and 50W/m^2. A floor to ceiling height of 3m was assumed. Of the 1320 hours representing the occupied period between 08:00 and 18:00 from May to October, Givoni's BBCC indicate that 918hrs lay within the DEC boundaries for developed countries whereas 1254hrs lay within the DEC boundaries for developing countries. Givoni's BBCC thus

suggest that PDEC would be effective at maintaining thermal comfort for 70% to 95% of the occupied hours during the cooling season depending on the degree of acclimatisation of the occupants, but that mechanical cooling assistance may be necessary in extreme conditions.

On the other hand, the CSAM suggests that PDEC would be effective at maintaining thermal comfort for around 33% (439hrs) of the same period for the PMV-PPD model. However, this figure significantly rises to 99% (1304hrs) if the ACM with the imposed upper humidity limit is considered. This marked increase in the potential effectiveness of PDEC is attributed to the difference between the upper boundaries of humidity in the two comfort models rather than to the difference between the upper limits of acceptable indoor temperatures. By way of illustration, if the upper limit of humidity for the PMV-PPD model was taken to be similar to that imposed on the ACM (i.e. 80% RH), the number of hours yielding comfort conditions rises from 33% (439hrs) to 93% (1227hrs) which indicates that the increase in the upper limits of acceptable indoor temperatures afforded by the ACM accounts for an increase of only 6% (77hrs) in the period yielding comfort conditions. Taking the highest input value for internal gains (50W/m^2), the CSAM also shows that average ventilation rates of 23.8ach^{-1} and 11ach^{-1} are needed to maintain thermal comfort during the period when PDEC may be applied if the PMV-PPD model and the ACM were considered respectively. Ventilation rates of more than 30ach^{-1} have been reported in PDEC buildings (Cunningham et al., 1987). Taking this value as a benchmark, around 83.3% and 98.5% of the calculated ventilation rates fall below for the PMV-PPD model and the ACM respectively. Given that even higher flow rates are anticipated in high-rise

buildings due to the increased height of the stack, it seems that the estimated flow rates could well be achieved in a purpose-built PDEC building.

It has to be noted however that the results show large discrepancies in the predicted number of hours yielding comfort conditions between the DEC boundaries for developed and developing countries in Givoni's BBCC and between the PMV-PPD model and the ACM in the CSAM. This indicates that the choice of comfort criteria to be adopted in general and the upper limits of humidity to be imposed in particular have a significant impact on the outcome of the analysis and ultimately on the decision of whether or not to proceed with the PDEC strategy. Nevertheless, in general, the results of the two methods suggest that PDEC could potentially be very effective in achieving thermal comfort in buildings located in Cairo provided that the occupants are highly acclimatised as suggested by Givoni (1992) to the ambient thermal environment and that the buildings are optimally configured to incorporate PDEC.

3.5 Overview of office building design and energy use in Cairo

A brief review on the current state of office building design and practice in Egypt was carried out. With the absence of any published data on the current office building stock in Cairo, data was mainly obtained from a series of personal communications with the heads of the architectural design departments of two of the leading architecture and engineering firms in Egypt and the Middle-east in addition to the review carried out by Hamza N. (2004) on office buildings in Cairo. The main findings of the review are as follows:

- The most prevalent construction methods for office buildings are reinforced concrete frames with brick infill or reinforced concrete frames with curtain walling systems.
- The average U-value of external walls using materials available within the Egyptian market is 1.7 $W/m^2.K$. It should be noted that within the limits of the current Egyptian thermal code for buildings, the limit of a façade construction (including window areas) should not exceed 1.5 $W/m^2.K$.
- Typical floor to floor heights range between 3m and 3.7m with the higher value typically associated with the existence of ductwork. This can be further elaborated as; 3m floor to ceiling, 0.5m clearance above ceiling and 0.2m slab thickness.
- Internal partitions and walls are usually made up of two layers of 19mm plaster board separated by a 10cm air gap.
- Most of the newly built office buildings incorporate an open-plan layout with only 10-15 % of the net lettable area allocated for cellular offices to house executives.
- Window to wall ratios WWR range between 40-60% in the case of brick infill façades to more than 90% in curtain walled constructions. These values are likely to increase in high-rise buildings to benefit from the exterior views afforded by such heights.
- From experience with workmanship levels in Egypt, a value of 0.5 ach^{-1} is reasonable to account for infiltration rates.

These findings were considered in the construction of the base case model as discussed in Chapter Five.

3.6 The case for Tall Buildings in Cairo

Since the beginnings of the high-rise building movement in Chicago at the end of the 19th century, tall buildings have been primarily dictated by commerce and pre-occupied with their role as a piece of sculptural urban imagery (Oldfield, Trabucco, & Wood, 2008). There has been very little consideration of appropriateness to their climate, culture. and physical setting.

At present, we are witnessing an unprecedented tall building boom with ever-denser cities and ever-taller buildings being built in different parts of the world in Europe, North America, Asia and the Middle East. Such a boom is not only in terms of number and height but also in terms of change in location, function, material, title, and motivation and finally in terms of aesthetics (Oldfield et al., 2008).

This section aims at casting some light upon the existing tall buildings paradigm worldwide and in Cairo, Egypt in terms of driving forces, the argument for and against, and their role in sustainability and future aspiration.

3.6.1 Driving Forces Worldwide

A number of driving forces is behind this boom; population/urbanization and density, land price, global icons, and finally sustainability and climatic change.

Population Growth

The Population Division of the United Nations has predicted that the urban population will grow by 68% by the year 2050 (United Nations, 2015). This means that not only is the world population growing but also that the percentage of

people living in the city is increasing even faster. In addition to that, the second half of the twentieth century has witnessed massive population shifts from the cities to the suburbs occurring in all parts of the developed world (Ali, 2008). In recent years, this trend of “urban dispersal” is returning to “densification” of urban areas through redevelopment programs, often invoking tall buildings of all kinds, whether commercial, residential, or mixed-use (Abel, 2003).

Growth is not something that can be stopped, only contained and influenced. Despite the global and local effects, cities will always thrive and continue to exist. The places they thrive will be the cities best prepared to deal with growth. Supertall buildings and megastructures are the likely solutions to the problems that megacities will face in the not-too-distant future (Ali, 2008).

Land value

High land values are playing a larger role in many cities in the United States, U.K. and all other countries seeking to repopulate urban centres with residential/recreational complements to the predominantly commercial/retail central business district building stock. These represent new markets which drive up city centre land prices which makes building tall for investment return increasingly necessary (Wood, 2007).

Global Icons

The focus behind building tall has been shifting from creating an architectural icon to project the identity of a corporation to that of reflecting the vitality of a city on a global scale to create sky lines with international recognition (Wood, 2007), an example of which is the Burj Khalifa in Dubai.

Sustainability and Climate Change

It is predicted that the impact of climate change emissions will result in a likely increase in average global temperatures between 1.1K and 6.4K during this century and that the critical level of CO_2 concentration in the atmosphere could reach 750-1000 ppm by the latter part of the century (IPCC, 2008).This is, without doubt, going to have a significant impact on the planet we inhabit. The governments of the world now realize that the international community needs to achieve an 80% cut in anthropogenic CO_2 emissions globally to allow the atmosphere to be stabilised at a level below that needed to avoid catastrophic climate disruption (Wood, 2007).

The built environment is recognised as being the largest single contributor to climate change, with the creation, running and maintenance of buildings estimated to account for 50% of all energy usage and more than 50% of all climate-change emissions globally (Smith, 2005).

Denser, more concentrated cities, sometimes referred to as sustainable compact cities (Shin, 2009), are seen as an essential part of a more sustainable way of living because they cut energy consumption and climate change emissions by reducing the suburban spread of cities, and thus the need for new transportation and infrastructure network (AIJ & IBEC, 2005). Tall buildings are seen to play a key role in creating these denser cities by accommodating more people on smaller parcels of land with the benefit of centralizing numerous functions of the city in one place (Shin, 2009). In addition, the investment in every tall building—both financial and professional—provides the opportunity to embrace sustainable designs and technologies that could lead the way for other

building types (Wood, 2007). Canary Wharf is known as a symbol of the changed economic geography of the UK that promotes the city's competitiveness (Je, 2006).

3.6.2 The Case for and against

Against this background, both the international and professional/academic communities are still divided on the sustainability credentials of Tall Buildings as an appropriate typology in our existing and future urban centres. There are those that believe that the concentration of population through high-density (therefore reducing transport costs and urban / sub-urban spread) combined with the economies of scale of building tall, make the typology an inherently sustainable option (Shin, 2009) whilst others believe that the embodied energies involved in constructing at height, combined with the impact on the urban realm, make them inherently anti-environmental (Roaf, Crichton, & Nicol, 2009).

Ken Yeang is one of those who advocates that Tall Buildings play a major part in a sustainable strategy if the density is high enough, and the land cost, the building's programme, location, transportation links and its proper bioclimatic design can produce quantifiable benefits and outweigh the embodied energy cost of building tall (Yeang, 2002). In Yeang's view, tall buildings seem to be unavoidable in dense cities and must be considered as integral to the quest for the sustainability of future cities. Wood (2007) however, has raised three challenges and three goals for future tall buildings in order to play a positive role in sustainability. A minimum goal should be zero net energy consumption, but a better goal would be true carbon neutrality through the creation of an energy

surplus that eventually could offset the embodied energy use/carbon emissions involved in the building's construction. A second challenge is to advance in design terms regarding the building's relation with its urban location. The third challenge lies in the building's functional programs to innovate beyond the standard functions of office, residential and hotel.

Those who have conservations against Tall Buildings, for instance (Roaf et al., 2009) have raised a number of issues that may be summarized as follows;

- High Energy Consumption in Operation.
- Structure and Embodied Energy.
- Wind and Occupation Comfort.
- Net-to-Gross Issues.
- Anti-Social Internal Environment.
- Sealed Environment at Height.
- Safety and Security Fears.
- Power Failure Implications
- Impact on Urban Scale
- Wind Draft & Pedestrian
- Overshadowing and Rights of Light

3.6.3 The Case for High-Rise Buildings in Cairo

Cairo, the capital of Egypt for hundreds of years, is the largest city in both Africa and the Middle East (Sims, 2003). Developments during the 19th and early decades of the 20th century have resulted in transforming Cairo by the beginning of the 20th century into a more familiar model of a modern metropolis (Abu-Lughod, 1971). These transformations had brought about two kinds of problems,

'…ones which were not unique to Cairo as a Middle-Eastern city, nor an Islamic one, nor even a prototype of a preindustrial city, but familiar problems faced by any major city in the twentieth century Western world'.

The other kind of problems are those related to what Sims (2003) refers to as Cairo's national context which comprises history, geography, demography, and its urban economy.

Overpopulation is one of the major problems Cairo is suffering from. This is where the unique geography and demography of Cairo seem to play the major role in making Cairo one of the most populated cities in the world.

3.6.3.1 Geography and Demography of Cairo

Cairo is situated on the Nile at a point where the flat flood plain, constricted by desert hills both to the west and the east, begins to open out into the Nile Delta. According to Sims, it is rare to find a report on Egypt's development that does not include a statement like "95 percent of the population lives on 4 percent of the land area" referring to the Nile Delta and Valley (Sims, 2012). Most of Cairo's expansion has been on rich agricultural land. Only the eastern districts, most notably 'Madinet Nasr', 'Nozha' (and earlier 'Abassia' and 'Heliopolis' have been created on what was desert land) (Sims, 2012).

In spite of the fact that the net in-migration has almost stopped since the 1980s, the metropolis's expansion is fuelled by natural increase and the incorporation of surrounding rural populations. According to the Egyptian Central Agency for Public Mobilization and Statistics (CAPMAS), Egypt's population

reached 94 million in 2017 with an estimated number of over 18 million living in the metropolitan region of Greater Cairo (CAPMAS, 2017). This means that almost 20% of Egypt's population are now living in Greater Cairo. According to the Ministry of Housing, Utilities and Urban Development of Egypt (MOHUUD) it is also projected that the total population of Egypt will be 103 million by the year 2027 with an estimated 27 million living in Cairo (MOHUUD & JICA, 2008). This means that almost 22% of Egypt's population will be living in Greater Cairo Region (GCR).

3.6.3.2 Driving Forces for High-Rise Buildings in Cairo

Similar to what happened in North America and most major cities in Europe the process of urbanization and the need to repopulate high density has resulted in raising the land price particularly in commercial/business areas in downtown Cairo, in residential/commercial/business areas in 'Muhandseen' district, in affluent residential districts such as 'Zamalek' & 'Heliopolis' and along the Nile front from 'Maadi' district in the south of Cairo up to 'Maspero' and 'Ramlat Boulack' districts to the north of Cairo.

However, unlike the process of urban densification in global cities in Europe, Australia and Asia involving the partnership and commitment of governments, policy makers, experts and the involvement of citizens, the process of densification in Egypt was left to individual initiatives of two different kinds of motivations; investors who are exclusively profit-oriented and ordinary new comers who simply need a residence. This has resulted in making building tall for both investment return and housing almost inevitable in dense locations.

The tendency towards increase in height has always been associated with several changes in building laws and legislations to facilitate the process of densification. According to Egyptian building regulations, multi-storey buildings are allowed to go as high as 1.5 times the street width provided that the height does not exceed 36 meters above ground level (about 12 floors). According to the CTBUH height criteria, buildings of this height are not considered high-rise. However, locations along the Nile front and around big squares (such as Tahrir Square in the heart of Cairo) are exempted from these regulations and can rise as high as the design brief requires.

It was not until 2008 that a strategic urban development master plan was proposed by MOHUUD in collaboration with Japan International Cooperation Agency (JICA) for the development of a sustainable Greater Cairo Region (MOHUUD & JICA, 2008). Although high-rise buildings were not explicitly addressed as part of the sustainable agenda, it was clear from the images of the future proposed projects, aiming at creating new business districts and vitalizing old ones, that high-rise office buildings of more than 50 floors were the essential building typology in those districts. Images of High-rise offices and multi-use buildings were also proposed along both sides of the Nile banks.

However, whilst the report has indirectly (through images) emphasised the role of tall Buildings in providing intensified development for the proposed international business/industry centres as well as projecting global icons for touristic/residential purposes, their important role in the climatic sustainability agenda was completely overlooked. In fact, the strategic sustainable plan for Cairo has categorically overlooked the important issues of pollution, energy

consumption and CO_2 emissions as major problems that require attention to maintain a sustainable development. Accordingly, the environmental sustainability credentials of tall buildings as an appropriate typology in existing and future urban development were not even raised.

In conclusion, Cairo is one of the most populated mega cities in the world. An action plan to densify projected locations targeted for both international business/industry and touristic/residential purposes is apparently undergoing. Building tall seems to be inevitable in these locations provided that the land value, the programme, location, transportation links and proper bioclimatic design can produce quantifiable benefits and outweigh the embodied energy cost of building tall. Given the pressing demand on curbing CO_2 emissions and providing high-quality office space in those locations or any other potential office locations in Cairo, it is anticipated that extending the application of PDEC to high-rise office buildings is imperative if PDEC is to be widely adopted as an alternative to conventional air-conditioning in those buildings.

3.7 Summary

An overview of Cairo's climate was presented and showed that the annual temperature range is 35K and that the diurnal range reaches 14K in July and August. Mapping monthly average hourly values of relative humidity over dry-bulb temperatures suggests the potential effectiveness of direct evaporative cooling during the cooling season which extends from May to October. Wind rose analysis also shows that north-western winds are dominant in the hot summer periods.

Review on thermal comfort requirements in PDEC buildings showed that very few studies have specifically addressed that topic. With regards to the two widely accepted models of thermal comfort, whilst field studies have shown that the heat balance model is a good predictor of comfort in mechanically cooled buildings, and the ACM in free-running buildings, it is not that obvious under which category should PDEC buildings fall. It is argued that due to the strong coupling between indoor and outdoor conditions and the fact that the driving forces are natural as opposed to mechanical, the ACM could equally be applied to PDEC buildings.

Preliminary analysis of climate suitability was carried out using Givoni's BBCC and an adapted version of the CSAM. Results indicated that the choice of comfort criteria to be adopted in general and the upper limits of humidity to be imposed in particular have a significant impact on the decision of whether to proceed with the PDEC strategy. Generally, the results of the two methods suggest that PDEC could potentially be very effective in achieving thermal comfort in buildings located in Cairo.

The case for high-rise office buildings in Cairo was also argued. With an action plan to densify projected locations targeted for both international business/industry and touristic/residential purposes apparently undergoing, building tall seems to be inevitable. That, and the pressing demand on curbing CO_2 emissions and providing high-quality office space in those locations, it is anticipated that extending the application of PDEC to high-rise office buildings would offer a more sustainable alternative to conventionally air-conditioned tall buildings.

Chapter 4: Plan for the design of PDEC multi-storey office buildings

4.1 Chapter Overview

In this chapter a proposed plan for the design of PDEC multi-storey office buildings is outlined. The plan proposes four stages. The first, henceforth referred to as the conceptual design stage, is where the ventilation strategy of the model is proposed and the generic prototype of the building that allows for such a strategy to work is developed. The second stage is that of design development and is where the initial sizes of the vents proposed in the generic prototype are calculated. The third and most important stage is that of performance assessment in which the airflow behaviour, resulting thermal conditions and environmental costs are established. The fourth and final stage of the design process is that of optimisation. Each stage requires different research tools and methods. The conceptual design stage entails knowledge of the ventilation strategies, flow patterns, and modes of operation involved. Knowledge of the building configuration that gives rise to such behaviour is however a prerequisite. Accordingly, analysis of precedents of PDEC buildings and NV tall buildings is presented in section 4.2 which then culminates in the development of the generic prototype of the PDEC multi-storey office building.

The second and third design stages require knowledge of the modelling techniques and assessment tools available for PDEC and NV. A review of those tools is therefore presented in section 4.3. Each modelling technique is described,

and examples of its application given. Suitability of each modelling technique for the various design stages is highlighted together with its advantages and limitations. The review concludes with the selection of an analytic model (Envelope flow models) for the initial sizing of the vents of the generic PDEC prototype (design development stage) and of an integrated dynamic thermal and airflow model (EnergyPlus) for the performance assessment stage. In section 4.4, description of Envelope Flow Models (EFM) and the procedure used to calculate the initial sizes of the generic prototype is presented. In section 4.5, a brief description of EnergyPlus is given, previous work on the validation of its results presented, and the procedure used to simulate PDEC described.

4.2 Conceptual Design: Ventilation Strategies and Modes of Operation

In Chapter 2, a general preview of the different issues involved in natural ventilation was presented. However, the application of these principles to a building will vary significantly depending on the building's form and function as well as the climatic wherein the building is located. This section will discuss the potential problems that might occur in the application of natural ventilation to buildings from two different aspects; the building's height, i.e. application to tall buildings, and the building's climatic context, i.e. application in hot-dry climates.

According to Etheridge and Ford (2008), it is not surprising that the adoption of natural ventilation in tall buildings is less common in view of the potential risks to a successful design. This is primarily because the potential magnitudes of the driving forces become greater and their relative magnitudes can vary over a wider

range. In applying the ventilation strategies presented in Chapter 2 to tall buildings, different problems occur depending on the adopted strategy.

For isolated spaces, that is, where single sided and cross ventilation strategies are adopted, the advantages and limitations (Etheridge & Ford, 2008) are:

- From a technical point of view, the design for one floor can be studied in isolation and then replicated for the other floors (with allowance for different pressures). However, practically, it may be difficult to achieve complete isolation due to the presence of lifts, service shafts, and stairwells.
- High wind pressures are likely to be encountered in tall buildings, whereas the buoyancy pressures remain low, because they are determined by the height which is in this case limited to the floor to ceiling height. This leads to large differences between the open areas required to achieve the flow rates under wind alone and buoyancy alone conditions.
- The height to width ratio of the building is limited. Owing to the fact that cross ventilation is only effective when the depth of a space D does not exceed 5 times its height h, i.e. D/h = 5, then the aspect ratio H/D of a 10-storey building, where H is the buildings total height, will need to be greater than two, but for a tall building with 50 storeys it will need to be greater than 10.

For connected spaces, that is, where buoyancy driven stack ventilation strategy is adopted, the advantages and limitations (Etheridge & Ford, 2008) are:

- That wind and buoyancy will act in unison, provided the outlet opening is in a region of relatively low wind pressure and the internal temperature is higher than the external.
- Since the overall height is the determinant of the buoyancy force. Thus, the main problem with applying this approach to tall buildings arises from the high-pressure differences that can be generated by buoyancy, due to the large height of the stack. This can lead to high discrepancies in airflow rates between the upper and lower floors and to difficulties in opening doors and windows in the lower floors.

The previous problems are further complicated if the building is to be located in a hot-dry climate. In this situation, since natural ventilation provides a heat transport mechanism between the external and internal environments, and since external temperatures are higher than internal ones, a rise in internal temperatures will eventually take place, rendering natural ventilation unsuitable unless the incoming air is pre-cooled. Furthermore, if a wind-driven ventilation strategy is adopted, any attempt to pre-cool air will lead to very high pressure drops and hence a huge reduction in airflow rates.

4.2.1 Precedents and Case Studies

In theory, there are several ways around the aforementioned problems; however, it is the means through which these solutions are put to practice in real buildings that is of great relevance to this study if a preliminary model of the PDEC high-rise building is sought. To investigate this, a review on PDEC as a means to overcome the problems associated with natural ventilation in hot-dry climates has

been carried out. Furthermore, a discussion on the prospects of natural ventilation in relation to its application to high-rise buildings and a review on a number of prominent mixed-mode tall buildings have also been carried out highlighting the key design features employed to overcome those problems. These are presented below.

4.2.1.1 PDEC Buildings

In the past decade, an increasing number of buildings have adopted PDEC or PHDC as their main passive cooling and ventilation strategy applying it to the entire building or to a select number of spaces. The application of downdraught cooling to buildings could be categorised into four generic cases (Ford et al., 2010):

1- *Open Central Atrium*: can be considered as a single cell, where the supply zone and the delivery zone are the same and surrounding spaces are not served by the downdraught cooling system.

2- *Open Central Concourse or Enclosed Central Tower*: can be considered as the supply zone which serves a number of surrounding zones and is therefore a 'multi-cell' building when considering airflow and thermal performance simulations. The main difference between an open concourse and an enclosed tower is that in the former the supply zone is big enough to be occupied and so can have a spatial function such as circulation, while the latter only functions as a supply zone.

3- *Attached Perimeter Tower*: A perimeter tower attached directly to the served space or spaces can be considered a multi-cell case. While a

central shaft has the potential to deliver air to all the spaces around it, a perimeter shaft can only deliver cool air to one side.

4- *Detached Perimeter Tower*: A detached perimeter tower is a variant of Case 3, where for various reasons the PDEC tower cannot be located immediately adjacent to the served space. The disadvantage of this arrangement is that the reversal of the pattern of air flow (to achieve night time convective cooling) will not take place as effectively as with the attached tower, where a vent opening can be located at high level between the room and the tower.

This research will focus on the second and third cases which are the central enclosed shaft and the attached perimeter tower. They are the only cases where a single element (tower or shaft) can serve several spaces on more than one floor rendering them the only cases relevant to the building type under consideration. Five buildings implementing one of those two cases are briefly described and analysed below. The five selected PDEC/PHDC buildings are located in five different locations around the world, namely Ahmadabad and Gulbarga in India, London in the UK, Seville in Spain, and Catania in Italy. It demonstrates how each building with its corresponding ventilation concept was designed to overcome the overheating problems associated with the natural ventilation of buildings when external temperatures exceed internal ones.

4.2.1.1.1 The Torrent Research Centre

- *Location*: Ahmadabad, India. 23.03 °N – 72.58 °E.
- *Year of completion*: 1998
- *Building Type*: Office building and Laboratories
- *Architect*: Nimish Patel, Parul Zaveri - Abhikram
- *Building Services*: Brian Ford and Associates
- *Total gross floor area*: 14000 sqm.
- *Number of storeys*: 3
- *Type of evaporation*: Misting nozzles
- *PDEC Strategy*: Open central concourse



Figure 4-1 The Torrent Research Centre. Source (Ford et al., 1998)

General

The project comprises a research and development centre for the Torrent Pharmaceutical Company. The laboratories provide facilities for a range of different disciplines including Molecular Biology, Cell Biology and Tissue Culture, Histology, Biochemical analysis, and the development of disease models for screening of new compounds. The design of the buildings in the Torrent Research Centre was aimed at integrating spaces requiring highly controlled conditions with those requiring less controlled conditions, while minimising the presence of dust in the internal environment (Ford et al., 1998).

Climate

Under the Köppen-Geiger climate classification (Kottek et al., 2006), Ahmadabad has a semiarid climate. There are three main seasons: summer, monsoon and winter. Aside from the monsoon season, the climate is dry. Annual average temperature is 15.9 °C. The weather is hot through the months of March to June. The average summer maximum is 45 °C, and the average minimum is

23 °C. From November to February, the average maximum temperature is 30 °C, the average minimum is 15 °C, and the climate is extremely dry. Cold northerly winds are responsible for a mild chill in January. The southwest monsoon brings a humid climate from mid-June to mid-September.

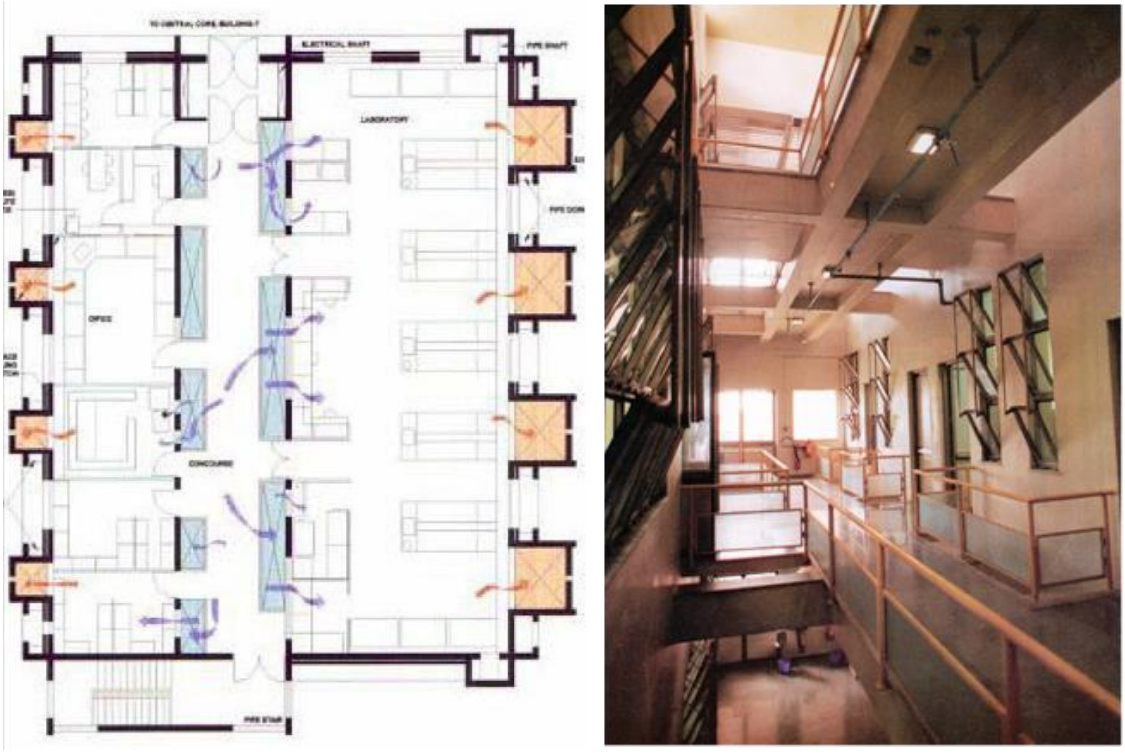

Figure 4-2: Ventilation concept of the TRC (left) and the Central open concourse (right) Source (Ford et al., 1998)

Ventilation concept

The building's basic ventilation concept depends on a central open concourse on three levels which allows evaporatively cooled air to be introduced to laboratories and offices and then exhausted through the perimeter stacks (Figure 4-2). However, the building operates at different modes depending on the time of year and day as described below.

Summer Mode:

During the day from late February to mid-June the building is naturally ventilated by stack or wind pressure differences. However, when the external air temperature is several degrees above internal, misting nozzles fixed at the top of three 4m x 4m towers are activated and the cool air descends slowly through the central corridor space via the openings on each side of the walkway. At each level, sets of hopper windows designed to catch the descending flow, divert some of this cooled air into the adjacent space. The cool air passes through the spaces and then exists via high level glass louvered openings which connect directly to the perimeter exhaust air towers. The perimeter stacks are designed to exhaust air at both high and low level, depending on the existence (or absence) of wind. At night, the airflow path is reversed to flush out any residual daytime heat gains (Figure 4-3).

Monsoon Mode

When the monsoon breaks in mid-June, the external temperature drops significantly, but the humidity rises. In these conditions, the client was happy initially to rely on air movement induced by natural ventilation alone. However, after the first year, following staff comments of ‘stuffiness’, it was decided to augment natural ventilation with the use of ceiling mounted low-speed fans.

Winter Mode

During the day, natural ventilation (from low to high level) is able to remove internal heat gains, while at night vents at the top of the building are closed to prevent excessive heat loss.

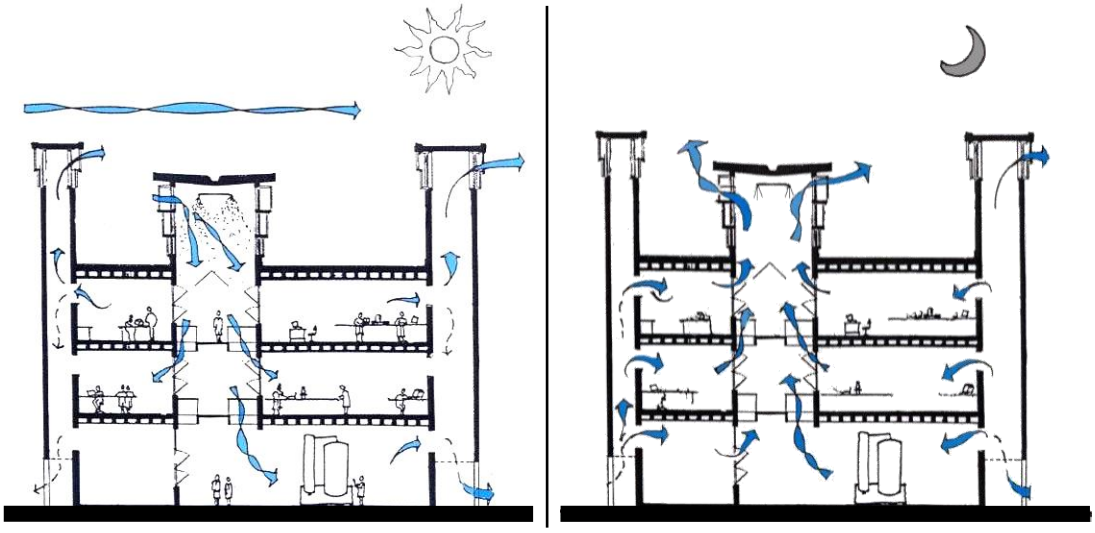

Figure 4-3 Summer day and night modes of operation in the TRC.
Source (Ford et al., 1998)

Measured Performance

Monitored temperatures have indicated that internal maximum temperatures could be maintained 12-14K below the external peak and that internal temperatures were around 5K lower than average external temperatures (Bowman et al., 2000).

4.2.1.1.2 Inspector General of Police Complex (IGP)

- *Location:* Gulbarga, India. 17.33 °N – 76.83°E.
- *Year of completion:* 2006
- *Building Type:* Office building
- *Architect:* Kembhavi Architecture Foundation
- *Floor area to be cooled:* 1100 sqm.
- *Number of storeys:* 3
- *Type of evaporation:* Shower tower
- *PDEC Strategy:* Enclosed Central tower + Attached perimeter tower



Figure 4-4 Inspector General of Police Complex. Source (Prajapati, 2007)

General

This building, designed to house the offices of the Inspector General of Police, employs a number of energy-conscious features. Apart from the PDEC system, the building is constructed using innovative materials such as composite walls to reduce heat gain and filler slabs to reduce the quantity of concrete in the structure. The building is roughly rectangular with the longer axis along the north-south direction with a central atrium to enhance cross ventilation and provide daylighting. Additionally, solar PVs, lighting and pumps, rainfall harvesting, and water conservation facilities are incorporated (Nayak & Prajapati, 2006).

Climate

According to the Koppen climate classification (Kottek et al., 2006), Gulbarga has a semiarid climate. There are 3 main seasons, summer which spans from late February to mid-June with average temperatures of 43 °C, monsoon which spans from late June to late September with relatively lower temperatures with

an average of 30 °C associated with high levels of relative humidity, and winter which extends to mid-January with average temperatures of 16 °C.



Figure 4-5 Ten enclosed shafts within the plan are used to cool the IGP. Source (Prajapati, 2007)

Ventilation concept

The offices of the Inspector General of Police (IGP), Gulbarga, India are cooled by a shower tower system, configured as ten enclosed shafts within the plan of the building (Figure 4-5). At the very top of each tower, cross baffles are used to divert wind into the tower. Air then passes through the water sprinklers which are placed just below the air inlets. The relatively denser air then flows downwards and is filtered through a wood charcoal layer installed to keep out dust and insects. Another type of baffle is used to divert some of the cool air into the occupied spaces on the first floor while the remaining cool air continues downwards to enter the adjacent ground floor spaces. Due to the large size of

droplets, water is not completely evaporated, and so excess water is collected at the bottom of the tower and then recirculated.

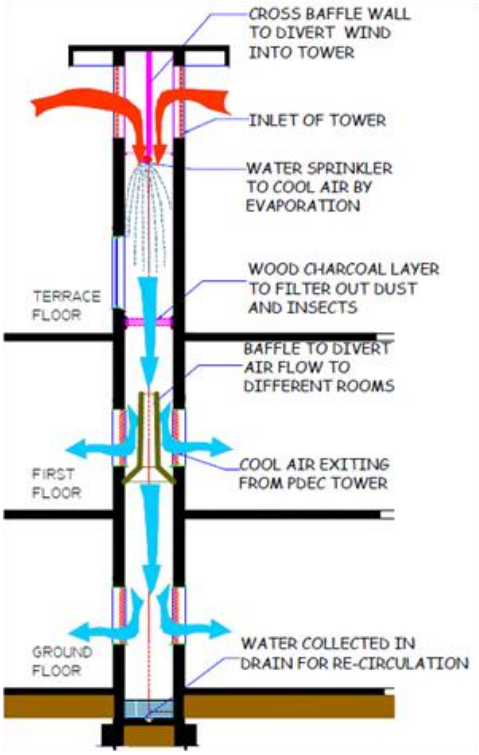

Figure 4-6: Detail of the shower tower. Source (Prajapati, 2007)

Measured Performance

Preliminary measurements taken in May and September 2005 have shown that the temperature of the air exiting from the tower is lower by about 10°C and 4°C respectively, compared to that of ambient air. It has also shown that the performance of the cool-towers appears to be satisfactory in the summer months and that the drop in temperature is about 12 - 13 °C in March, April and May (Ford et al., 2010).

4.2.1.1.3 School of Slavonic and Eastern European Studies (SSEES)

- *Location:* London, UK. 51.5 °N – 0.12 °E.
- *Year of completion:* 2006
- *Building Type:* Office building
- *Architect:* Short and Associates
- *Building Services:* Malcolm Cook, IESD Andrew Woods, BP Institute
- *Total gross Floor area:* 3500 sqm.
- *Number of storeys:* 5 + lower ground
- *Type of cooling:* Chilled water pipes
- *PHDC Strategy:* Enclosed Central atrium



Figure 4-7 The SSEES Building. Source (www.shortandassociates.co.uk)

General

The building that houses the School of Slavonic and Eastern European Studies (SSEES) is a typical example of a PHDC building. Although the building is located in the eye of London's heat island, the designers opted for a low-carbon, low-energy mechanism of cooling. Due to climate incompatibility, evaporative cooling was not employed but rather an active source of cooling (chilled water coils) is used to generate a downdraught sufficient enough to drive the air throughout the building's spaces. The building has five storeys punctured by a triangular light well in the centre of the plan which is zoned into a core zone, an open plan area, and a perimeter zone that could be cellularised into offices if necessary (Figure 4-8).

Climate

London has a temperate marine climate (Köppen-Geiger climate classification Cfb) (Kottek et al., 2006), so the city rarely sees extremely high or

low temperatures. Summers are warm with average high temperatures of 21-24 °C and lows of 11-14 °C. But temperatures can exceed 25 °C on many days, and in almost every year they exceed 30 °C on some days. Winters in London are chilly, but rarely below freezing with daytime highs around 5 °C - 8 °C, while spring has mild days and cool evenings. Autumn is usually mild but often unsettled as colder air from the north and warmer air from the south meet.

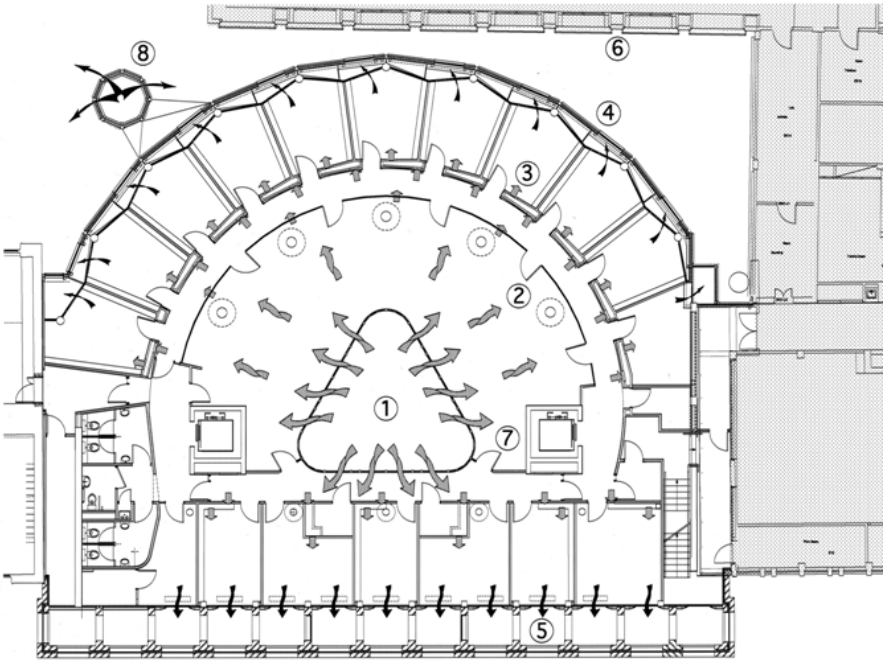

Figure 4-8 Typical floor plan configured as a core zone, an open plan area, and a perimeter zone. Source (Lomas, Short, et al., 2004)

In a large city such as London, a substantial urban heat island can be generated further raising the air temperature around city buildings. This elevation in temperature is most significant on still summer nights, with the eye of the heat island being near the British Museum, which is approximately 600m from the site of the SSEES building. When assessing a building to be sited in this location, the effects of the heat island must be considered. This indicates that some form of

cooling must be used to maintain comfort in the SSEES building. The design challenge was to provide this in an energy-efficient manner.

Ventilation concept

The five-storey building is punctured by a triangular light well in the centre of the plan. Fresh air is introduced into the light well either through a plenum located between the upper and lower ground floors or from the top of the light well depending on the time of year and day. The air then enters the adjacent spaces and finally exits from the exhaust stacks distributed around the rear elevation which serve each (potential) office, or from a continuous double façade rather than individual stacks on the front elevation. A BEMS automatically controls the dampers and openable windows of the entire building, as shown in Figure 4-9a. The seasonal operational modes are as follows (Lomas, Short, et al., 2004).

Winter Mode

In winter, finned emitters located around the light well and at the parameter of the building are used to warm the building before the arrival of occupants and all dampers are closed. During occupancy, air enters the plenum at the base of the building to satisfy IAQ requirements. It is introduced into the base of the light well through dampers and across heating coils. Finer control of space temperatures is achieved by heating elements located at the point of entry into the occupied spaces. This allows the amount of heat delivered to be controlled on a space-by-space basis, taking into account the varying levels of heat gain and occupancy across the building. The building is in its pure buoyancy-driven mode. The top of the light well is sealed to prevent leakage of the warm buoyant air (Figure 4-9b).

Mid-season Mode

In mid-season, air is admitted via the low-level plenum and to provide the additional volumes of air needed for ventilation cooling, the top of the light well is opened. The same top- and bottom-venting strategy will be exploited to achieve purging of the unoccupied structure during summer nights. The light well top can be ventilated during the day to prevent the accumulation of solar heat gains (Figure 4-9c).

Summer Mode

In peak summer conditions, the windows and the ring of dampers above the cooling coils are open, allowing air to pass across the coils and directly into the light well. The chilled water in the cooling coils lowers the temperature of the air, which falls freely, under negative buoyancy, filling the light well. The air flows from the reservoir into each floor through conventional bottom-hung windows. These are controlled so that the desired amount of cooling is achieved. In cooling mode, the dampers between the plenum and the outside are tightly sealed to avoid leakage of cool air, which would prevent the light well from being filled up. The airflow across the floor plate to the rear of the building, and into the third and fourth floors at the front, will be assisted by injecting heat into the head of the stacks. Alternatively, at the rear of the building, dampers can be opened at the bottom of each stack (Figure 4-9d).

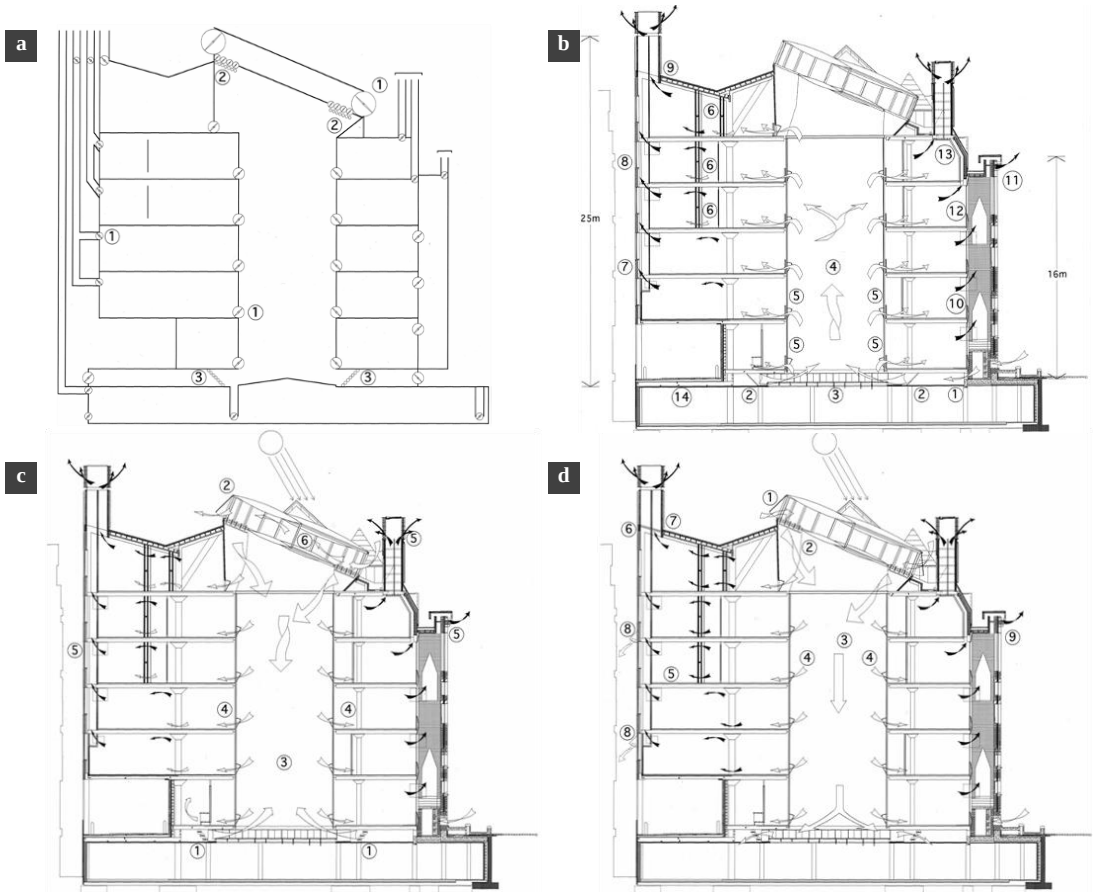

Figure 4-9 a) BMS controlled openings b) winter mode c) mid-season mode d) summer mode. Source (Lomas, Short, et al., 2004)

Building Performance

The results of a POE conducted in 2008 show that occupants generally have a fairly negative perception of the building which according to Short, Cook, & Lomas, (2009), can be attributed to the fact that the building was occupied early and underwent a prolonged commissioning period and difficulties. On the positive side, comparing the cooling energy consumption of the SSEES building with that of a typical A/C building (approx. 30kWh/m^2), a saving of 28kWh/m^2 is achieved by using downdraught cooling alone.

4.2.1.1.4 Office building in Seville

- *Location:* Seville, Spain. 37.37 °N – 5.98 °E.
- *Building Type:* Office building
- *Architect:* Brian Ford Associates
- *Building Services:* IESD
- *Number of storeys:* 5
- *Type of evaporator:* Misting nozzles
- *PHDC Strategy:* Enclosed Central atrium /s

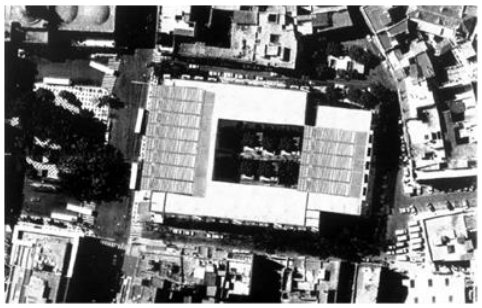

Figure 4-10 Office building in Seville. Source (Ford, 2001)

General

As part of the PDEC research project referred to above, detailed design studies for a speculative office building in Seville were performed by BFA (Ford et al., 2000). The proposed building deals simultaneously with the commercial requirements of the brief, the constraints of the urban site and geometrical implications of the PDEC strategy providing both open-plan and cellular office space without compromising the PDEC system. The design attempts to achieve an essentially deep plan office floor plate (overall width 27m) incorporating substantial (6m wide) light wells, which also serve as the transitional space through which evaporatively cooled air is distributed to each floor. The open shafts in the centre of the building are surrounded by open-plan offices, with cellular offices and meeting rooms around the perimeter (Figure 4-11)

Climate

Seville has a hot-summer Mediterranean climate (Köppen-Geiger climate classification Csa), with Semi-arid climate (BSh) influences (Kottek et al., 2006). The annual average temperature is 18.6 °C, which makes this city one of the

warmest in Europe. Winters are mild; January being the coolest month, with average maximum temperatures of 15.9 °C and minimum of 5.2 °C. Summers are very warm; July being the warmest month, with average maximum temperatures of 35.3 °C and minimum temperatures of 19.4 °C. Every year the temperature exceeds 40 °C on several occasions while the average number of days above 32°C is 88 and below 0°C is 6. The average morning relative humidity is 84%, while the average evening relative humidity is 46%.

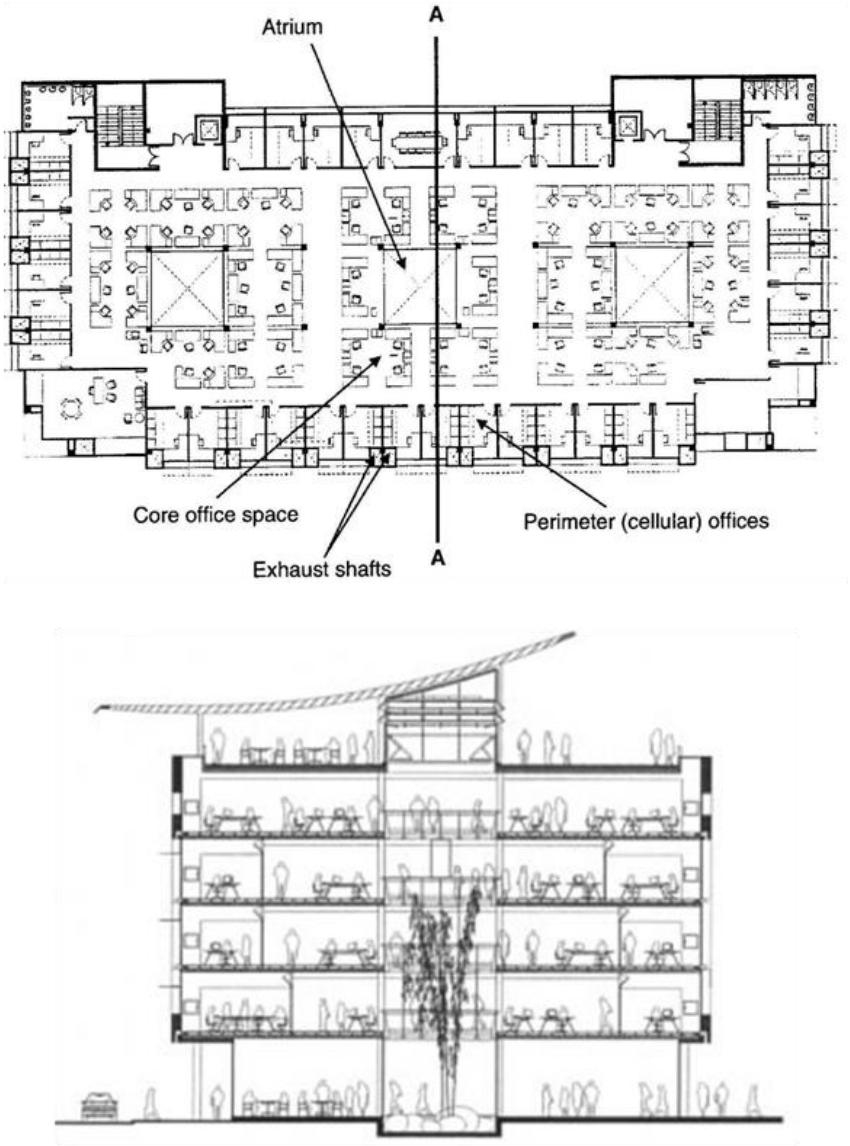

Figure 4-11 Typical plan (top) and cross section (bottom) of the Seville office building. Source (Ford, 2001)

Ventilation Concept

Air is introduced to the building at high level, where the concentration of pollutants is significantly lower than at street level. It is evaporatively cooled at the top of the lightwells and then enters the separate office floors. Exhaust air from open-plan offices passes through a bulkhead duct located in the perimeter cellular offices, and out via automatically controlled top hung ventilators into the perimeter shaft. These shafts, expressed fully in the Torrent building, are deliberately suppressed in the Seville office building, terminating in a relatively low continuous parapet. Part of the design task was to establish a threshold for the depth of plan and the degree of cellularisation which can be achieved using PDEC (Ford et al., 2000).

In summer the volume of supply air is controlled by glazed motorised louvers which respond to wind direction and ambient temperature. Distribution of air from core to perimeter employs two routes: either through a dedicated bulkhead direct to vertical shafts at the perimeter or via perimeter cellular offices Figure 4-11. Performance simulation using computational fluid dynamics has confirmed the viability of this strategy (Cook, Lomas, & Eppel, 1999b). Night-time convective cooling coupled with the mass of the building is part of the strategy for PDEC to be successful in the climate of Seville. This is achieved by encouraging flow reversal in both still and windy conditions. Control of louvers at high level is necessary to ensure negative pressure at the outlet.

Winter daytime ventilation is achieved via trickle vents located in the soffit of the cantilevered slab at each level. This detail provides protection from the prevailing wind and allows pre-heating if required. Stale air is exhausted via the

light-wells and high-level vent. Motorised louvers would be controlled to block the prevailing wind in winter in order to encourage air to exhaust on the leeward side.

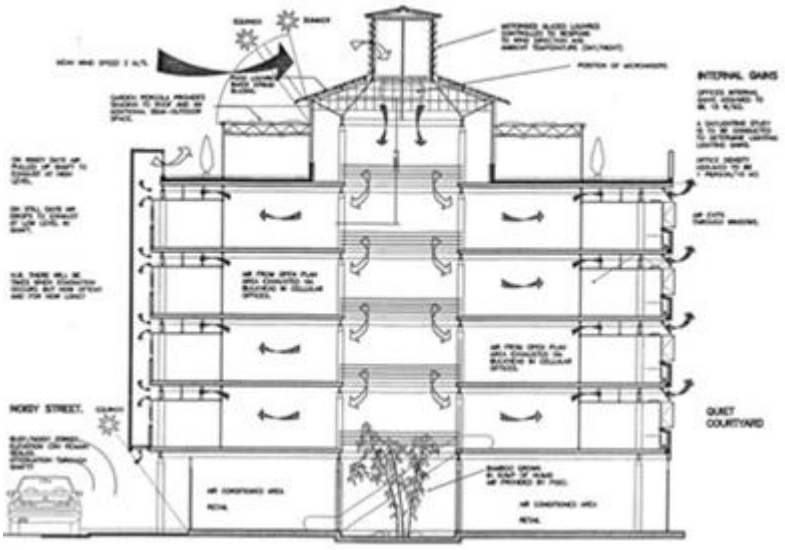

Figure 4-12 Summer day ventilation Concept. Source (Ford, 2001)

Building Performance

Performance analysis undertaken at De Montfort University revealed that for the Seville Office Building, the wet bulb temperature is sometimes too high to rely on evaporative cooling (Cook et al., 2000; Robinson et al., 2004). Mixed mode operation is therefore proposed for this office building to maintain internal air temperatures below 26°C. Nevertheless, simulation results indicate energy consumption approximately 75% below the air-conditioned reference building. Also, overall building costs have been estimated to be 6% below the air-conditioned reference building.

4.2.1.1.5 Office building in Catania

- *Location:* Catania, Italy. 37.5 °N – 15.1 °*E.*
- *Building Type:* Office building
- *Architect:* Mario Cucinella Architects
- *Total gross Floor area:* 4000 sqm.
- *Number of storeys:* 4
- *Type of Evaporator:* Misting Nozzles
- *PHDC Strategy:* Enclosed Central atrium/s

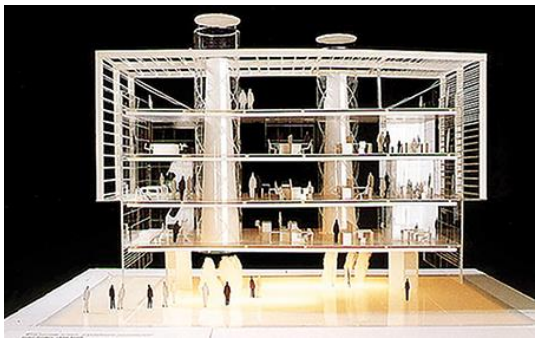

Figure 4-13 1:50 Scale model of the PDEC Catania office building.
Source (Francis, 2000)

General

In parallel with the design of the Seville office building, Mario Cucinella Architects designed a new office building for Catania, Sicily, as part of the same PDEC research project.

Despite being the final building to be demonstrated, the outcome of this project seems to be the most relevant to the study at hand. Not only does it provide a viable exemplary PDEC office building, the project has also provided a methodology for architectural research by exploring the potential of a scientific phenomenon through design. This is vital to the current enquiry as it presents a very similar stance to the one proposed and adopted by this study, that is, to develop a systematic approach to a technical problem combined with a creative architectural design process.

This project followed the construction and testing of a full-scale prototype experimental building. The performance of the experimental building was extensively monitored, and the data collected helped to inform the design of the new office building.

Climate

The climate in Catania is hot and dry in the summer months, although the wet bulb occasionally goes above 24ºC, reducing the time during the summer when evaporative cooling is effective.

Ventilation Concept

An initial proposal with a central atrium spanning the four-storey building presented difficulties in terms of efficiency and control of the air between the atrium and the office spaces. This is because a large volume of air needed to be cooled even at times when the cooling demand was low or varied between different office spaces. It was difficult to control the movement of air into the lower floor spaces and to achieve uniform air speeds across the office spaces. The atrium typology was also inefficient in terms of the construction costs and usable floor area thus decreasing the overall sustainability of the design.

Instead of having a central atrium and a volume of cooled air, the final proposal is comprised of a number of PDEC towers crossing the building vertically. In terms of cooling and air distribution, this strategy has the benefit of serving different areas of the building at different times depending on the actual needs of the occupants.

The project also investigated how the design of the towers could contribute to the uniformity of air velocity and temperature distribution throughout the office spaces. It was found that openings in the tower with a low aspect ratio (width over height) close to 0.1, reduced problems such as the direction of the air flow leaving the opening into the building, the differences existent between the top floors of the building and the bottom floors and the existence of reverse flow conditions.

Increasing the height of the tower further reduced the difference between the opening areas required at the different floors.

Furthermore, the project investigated the influence of layout configuration on internal conditions. The most efficient configuration was found to be (Francis, 2000):

- Exclusion of the effects of the wind so the air entering the towers is considered to be a zero velocity. A tower 5m high above the roof level allows complete evaporation of the water from the micronisers before the air enters the offices.
- Two towers with high level inlets and low-level outlets gave the best results in terms of temperature and air velocity distribution throughout the spaces.
- A layout with towers placed alternatively throughout the building floors at 6m centres and 27m wall to wall.
- A tower diameter of 3m.
- 200mm high uniform openings around the top of each tower.

Building Performance

A strategy for extra cooling and heating was defined to cover all the seasons and to establish the energy consumption over twelve months. The figures resulting from the simulation were encouraging as the overall energy consumption of this building was estimated to be 15% of that of a conventional building of the same size. Simulations also showed that the temperature and air speed were reasonably uniform throughout the office spaces.

4.2.1.2 Naturally Ventilated (NV) Tall Buildings

As mentioned previously, the posed problems highlighted in §4.2.1 related to the application of natural ventilation to high-rise buildings can theoretically have a number of solutions of which the most common are the use of internal resistances (small openings) and the use of segmentation, i.e. to divide a building into several segments that are isolated from one another by open spaces. Over the last decade, a number of prominent high-rise buildings have applied these solutions in practice. However, not all buildings are relevant to this study, and therefore, in order to narrow down the number of those to be reviewed, the selected buildings had to fulfil the following two criteria;

- That the building's delivery zones are connected to each other and to outside in terms of airflow via a central supply or exhaust path, i.e. a distribution or extract zone (connected spaces).
- That they present an innovative architectural or technical solution to a recurring problem associated with natural ventilation in high-rise buildings such as the variability of driving forces.

Accordingly, four buildings have been selected; The Deutsche Post Tower in Bonn, The Commerzbank in Frankfurt, The Liberty Tower of Meiji University in Tokyo, and The New Headquarters of the European Central Bank in Frankfurt. Following is a review of the selected high-rise buildings.

4.2.1.2.1 The Deutsche Post Tower

- *Location*: Bonn, Germany. 50.4°N - 7.1°E.
- *Year of Completion*: 2002
- *Architect*: Murphy Jahn
- *Building Services*: Matthias Schuler
- *Total gross floor area*: 107,000 sqm
- *Number of storeys*: 42



Figure 4-14 The Deutsche Post Tower. Source (www.jahn-us.com)

General

The design of the tower was the outcome of an open design competition which was held in 1997 for the new corporate headquarters of the Deutsche Post later named World Net (Wells, 2005). The building is crowned by an oval structure which is used as a conference centre. The three-storey annex building to the north of the tower houses conference rooms, the canteen, a postal retail outlet, a gallery, and an exhibition space (Wood & Salib, 2013b)

Climate

Bonn's climate is classified as mild and temperate (Cfb according to the Köppen-Geiger climate classification) (Kottek et al., 2006). The average annual temperature in Bonn is 10.0°C whilst rainfall averages 742 mm (Alexander Merkel, 2014). Summers have an average temperature of 17°C, while winters can feel cold with average temperatures of 4 °C. However, temperatures can drop down to -13.3°C and rise up to 33.4 °C. During the summer, the average diurnal range is approximately 11°C. Winds from the Southeast prevail during most of the year but are mostly from the East and West from April through to July.

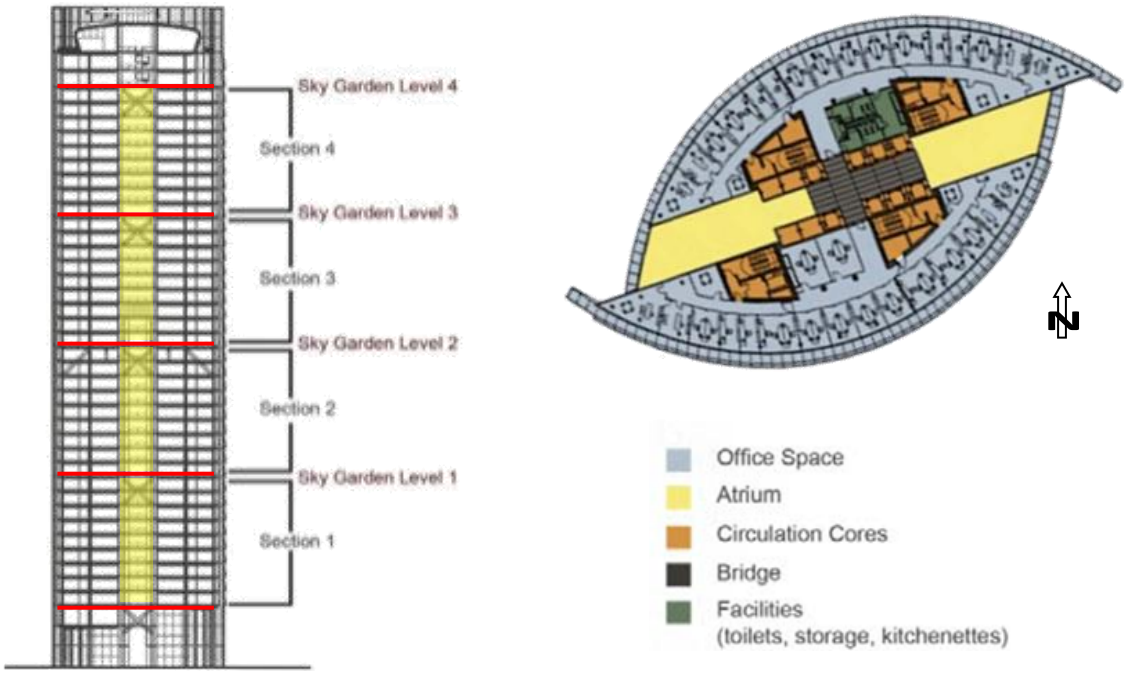

Figure 4-15 Cross section showing the segmentation (left) and typical floor plan (right). Source (Jahn, 2003)

Spatial configuration

The tower consists of two elliptical segments which are slightly offset and separated from each other by a 7.2m atrium which houses the circulation cores and the sky-gardens (Castillo, 2001). In each elliptical segment, the building mainly accommodates cellular offices around the perimeter, and conference rooms towards the centre. Vertically, the building is divided into four sections by means of nine-storey-high sky-gardens. The two elliptical halves of the tower are connected to each other by steel structured glazed bridges on every floor and translucent sky-garden platforms every nine floors.

Ventilation Strategy

A key component of the tower's natural ventilation concept is its double-skin façade which extends vertically and horizontally along the length of the façade

with horizontal divisions only existing at the levels of the sky gardens. The overall ventilation strategy relies on cross-ventilation where air enters the building through the double-skin façade, flows through the offices and into the corridors via the double-dividing glass walls of the offices (Figure 4-16a, b). The corridors act as exhaust air collectors, allowing spent air to pass into the nine-storey atrium via the raised floor grilles (Figure 4-16c). Finally, spent air is extracted through the windows and vents located on the topmost level of the atrium (Figure 4-16d).

Summer mode

In summer, the moveable flaps of the outer skin are opened to the maximum to ensure sufficient airflow within the air cavity. The vertical continuity of the DSF allows the stack effect to draw heat off at high levels reducing the risk of overheating. The airflow then follows the same route as described above until it is exhausted via the sky-garden vents. However, during extreme high temperatures, a mechanical displacement system consisting of decentralized air supply units serves to cool the incoming air along the perimeter of the building. The air supply units have perimeter convectors and air intake fan coils to drive the pre-cooled air into the office spaces via the floor grilles. Additionally, the floor slabs of the Deutsche Post tower are equipped with radiant thermal regulators consisting of cast-iron water pipes which draw relatively colder groundwater from the nearby Rhine River. Cooling is achieved by allowing the whole slab to act as a thermal radiator to the surrounding spaces (Figure 4-17). Due to the high thermal capacity of concrete, the exposed building components (floors, ceilings, walls) absorb and store a large amount of heat energy during the day. Consequently, night ventilation is used to cool the building structure at night,

allowing it to release the heat energy accumulated throughout the day. This helps in regulating the internal temperatures and reducing the cooling loads during the summer. Cool night air is allowed to flow into the building via the double-skin façades and is channelled across the slabs to remove excess summer heat.

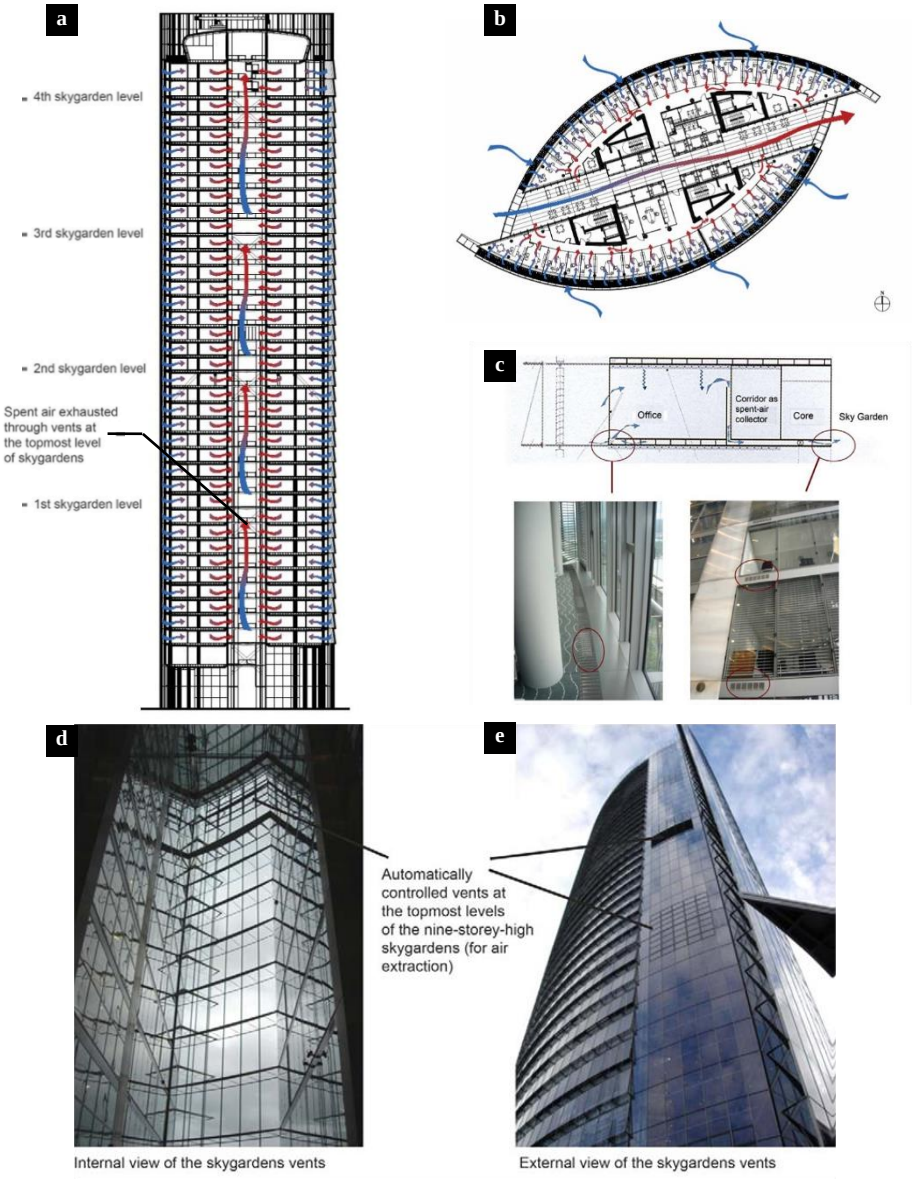

Figure 4-16 a) Ventilation concept in section b) Ventilation concept in plan (Wood & Salib, 2013b) c) Exhaust of air from the offices to the atrium via raised floor grilles (Jahn, 2003) d) Automatically controlled vents at the top of the atrium (Salib, 2008)

Winter mode

During winter, the moveable flaps of the outer skin are closed down to a minimum, allowing the façade's intermediate space to act as a thermal buffer to reduce heat loss.

At extreme cold temperatures, the perimeter mechanical displacement system is turned on and the air is preheated before being allowed to enter the spaces. Additionally, water running through the water-pipes embedded in the floor slabs is heated to provide additional radiant space heating (Figure 4-17).

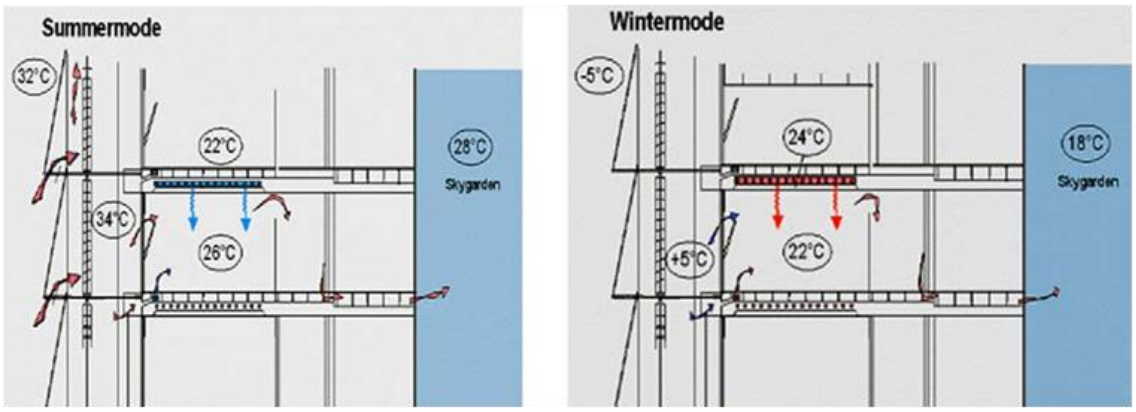

Figure 4-17 Extreme summer and winter modes of operation. Source (Salib, 2008)

Characteristic design feature

The central and most significant design feature of the Deutsche Post tower is the use of segmentation. Airflow in the tower benefits from the stack effect caused by the height of the atria. However, the building is segmented so as to overcome the problem of high-pressure differences in the lower levels and discrepancies in magnitude between the driving forces along the height of the tower which would have otherwise occurred had the atrium been continuous throughout the building height.

4.2.1.2.2 The Commerzbank

- *Location*: Frankfurt, Germany. 50.1°N – 8.6°E.
- *Year of Completion*: 1997
- *Architect*: Foster and Partners
- *Building Services*: Pettersson & Ahrens Ingenieur-Planung GmbH
- *Total gross floor area*: 121,000 sqm
- *Number of storeys*: 56



Figure 4-18 The Commerzbank Headquarters Building. Source (www.fosterandpartners.com)

General

This building is the result of a limited international competition held in 1991 for the design of the new headquarters of the Commerzbank to be erected adjacent to the existing office tower in the financial quarter of Frankfurt, between the main train station and the historic centre. The new building was to be ecologically oriented, through energy conservation, operability and flexibility in workspace, and present a positive corporate image.

Climate

The city of Frankfurt has a temperate continental climate characterised by warm summers with occasional wet days, and cold winters. Temperatures are not extreme and never severe, but winters can bring occasional violent storms. The average annual temperature in Frankfurt is 10 °C fluctuating between an average minimum of 6 °C during the coldest months (November to February) and an average maximum of 14 °C during the hottest months (May-August). The

average annual wind speed in Frankfurt is 4.2 m/s with prevailing winds typically coming from the southwest.

Spatial configuration

The overall shape of the building is triangular in plan with three main arms of office floors surrounding a central triangular atrium that runs along the whole height of the building and separated every 12 storeys by glazed decks. Services and circulation cores are located at each corner of this triangle and also act as the vertical load support for the entire structure leaving an open, column-free space for the offices. The shallow office floor plates, only 16.5m deep, have either an open-plan or a double loaded configuration. In the latter, the offices on the interior have access to daylight and clean air provided by sky-gardens which are four storey tall interior plantings completely open to the central atrium. There is a total of nine sky gardens, three on each elevation, spiralling around the tower (Figure 4-19).

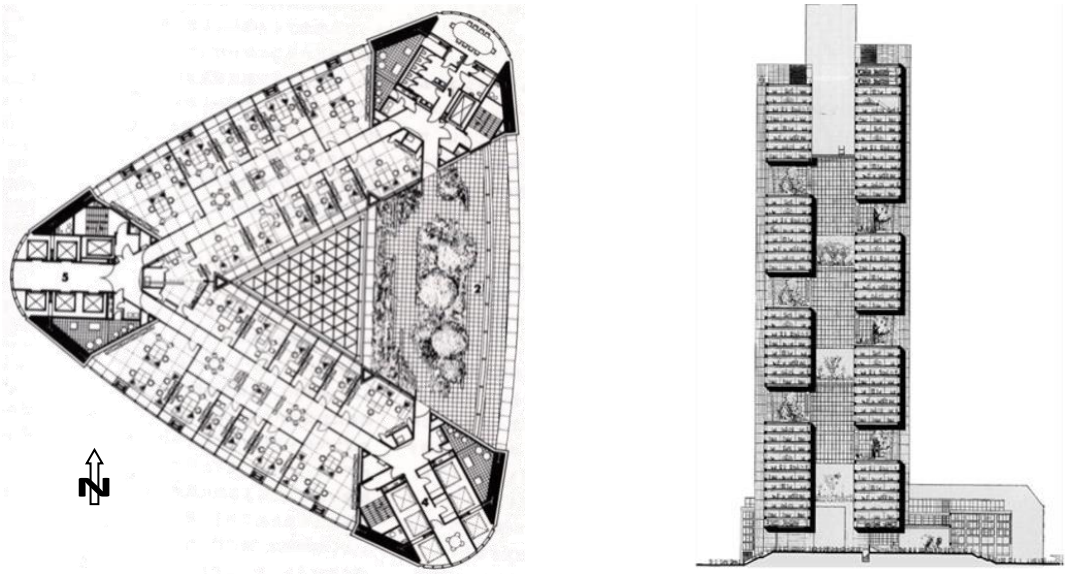

Figure 4-19: Plan and section of the Commerzbank. Source (Buchanan, 1998)

Ventilation Strategy

Natural ventilation in the Commerzbank occurs at multiple scales ranging from individual rooms to several building storeys. The atrium is segmented by glass decks into four 12-storey segments to overcome the powerful up-draught of air that would otherwise occur due to the tower's height. Each segment consists of three deliberately positioned sky gardens (Figure 4-20). The ventilation strategy adopted varies depending on the office layout configuration. In an open plan configuration cross ventilation occurs between the external façade and the atrium façade while in a double-loaded configuration, offices on both sides of the corridor are ventilated using a single-sided ventilation strategy assisted by the stack effect generated by the atrium or the external façade system.

For offices facing inwards, stale air is exhausted to the main atrium space which then rises and is exhausted out of the building through operable panels in the topmost garden of the 12-storey segment. As for the offices on the exterior face, a double layered cladding system is used to enhance natural ventilation as well as sun shading. This system consists of a 165mm ventilation shaft running the entire face of the tower enclosed to the exterior by a single-glazed wall acting as a rain screen, and to the interior by a double-glazed wall. This system allows for ventilation on the scale of the office just as the sky gardens provide ventilation for the entire building. Fresh air enters the cavity through aluminium transoms in this exterior wall, which are located above and below the clear view glazing of the interior wall. The air enters the bottom transom, and by convection is pulled out at the top along with the stale, hot air venting from the open interior wall.

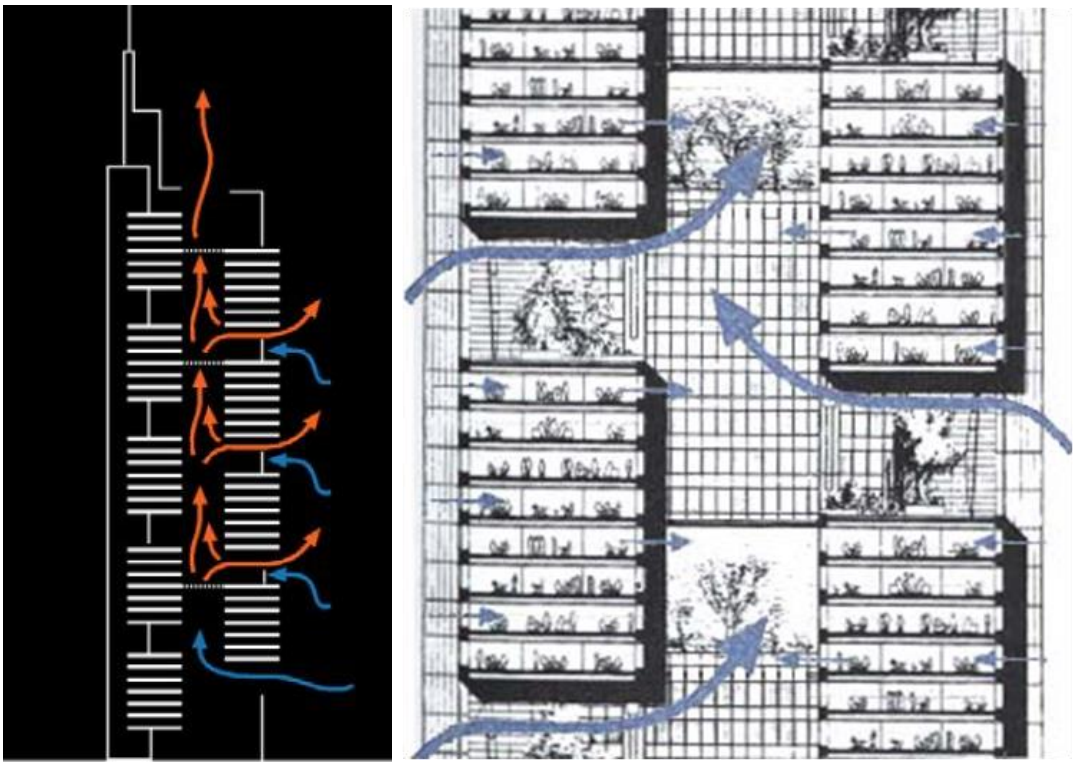

Figure 4-20: Ventilation on the level of the sky-gardens and atrium.
Source (Buchanan, 1998)

Summer mode

In summer, the bottom-hung windows located on the inner wall of the double skin façade tilt open 30 cm to ventilate the offices on the exterior face, and immediately, cooler air as well as a slight breeze is felt in the office (Figure 4-21a). To provide additional cooling for offices facing the atrium, the panels in the lowest garden of the segment are opened, to allow cool fresh air to be drawn in (Figure 4-21c). When passive cooling and ventilation are not effective, the windows are closed and a mechanical ventilation system is turned on to provide fresh air while chilled water panel ceilings are used to cool the space (Figure 4-21b). During unoccupied hours, windows can be left open to allow the night air to flush out the hot air of the building, thus saving energy used by the chillers as well as the mechanical system.

Winter mode

In winter, the bottom-hung windows are open to a minimum to provide fresh air. The panels of the topmost garden of the segment are also left open while those of the middle and lower gardens are kept closed (Figure 4-21d). During extreme cold conditions, the office windows are closed and the mechanical system takes over to provide ventilation while heat is provided through conventional radiators located at the sides of the windows (Figure 4-21b).

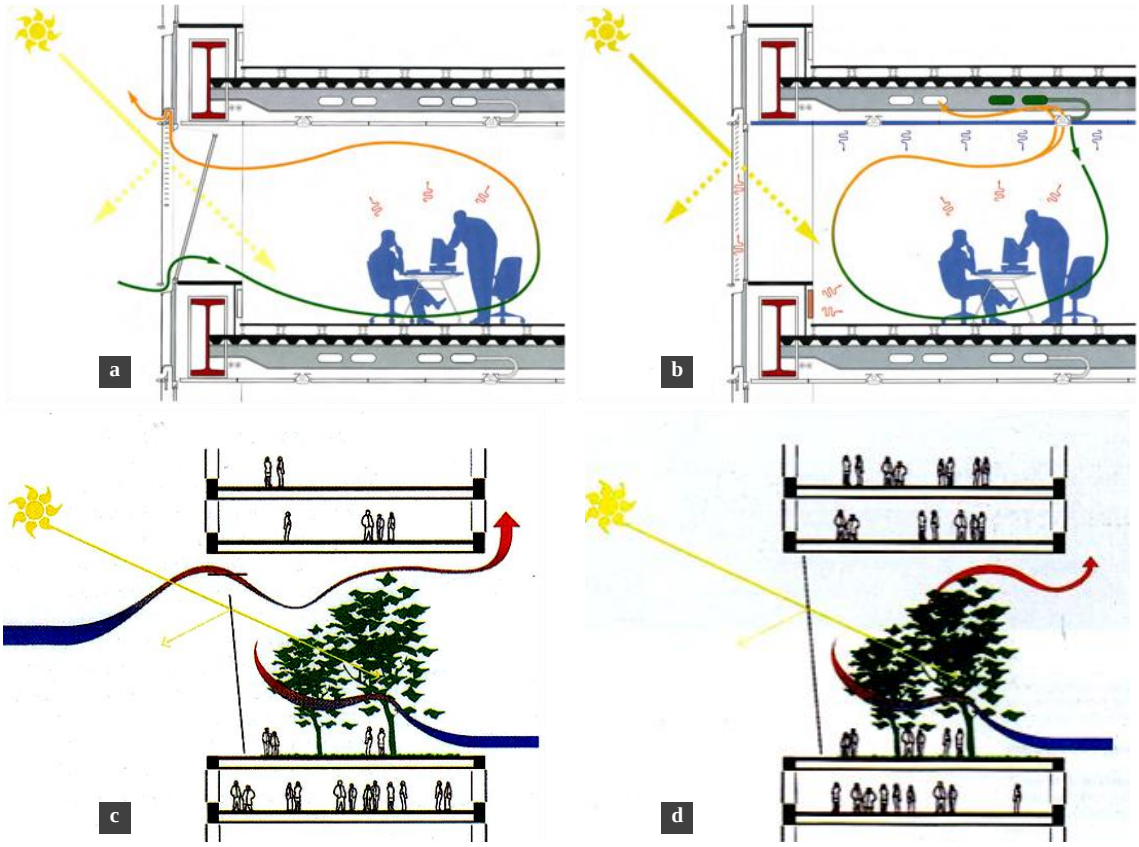

Figure 4-21: Modes of operation in offices and sky-gardens a) office ventilation in natural mode b) office ventilation in mechanical mode c) sky-garden ventilation in summer d) sky-garden ventilation in winter. Source (Davey, 1997)

Characteristic design feature

As with the Deutsche Post Tower, the sky-gardens have proven to be a vital element in the design of the Commerzbank Tower. Not only do they assist in the natural ventilation strategy, but also provide mass quantities of natural light directly to the centre of the building from top to base giving offices facing the atrium access to daylight and exterior views through the gardens. Finally, the garden spaces provide a high-quality microenvironment to the interior tower offices, with air quality equal to or even better than ambient city air quality due to the purification effect of the plants creating a much greener, natural, meeting place for those working in the building.

4.2.1.2.3 The Liberty Tower of Meiji University

- *Location*: Tokyo, Japan. 35.7 °N – 139.7 °E.
- *Year of Completion*: 1998
- *Building Type*: Educational
- *Architect*: Nikken Sekkei Ltd.
- *Building Services*: Nikken Sekkei Ltd.
- *Total gross floor area*: 59,000 sqm
- *Number of storeys*: 23



Figure 4-22 The Liberty Tower of Meiji University. Source (Chikamoto et al., 1999)

General

Located in the centre of the Tokyo Metropolitan area, this building introduces the hybrid air-conditioning (cooling) system utilizing natural ventilation for controlling the indoor climate in temperate seasons especially to rooms with high occupational densities and high internal loads caused by computers, such as lecture rooms.

Climate

Tokyo has a Humid Subtropical Climate zone (Köppen-Geiger climate classification Cfa) (Kottek et al., 2006), with hot humid summers and generally mild winters with cool spells. The annual average mean temperature is 15.9 °C. Winters are mild; January being the coolest month, with average maximum temperatures of 9.8 °C and minimum of 5.8 °C. Summers are very warm; August being the warmest month, with average maximum temperatures of 30.8 °C and minimum temperatures of 24.2 °C. The prevailing wind direction is Northeast/North with an annual average speed of 2.6 m/s.

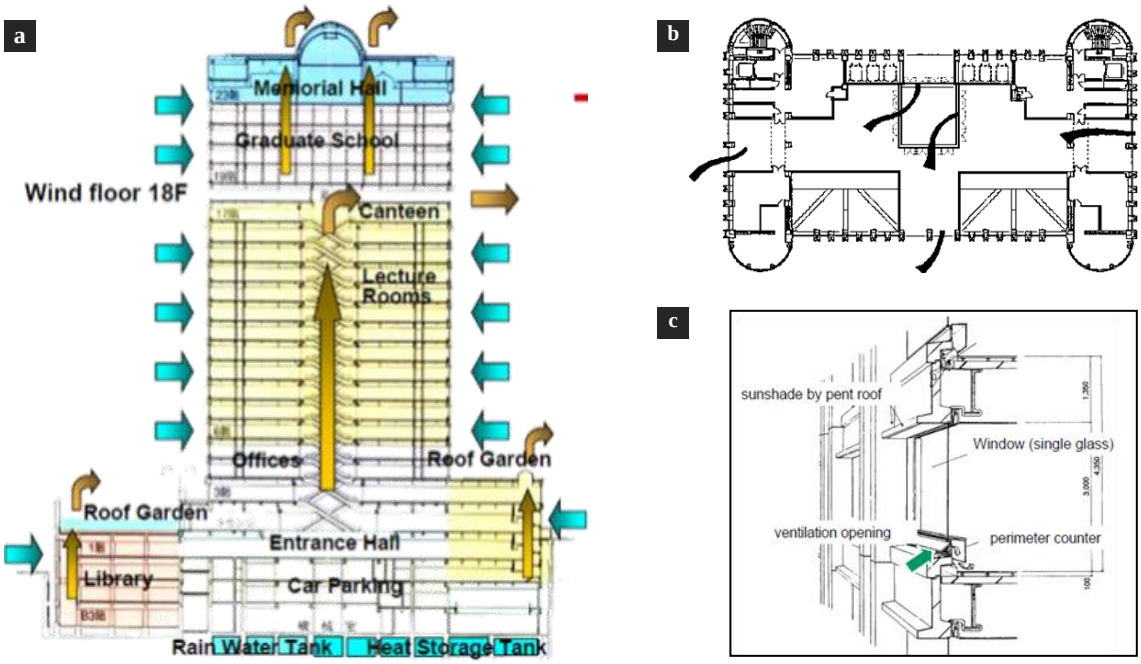

Figure 4-23: a) Ventilation concept in section b) Ventilation concept in plan c) Perimeter counter units. Source (Chikamoto et al., 1999)

Ventilation Strategy

During mid-seasons, the stack effect caused by the central void (wind-core), which is basically the escalator space between the 1st and 17th floor (Figure 4-23a), is used to draw stale air from the surrounding spaces which is in turn replaced by fresh air entering via dedicated intake perimeter counter units on each floor (Figure 4-23c). The rising stale air is exhausted at the top of the wind-core which terminates on the 18th floor (wind-floor) where it exits the building via 4 designated wind paths located on the 4 different façades (Figure 4-23b). When the external temperatures rise or fall beyond a certain limit and natural ventilation does not suffice, the perimeter openings are closed and an alternative air-conditioning system is used to deliver comfort conditions (Chikamoto et al., 1999).

Characteristic design feature

One characteristic design feature of this building's ventilation strategy is the wind-floor located on the 18th floor. External air passing through this wind-floor utilises the Venturi effect to create a suction force that further promotes the wind-core's stack effect. CFD simulations have shown that wind enters the wind-floor without any decrease in speed (Figure 4-23a). Moreover, as previously mentioned, air leaving the wind-core is exhausted via four designated wind paths located on four different façades. The wind floor is intentionally open to these four different directions in order to stabilise the driving forces irrespective of wind direction. Another design feature employed in the wind-floor is the use of wind fences located near the exits atop of the wind-core to prevent outdoor air passing through the wind-floor from disturbing the smooth exhaust of air (Figure 4-23b).

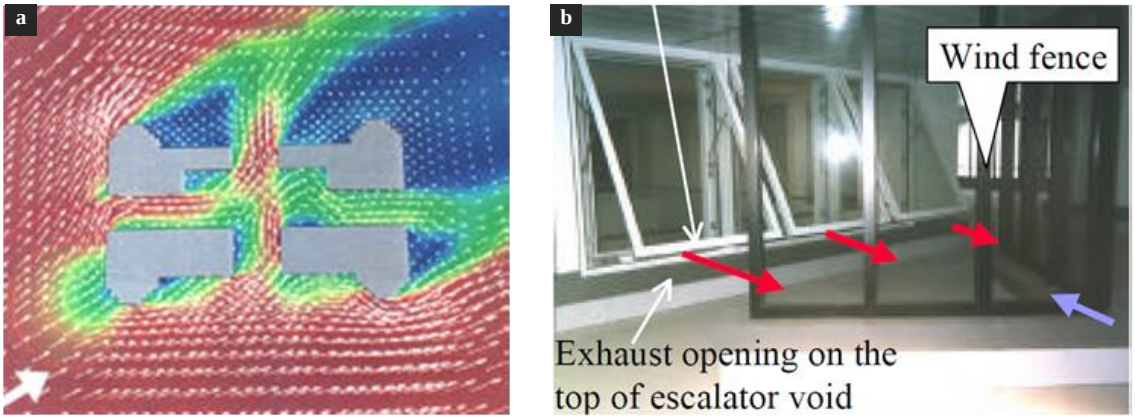

Figure 4-24: a) CFD simulation of the wind floor b) Wind fences.
Source (Chikamoto et al., 1999)

4.2.1.2.4 The New European Central Bank Headquarters (ECB)

- *Location*: Frankfurt, Germany, 50.1°N – 8.6°E.
- *Year of Completion*: 2014
- *Building Type*: Office Building
- *Architect*: Coop Himmelblau
- *Building Services*: Brian Cody - Arup
- *Total gross floor area*: 120,000 sqm
- *Number of storeys*: 45



Figure 4-25 The New European Central Bank Headquarters (ECB).
Source (www.coop-himmelblau.at)

General

This building is a result of an international competition held in 1999 to house offices of the ECB staff currently located in three separate buildings in Frankfurt. The building is approximately 185 meters tall accompanied by other secondary buildings on a landscaped site on the site of the former wholesale market in the eastern part of Frankfurt.

Climate

The city of Frankfurt has a temperate continental climate characterised by warm summers with occasional wet days, and cold winters. Temperatures are not extreme and never severe, but winters can bring occasional violent storms. The average annual temperature in Frankfurt is 10 °C fluctuating between an average minimum of 6 °C during the coldest months (November to February) and an average maximum of 14 °C during the hottest months (May - August). The average annual wind speed in Frankfurt is 4.2 m/s with prevailing winds typically coming from the south/southwest.

Ventilation Strategy

The form of the ECB building is optimised to employ wind, thermal, and solar power to provide controlled natural ventilation of the offices. The building is comprised of two optimally orientated towers with their main façades facing north/south positioned on the site so that an effective shading of the first tower is provided by the second. An additional skin is wrapped around the two towers to create a central atrium and the double-skin façades on the external sides (Figure 4-26a). In contrast to the ventilation strategy employed in the Deutsche Post Tower, air flows from outside into the atrium and from there across the office floors before leaving the office spaces on the external sides of the towers, thus ensuring effective cross ventilation of the office floors. The double façade on the external sides of the towers also acts as a solar thermal exhaust flue. The less dense warmer air rises up through the flue and is replaced by cooler heavier air flowing through the office floors (Figure 4-26b). On account of the height of the building, the façade is vertically divided by horizontal separators into 3 sections with a height of approximately 50m each, in order to keep the pressure differences between floors manageable (Figure 4-26c).

Characteristic design feature

The characteristic design feature in this building is the tower's form itself. The atrium façades are designed to act as wind scoops to channel wind into the atrium. In the external façades of the office towers the negative pressure at the specially designed "suction gaps" ensures that the used air is drawn out of the building independent of wind direction (Figure 4-27a). Dampers in the external skin of the atrium and office façades are operated to control the pressure

difference acting across the office floors and so regulate the natural ventilation of the offices. Due to the special design of the suction gap elements in the external façades of the office towers the pressure coefficient at the air exhaust points is always lower than the pressure coefficient at the air inlet points on the atrium façade regardless of wind direction (Figure 4-27b). In contrast to the high-rise buildings using natural ventilation built thus far this concept eliminates the need for mechanical ventilation in the office spaces completely and thus offers enormous advantages in capital cost and grey energy terms (mechanical systems, plant rooms, shafts) as well as energy savings and maintenance costs.

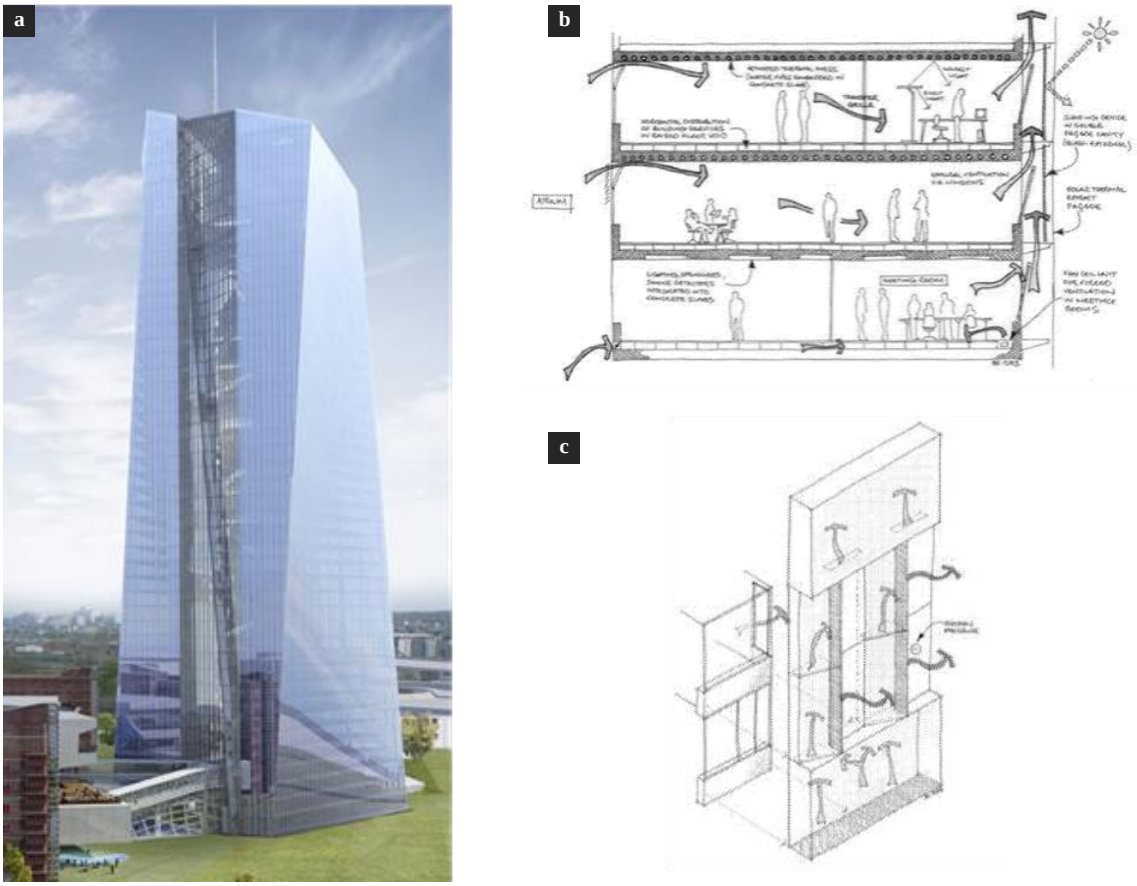

Figure 4-26: a) A double skin façade is wrapped around the two buildings to create a linear atrium between them b) ventilation concept of offices c) the double skin acts as a thermal stack that extracts air from the offices. Source (Cody, 2008)

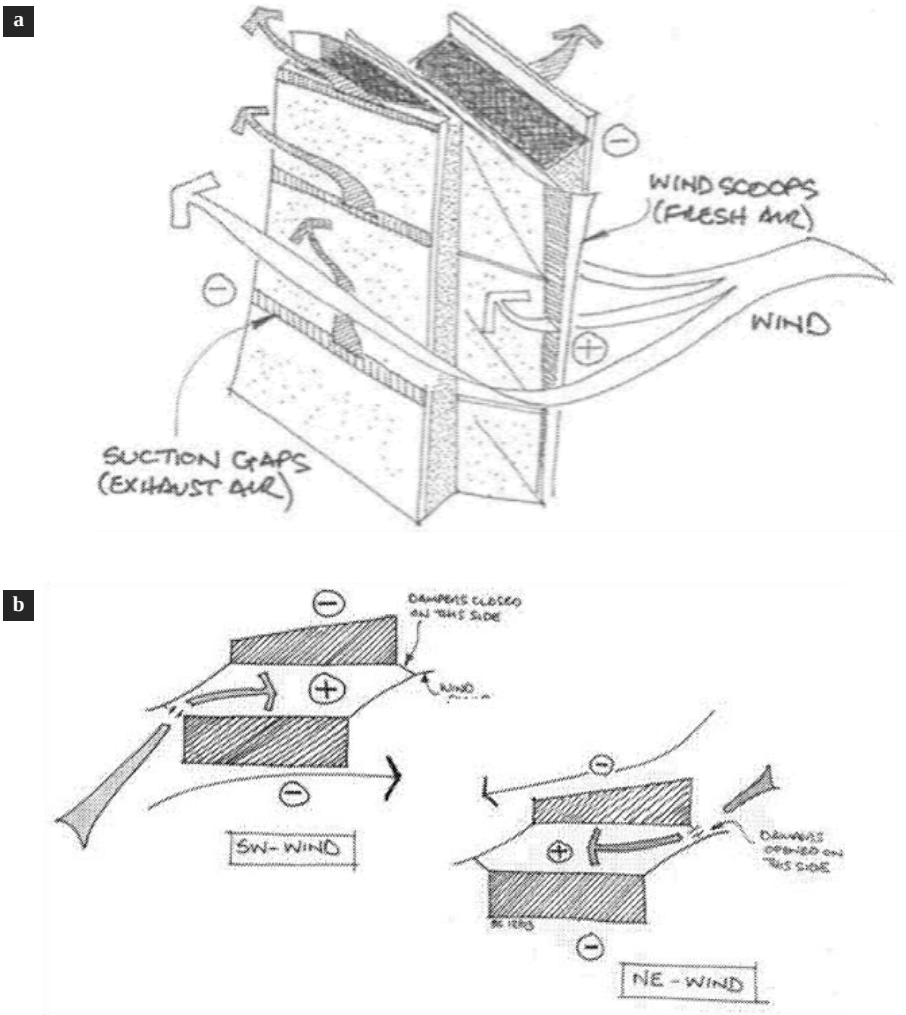

Figure 4-27: The form of the building is designed to create areas of high and low pressures at the inlets and outlets respectively. Source (Cody, 2008)

4.2.2 Application of PDEC to office buildings

For this study to fully benefit from the review, the buildings have to be further analysed in order to highlight common features (if present) and characteristic design features. The analysis is performed on three different levels as follows:

4.2.2.1 Ventilation Concept

Ventilation strategy:

All buildings adopt a buoyancy-driven stack ventilation strategy, where a downdraught is generated by the negative buoyancy of air which is cooled either by evaporation or by active components such as chilled water pipes at the top of the supply zone before being distributed to the occupied spaces. This downdraught of relatively cold air is then introduced to the adjacent spaces (delivery zone) replacing the warm stale air which is extracted by the exhaust zone before leaving the building.

It has to be noted that in all buildings, the two processes of cooling and distribution take place in the supply zone, i.e. the inlet and distribution zones are both housed in one single space (supply zone). However, in the SSEES, a separate inlet zone exists (an air plenum in this case) which only functions in certain modes of operation.

Flow direction:

Apart from the IGP, the horizontal flow direction in the reviewed buildings is centre-in edge-out (C-E), where incoming air enters through the supply zone located at the centre of the building, passes through the delivery zone and

then leaves the building via the exhaust zone located at the building's perimeter. However, in the IGP, multiple flow directions co-exist at the same time such as (C-E) and (E-C). As for the vertical flow direction, it has to be noted that, although the supply direction in all buildings when operating in cooling mode is downwards, the exhaust flow direction differs depending on the relation between internal and external temperatures. In temperate climates such as London, where internal temperatures are usually higher than external ones, the exhaust flow direction is upwards, whereas in hot climates such as India and southern Europe, daytime external temperatures usually exceed internal ones and so the exhaust flow direction is downwards.

Ventilation principle:

The ventilation principle adopted in most of the buildings is that of displacement ventilation wherein air is introduced to the delivery zone from bottom inlets displacing warm used air inside the space upwards to be exhausted from a top located outlet.

Modes of Operation

In addition to adopting basic principles of bioclimatic design to minimise solar gains such as the proper orientation of the building and the use of solar shading, all the reviewed buildings are designed to operate in different ventilation modes depending on the time of day and year. At out-of-work hours when external temperatures drop, the buildings are flushed with outdoor air cooling down the structure which has stored heat throughout the course of the previous day. In this mode, the flow direction changes from

(C-E) to (E-C) whereby the supply and exhaust zones reverse functions. This strategy is central to the success of the downdraught cooling strategy.

4.2.2.2 Spatial Configuration

Although all selected buildings generally have a similar ventilation concept, nevertheless, they can be divided into two distinct categories owing to the configuration of the supply zone within the building (Figure 4-28):

- The *Single-atrium or concourse* type where the supply zone is one single space centred within the building and surrounded by the delivery zone. This type is represented by the TRC and the SSEES
- The *Multi-tower or shaft* type where a number of supply zones are *distributed* within the delivery zone. This type is represented by the IGP, the Seville office building, and the Catania office building.

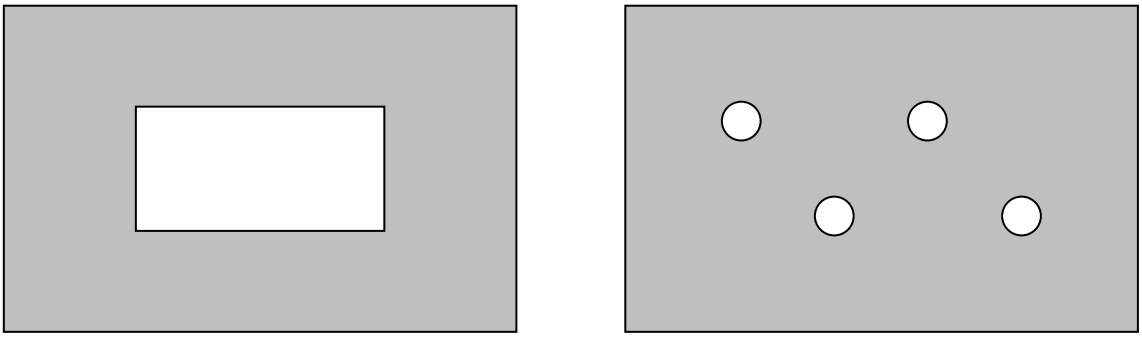

Single-atrium or concourse *Multi-tower or shaft*

Figure 4-28: The two different types of PDEC/PHDC buildings

Both categories have their relative advantages and drawbacks. These have been investigated in the Catania project and are summarised as follows (Francis, 2000):

- The multi-tower type combines and exploits the concepts of evaporative cooling with the downdraught effect making it more efficient in terms of resources and cooling power than the single-atrium type which relies on creating a cold-air reservoir that necessitates a large volume of air to be cooled even at times when cooling demands are low.
- The multi-tower type provides more flexibility by allowing different areas of the building to be cooled at different times to satisfy actual needs.
- In the multi-tower type, each individual tower can be defined to provide the cooling power required by the area it serves only. Moreover, the evaporation system in each tower can be controlled to meet the varying cooling requirements of this area.
- The building management system in the multi-tower type can be more accurate owing to the increased sensitivity of the system.
- Natural light in the multi-tower type can be evenly distributed allowing an increase in the floor depth without reducing comfort.
- In the multi-tower type, it is possible for the PDEC towers to have a double function by providing structural support together with the façade columns leaving the plan free from columns which allows for more flexibility in terms of internal layouts.
- The single-atrium type however, offers savings in initial costs since all system components are located in one central place.

The previous points indicate that the *multi-tower* type has advantage over the *single-atrium* type in terms of performance, energy-efficiency, controllability, and architectural quality which can be attributed to the fact that for a given

distribution zone area (lightwell area) the former type offers better distribution than the latter. However, the *multi-tower* type can be seen as a number of connected *single-atrium* configurations and as such can be described in terms of the latter. Moreover, since the *single-atrium* type cannot be further abstracted, accordingly, it will be taken to represent the basic morphology of the PDEC building upon which the initial model will be based.

4.2.2.3 Critical design considerations

Having reviewed and analysed the ventilation concept and spatial configuration of PDEC/PHDC buildings, the following design considerations have been inferred and should be taken into consideration when developing the initial model;

1- The air inlet is located at the top of the building above the distribution zone and should not be obstructed. This zone together with the evaporation zone should extend above the upper floor by a distance sufficient to guarantee the full evaporation of water and generate a driving force that would draw the air into the upper floor of the building. According to the studies performed in the Catania project, this distance should not fall below 6 meters (Francis, 2000).

2- Similarly, since used air leaving the delivery zone is usually exhausted downwards, the outlet zone should extend below the building's lower floor.

3- Air inlets and outlets should preferably be inured to the effects of wind. However, should that prove to be difficult, it is best that inlets be located

at areas of high-pressure coefficients while outlets at areas of low-pressure coefficients. Furthermore, wind baffles are added to the exhausts to ensure that the flow through the outlet zone is unidirectional from inside to outside.

4- The system should be designed to allow for the reversal of flow direction in different modes of operation.

5- Any given point in the delivery zone should be located between a distribution and extract zone to generate a cross flow.

6- The number of floors that can be served by a single distribution zone is limited, and thus needs to be accurately established.

4.2.3 Application of Natural Ventialtion to high-rise office buildings

A building precedent study of four buildings was performed. The building precedent study demonstrated how each building with its corresponding ventilation concept was designed to overcome the problems associated with the natural ventilation of high-rise buildings raised. However, for this study to fully benefit from the review, the buildings have to be further analysed in order to highlight any common features (if present) and characteristic design features. The analysis is performed on three different levels as follows:

4.2.3.1 Spatial Configuration

Although it might not seem apparent from the preliminary review, all the selected buildings share the same basic configuration where a central void (either a distribution or extract zone depending on the flow direction) is

surrounded by the occupied spaces (delivery zone) while also being connected to the external façade. However, it is the degree or frequency of this connection along the height of the building together with the path that air follows between the external envelope and the distribution zone, i.e. the inlet/outlet zone, which varies from one building to another. This ranges from a single connection on one floor only via an outlet zone as is the case with the wind floor in the Liberty Tower, to a full connection over the course of the building's height where the inlet/outlet and the supply/extract zones are the same as is the case with the Deutsche Post and the ECB. However, in the Commerzbank, although in terms of frequency, the atrium is connected to the external façade every single floor, an inlet/outlet zone is created due to the rotation of the sky-gardens on the different façades of the building.

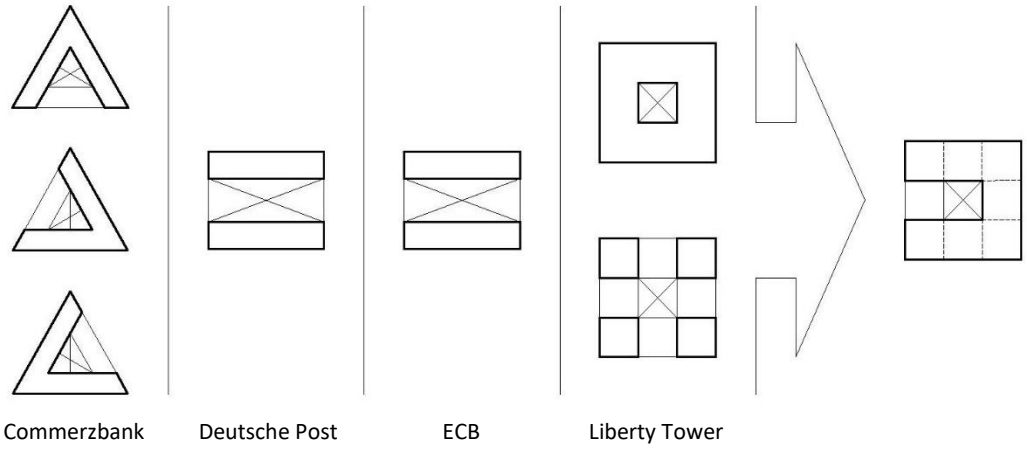

Figure 4-29: The four reviewed buildings have a similar configuration

4.2.3.2 Ventilation Concept

All buildings share the same ventilation concept of buoyancy driven stack ventilation generated either by the central atrium or DSF assisted by wind forces acting on the external envelope. However, an important distinction

between the selected buildings can be made relative to the flow direction. Accordingly, the reviewed buildings can be classified into two categories in terms of airflow direction:

- *Edge in – Centre out* (E-C) represented by the Commerzbank, the Deutsche Post and the Liberty Tower where the supply zone on both buildings is located at the building's perimeter (DSF) while the extract zone is located at the centre (atrium).
- *Centre in – Edge out* (C-E) represented by the ECB where the supply zone is located at the building's centre (atrium) while the extract zone is located at the perimeter (DSF).

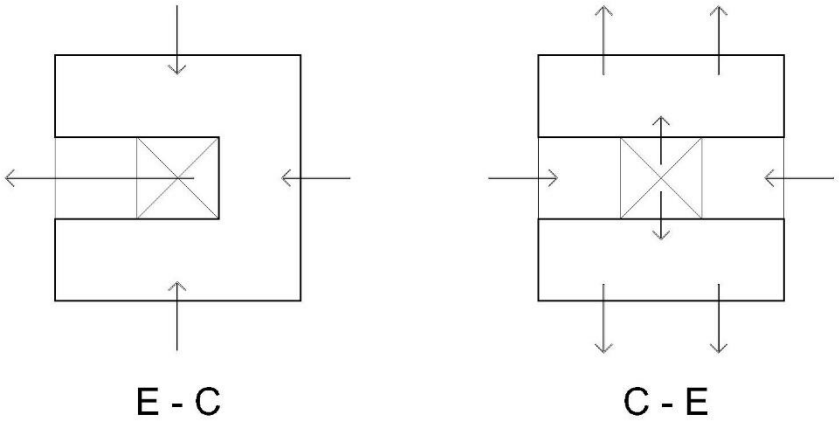

Figure 4-30: Flow Directions in the high-rise towers

4.2.3.3 Characteristic Design Feature

By analysing the selected buildings, it is noticeable that they all share three characteristic design features rendering them fundamental to natural ventilation in high-rise buildings;

Segmentation: The Liberty tower aside, all reviewed buildings have adopted the segmentation strategy to overcome the problem of discrepancies in airflow rates that would otherwise occur between the upper and lower floors due to the considerable stack height.

Orientation of inlet and outlet zones: To overcome the problem of variability in wind direction, the openings connecting the atrium of the four buildings to the external façade are directed towards at least two different orientations. This is the case in the Deutsche Post tower and the ECB where the atrium is open to two opposite orientations, while in the Commerzbank, the atrium is connected to three different facades, and four in the Liberty tower. It is interesting to notice that in the Commerzbank, all the inlet openings (lower sky-garden in a segment) are located on the same façade while the outlet openings (upper sky-garden) are all located on another. This allows for the possibility of inlets to be directed windward and outlets leeward.

Double envelope: to overcome the problems of noise and discomfort associated with high wind speeds likely to be experienced in high-rise buildings, the selected examples have employed double skin façades which also act as a thermal buffer between the internal and external environments and in some cases as an extract and outlet zone.

There are also design features that are unique to a building or two of which the form of the tower in the case of the ECB and the Deutsche Post is a good example. The ECB form is designed to create areas of high pressure at the atria's inlet zones and low pressure at the suction gaps where used air is

exhausted from the building. Moreover, the dual curvature in the form of the Deutsche Post tower lends itself well to aerodynamics by allowing for air to move more freely from the windward to the leeward side of the building on each floor assisted by the horizontal continuity of the double-skin façade cavity (due to the absence of vertical partitions) which helps in dissipating the pressure differences across the faces of the building.

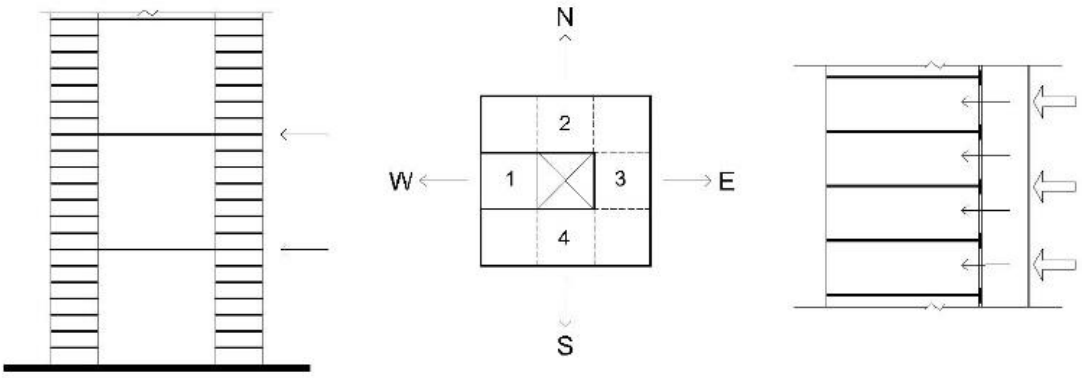

Segmentation Orientation of inlet/outlet Double envelope

Figure 4-31: Design considerations in High-rise buildings

4.2.4 Developing the PDEC multi-storey office building prototype

To perform the required analysis, a preliminary model of the PDEC high-rise office building had to be developed. The proposed model had a square shaped floor plan of a typical high-rise office building with a central atrium replacing the central core. The model was vertically divided into isolated segments (in terms of airflow) each comprising the same number of floors. However, the model was further modified into a more generic form.

The floor plan of each segment (Figure 4-32a) is rectangular in shape with two 12m deep floor plates separated by an atrium running along the length of the

building. The external envelope on either side of the floor plates opposite the atrium consists of a ventilated double-skin facade (DSF). To guarantee the full evaporation of water and potentially achieve the required flow rates in the upper floor of each segment, the atrium is allowed to extend above the segment's upper floor whilst the DSF is also allowed to extend below the segments lower floor to increase the stack height between the lower floor and the outlet (Figure 4-32b). The height of the atrium's and DSF's extension beyond the segments upper and lower floors respectively will be discussed later. This configuration is intended to induce two different flow patterns;

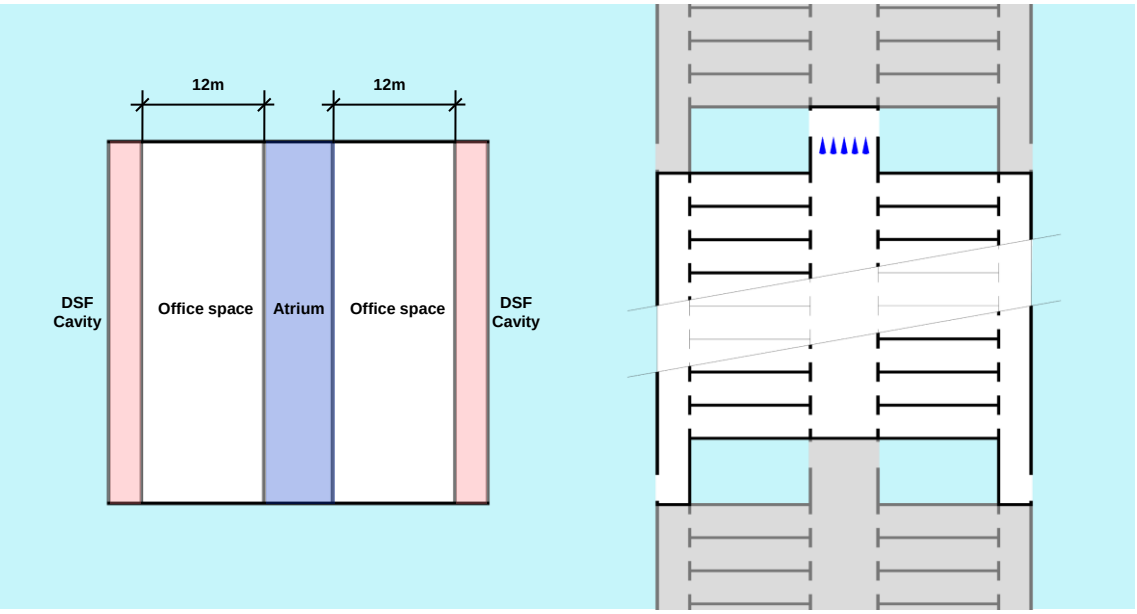

a. Floor Plan **b.** Section

Figure 4-32: PDEC high-rise model

A Top-down (T-D) flow pattern (in passive downdraught evaporative cooling PDEC mode): As shown in Figure 4-33a, fresh ambient air enters each segment from the opening at the top of the atrium where it is cooled (either passively or actively) creating a downdraught. The cooled air then enters the different floors

through individual high-level vents at the atrium/office interface whereas used air is discharged to the DSF cavity through high-level vents at the office/DSF interface. Since used air is presumably cooler, hence denser than ambient air, it will flow downwards and exit the segment via the outlet opening located at the bottom of the DSF cavity. This centre-in edge-out (C-E) flow direction has two major advantages over the edge-in centre-out (E-C) approach. The first is that the cool zone (atrium) is located at the centre of the building and is thus protected from direct exposure to the hot external environment. The other advantage is that used air leaving the office space is relatively cooler than ambient and thus creates a cold buffer which is assumed to reduce heat gains through the external envelope and also help reduce the overheating risk of the DSF cavity.

A Bottom-up (B-U) flow pattern (in night cooling and daytime ventilation mode when internal temperatures are higher than external ones): At instances when internal temperatures are higher than ambient (e.g. summer night-time or temperate/cold seasons), it is likely that flow reversal occurs, that is the flow pattern changes from T-D to B-U. Used air from the occupied floors is, in this case, warmer hence less dense than ambient air and is therefore discharged to the atrium where it flows upwards to exit the segment from the opening at the top of the atrium (Figure 4-33b). It is then replaced by fresh cooler air entering from the bottom of the DSF. In this mode, the flow direction changes from C-E to E-C whereas the atrium and DSF exchange roles to act as exhaust and supply zones respectively. It has to be noted that changing the flow direction in this manner could create airflow control difficulties and could be confusing for the occupants and facility managers.

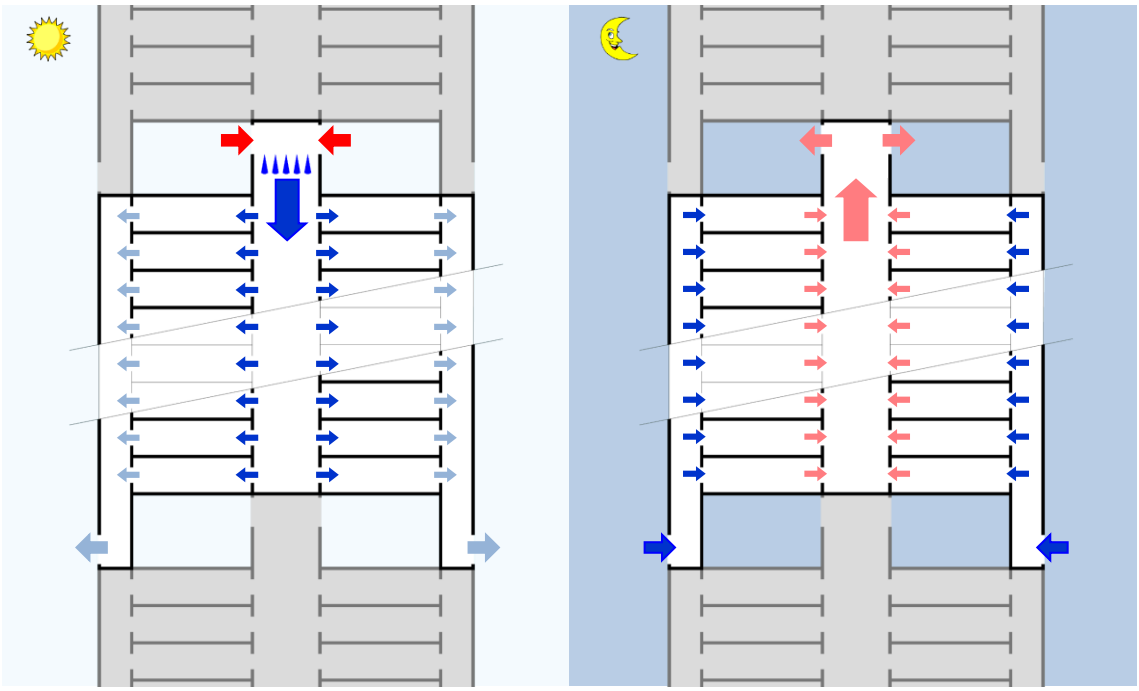

a. Top-down C-E flow pattern (PDEC operation)

b. Bottom-Up E-C flow pattern ($t_{db} > t_x$)

Figure 4-33: Top-down and Bottom-Up modes of operation

An alternative configuration exists (Figure 4-34) in which the atrium and DSF preserve their functions as supply and exhaust zones respectively whereby used air is discharged from the top of the DSF and replaced by fresh air entering from the bottom of the atrium. From the point of view of an occupant inside the delivery zone (offices), this B-U, C-E flow pattern allows fresh air to always flow from the atrium to the DSF. This flow direction also has the added benefit of making use of any air treatment measures (such as vegetation) employed in the T-D operating mode to filter out dust and other undesirable airborne particles.

To achieve this B-U, C-E flow pattern without the need to add any openings at the top and bottom of each segment's atrium and DSF respectively, the atria and DSFs of all the segments of the high-rise are assumed to be connected. Two

sets of horizontal dampers located inside the atria and DSF above and below each segment's inlet and outlet opening are added to provide control. These dampers are opened and closed in an alternating fashion to switch between the T-D and B-U operating modes. In the T-D operating mode (Figure 4-34a), the dampers below the inlets and above the outlets are open whilst those above the inlets and below the outlets are closed. This pattern is then reversed in the B-U operating mode (Figure 4-34b).

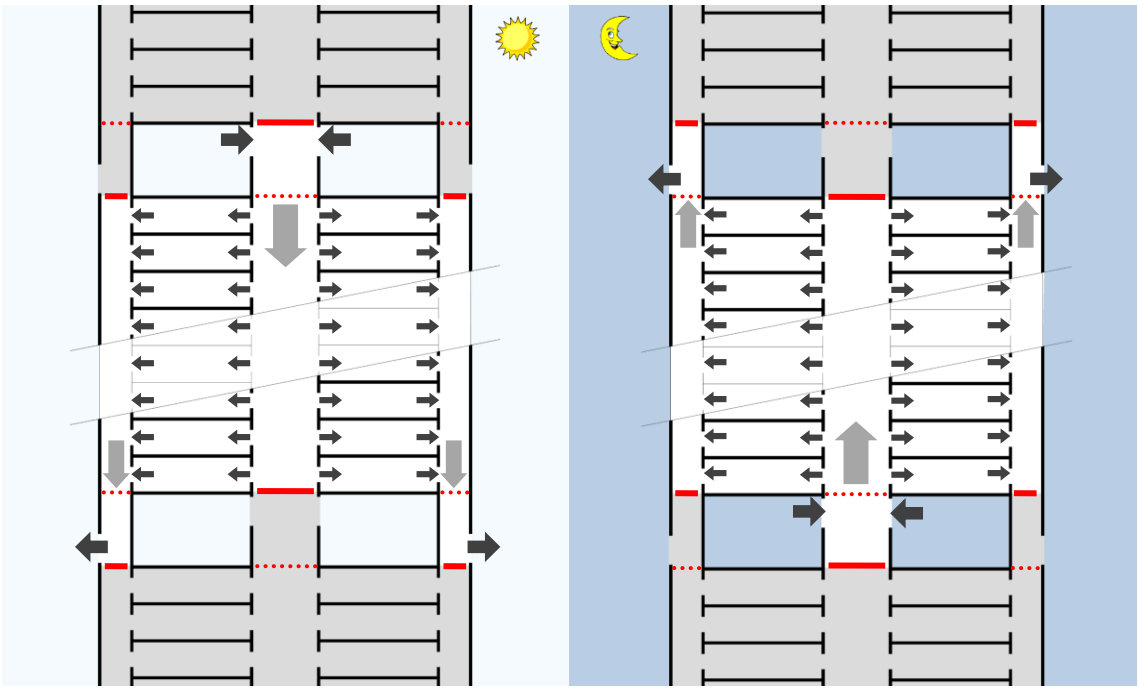

a. Top-down C-E flow pattern (PDEC operation)

b. Bottom-Up C-E flow pattern ($t_{db} > t_x$)

Figure 4-34: Alternative configuration for PDEC model

Despite the apparent advantages of the latter alternative, the model to be used in the simulations was configured to employ the former flow pattern, i.e. the E-C alternative, in the B-U operating mode due to its simplicity in terms of modelling owing to the fact that the airflow in this operating mode follows the exact same flow path of the T-D mode albeit in opposite direction.

Results of the Pilot model presented in Chapter Five revealed that occasionally, at the early hours of the working day (8am to 10am), indoor temperatures would rise, mainly as a result of internal heat gains, and would become warmer than the external dry-bulb temperature which, at the same time would not be low enough to allow for natural ventilation. At that point, even with PDEC in operation, internal temperatures would still remain higher than ambient. This temperature difference would cause the relatively warmer air leaving the offices to flow upwards through the DSF. If, in this case an exhaust vent exists at the bottom of the DSF only, the T-D flow pattern of the incoming air is interrupted, and a flow resistance occurs reducing the airflow rates. That is why an upper vent was introduced at the top of the DSF to induce a Top-Up (T-U) flow pattern (Figure 4-35). Accordingly, the lower and upper DSF vents are alternately opened depending on the air temperature inside the DSF.

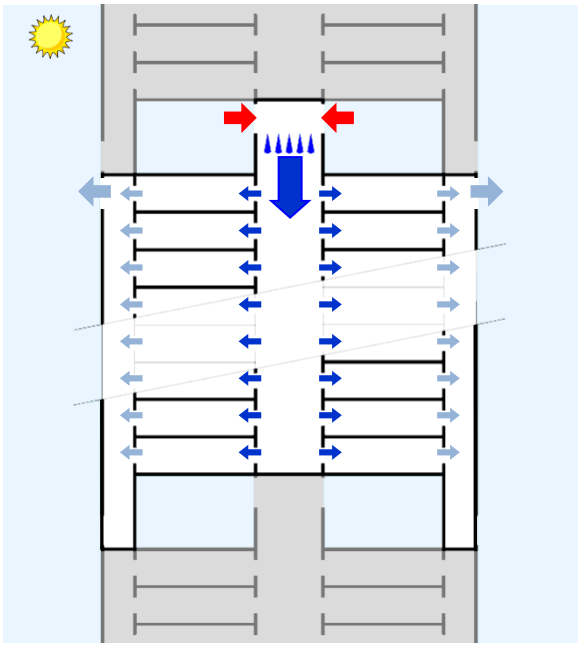

Figure 4-35 Top-Up mode of operation

4.3 Modelling techniques of Natural Ventilation and PDEC in buildings

The design of Passive and Hybrid Downdraught Cooling systems for buildings requires a suitable model to assess system performance. PHDC can be considered as a form of natural ventilation, driven by either buoyancy (stack effect) or wind or a combination of the two. As such, and in principle, most analysis methods that have been developed for natural or mechanical ventilation systems can be adapted for PHDC analysis. Li & Heiselberg (2003) posit three main issues that need to be addressed in modelling natural and mixed-mode (hybrid) ventilation;

- The variability of the driving forces

  Stack pressure, for example, is determined by the temperature difference between the indoor and outdoor air, which, in turn, is affected by ventilation flow rates. The pattern of wind flow around buildings is also very complex. Wind flow is unsteady (i.e. time varying) and wind pressure is strongly affected by the microclimate around the buildings, which is again affected by landforms, vegetation and other surrounding buildings (Li & Heiselberg, 2003).

- Control Strategies and occupant interactions

  The task of the control strategy is to identify when natural mode, mechanical mode or both modes should be active. Although modelling of the control strategy itself may not be difficult for a particular building, provided that the control strategy can be clearly defined, it is, however, not easy to develop a general algorithm that covers the modelling of all possible control strategies. One such example is the indeterministic nature of the occupants' behaviour

in response to indoor stimulus which can have a profound influence on the accuracy of results (Li & Heiselberg, 2003).

- Non-Linear Dynamical Phenomena such as Solution Multiplicity

  As with many other physical systems, airflow in buildings can exhibit non-linear dynamical phenomena such as the existence of multiple steady states. This means that, for a given set of boundary conditions, the air flow pattern in the space can adopt one of several possibilities, or that the pattern can oscillate between one solution and another (Li & Heiselberg, 2003).

In order to address these issues, a large number of design and analysis tools have continuously been developed over the last two decades. They can be categorised as follows:

- Simple Analytical and Empirical models
- Small-scale physical models
- Combined thermal (DTM) and airflow models (AFN)
- Computational fluid dynamics (CFD)

There are basically two sets of fluid dynamics equations that are primarily used to model the ventilation process (Li & Heiselberg, 2003), these are:

- Bernoulli's Equation for flow through an opening. In this equation, the effects of wind flows around buildings are generally included by using a wind pressure coefficient and the air flow in the room is assumed to be stagnant.
- The Navier–Stokes Equations. These equations apply to both laminar and turbulent flows. Reynolds-averaged or space-filtered equations are

generally used to model turbulent flows. This approach allows for the movement of air within a room or zone to be represented.

Bernoulli-Equation approaches include simple analytical models and network (multi-zone) models. Navier–Stokes Equations are applied to computational fluid dynamics (CFD) methods.

A detailed review of the available design and analysis tools for NV and PDEC can be found in Appendix A wherein their relative advantages and limitations together with some examples of their application in the design of NV and PDEC buildings is presented. A summary of that review is presented in Table 4-1. Each modelling technique is outlined and its relative advantages, limitations, and proposed utilisation in this study presented.

Having reviewed the available methods of analysis and performance prediction and their potential applications, and in light of the research questions posed in this study, two modelling techniques were chosen; Envelope Flow Models (EFM) (Etheridge, 2011b; Irving et al., 2005), to determine the initial sizing of the PDEC components (vent sizes), and EnergyPlus (Crawley et al., 2000), a dynamic thermal simulation program (DSP) coupled with an airflow network (AFN) to provide overall evaluation of PDEC cooling potential and to give details on ventilation rates and general airflow patterns. Following is a description of the two methods.

Table 4-1 Summary of review of modelling techniques of NV and PDEC

Technique	Advantages	Limitations	Utilisation in design
Envelope Flow Models (EFM)	Very simple, quick, and cheap to use	Very approximate predictions	Initial sizing of openings at chosen design conditions
Salt-Bath technique	Provides dynamic and visual demonstrations of natural ventilation processes Can identify the different possible flow regimes The ability to cope relatively easily with complex geometries and complex ventilation flows	Gives qualitative rather than quantitative results Practical experience required Adiabatic room envelopes Not all Mechanisms of heat transport are considered Simplified heat sources	_____
Fine-Bubble technique	Setup and operation of experiment are simple Does not require a big liquid reservoir heating elements are involved	application limited to the modelling of natural ventilation due to buoyancy in single-cell buildings only	_____
Wind Tunnels	Offers relatively high accuracy in the determination of ventilation rates due to wind Models can be subjected to varying and controlled wind speeds and directions Flow visualisation possible	Poses limitations on the size of the building to be modelled, especially on its height Very difficult to model internal flows	_____
Combined Thermal (DTM) and Airflow Models (AFN)	Only acceptable model for analysing ventilation performance for moderately and large-sized buildings Can be used to provide boundary conditions for CFD applications.	Limited to the predictions of the average characteristics of airflows and contaminant distributions within each zone	Understand the time-varying behaviour of the building Determine the number of hours in which the simulated indoor air temperature exceeds a set of predetermined temperatures Provide boundary conditions for CFD
Computational Fluid Dynamics (CFD)	Potentially very accurate. Able to predict spatial information giving values for variables throughout the entire flow domain Easy to investigate changes in geometry and operating conditions. Additional physical models (e.g. radiation models and contaminant dispersion) can be added with relative ease.	Require a high level of expertise in terms of data input, assumptions and interpretation Very computationally intensive prohibiting detailed simulations of entire building Can only model a snap-shot scenario Development is still required especially in the area of turbulence modelling and heat transfer, particularly close to surfaces	_____

4.4 Initial Sizing of the PDEC Components using EFM

As mentioned above, Envelope flow models are used for the initial sizing of openings at the chosen design conditions in the early stages of design. Envelope flow models solve the equations that govern the flow of air through openings in the envelope of a building. Using the explicit method of solution for a multi-cell building (Etheridge, 2011a), the areas of openings for given volume flow rates and flow directions can be determined. The method as described in (Etheridge, 2011a) can be summarised in the four stages below.

Stage 1: Selection of a ventilation strategy

In this stage, the intended flow direction that corresponds to the building configuration and external conditions is selected. For the PDEC multi-storey building, the three flow patterns described in section 4.2.1 are used. Figure 4-36 shows a three-storey segment with a supply and exhaust zone operating in each of the aforementioned flow patterns. This five-cell configuration will be used to demonstrate how EFMs are used to calculate the areas of the openings.

The three floors are denoted by cells A, B, and C; the Atrium by S; and the DSF by X. The openings are denoted by numbers 1 to 8 as shown in the figure.

Stage 2: Specification of data relating to boundary conditions

Boundary (design) conditions are selected at this stage. These include external and internal temperatures, anticipated heat loads that are required to be offset, wind speed and direction, and surface pressure coefficients. Since the three flow patterns are likely to have different design conditions, these are individually specified.

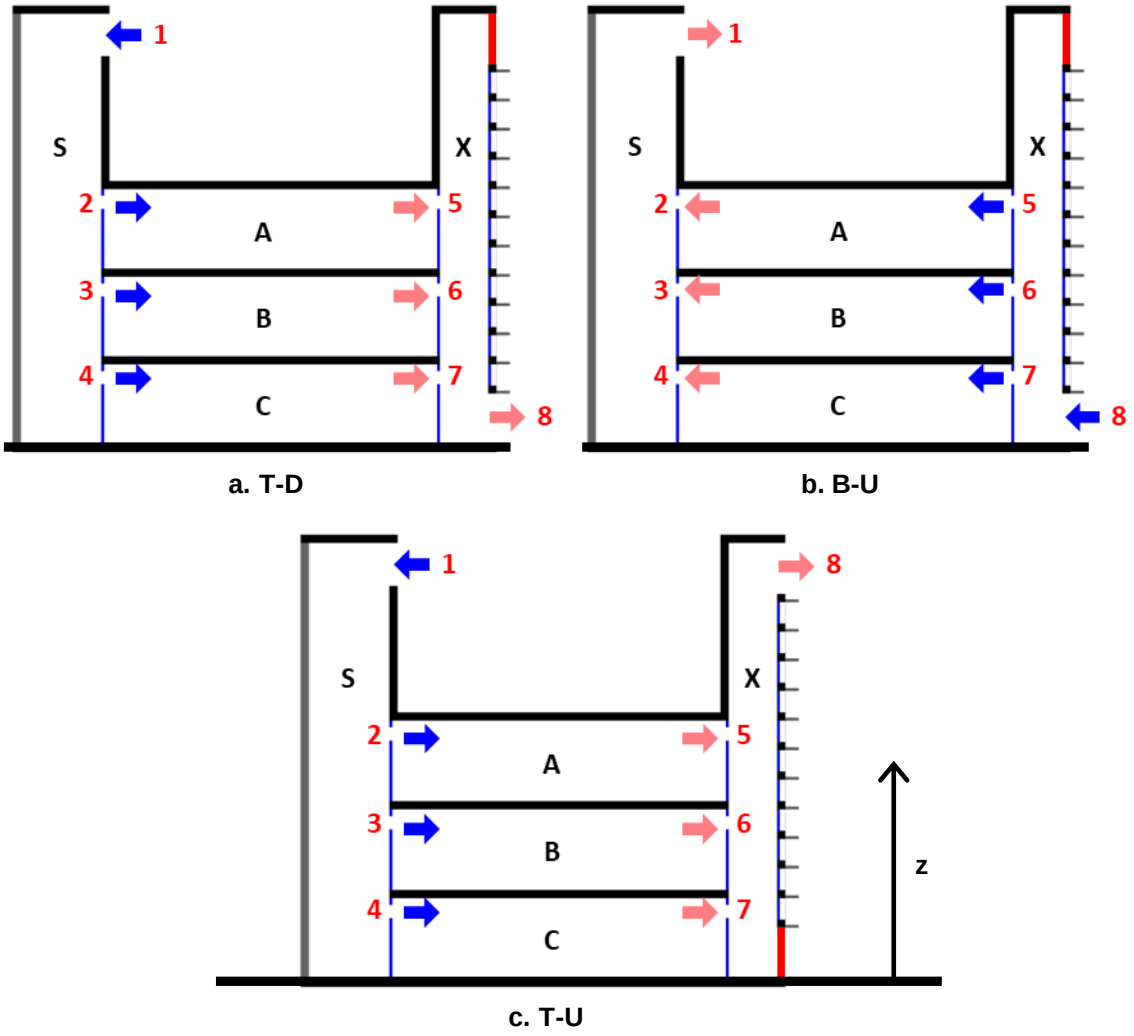

Figure 4-36 Five-cell representation of a three-storey model of the PDEC building during a) the T-D flow pattern, b) the B-U flow pattern, and c) the T-U flow pattern

Stage 3: Calculation of required flow rates

For each floor (cell), the volume flow rate of air q_{vi} (m^3/s) that is required to offset a sensible heat gain of B (W) is given by

$$q_{vi} = \frac{B}{\rho\, c_p\, (t_{db} - t_s)} \qquad \text{Equation 4-1}$$

where i denotes the opening, ρ is the density of air (kg/m^3), c_p the specific heat capacity of air (J/kg.K), t_{db} the internal air temperature of that floor (C°), and t_s the

supply air temperature which is equal to the external temperature in NV mode (B-U mode) and to the PDEC outlet temperature in PDEC modes (T-U and T-D modes).

Applying the principle of mass conservation to the fixed volume gives the continuity equation for the complete envelope as

$$\sum \rho_i \, q_i = 0 \qquad \text{Equation 4-2}$$

which can be reduced to conservation of volume without significant error:

$$\sum q_i = 0 \qquad \text{Equation 4-3}$$

Stage 4: Application of explicit method to determine the sizes of openings

The relationship between the area of an opening and the volume flow rate through the opening can be expressed by

$$C_d \, A_i = q_{vi} \sqrt{\frac{\rho}{2 \, |\Delta p_i|}} \qquad \text{Equation 4-4}$$

where *i* denotes the opening, C_d is the discharge coefficient (dimensionless), A_i the area of the opening (m^2), q_{vi} the volume flow rate through the opening (m^3/s), Δp_i the pressure difference across the opening (Pa), and ρ is the air density (kg/m^3).

The only unknown term on the RHS of $C_d \, A_i = q_{vi} \sqrt{\frac{\rho}{2 \, |\Delta p_i|}}$ Equation 4-4 is Δp_i.

For the T-D flow pattern, the equations for Δp_i are

$$\Delta p_1 = P_{E0} - P_{I0S} - (\rho_E - \rho_S) \, g \, z_1 + p_{W1} \qquad \text{Equation 4-5}$$

$$\Delta p_2 = P_{I0S} - P_{I0A} - (\rho_S - \rho_A)\, g\, z_2 \quad \text{Equation 4-6}$$

$$\Delta p_3 = P_{I0S} - P_{I0B} - (\rho_S - \rho_B)\, g\, z_3 \quad \text{Equation 4-7}$$

$$\Delta p_4 = P_{I0S} - P_{I0C} - (\rho_S - \rho_C)\, g\, z_4 \quad \text{Equation 4-8}$$

$$\Delta p_5 = -P_{I0X} + P_{I0A} + (\rho_X - \rho_A)\, g\, z_5 \quad \text{Equation 4-9}$$

$$\Delta p_6 = -P_{I0X} + P_{I0B} + (\rho_X - \rho_B)\, g\, z_6 \quad \text{Equation 4-10}$$

$$\Delta p_7 = -P_{I0X} + P_{I0C} + (\rho_X - \rho_C)\, g\, z_7 \quad \text{Equation 4-11}$$

$$\Delta p_8 = -P_{E0} + P_{I0X} + (\rho_E - \rho_X)\, g\, z_8 - p_{W8} \quad \text{Equation 4-12}$$

where z is the height of the opening (m), P_{E0} the external hydrostatic pressure at z = 0 (Pa), P_{I0} the internal hydrostatic pressure of the corresponding cell (Pa), ρ_E the external air density (kg/m^3), ρ_A, ρ_B, ρ_C, ρ_S, and ρ_X are the internal air densities of their respective cells (kg/m^3), and p_{W1} and p_{W8} are the wind pressures at their respective openings and are taken to be equal to zero assuming a no-wind scenario. Note that the signs of the terms are dictated by the intended flow direction across the opening.

To solve the equations some requirement has to be specified. The pressure difference across opening 1 is taken to be equal to the sum of the pressure difference across openings 2 and 5. Thus

$$\Delta p_1 = \Delta p_2 + \Delta p_5 \quad \text{Equation 4-13}$$

Furthermore, for each internal opening on the DSF, the pressure difference is specified to be a factor K of its corresponding internal opening on the Atrium. Thus

$$\Delta p_5 = \mathrm{K}\,\Delta p_2 \qquad \text{Equation 4-14}$$

$$\Delta p_6 = \mathrm{K}\,\Delta p_3 \qquad \text{Equation 4-15}$$

$$\Delta p_7 = \mathrm{K}\,\Delta p_4 \qquad \text{Equation 4-16}$$

Finally, with 13 unknowns and 12 equations, a further equation is required. This is taken to be

$$\Delta p_1 = \Delta p_8 \qquad \text{Equation 4-17}$$

So that the areas of opening 1 and 8 will be equal.

By solving equations 4-5 to 4-17 simultaneously, the values of Δp_i are calculated, and the sizes of the corresponding openings obtained.

4.5 Modelling PDEC using the AFN integrated DTM program EnergyPlus

Developed by the US department of energy DoE, EnergyPlus solves a range of problem types including building fabric, mass flow and detailed plant systems, sequentially or simultaneously (Crawley et al., 2000). The airflow network model in EnergyPlus (Gu, 2007) was developed based on AIRNET, a detailed description of which may be found in the work of (Walton, 1989; Walton & Dols, 2003) The model consists of a set of nodes linked by airflow components through linkages. The node variable is pressure and the linkage variable is airflow rate. The nodes are mapped on thermal zones while the linkages represent flow components such as windows, vents and cracks. Based on the airflow calculated for each linkage, the model then calculates node temperatures and humidity ratios. A mass balance is expressed for each node in the building. The resulting

system of equations is solved to yield nodal pressures and the flows through the connections.

As a tool, EnergyPlus has been tested and validated for the modelling of natural ventilation in multi-storey buildings. Zhai, Johnson, & Krarti, (2011) assessed the accuracy and usability of EnergyPlus in modelling hybrid ventilation by simulating three selected real buildings that were supplied with the most detailed building and measurement information available. Although results of their validation were inconclusive due to the lack of some data pertaining to the actual effective vent areas and field measurements of ventilation flow rates, however, in cases where those were available, simulated results showed excellent agreement with measured data (Zhai et al., 2011).

Furthermore, Anđelković, Mujan, & Dakić, (2016) compared field measurements to simulated values of cavity air temperature and velocity of a multi-storey naturally ventilated DSF using EnergyPlus. The validation was done for winter, transitional seasons, and summer. Results highlighted a very good overall agreement and a high level of matching between measured values and simulated results in terms of temperature and flow rates (Anđelković et al., 2016).

Johnson, Zhai, & Krarti, (2012) investigated the capability and accuracy of four network airflow models—of which EnergyPlus was one—to simulate a wide range of natural ventilation scenarios, with varying combinations of geometry and natural ventilation driving forces. Measured values were gathered from a selected body of experimental data. Of the eight test cases investigated in their study, only two were of interest here, namely, Buoyancy-driven atrium ventilation and

Combined-driven atrium ventilation. Average errors for the two case were found to be 2.5% and 5% respectively (Johnson et al., 2012) indicating the high accuracy of network airflow models.

The previous validation studies give sufficient confidence to proceed with using EnergyPlus with its integrated airflow network model to accurately predict internal conditions in terms of temperature and bulk airflow rates inside the generic PDEC multi-story office building developed in this chapter.

In this study, the modelling procedure of PDEC reported in (Robinson et al., 2004) is adopted. Although their simulations were carried out using ESP-r, the same procedure can be followed in EnergyPlus. It has to be noted that although a dedicated module for simulating PDEC exists in EnergyPlus, it is only restricted to a single zone and cannot be incorporated in a multi-zone airflow network model (Kang & Strand, 2009). The modelling procedure adopted in this study is described as follows:

A simple approximation is used to emulate the performance of a well-designed and controlled microniser array. Two important physical processes need to be considered:

i- The reduction of incoming ambient air temperature due to droplet evaporation

ii- The mass flows resulting from the relative density difference between internal and ambient air.

Since the latter is strongly coupled with the former, it is imperative to predict the post-evaporation internal air temperature. Robinson et al., (2004) suggested the target air state to be defined in cooling efficiency terms as 70% of the wet bulb temperature depression:

$$t_{pdec} = t_x - 0.7(t_x - t_{wb}) \quad \text{Equation 4-18}$$

where the wet bulb temperature depression t_{PDEC} is the dry bulb temperature difference between two points along a line of constant enthalpy on the psychrometric chart. The first point t_x represents ambient dry-bulb temperature and the latter t_{wb} the wet bulb temperature.

The evaporation process can be approximately emulated by cooling a zone in the model to t_{PDEC} at each simulation time-step. This can be achieved in EnergyPlus by creating a boundary file that defines the set-points for mechanical cooling of a transient zone at each time-step. The transient zone is controlled by an Ideal Loads Air System (ILAS).

At each time-step it is also possible to calculate the water usage at the prevailing air change rate. The volume, in litres, of water V_w required to reduce the temperature of a given volume of air V_a of known density ρ_a, to 70% of the ambient air wet bulb temperature depression t_{PDEC}, i.e. from moisture content W_{db} up to W_{PDEC} for each time-step is given by:

$$V_w = \rho_a V_a (W_{PDEC} - W_{db}) \rho_w^{-1} \times 10^3 \quad \text{Equation 4-19}$$

The water delivery rate V_m is quoted by the manufacturers of micronisers. The number of micronisers n_m that must operate at each airflow rate is given by:

$$n_m = Int\left(\frac{V_w}{V_m}\right) + 1 \qquad \text{Equation 4-20}$$

4.6 Summary

In this chapter a four-stage plan for the design of a PDEC multi-storey office building was presented, namely; a conceptual design stage, a design development stage, a performance assessment stage and a design optimisation stage. For each stage, the respective research tool or modelling technique was presented. For the first a building precedents study was conducted to provide an *a priori* of the generic PDEC office building prototype the outcome of which was the development of that generic prototype. A literature review was then presented for the various tools available for modelling PDEC and natural ventilation and their suitability for each design stage. Envelope flow models were selected for the design development stage and the procedure used to calculate the initial sizing of the PDEC components described. To assess the time-varying performance of the generic model, the dynamic simulation program with integrated airflow modelling 'EnergyPlus' was selected. A description of the program was given, and the methodology used to simulate PDEC described.

Chapter 5: Simulation of the Base Case Model

5.1 Chapter Overview

In this chapter, results of the integrated thermal and airflow simulations of the Base Case Model (BCM) of the proposed PDEC Multi-storey Office Building are presented. The BCM represents the foundation to which the model variants and the parametric investigations performed in the following chapter are compared. To assess the preliminary validity of the proposed model in EnergyPlus and accordingly allow for any necessary refinement, a pilot model was deemed necessary. Section 5.2 describes the Pilot Model (PM), its modelling assumptions, construction profiles, occupancy and Internal heat gains schedule, aperture control logic, and initial sizing of PDEC components (i.e. the size of openings throughout the model). Results of the preliminary investigation are also presented in this section. Based on the results of the PM, a process of refinement was performed to reach the BCM, details of which are presented in Section 5.3. Analysis of the results of the BCM is presented in Section 5.4 together with a discussion on the thermal and airflow behaviour of the model. In Section 5.5, conclusions on the overall performance of the BCM are drawn and issues raised from the analysis of the results of the BCM are highlighted to be investigated in the following chapter.

5.2 Pilot Model

As previously mentioned, to assess the preliminary validity of the proposed PDEC multi-storey office building model in EnergyPlus and accordingly allow for

any necessary refinement, a PM was deemed necessary. The PM was configured such that it comprises the least number of floors in a segment that would capture the thermodynamic essence of the problem being addressed. A segment made up of three storeys; an upper floor, a lower floor, and a single middle floor to account for mid-height storeys in the segment was thus chosen (Figure 5-1). To avoid long simulation runs, only half the building and of this only a 10m wide slice of its total length was considered, giving a floor area of 120m^2 (12m x 10m). The floor to ceiling height assumed was 3m. For the PM, an initial east-west orientation for the building axis was assumed with the DSF (the only façade with an external exposure) facing south. This orientation was arbitrarily chosen on the backdrop of the fact that the effect of orientation on performance will further be investigated (see Section 6.4). Finally, given that the aperture at the top of the Atrium acts as the segment's inlet during PDEC operation and outlet during NV, the Atrium was allowed to extend two storeys above the segment's upper floor to increase the stack height between the aperture at the top of the atrium and that at the upper floor's atrium/office interface. Note here that the height of the Atrium's extension beyond the upper floor was intentionally chosen to be a multiple of the height of one storey to facilitate any architectural intervention in the intermediate zone between segments.

5.2.1 Modelling assumptions

In many cases where NV, and by extension PDEC, are considered, design conditions wherein average wind speeds approach zero are considered to be worst case scenarios (Etheridge, 2011a). For the proposed PDEC model, it seemed reasonable to investigate whether sufficient airflows can be generated

under a buoyancy only scenario, that is, with no assistance from wind forces. To predict the performance of the PM under buoyancy forces only, the effects of wind needed to be eliminated. This was achieved in EnergyPlus by setting the values of all wind pressure coefficients to near-zero values.

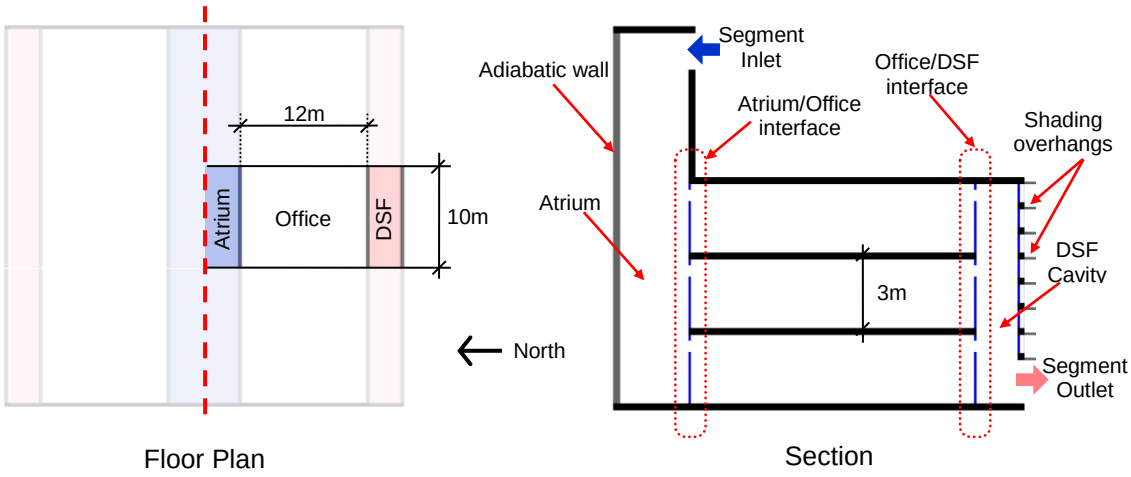

Figure 5-1 Pilot Model

5.2.1.1 Construction Profiles and Shading

As a starting point, commonly used construction profiles for external walls in newly built office buildings in Egypt were considered and the building was assumed to be of heavy-weight construction. However, to represent good passive building design practice and to comply with the requirements of the Egyptian Code for improving the Energy Efficiency of Commercial Buildings (HBRC, 2005), an additional layer of insulation was added to give a total U-value of 0.4W/m^2.K. Transparent components of the envelope were assumed to be double-glazed with a U-value of 2.2W/m^2.K and a solar heat gain coefficient (SHGC) of 0.14. To take advantage of the external views likely to be afforded by high-rise buildings, a relatively high window to wall ratio (WWR) of 70% was used. However, overhangs with a projection factor (PF) of 1.0 were added above all glazed areas

to compensate for this relatively large WWR as recommended by the Egyptian Code. It is noteworthy that the final SHGC and U-values used here also comply with the requirements of ASHRAE standard 90.1 (ASHRAE, 2004b) and the International Energy Conservation Code (ICC, 2012).

Furthermore, all internal surfaces apart from the Atrium/Office and Office/DSF interfaces were considered adiabatic. These also include the ceiling and floor of the upper and lower level floors respectively. Infiltration was defined so that the permissible air leakage for the whole building does not exceed $7m^3/h/m^2$ at 50Pa pressure differential as recommended by the British Council for Offices (BCO, 2014). This was achieved by creating cracks with appropriate flow properties around the external openings.

5.2.1.2 Occupancy and internal heat gains

Office hours run from 8:00 to 18:00 five days a week. Based on an occupancy density of $8m^2$/person, typical sensible internal heat gains during occupied hours were assumed to be 10 W/m^2 for occupancy, 14 W/m^2 for lighting and 25 W/m^2 for office equipment with an approximate total of 50 W/m^2 (BCO, 2014). The Egyptian Typical Meteorological Year ETMY for Cairo was used as the weather data file for all simulations.

5.2.1.3 AFN Control-logic

In Chapter 4, it was shown that the prototype for the multi-storey PDEC office building was configured to allow it to alternate between three passive modes of operation; Nighttime Cooling (NC), Natural Ventilation (NV), and Passive Downdraught Evaporative Cooling (PDEC). Should passive modes make internal

conditions untenable for occupants, it seemed sensible to allow for an auxiliary active mode in the form of Mechanical Air Conditioning (AC), which would also serve to establish any potential energy savings in comparison to conventional fully air-conditioned buildings.

As with any Mixed-Mode (MM) building, the ultimate aim of the control logic for the multi-storey PDEC office building was to maintain a satisfactory thermal environment during occupied hours whilst minimising environmental costs, in this case, water (PDEC) and energy (AC). To achieve that, a control logic would principally be set up to determine the appropriate mode of operation for any given combination of internal and external conditions by defining a number of setpoints around which the different modes of operation would alternate, PDEC and AC included. This implies that the values of those setpoints have direct implications on water and energy consumption; the lower the setpoint, the higher the consumption. But to achieve that critical balance between maintaining comfort and avoiding overconsumption, the values of those setpoints need to be linked to the comfort boundaries of each mode (Rijal, Humphreys, & Nicol, 2009). It is therefore clear that knowledge of the internal conditions that are likely to be acceptable to the majority of occupants in PDEC buildings is a prerequisite to the determination of the required setpoints and in turn, to the development of an appropriate control logic.

Discussions in Chapter 3 have shown that comfort conditions in PDEC buildings do not strictly conform to the applicability criteria of either of the two main models of thermal comfort: the Fanger PMV-PPD model (Fanger, 1970) and the Adaptive Comfort Model (Auliciems, 1981; de Dear & Brager, 2001;

Humphreys, 1975; Humphreys & Nicol, 1996) as codified in ASHRAE Standard 55 (ASHRAE, 2010), EN15251 (CEN, 2008), and ISO 7730 (ISO, 2005) but are likely to lie somewhere in between. However, the control logic of the PM was set up on the premise that comfort conditions in PDEC buildings could be considered to be equally in conformity with the predictions of the ACM as those in naturally ventilated and mixed-mode buildings. Accordingly, the control logic was set up to maintain internal conditions within the 90% acceptability range of the ACM as defined by ASHRAE standard 55 (ASHRAE, 2013b).

Since the single main purpose of creating a PM in the first place was to assess the feasibility of modelling the PDEC office building prototype in EnergyPlus and refine it accordingly, only passive modes were considered. A fairly basic control-logic was thus used. Priority here was given to NV during occupied hours as well as nighttime cooling (NC) to reduce radiant heat gains from the building's structure during the following day. The intention was to minimise water consumption by resorting to PDEC only to maintain internal temperatures within the comfort range. During office hours, the control logic assumes all apertures remain closed and ambient air is only supplied at minimum fresh air rate requirements if internal temperatures in all floors remain lower than a predefined setpoint, henceforth referred to as the initiation setpoint temperature (t_{isp}). As previously discussed in Chapter 3, indoor operative temperatures offer a more accurate index of thermal sensation than dry-bulb temperatures (Nicol et al., 2009). Control setpoints for the PM were therefore based on internal operative temperatures (t_{op}) rather than dry-bulb temperatures (t_{db}) and t_{isp} was taken to be equal to ASHRAE's adaptive comfort temperature (t_{cmf_ASH}). Preliminary runs

showed that the difference between t_{db} and t_{mr} (mean radiant temperature) remained under 4K. t_{op} was therefore approximated as their mean value in accordance with ASHRAE standard 55 (ASHRAE, 2013b).

Once t_{op} exceeds t_{isp}, PDEC is switched on or off depending on ambient conditions. If the concurrent external dry-bulb temperature (t_x) is simultaneously lower than both the internal dry-bulb temperature (t_{db}) and a predefined upper limit for the supply air temperature (t_{s_max}), NV is allowed. For the PM, t_{s_max} was taken to be the temperature at the lower boundary of the 90% acceptability range of the adaptive comfort model as defined by ASHRAE Standard 55 (t_{lb_ASH}). However, if either of the above conditions is not met on any floor, that is if $t_x > t_{db}$ or $t_x > t_{s_max}$, PDEC is initiated. Note here that for PDEC to be allowed, the outdoor relative humidity (*RH*) needs to be below 80%. As discussed in Chapter 3, this condition was imposed to avoid moisture build-up in internal spaces as well as uncomfortable internal conditions due to elevated humidity levels. If $RH > 80\%$, PDEC is not allowed and the segment continues in NV mode even if $t_x > t_{s_max}$ so long as $t_x < t_{db}$. If, after either NV or PDEC has been initiated, t_{op} in any floor drops below t_{isp}, apertures at the atrium/office and office/DSF interfaces of that floor are closed.

During unoccupied hours, nighttime ventilation is allowed for a specific floor provided that the internal dry-bulb temperature for that floor is higher than the external dry-bulb temperature. The control logic described above was written in the EMS language created in EnergyPlus (Crawley et al., 2000).

5.2.1.4 Sizing of PDEC Components

The initial sizing of the PDEC components were calculated using the EFM method described in Section 4.3.5.1. For the boundary design conditions required for the EFM calculation, t_S was taken to be the PDEC outlet temperature value that is exceeded on average by only 1% of the total number of hours in a year (i.e. 87 of 8760) in coherence with the ASHRAE handbook of fundamentals (ASHRAE, 2013a). The outdoor temperature was accordingly taken to be the mean coincident dry-bulb temperature. Internal temperatures were taken to represent the upper limit for internal comfort conditions at the upper limit of relative humidity 80% (Martínez et al., 2000). Finally, it seemed logical to assume that t_{DSF} is higher due to solar gains but only by a 0.2K difference due to the anticipated high airflow rates. Accordingly, a fixed size of $8m^2$ was used for the openings on both the atrium/office and office/DSF interfaces. The size used for both the inlet and outlet openings at the top of the atrium and the bottom of the DSF respectively was $18m^2$. The cross-sectional area used for both the atrium and DSF was also $18m^2$.

5.2.2 Preliminary run

The week commencing August 13th (day 225) is reasonably typical of summertime conditions. Throughout this week, ambient temperatures peak at 38°C. Results for this week (Figure 5-2) highlight two main issues. The first concerns the unusual rise in temperature during the early office hours on a number of days whilst the second relates to the great deal of fluctuation that occurs when indoor operative temperatures approach t_{isp}.

5.2.2.1 Flow reversal

It is worth noting that although implementing PDEC has largely maintained indoor operative temperatures between 27ºC and 29ºC during office hours, an unanticipated increase in indoor operative temperatures occurred in the early hours of the working day on the 13th, 14th, 16th, and 17th of August. To appreciate this in more detail, focus was shifted to a 24-hour period. Figure 5-3 shows the volume flow rate profiles for the three different office floors of the PM on the 14th of August as it represents the most pronounced occurrence. The volume flow rates are of positive values (> 0 m^3/s) when the flow direction is from the atrium to the DSF which mainly occurs in the T-D/C-E flow pattern and of negative values when the flow is in the opposite direction most likely occurring in a B-U/E-C.

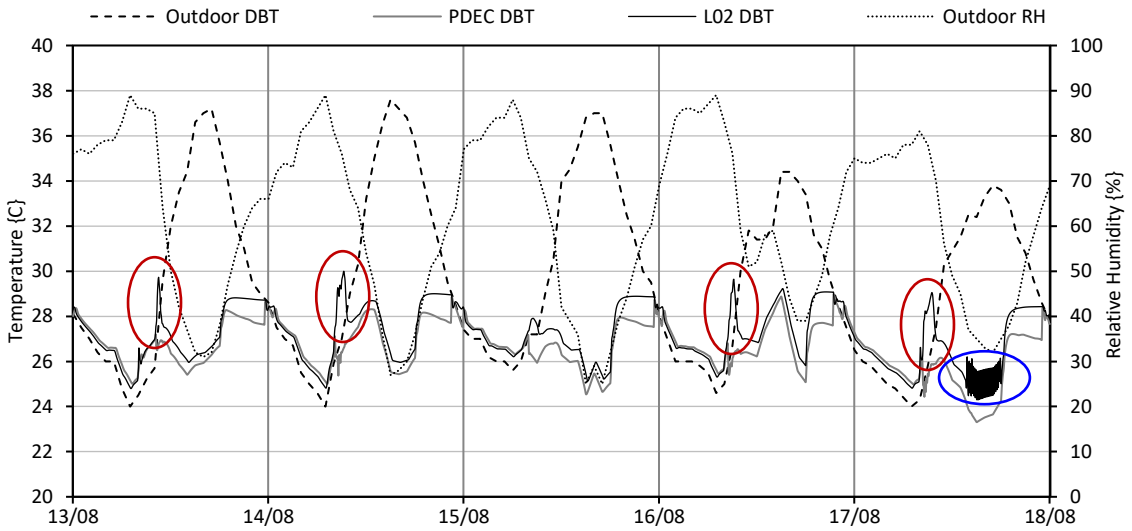

Figure 5-2 Dry bulb temperature profile for middle floor throughout extreme summer week (from 13/8 to 18/8)

After 08:00, the indoor temperature profile rises corresponding to ambient temperature to reach a peak of 29.7ºC at around 09:30 on the upper level and then suddenly drops back to follow the PDEC outlet temperature profile. Indoor

temperatures would normally increase at this time due to gains from occupants, lights, and equipment. However, it is the sharp and prolonged rise in the temperature profiles that seems peculiar. A closer look at the airflow pattern indicates that during the previous night around midnight, internal temperatures slightly exceed ambient temperatures allowing for nighttime ventilation. The temperature differential causes air to flow up the DSF through the offices and exit the building from the opening at the top of the Atrium (i.e. a B-U/E-C flow pattern occurs indicated by negative airflow values). It was anticipated that when PDEC was allowed to operate at around 08:00, the flow would change to a T-D/C-E pattern and the internal temperature profile would resemble that of the PDEC outlet temperature with a slight offset due to internal heat gains.

However, this was not the case. Despite PDEC being in operation, the airflow profiles for the whole segment as well as for individual floors kept fluctuating between negative and near zero values until about 09:30. One explanation could be that, at the early working hours of the day, when external temperatures are still relatively low, the temperature of used air leaving the offices is slightly higher than ambient and therefore less dense causing it to flow upwards rather than downwards. As a result, exhaust air cannot exit the segment from the opening at the bottom of the DSF.

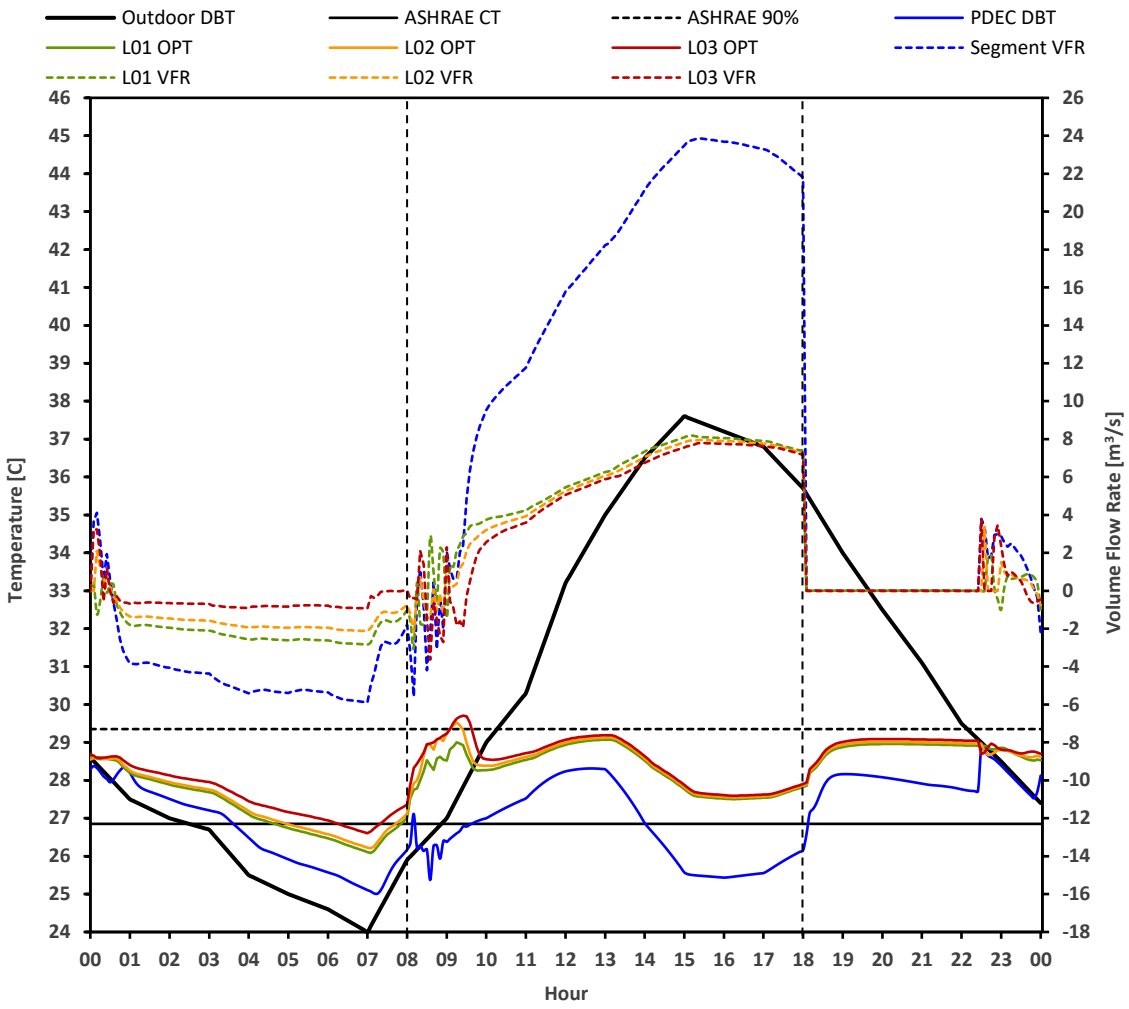

Figure 5-3 Dry bulb temperature and Volume flow rate profiles on the 14th of August for the Pilot model

Instead, used air from the lower floor level mixed with fresh air entering from the opening at the bottom of the DSF flows up the DSF and enters the middle and upper floors. A reverse flow is thus created in both floors as well as in the whole segment indicated by the negative values of the airflow rates (Figure 5-4a). When the pressure differences at openings on the atrium/office and office/DSF interfaces are equal, air ceases to flow through the floor plates and airflow through the whole segment is brought to a halt (indicated by near zero values) (Figure 5-4b). The alternating airflow pattern between negative and zero values

continues until external temperatures start to rise significantly. Only then does the flow change to a T-D/C-E pattern (positive values) and the internal temperature profiles follow that of the PDEC outlet temperature with a slight offset due to heat gains.

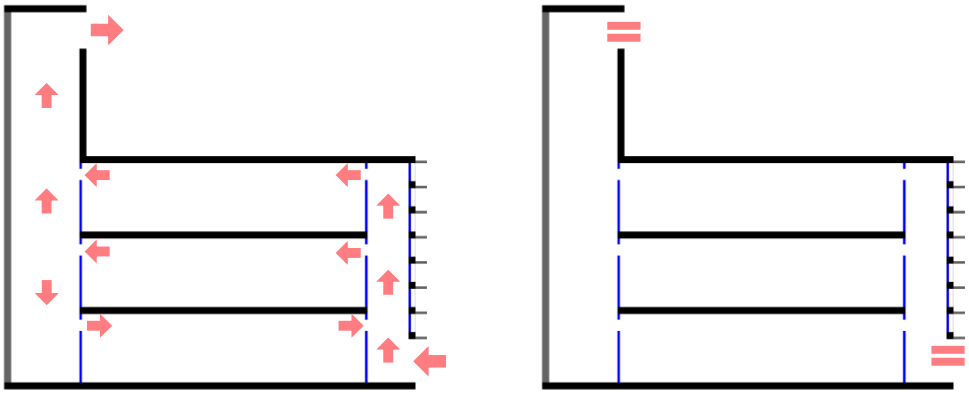

a. Reverse flow b. No flow

Figure 5-4 Alternating flow patterns during PDEC operation in the early working hours for the Pilot model

5.2.2.2 Temperature Fluctuation

Figure 5-5 shows the temperature and airflow profiles of the middle floor on the 17th of August. The graph clearly illustrates the other issue highlighted by the results of the PM; that of the rapid fluctuation in internal conditions as operative temperatures approach t_{isp}.

The PM contains no modulation but rather a simple on/off control logic implemented by fully opening the Segment's inlet and outlet openings as well as the apertures at both sides of the office floor when t_{op} in that floor exceeds t_{isp}. The fluctuations correspond to the rapid alternate opening and closing of the PDEC aperture to its maximum area. To give an example, if at a certain time-step the internal air temperature rises from (t_{isp} - 0.2) to (t_{isp} + 0.2), in an on/off control

logic, the apertures are fully opened. This induces a large volume of cold air causing a sudden drop in temperature to a value below t_{isp}. This in turn causes the apertures to close at the following time-step. Due to heat gains, temperatures rise again above ti_{sp} and the process is repeated. This on and off behaviour generates a great deal of fluctuation in internal dry-bulb temperatures of up to 2K in a five-minute interval.

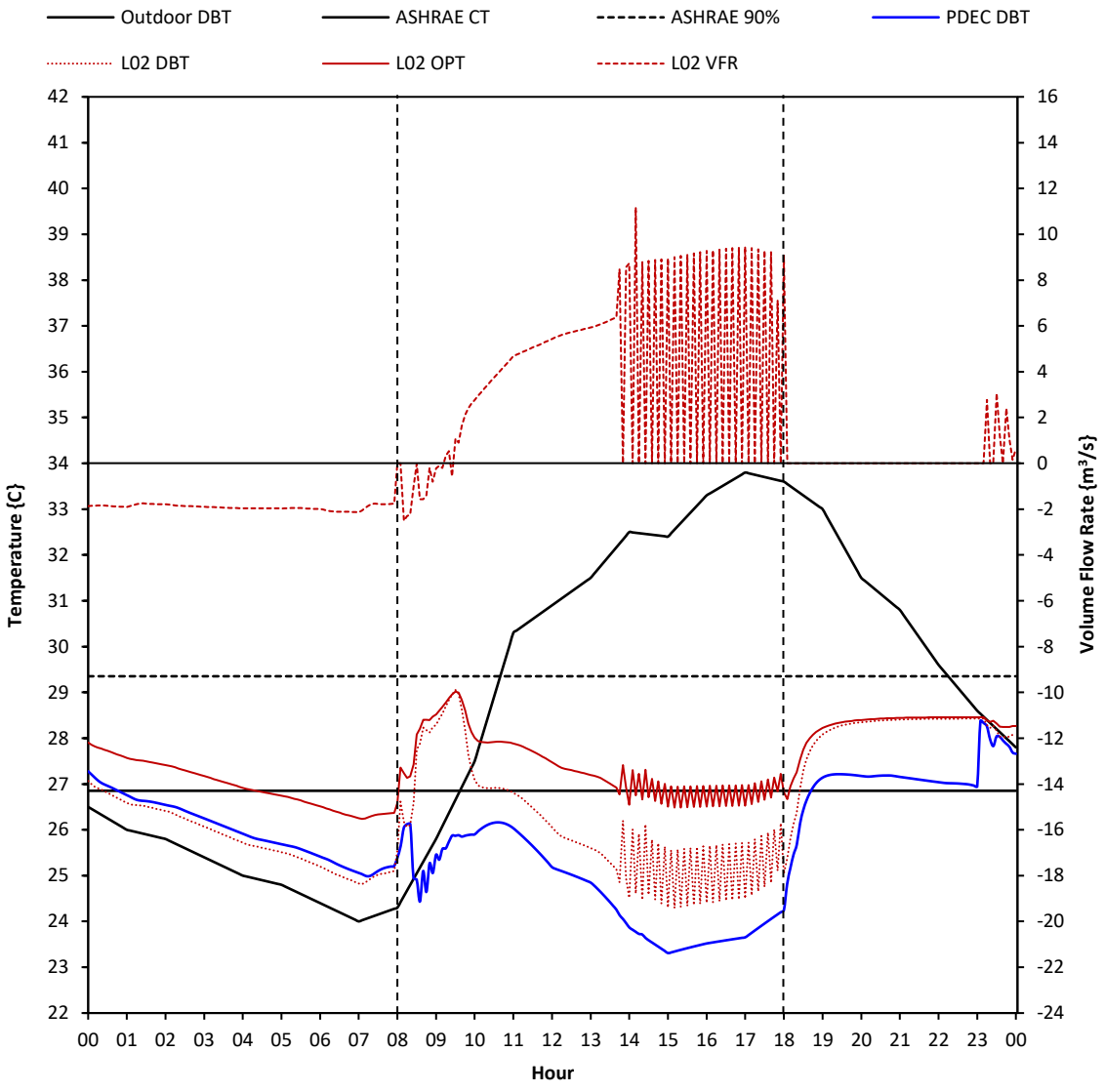

Figure 5-5 Dry-bulb temperature and Airflow rate profiles for the middle floor of the Pilot model on the 17th of August

5.3 Model Refinement: The Base Case Model

Both issues highlighted above; namely, the occurrence of a flow reversal at the early working hours and the rapid fluctuations in internal temperatures had to be addressed before the main investigations were to be carried out. This has prompted the refinement of the PM, which has been modified as described below to obtain the BCM.

5.3.1 Addition of a second outlet to the DSF

Results of the PM suggest that in some incidences, at the early hours of the working day (8am to 10am) internal temperatures would remain higher than ambient even if indoor temperatures exceed the PDEC operating setpoint and PDEC is turned on. It was thus suggested that adding another opening vent at the top of the DSF would allow relatively warmer-than-ambient air leaving the offices to flow upwards through the DSF and exit the building. This Top-Up (T-U) flow pattern would likely prevent any overheating to occur due to flow reversal. Using this configuration, the lower and upper DSF vents are alternately opened and closed depending on the air temperature inside the DSF (Figure 5-6). To provide enough stack height to induce sufficient flow rates through the upper floors during the T-U flow pattern, the DSF and in turn the opening at its top were allowed to extend two floors above the segment's upper floor in the same manner as the opening at the top of the atrium.

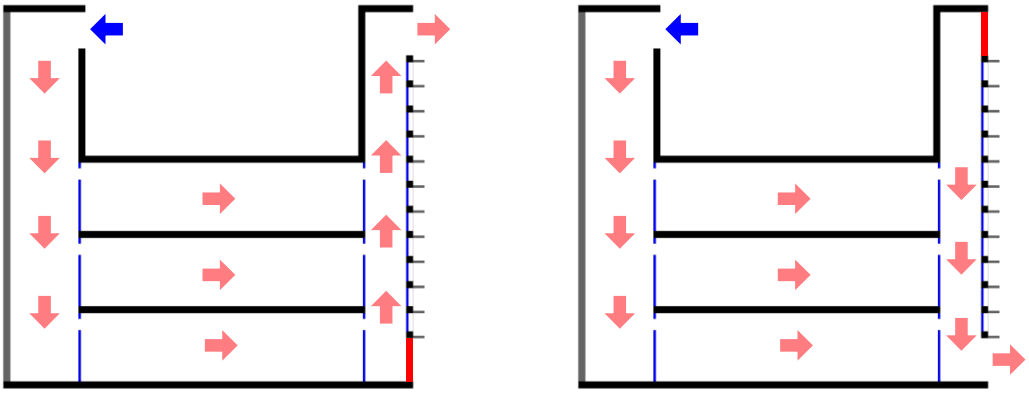

T-U/C-E Flow Pattern

T-D/C-E Flow Pattern

Figure 5-6 Flow Patterns for the Base Case model during PDEC operation in the early working hours

5.3.2 Resizing of the PDEC Components

Due to the introduction of another vent at the top of the DSF, a readjustment of the opening sizes of the PDEC components had to be carried out to achieve the required flow rates during the T-U/C-E flow pattern. For the sake of simplicity, the area of the opening at the top of the DSF was assumed to be equal to the area of both the opening at the top of the Atrium and the opening at the bottom of the DSF. The EFM method described in Section 4.3.5.1 was again used. The same boundary conditions for the T-U flow pattern were also used but external and supply temperatures were taken as their respective averaged values over the duration of flow reversal in the Pilot model. Heat gains were also reduced to account for relatively smaller solar gains during the same period. It was found that the opening sizes calculated for all PDEC components during the T-U/C-E flow pattern were smaller than those that were previously calculated for the other modes of operation. Accordingly, the sizes of the PDEC components used for the PM were maintained for the BCM.

5.3.3 Aperture Modulation and Control Logic

The large and rapid fluctuations in temperatures resulting from the alternate on and off switching of PDEC when internal temperatures approach t_{isp} in the PM implies the need for close control of aperture opening size. If the PDEC system were to serve a single floor, airflow modulation could have been achieved by either modulating the size of the aperture at the segment's inlet opening or by controlling the quantity of water supplied for evaporation, i.e. by controlling the number of misting nozzles in operation. However, since the PDEC system is designed to serve multiple floors, modulation is individually delegated to each floor's aperture at the atrium/office interface. The control logic implemented in the BCM was thus developed to comprise a Global Logic for determining the appropriate mode of operation and the consequent opening and closing of the segment's inlet and outlet openings and a Local Logic for individually controlling the apertures at the atrium/office and office/DSF interfaces at each floor.

As with the PM, the aim of the BCM's control logic is to maintain internal conditions within the adaptive comfort boundaries as defined by ASHRAE standard 55. One other aspect that also needed to be factored in before setting up the control logic was the choice of overheating criterion to be used to assess the performance of the BCM. The overheating criterion has a bearing on the control logic because it would be differently set up if, for example, Exceedance_M (Borgeson & Brager, 2011), which refers to the number of hours during which internal conditions exceed a specific threshold, is used rather than the magnitude and duration of departure of internal conditions from the comfort/neutral temperature (Nicol et al., 2009). A control logic appropriately based on the former

criterion is likely to result in operative temperatures stacked closely under the upper boundary of the 90% acceptability range for the majority of the occupied hours whereas one based on the latter is likely to result in internal conditions more normally distributed around the neutral/comfort temperature. Applying the latter criterion on a model with a control logic based on the former would likely result in an overestimation of overheating whilst the opposite would likely result in overconsumption of water and/or energy with no significant reduction in overheating.

For the BCM, it was decided that the magnitude and duration of departure of operative temperatures from the neutral/comfort temperature of the ACM as defined by ASHRAE standard 55 would be used for assessment and so, the control logic was set up accordingly. The effect of adopting other overheating criteria and comfort models will be investigated in the next chapter.

5.3.3.1 The Global control logic

As mentioned above, the global control logic determines the segment's mode of operation at each timestep. Here, in addition to the three passive modes used in the PM, namely; NC, NV, and PDEC, the BCM is also allowed to employ the auxiliary AC mode to maintain satisfactory internal conditions should these become untenable for occupants under passive modes. This would also enable quantification of potential energy savings compared to a conventional fully air-conditioned building. Moreover, for the sole sake of convenience in describing the global control logic in the following section, the period wherein all apertures are closed, and no passive or active cooling is

required will be considered here as a mode in itself and will be referred to as the Neutral Mode (NM). The global control logic assumes the following:

For occupied hours (8:00 to 18:00 on weekdays)

During occupied hours, determination of the segment's mode of operation for the current timestep depends, not only on concurrent external and internal conditions, but also on the segment's preceding mode of operation that had given rise to those internal conditions. In other words, for the same set of concurrent external and internal conditions, the control logic would select different modes of operation for the current timestep for different modes of operation at the preceding timestep. So, for instance, if the external dry-bulb temperature exceeds a predefined upper limit, the segment would not be allowed to operate in NV provided that all other conditions for NV are met if it were operating in NM at the previous timestep but would be allowed otherwise. The global control logic is described below by showing how it was set up to respond to external and internal conditions for each of the possible modes of operation at the preceding timestep.

Segment in Neutral-mode (NM)

1- Similar to the PM, if the segment was in NM when the operative temperature (t_{op}) in any office floor of the segment exceeds the initiation setpoint temperature (t_{isp}), also taken here to be equal to t_{cmf_ASH}, either NV or PDEC could be initiated depending on external conditions. NV is allowed if the following conditions are met:

i. If the supply temperature, in this case the coincident external dry-bulb temperature (t_x), is lower than the internal dry-bulb temperature of that office floor (t_{db}).

ii. If t_x does not exceed the predefined upper limit for the supply air temperature (t_{s_max}) taken here to be equal to t_{lb_ASH}. However, t_{s_max} can be increased to t_{cmf_ASH} if the coincident outdoor relative humidity (RH) is greater than 80% to compensate for the fact that PDEC is not allowed to operate beyond that level.

Therefore, when t_{op} exceeds t_{cmf_ASH}, NV is only initiated if $t_x < t_{db}$ and $t_x < t_{s_max}$, in which case the segment is expected to operate in a B-U/E-C flow pattern wherein the openings at the bottom of the DSF and top of the Atrium are fully opened.

2- Otherwise, if $t_{op} \geq t_{isp}$ and at the same time $t_x \geq t_{db}$ and/or $t_x \geq t_{s_max}$, PDEC could potentially be initiated if the following two external conditions are satisfied:

i. If the outdoor relative humidity (RH) is lower than 80%.

ii. If the coincident supply temperature, this time the PDEC outlet temperature (t_{PDEC}) is lower than the internal dry-bulb temperature of that office floor (t_{db})

That is, if $RH < 80$ and $t_{PDEC} < t_{db}$, PDEC is initiated. During PDEC operation, if the dry-bulb temperature in the DSF (t_{DSF}) is lower than t_x, the vent at the bottom of the DSF is fully opened and the building operates in a T-D/C-E flow pattern. Otherwise, the vent at the top of the DSF is fully opened and the building operates in a T-U/C-E flow pattern.

3- If conditions for NV and PDEC as described above are not satisfied, the segment remains in NM wherein all apertures of the segment are closed, and ambient air is only supplied at minimum fresh air rate requirements. In this case, if t_{op} in any floor exceeds another predefined setpoint, this time for mechanical air conditioning (t_{AC}), AC in that floor is activated. To maintain internal conditions within the 90% acceptability range of the adaptive comfort model as defined by ASHRAE standard 55 before AC activation, t_{AC} was taken to be 0.2K lower than the temperature at the upper boundary of that range (t_{ub_ASH}), that is, $t_{AC} = (t_{ub_ASH} - 0.2)$. During AC mode, the thermostat was set to maintain internal conditions just below a PMV value of +0.5, i.e. at a PPD of just under 10%.

Segment operating in Natural Ventilation mode (NV)

1- In this case, the segment continues to operate in NV mode if t_{op} in all floors remains lower than t_{isp} irrespective of any other condition. It has to be noted that no upper limit was imposed on the supply temperature once NV is initiated. This means that the segment is allowed to continue in NV mode even if $t_x > t_{s_max}$.

2- Otherwise, PDEC is initiated if t_{op} in any office floor continues to rise above t_{isp} with the aperture at the atrium/office interface of that floor fully opened for two consecutive timesteps provided that $RH < 80\%$. This measure was taken to prevent excessive overheating because although NV in this case is operating at full capacity, internal temperatures continue to rise above t_{isp}.

3- In the meantime, if t_{op} in any office floor exceeds another predefined setpoint, henceforth referred to as the changeover setpoint temperature (t_{csp}), PDEC is initiated, again provided that RH < 80%. In keeping with the selected overheating criteria, t_{csp} was taken here to be only 1K above t_{cmf_ASH}, i.e. $t_{csp} = (t_{cmf_ASH} + 1)$.

4- If, however, $RH \geq 80\%$, then the previous conditions are ignored, and the segment continues to operate in NV mode so long as $t_x < t_{db}$ until t_{op} in any floor exceeds t_{AC} when at that point, AC is activated on that floor. Note here that the segment continues to operate in NV mode to serve all other floors. If t_{op} in all floors exceeds t_{AC}, all apertures are closed and all floors in the segment operate in AC mode.

Segment operating in Evaporative Cooling mode (PDEC)

1- When the segment is operating in PDEC mode then it is possible to revert to NV mode under certain circumstances. The fact that the segment has already been switched to PDEC mode implies that the external dry-bulb temperature has risen to a degree that renders NV insufficient to sustain a comfortable internal environment. As the day progresses, external temperatures would continue to rise and the conditions unfavourable for NV operation are likely to prevail until late in the afternoon when external temperatures start to drop again. Only then is the segment allowed to revert to NV and is restricted to instances when $t_x < t_{s_max}$ at the current timestep and $t_x \geq t_{s_max}$ at the previous timestep.

2- If either of the previous conditions is not satisfied, the segment continues to operate in PDEC mode provided that RH remains lower than 80%.

3- However, if *RH* exceeds 80% or if t_{op} in any office floor exceeds t_{AC} and continues to rise while the aperture at the atrium/office interface of that floor is fully open, AC is activated. If the reason for activating AC is the latter rather than the former, the segment continues to operate in PDEC mode to serve the other floors. If t_{op} in all floors exceeds t_{AC}, all floors operate in AC mode and the apertures in the whole segment are closed.

Floor operating in Air Conditioning mode (AC)

1- Again, similar to the case when PDEC is in operation, if a floor is operating in AC mode then it is possible to revert to NV mode if external conditions for NV become favourable again, that is if $t_x < t_{s_max}$ at the current timestep and $t_x \geq t_{s_max}$ at the previous timestep.

2- If not, the floor could alternatively revert to PDEC mode if the following two conditions are satisfied;

   i. It was anticipated that at some instances, AC could be activated not because t_{op} had exceeded t_{AC} but because *RH* had exceeded 80% rendering PDEC inapplicable. It is for these instances that the control logic was assumed to allow the segment to revert to PDEC from AC mode if *RH* drops below 80%.

   ii. Moreover, although no upper limit was imposed on t_{PDEC} (the supply temperature during PDEC operation), it was envisaged that it would be more fitting to assume one when reverting to PDEC from AC mode as a conservative measure. Reverting to PDEC mode was therefore also restricted to instances when $t_{PDEC} < t_{cmf_ASH.}$

Accordingly, in order for the segment to revert to PDEC from AC mode, then, for the current timestep, *RH* must be lower than 80% and t_{PDEC} lower than t_{cmf_ASH} when either RH was greater than 80% or t_{PDEC} was greater than t_{cmf_ASH} at the previous timestep.

3- Otherwise, the floor continues to operate in AC mode.

For unoccupied hours

1- When the external dry-bulb temperature drops below the internal dry-bulb temperate in any office floor and the latter exceeds t_{lb_ASH}, nighttime ventilative cooling (NC) is allowed. As with NV mode, the openings at the bottom of the DSF and top of the Atrium are fully opened and the segment operates in a B-U/E-C mode.

2- Otherwise, all apertures are closed, and no intentional airflow is allowed.

3- Note here that for the Base Case, PDEC was not allowed to operate outside occupied hours. However, this alternative has been explored in the following chapter (Section 6.3) to determine the benefits of cooling the building's structure during the night to reduce radiant heat gains the following day.

5.3.3.2 The Local control logic

The local control logic assumes that airflow control for each office floor is located at the aperture on the atrium/office interface. This is achieved by ensuring that the aperture has the smallest opening size, i.e. induces the

largest pressure drop in the office floor's airflow path at any given timestep. To maintain the required thermal conditions inside the office at each timestep, the area of the aperture is set to vary according to a set of criteria that correspond to prevailing internal and external conditions.

Given the scale of the building and the complexity of integrating the airflow network model with the thermal model as discussed in Chapter 4, a 5-minute timestep was assumed (Robinson et al., 2004). This was considered a reasonable compromise between exhaustive computational demands and the high levels of accuracy required. However, even with this relatively small timestep, the area of the aperture at each timestep needed to be carefully calculated.

At each timestep, the area of the aperture at the atrium/office interface was taken to be equal to the maximum area of the aperture multiplied by an opening factor and is given by the following relation

$$A_A = A_{MAX} * OF \qquad \text{Equation 5-1}$$

where A_A is the area of the aperture at the atrium/office interface at a given time-step, A_{MAX} the maximum area of the aperture as calculated by the EFM method in Section 5.3.2, and *OF* the opening factor at that time-step. *OF* ranges between 0.0 when the aperture is closed (so that A_A = 0.0) and 1.0 when the aperture is fully open (so that $A_A = A_{MAX}$).

The increase in aperture size from 0.0 to A_{MAX} (corresponding to an increase in *OF* from 0.0 to 1.0) occurs in discrete steps rather than in a continuous fashion to emulate the action of window actuators in actual buildings. It was

assumed that the increments by which the area of the aperture increases from one step to the next would start small and increase progressively. This was implemented in anticipation of the abrupt variations in internal conditions likely to occur when the aperture is initially opened during occupied hours or when a sudden change in the supply temperature occurs (as is the case when the mode of operation changes from NV to PDEC). Accordingly, the value of *OF* was set to increase from 0.0 to 1.0 in 6 progressively increasing steps; 0.05, 0.1, 0.2, 0.4, 0.65, and 1.0.

At each timestep, the value of *OF* is determined as follows:

<u>For occupied hours</u>

1- Once t_{op} in any office floor exceeds t_{isp} and either NV or PDEC is initiated (depending on coincident external conditions as discussed in the global control logic), the aperture at the atrium/office interface of that floor is opened to its initial size (*OF* = 0.05).

2- If this initial increase in *OF* induces sufficient flow to maintain t_{op} at or below its previous value, *OF* remains the same. However, if t_{op} continues to rise, *OF* increases by another increment and so on. This pattern continues until *OF* reaches its maximum value of 1.0.

3- If t_{op} continues to rise beyond this point for two consecutive timesteps and the segment was operating in NV mode, PDEC is initiated. In this case, if the difference between the supply air temperature in NV mode and PDEC mode is more than 2K (i.e. $t_x - t_{PDEC} > 2$), *OF* reverts to its

minimum value of 0.05 to avoid abrupt changes in internal conditions. Otherwise, the value of *OF* remains the same. This last condition also applies to the apertures of all the other floors, which may not have necessarily reached their maximum opening size when the mode of operation had changed from NV to PDEC.

4- On the other hand, if the segment was operating in PDEC mode when *OF* in any floor reaches its maximum value of 1.0 and t_{op} continues to rise, then PDEC is allowed to continue until t_{op} exceeds t_{AC}. At that point AC is activated on that floor and the aperture is closed (*OF* = 0.0).

5- If at any time during NV or PDEC operation, t_{op} drops below t_{isp}, the value of *OF* remains the same until t_{op} exceeds t_{isp} again and the pattern described above is then repeated.

6- However, if t_{op} drops to a temperature lower than 1K below t_{isp}, the value of *OF* decreases incrementally and continues to do so until t_{op} starts to rise again. In the meantime, if at any point t_{op} drops below t_{lb_ASH}, *OF* is set to its lowest value of 0.05. These two measures were taken to prevent overcooling and minimise water consumption.

7- At certain instances during NV or PDEC operation, *OF* is set to its maximum value of 1.0 irrespective of any other condition in a measure to maintain internal conditions as close as possible to t_{cmf_ASH} as follows;

   i. If the segment reverts to NV or PDEC from AC, or to NV from PDEC.

   ii. If t_{op} exceeds t_{csp} during PDEC mode (or during NV mode only if *RH* > 80, i.e. when PDEC cannot be used and $t_{op} < t_{AC}$).

iii. If, after the segment had been operating in NC mode, the difference between the supply air temperature in NC mode and PDEC mode is less than 2K (i.e. $t_x - t_{PDEC} < 2$) and PDEC is required at the beginning of the day (which, according to the global control logic, means that $t_{op} > t_{isp}$ while $t_x > t_{db}$ and/or $t_x > t_{lb_ASH}$).

For unoccupied hours

The local control logic for unoccupied hours is much simpler than the one employed during occupied hours and assumes the following

1- Night time cooling (NC) is only allowed when the internal dry-bulb temperature is higher than t_{lb_ASH} and higher than the external dry-bulb temperature

2- In this case, if the difference between external and internal dry-bulb temperatures is more than 3K ($\Delta t \geq 3$), the value of *OF* is limited to 0.05 (*OF* = 0.05)

1- Otherwise, the aperture is fully open and *OF* is set to its maximum value (*OF* = 1.0)

As with the PM's Control Logic, the complete algorithm for the BCM aperture modulation Control Logic can be found in the Appendix B.

5.4 Results and Discussion

To allow comparisons with the PM, the BCM in the following section was modified whereby the AC mode was omitted. To differentiate between the BCM with an auxiliary AC mode and that without, the former will henceforth be referred

to as BCM_AC. Figure 5-7 shows the internal conditions in the second floor (mid-floor) of the segment on the 17th of August for the BCM. Compared to profiles in Figure 5-5, it is clear that the two issues highlighted in the results of the PM have been resolved. The marked increase in internal temperatures that were present at the beginning of the day in the PM has not occurred in the BCM, despite having the same setpoint for NV/PDEC initiation, which suggests that the reduction could mainly be attributed to the addition of the upper DSF outlet. Furthermore, the fluctuations occurring in the PM when t_{op} was approaching t_{isp} in the PM have all disappeared as indicated by the smooth profile of t_{op}.

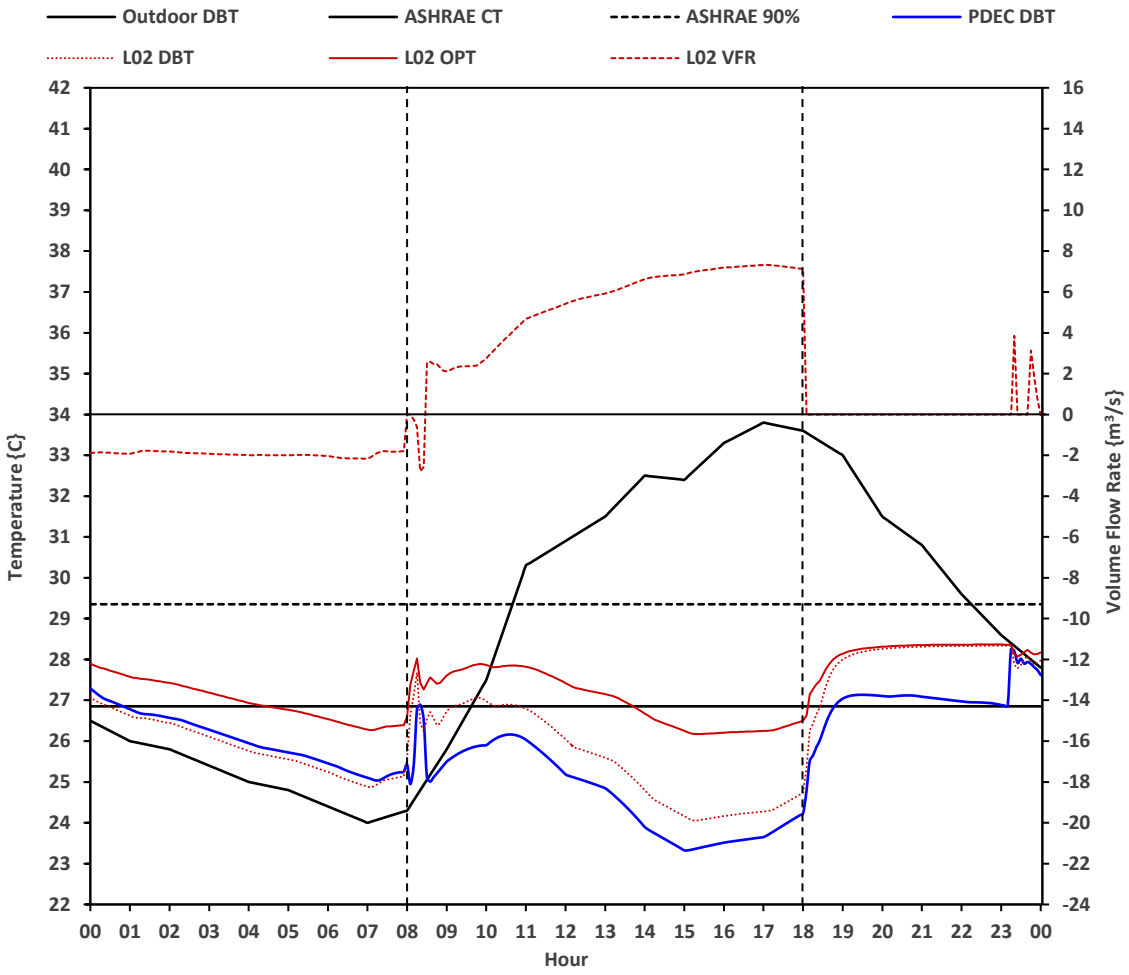

Figure 5-7 Dry-bulb temperature and Airflow rate profiles for the middle floor of the Base Case Model on the 17th of August

To highlight the effect of adding an upper outlet to the DSF, it is useful to compare internal conditions in the first third of the working day when it is most likely that the T-U/C-E flow pattern occurs in both models. Figure 5-8 shows the number of hours in which t_{db} exceeds 27°C during occupied hours of the cooling season for the segment's middle floor.

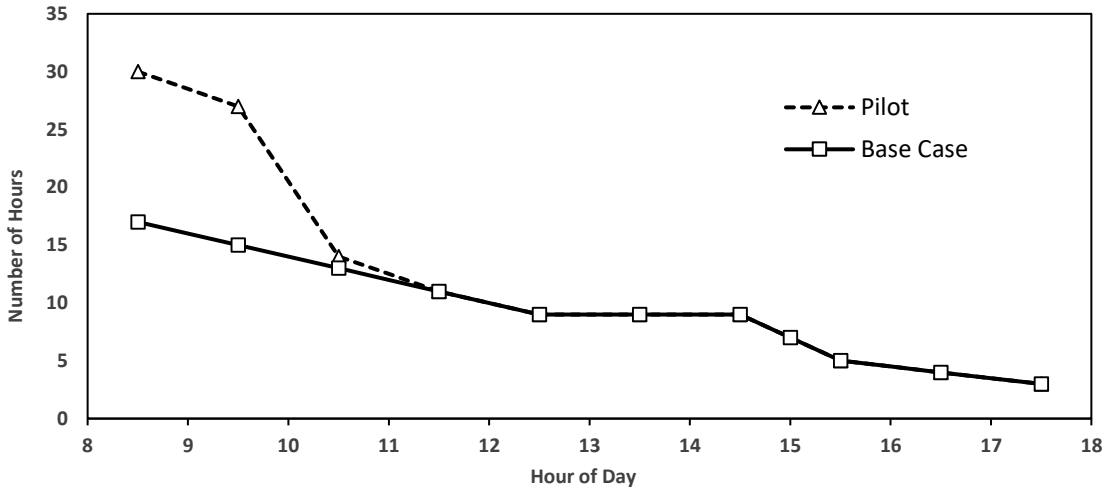

Figure 5-8 Number of hours in which t_{db} exceeds 27°C during occupied hours of the cooling season for the segment's middle floor

The number of hours above 27°C during the first hour of the working day for the BCM has been reduced from 30 to 17, a reduction of nearly 45%. This means that only 17 days during the cooling season witness an internal dry-bulb temperature higher than 27°C between the hours of 08:00 and 09:00 as opposed to 30 for the PM. This pattern continues for the first four hours of the working day albeit with a diminishing difference between the two models until midday when both equally perform, and the two profiles overlap.

On the other hand, to quantify the stability of internal conditions, the sum of the number of crests and troughs in the dry-bulb temperature profile of the

segment's middle floor was calculated. A crest occurs when the value of t_{db} at a certain timestep is higher than its values at both the preceding and following timesteps and a trough occurs when it is lower. The number and magnitude is only calculated when these fluctuations occur due to a change in the size of the aperture at the atrium-office interface instigated by the control logic. Figure 5-9 clearly shows the effect of aperture modulation in BCM on the stability of internal conditions as compared to the PM.

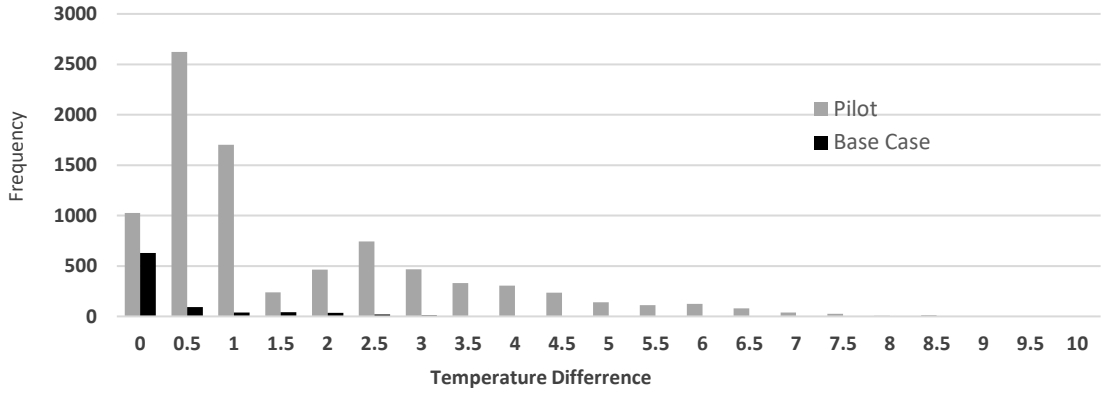

Figure 5-9 Number and magnitude of temperature fluctuations occurring during occupied hours of the whole year due to changes in the aperture size at the atrium/office interface of the segment's middle floor

5.4.1 Overall Performance

The main objective of the thermal simulations is to predict the performance of the PDEC strategy in terms of its capacity to provide the cooling required to achieve thermal comfort in all floors of the segment and accordingly, its capacity to deliver an even distribution of the required flow rates across the segment's floors. The associated environmental costs in terms of water and energy consumption are also assessed. It has to be noted that Instead of aggregating the results into hourly data, the 5-minute timestep implemented in the simulations

has allowed for a much finer temporal resolution and results are thus analysed and represented.

The energy required for mechanical cooling of the BCM_AC for the whole year is presented in Table 5-1. The main point beckoning to be highlighted is the fact that the longest duration in which AC mode operates in any floor does not exceed 0.5% (~12 hrs) of occupied hours for the whole year (resulting in near-zero values for the annual supply cooling energy per unit area). This has prompted a revisit of the results of the BCM to determine whether internal operative temperatures had actually exceeded the upper boundary of the 90% acceptability range and in turn, whether AC was required in the first place given that the control logic in the BCM_AC was set to initiate AC if t_{op} exceeds t_{AC} which was set to be 0.2K lower than t_{ub_ASH}.

Table 5-1 Annual cooling energy for the BCM_AC

Parameter	**L01**	**L02**	**L03**
Proportion of time AC Mode in Operation	0.2%	0.2%	0.5%
Annual Supply Cooling Energy (kWh/yr)	26.5	27.5	74.8
Annual Supply Cooling Energy per Occupied Unit Area (kWh/m^2.yr)	0.22	0.23	0.62

Accordingly, focus was shifted to the BCM of which the overall performance results for the whole year are summarised in Table 5-2. Simulations show that the internal operative temperatures of the BCM lie within the 90% acceptability range (t_{cmf_ASH} ± 2.5) for more than 99.9% of occupied hours during the cooling season for the upper floor of the segment and for nearly 100% of the time for the lower and middle floors.

Table 5-2 Summary of whole-year results for the BCM during occupied hours only

Parameter	L01	L02	L03
Proportion of time $t_{op} > t_{ub_ASH}$ (%)	0.0% (<1hr)	0.0% (<1hr)	0.1% (<2hr)
Annual Water Consumption per unit area (l/m^2)		420	
Daily Water Usage per Occupant (l/person/day)		9.1	
Maximum number of nozzles required (6 l/hr per nozzle assumed)		94	

The results also show that the predicted daily water consumption of the evaporation system calculated per occupant is 9.1 litres, a significant quantity when considered in isolation, but one that represents approximately 4% of the average per capita daily consumption of clean water in Egypt, currently at 211 litres (CAPMAS, 2015). Assuming that each microniser or misting nozzle in the evaporation system delivers 6 litres of water per hour, the number of nozzles required for the whole segment to deliver evaporative cooling at peak demand was estimated to be 94 (approximately 2 nozzles/person or 0.25 nozzles/m^2).

The proportion of time in which the segment operates in each mode (flow pattern) during occupied hours is presented in Figure 5-10. Operating for just over 50% of all occupied hours of the whole year, PDEC (T-D) is the most dominant mode of operation followed by NV (B-U) at 43%. It was not surprising to find that the segment operates in PDEC (T-U) mode for only 4% of occupied hours as internal temperatures during PDEC operation only exceed external temperatures in rare cases when both the wet-bulb depression is low, and NV is insufficient and even when this occurs it is usually short-lived. Overlaying the monthly mean external temperature profile on the chart clearly shows that the proportion of time in which PDEC operates during occupied hours for each month follows a very similar but reversed trend to that of the profile.

5.4.2 Overheating and Comfort

The Overheating Risk Index (ORI), is a measure that relates the magnitude of the departure of actual or predicted operative temperatures from the comfort temperature to the proportion of people (*P*) voting 'warm' or 'hot' on the ASHRAE comfort scale (the accepted definition of discomfort from heat) and is applied only for occupied hours in which the space is operating in a free-running mode; primarily NV but extended in this study to include PDEC as well (refer to §5.2.1.3 for more on this). It was first derived from a logistic regression analysis based on comfort surveys in European office buildings (Nicol et al., 2009) in which the difference between recorded operative temperatures and the adaptive comfort temperature as defined by the EN15251 standard was used. Another exercise was conducted (Carlucci, 2013) to derive a similar index, this time based on the adaptive comfort temperature as defined by ASHRAE standard 55. This index, henceforth referred to as ORI_{ASH} to differentiate it from the one above, was the one used to assess overheating in this analysis.

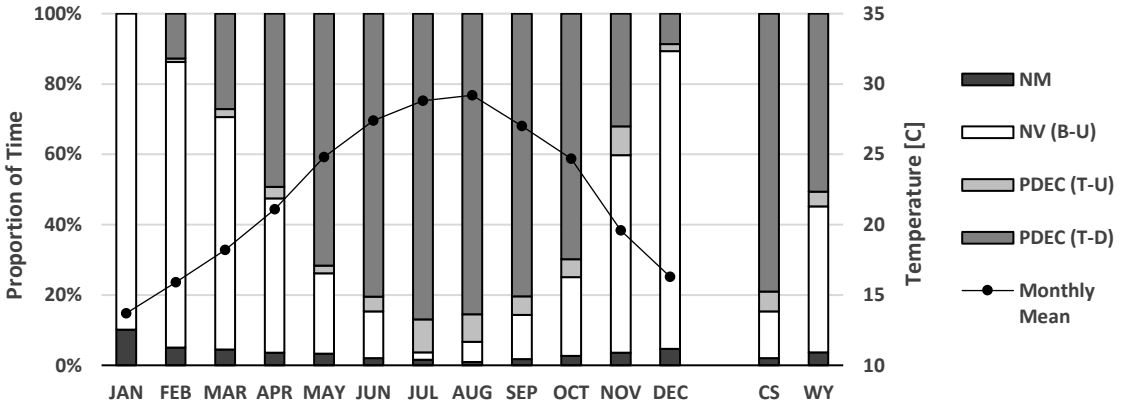

Figure 5-10 Monthly, seasonal, and whole-year proportion of time in which the segment operates in each mode (flow pattern) during occupied hours

Assessing the likelihood of overheating in the way ORI_{ASH} does, differs from one that merely relates overheating to a particular threshold such as the temperature at the upper boundary of the 90% acceptability range of ASHRAE's ACM. In this 'Exceedance Index' (EXI_{ASH}) as will be referred to henceforth, all instances in which the operative temperature does not exceed the threshold are considered to be equally comfortable and vice versa. As such, a timestep in which the operative temperature is just below the boundary would be counted towards the total duration in which comfort is achieved as much as one that is nearer to the comfort temperature. In reality, the proportion of occupants that would find internal conditions uncomfortable are likely to vary markedly in the two cases. Another advantage that stems from the way the two indices operate is that the ORI_{ASH} would potentially be more sensitive in identifying discrepancies in comfort conditions than the EXI_{ASH} and thus would be more apt for exercises that require ranking of, or comparison between, two spaces or models. For instance, given two spaces in which the operative temperatures for the whole duration of interest lie under the threshold. In one space, operative temperatures for the majority of the time are stacked below the upper boundary whilst in the other they are closer to the comfort temperature. The Exceedance Index would not pick up any difference between the two spaces in terms of comfort and overheating whilst the Overheating Risk Index would.

The overall results of the BCM represented above show that operative temperatures in all floors of the segment have remained within the boundaries of the 90% acceptability range of ASHRAE's ACM for nearly all occupied hours, which according to EXI_{ASH}, indicates that no overheating occurs in all three floors

of the segment. However, using the ORI_{ASH} shows a different picture. The proportion of subjects voting warm or hot (*P*) was calculated at each time step during occupied hours for all three floors of the segment. Aggregating those into a single value for each floor over the whole year by simply summing or averaging them to represent the ORI of that floor would have been tempting in the interest of simplicity and clarity. However, that figure is likely to be misleading because the same value of ORI in this case could have been equally arrived at by aggregating low values of *P* for long periods or high values of *P* for shorter periods which would not be very helpful in determining the severity and/or duration of overheating.

Another approach, adopted here, is to represent the ORI as a distribution of the values of *P* in terms of their frequency of occurrence. In this way, the duration and severity of overheating in each floor at various values of *P* can be determined in absolute terms as well as in relation to other floors. However, assessing the overall overheating risk in a straightforward way would still be difficult. For this, one could for example make use of percentiles in a manner similar to that used in CIBSE Guides A (CIBSE, 2006) and J (CIBSE, 2002) which suggest that temperatures inside offices should not exceed 28 °C for more than 1% of occupied hours and 25 °C for more than 5% of occupied hours respectively. Similarly, an index based on the distribution of *P* could require that, for a space to be considered comfortable, *P* should not exceed a certain maximum value for more than a specified limited proportion of occupied hours for the whole year and another intermediate value for a relatively longer duration.

In the absence of such guidelines, a visual assessment such as the one inferred from Figure 5-11 would suffice. The first thing to notice from the chart is that the average values of *P* in all floors (vertical lines) during occupied hours of the cooling season almost coincide with the value of *P* at t_{cmf_ASH} (dashed line at 4.5%) indicating that the average difference between predicted operative temperatures and the comfort temperature is not significant. Furthermore, the dotted line marking the value of *P* at the upper boundary of ASHRAE's 90% acceptability range just passes the 12% mark which is higher than the 10% PPD originally used to demarcate that range. This suggests that a revision of the acceptability ranges in ASHRAE's ACM might be required.

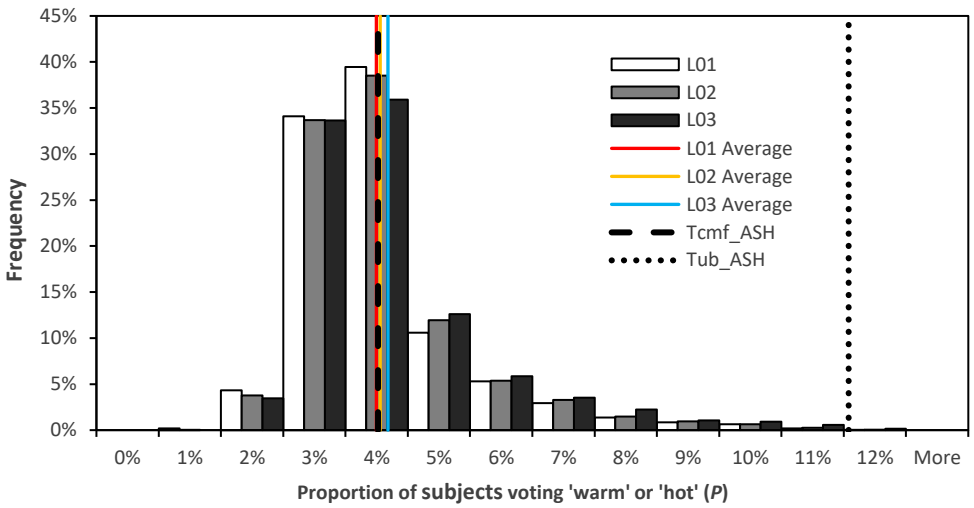

Figure 5-11 Distribution of the proportion of occupants voting 'warm' or 'hot' on the ASHRAE scale (*P*) during occupied hours of the cooling season

To determine whether the difference in overheating between the floors occurs at a specific time of the working day or is evenly spread over its course, the values of *P* where independently aggregated for each occupied hour during the cooling season as shown in Figure 5-12. The graph shows four sets of

profiles; the median of the hourly values of *P* (solid lines), values of *P* at the 75th (long dashed lines) and 95th percentile (dashed lines), and the hourly maximum values of *P* for the three floors of the segment (dotted lines).

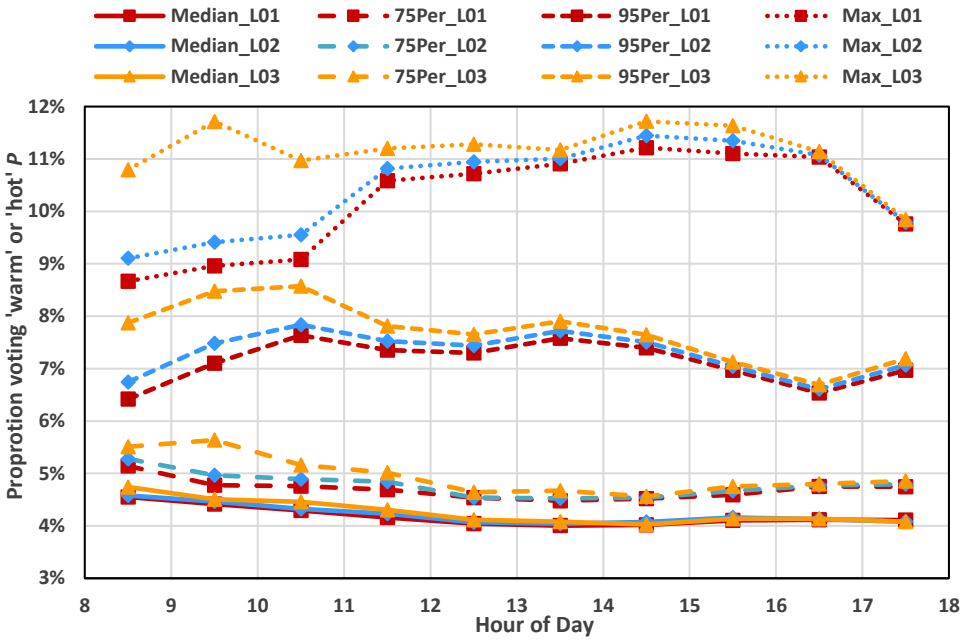

Figure 5-12 Percentile profiles for hourly aggregated values of the proportion of subjects voting 'warm' or 'hot' on the ASHRAE (*P*) scale for the three floors of the segment

It is clear that as the percentile increases, the difference in the values of *P* between the floors increases as well. This is generally the case for all hours of the working day although it is much more pronounced between the hours of 8:00 and 12:00. In light of the complex thermal exchanges taking place in buildings in general, it would be difficult to attribute this disparity in thermal conditions between the floors of the segment to one single cause. However, the fact that all assumptions about internal heat loads, occupancy patterns and the thermophysical properties of the envelope apply equally to all floors of the segment, suggests that this disparity, particularly in internal conditions at the early

hours of the occupied period, is likely to be caused by differences in airflow rates occurring in each floor due to its relative vertical position within the segment. Airflow rates influence internal conditions in each floor in two ways; directly in the form of convective heat exchanges during the day, or indirectly through their capacity to purge heat stored in the structure during the previous night which subsequently impacts radiant heat exchanges taking place the following day. To appreciate this in more detail, focus is shifted to the analysis of the bulk airflow rates in the segment.

5.4.3 Airflow rates

One of the objectives of the BCM was to investigate whether sufficient airflows can be generated under a buoyancy only scenario. A summary of the maximum achievable airflow rates in the segment are presented in Table 5-3.

Table 5-3 Summary of whole-year results for airflow rates in the BCM

Parameter	Value	Occurs on
Maximum airflow rate through segment inlet [m^3/s]	25.2	17 SEP
Maximum airflow rate through atrium/office aperture [m^3/s (ACH)]	9.2 (92)	11 SEP on Upper floor
Maximum air velocity at atrium/office aperture [m/s]	1.1	11 SEP on Upper floor
Maximum average air velocity traversing offices [m/s]	0.3	11 SEP on Upper floor

Figure 5-13a shows the monthly average volume airflow rates during occupied hours for the three floors of the segment. Note here that an airflow rate of 1 m^3/s is equivalent to 10 ACH given that the volume of each floor in the 10m slice of the segment is 360 m^3. Note also that since the BCM was developed to alternate between two modes of operation that have opposite flow paths and therefore opposite signs for their resulting airflow rates; and since within each operating mode, a reverse flow could potentially occur that would also result in

airflow rates with opposite signs; then, in order to calculate the average values of a period of interest, the sum of the values of airflow rates at each timestep had to be calculated separately for each mode and the absolute values of those two figures then added and divided by the total number of timesteps within that period.

The results indicate that average monthly airflow rates vary significantly from one month to the other and tend to increase as the average monthly external temperature increases (Figure 5-10), ranging from an average value of approximately 1.2 m^3/s in May to 5 m^3/s in August. This should be expected given that the cooling loads in the warmer months tend to be higher which in turn beget higher flow rates and consequently larger *OF* values as evident in Figure 5-13b. It could be argued however, that the extent to which the values of *OF* need to increase is likely to have been partially offset by the fact that when the temperature differential is quite large, as is likely to be the case during PDEC operation, and accordingly during months when PDEC is the predominant operating mode (Figure 5-10), the driving forces tend to be higher owing to the fact that in a no-wind scenario like the one assumed in the BCM, buoyancy—generated by temperature differences between internal, external, and supply air temperatures (in the case of PDEC)—is the only force driving airflow through the segment.

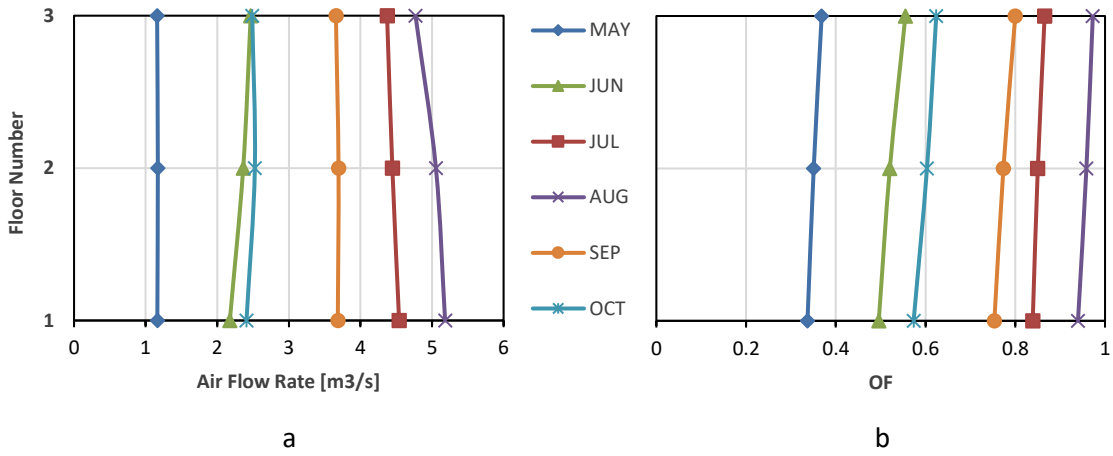

Figure 5-13 Monthly average volume flow rates (a) and monthly average *OF* values (b) during occupied hours of the cooling sea

With regards to the disparity in internal conditions between the three floors discussed in the previous section, the results show that not only do the average airflow rates in the whole segment increase with monthly average external temperatures, but that there is also a progressive, albeit slight, reduction in the average airflow rates on the upper, and less so in the middle, floors of the segment despite the fact that the monthly average values of *OF* on those two floors are consistently larger (Figure 5-13b). This pattern is reversed for the relatively more temperate months of the cooling season. A look at the average flow rates for each flow pattern independently (Figure 5-14) reveals that the flow rates during the T-D flow pattern (Figure 5-14c) tend to be consistently equal across the floors for all months of the cooling season. On the other hand, when the segment is operating in the B-U and T-U flow patterns (Figure 5-14a & Figure 5-14b respectively), the difference in flow rates between the upper and lower floor tend to progressively increase, ranging from a difference of only 0.1 m^3/s (representing a 16% reduction) and 0.2 m^3/s (25% reduction) in May to as much

as 1.2 m^3/s (54% reduction) and 1.75 m^3/s (66% reduction) in August for the B-U and T-U flow patterns respectively.

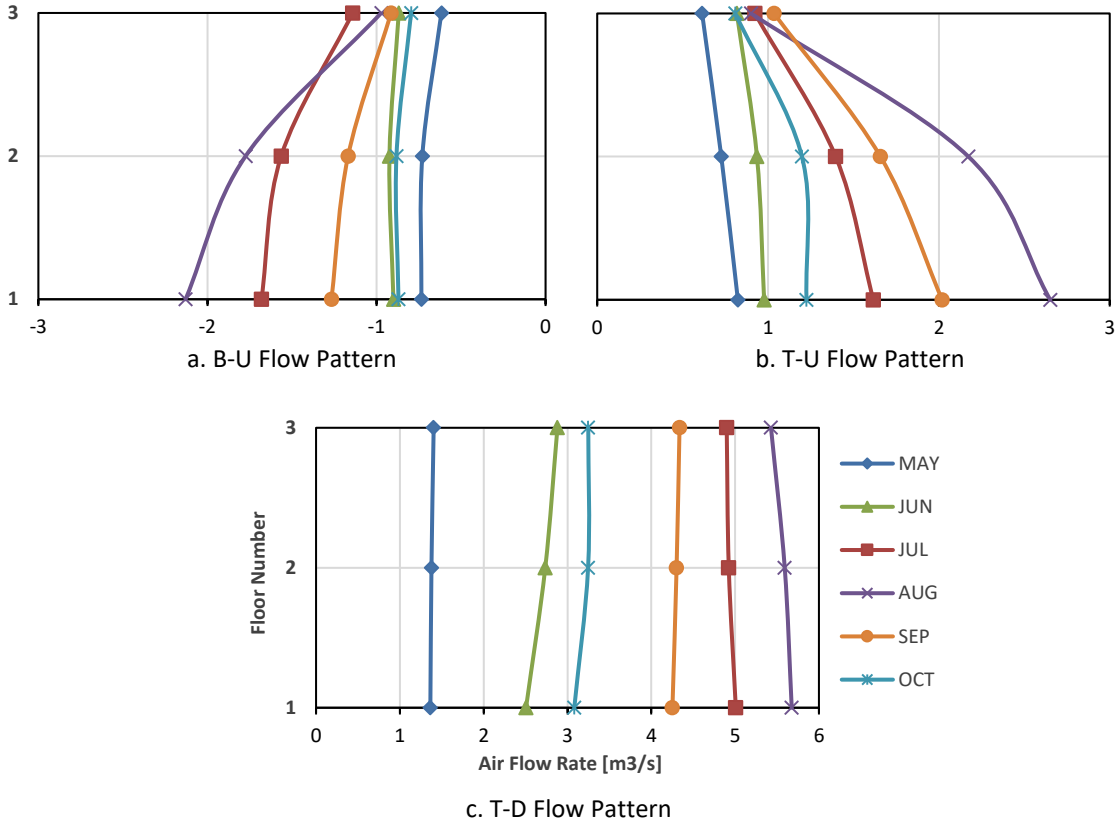

Figure 5-14 Monthly average airflow rates during occupied hours for a) B-U flow pattern, b) T-U flow pattern, and c) T-D flow pattern

Results presented in Figure 5-13 and Figure 5-14 suggest that there is a correlation between the average value of *OF* for a given month and the disparity in the average airflow rates between floors of that month; the larger the *OF* monthly average the greater the disparity. This can be demonstrated by looking at the airflow rates of the BCM aggregated for instances when the values of *OF* on all floors are equal (Figure 5-15). The averages were aggregated for each flow pattern independently over the duration of the cooling season.

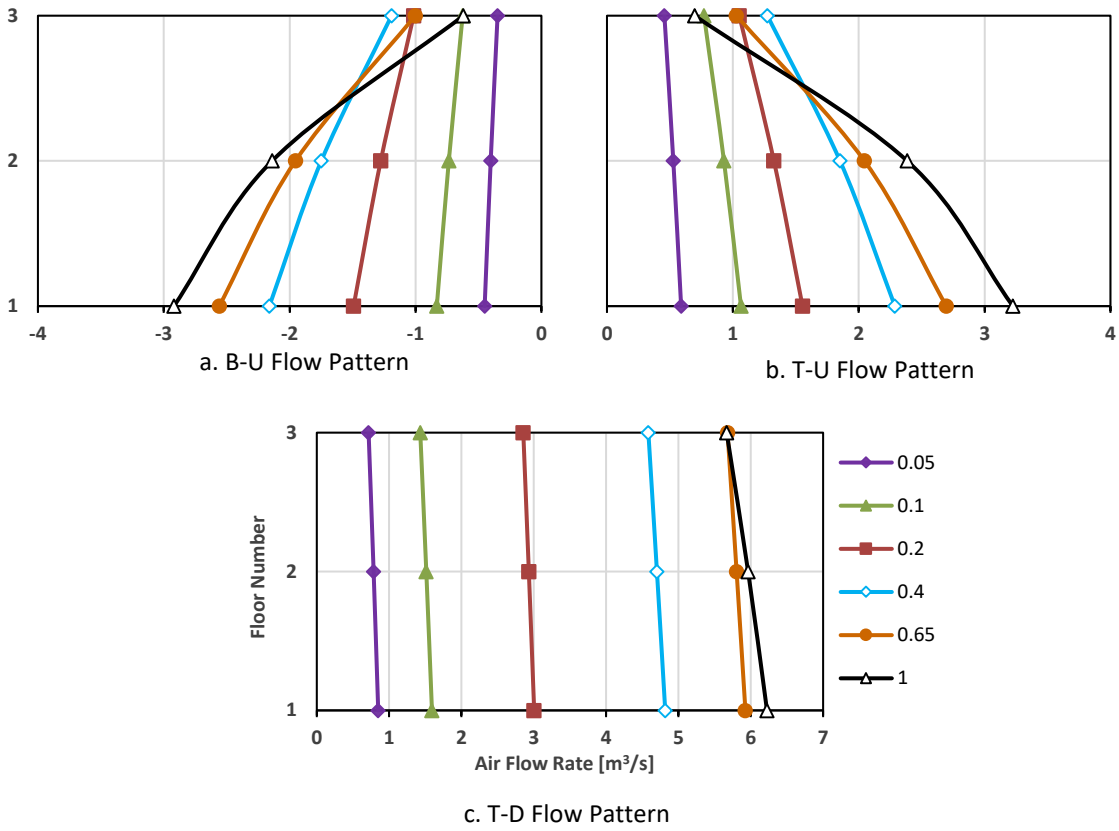

Figure 5-15 Average airflow rates at equal *OF* values during occupied hours for of the cooling season for a) B-U flow pattern, b) T-U flow pattern, and c) T-D flow pattern

For the T-D flow pattern, the results show that the average airflow rates on all floors equally increase with *OF* and as a result, the disparity in airflow rates between floors remains minimal for all values of *OF* other than 1.0 wherein the average airflow rate increases on the lower, and slightly less so, on the middle floor but not on the upper floor. However, for the B-U and T-U flow patterns, the results show that as *OF* increases, the variation in airflow rates between the floors progressively increases. This has significant consequences for the upper floor. When *OF* on all floors is equal, then for *OF* values greater than 0.4, average airflow rates on the upper floor tend to decrease rather than increase. This pattern is evident to the extent that when *OF* on all floors increases from 0.4 to 0.65, a

consequent increase in airflow rates occurs in the lower and middle floors but not in the upper floor which, to the contrary, actually witnesses a reduction in the average airflow rate dropping to the same average value as that when *OF* on all floors was 0.2. When *OF* on all floors increases to 1.0, again the same pattern occurs only this time the airflow rate in the upper floor drops even further to equal its value when *OF* on all floors was 0.1.

The sharp and progressive reduction in average airflow rates between the floors during the B-U and T-U flow patterns noted above explains the general trend seen in Figure 5-13a although it is less pronounced there because over the course of the cooling season, the predominance of the T-D flow pattern in terms of the proportion of time it occupies (Figure 5-10) dampens this effect. This disparity could also explain the marked difference in internal conditions occurring in the first 3-4 hours of the working day in the relatively warmer months (Figure 5-12), as it is only during that period of the day that the segment operates in either two before switching to a T-D flow pattern. This is clearly demonstrated in Figure 5-16 which shows the average volume flow rate profiles of the three floors aggregated over each timestep of the working day during the month of August plotted against the backdrop of the proportion of time in which each mode/flow pattern operates.

The graph shows that up until 9:00, the averaged airflow rates in all floors remain low and constant and the disparity between the lower and upper floor is nearly twofold. It is not surprising then to find that during that period of the day, the segment operates in a T-D flow pattern for only 10% of the total number of working days in August. The transition from a B-U or T-U flow pattern to a T-D

one mainly occurs during the period between 9:00 and 10:30, which is also the period when airflow rates in all floors start to pick up and the disparity between the three progressively decreases to completely diminish at around 12:00.

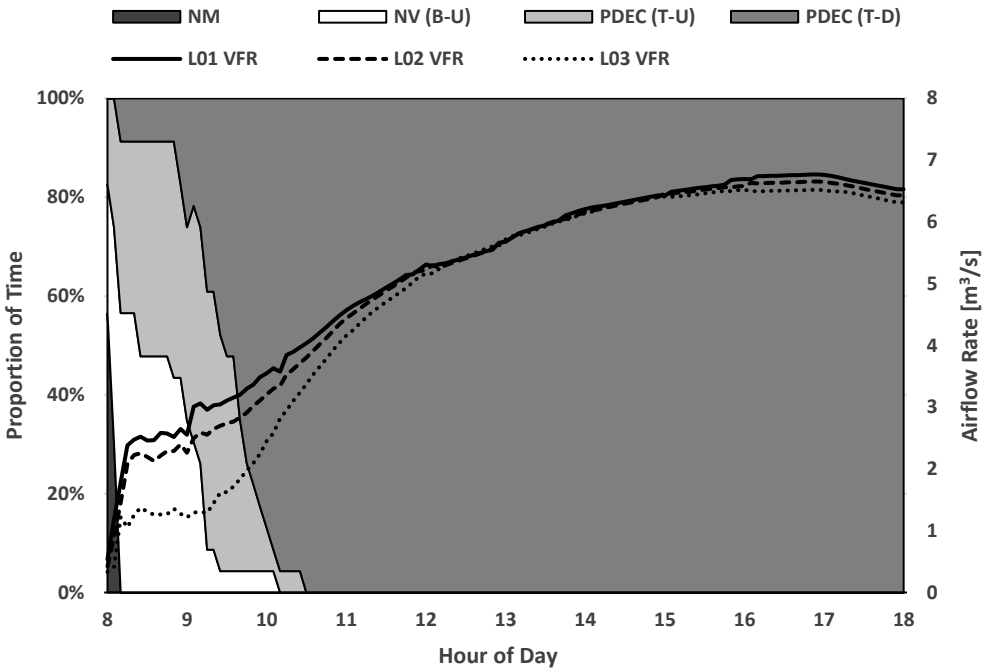

Figure 5-16 Timestep-averaged airflow rates and proportion of time operating modes/flow patterns occupy during the working hours of August

These observations confirm what had previously been suggested of the existence of a strong correlation between the mode of operation/flow pattern being employed and the disparity in airflow rates across the floors of the segment, especially during the warmer months of the cooling season. However, to understand why this to be the case, that is, why a disparity in airflow rates across the floors occurs in the first place during the B-U and T-U flow patterns and why it is more pronounced during the warmer months than it is during the relatively temperate periods of the cooling season, it was necessary to first identify the main factors that are likely to effect changes on the magnitude and distribution of

flow rates across the floors and that are also likely to have significantly different values for the two periods, and second to investigate how those factors actually influence the airflow behaviour of the segment.

It was beneficial here to make use of the simple mathematical model of stack ventilation flows in multi-compartment buildings developed by Acred and Hunt which elucidates the relationships between the core variables involved in such buildings, namely; flow rates, air temperatures, heat inputs and building geometry (Acred & Hunt, 2014). Although the model was developed for steady flows in buildings, it was still considered useful in providing a general picture of those relationships particularly because they are represented in a non-dimensional form.

Two factors were identified, the first and most obvious was the difference between external and internal air temperatures. This could be expressed more precisely as the ratio $R_{\Delta t}$ of the difference in air temperatures between the atrium and DSF Δt_S to the difference between the atrium and external air temperature Δt_A expressed as

$$R_{\Delta T} = \frac{|t_{DSF} - t_A|}{|t_X - t_A|} = \frac{\Delta t_S}{\Delta t_A} \qquad \text{(Equation 5-2)}$$

where t_A, t_{DSF}, and t_X are the dry-bulb temperature of the atrium, DSF, and external air respectively.

The other factor found to influence the distribution of airflow rates across the floors relates to the relative sizes of the openings in the segment, or to be more precise, to the vent area ratio R_A of the combined effective area of openings at

the atrium/office and office/DSF interfaces A^*_j to the combined effective area of the segment's inlet/outlet openings A^*_s.

$$R_A = \frac{A^*_j}{A^*_s} \quad \text{(Equation 5-3)}$$

The combined effective area A^*_j relates to the effective area of the openings at the atrium/office interface A'_{jA} and the office/DSF interface A'_{jDSF} by

$$\frac{1}{A^{*2}_j} = \frac{1}{A'^{2}_{jA}} + \frac{1}{A'^{2}_{jDSF}} \quad \text{(Equation 5-4)}$$

and the combined effective area A^*_s relates to the effective area of the segment's inlet/outlet openings A'_A and A'_{DSF} by

$$\frac{1}{A^{*2}_S} = \frac{1}{A'^{2}_A} + \frac{1}{A'^{2}_{DSF}} \quad \text{(Equation 5-5)}$$

The effective area of an opening A' relates to its geometric or actual physical area A by the following relation

$$A' = \sqrt{2} c_d A \quad \text{(Equation 5-6)}$$

where c_d is the opening's corresponding discharge coefficient.

Assuming the same configuration as that of the BCM and assuming an equal value of A^*_j on all three floors of the segment, the general equation of the mathematical model that relates $R_{\Delta T}$ and R_A to the volume flow rates across the floors when the segment operates in either a B-U or T-D flow pattern is

$$\frac{Q^2_{tot}}{A^{*2}_S} + \frac{Q^2_j}{A^{*2}_j} = \frac{|t_x - t_{DSF}|}{t_x} gjh + \frac{|t_x - t_A|}{t_x} g(n + 2 - j)h \quad \text{(Equation 5-7)}$$

which can be reduced by substituting with Equations 5-1 and 5-2 to

$$\frac{Q_{tot}^2}{A_s^{*2}} + \frac{Q_j^2}{R_A^2 A_s^{*2}} = \frac{\Delta t_A}{t_x} gh(n + 2 - R_{\Delta T} j) \qquad \text{(Equation 5-8)}$$

where Q_{tot} is the total volume flow rate for the whole segment (equal to the sum of flow rates on all floors), Q_j the volume flow rate on the jth floor, g the acceleration due to gravity, h the floor height, and n the number of floors in the segment. Note here that Equation 5-4 equally applies to the B-U and T-D flow patterns because the flow path in both is the same albeit in opposite directions.

As for the T-U flow pattern, the equation changes to

$$\frac{Q_{tot}^2}{A_s^{*2}} + \frac{Q_j^2}{A_j^{*2}} = \frac{|t_x - t_{DSF}|}{t_x} g(n + 2 - j)h + \frac{|t_x - t_A|}{t_x} g(n + 2 - j)h \qquad \text{(Equation 5-9)}$$

which can again be reduced by substituting with Equations 5-1 and 5-2 to

$$\frac{Q_{tot}^2}{A_s^{*2}} + \frac{Q_j^2}{R_A^2 A_s^{*2}} = \frac{\Delta t_S}{t_x} gh(n + 2 - j) \qquad \text{(Equation 5-10)}$$

By numerically solving the equations of the mathematical model, it was possible to represent the relation between the ratio of airflow rates in the middle and upper floors to the airflow rate in the lower floor on one hand and changes in $R_{\Delta t}$ and R_A on the other.

For the B-U and T-D flow patterns, a contour graph was plotted for each floor separately (Figure 5-17) showing the relationship between $R_{\Delta t}$ on the horizontal axis, R_A on the vertical axis (corresponding to values of *OF* between 0.05 and 1.0 in increments of 0.05), and the resulting ratio of the airflow rate in that floor to that in the lower floor expressed as contour lines in percentage values. The contour

plot generally shows that the variation in the ratio of airflow rates in both floors to the airflow rate in the lower floor increases almost linearly with both $R_{\Delta t}$ and R_A and is more pronounced in the upper floor than it is in the middle floor. To compare their effect on the variation in flowrates during the relatively temperate and hot months of the cooling season, the average values of $R_{\Delta t}$ and R_A were aggregated for each flow pattern (B-U and T-D) separately.

The months of May and August were taken to represent those two periods respectively. It has to be noted that given that the value of R_A for any floor can only be one that corresponds to the fixed values of *OF* used in the BCM, using the monthly averaged value of R_A for each flow pattern to represent that month could be considered a compromise, but one that nonetheless provides a reasonable approximation given that the relation between R_A and the variation in the ratio of the airflow rates in the middle and upper floors to that in the lower floor is almost linear for all values of $R_{\Delta t}$ as can be seen in Figure 5-18 which shows the relation at four different values of $R_{\Delta t}$.

As anticipated, during the B-U flow pattern (represented by circles), the disparity in the ratio of flow rates is greater in August, at 80% and 54% of the airflow rate in the lower floor for the middle and upper floors respectively, than it is in May, at 92% and 83% for the middle and upper floors respectively. This is more attributed to the difference in the average value of R_A for the two months (0.14 in May and 0.64 in August), than it is to the difference in the average value of $R_{\Delta t}$ (0.61 in May and 0.76 in August). For the T-D flow pattern however (represented by diamonds), the disparity in the ratio of airflow rates between the floors is not as significant and this applies to both months. For May, the ratio is

95% and 89% for the middle and upper floors respectively and is even less pronounced in August at 96% and 92% of the airflow rate in the lower floor for the middle and upper floors respectively.

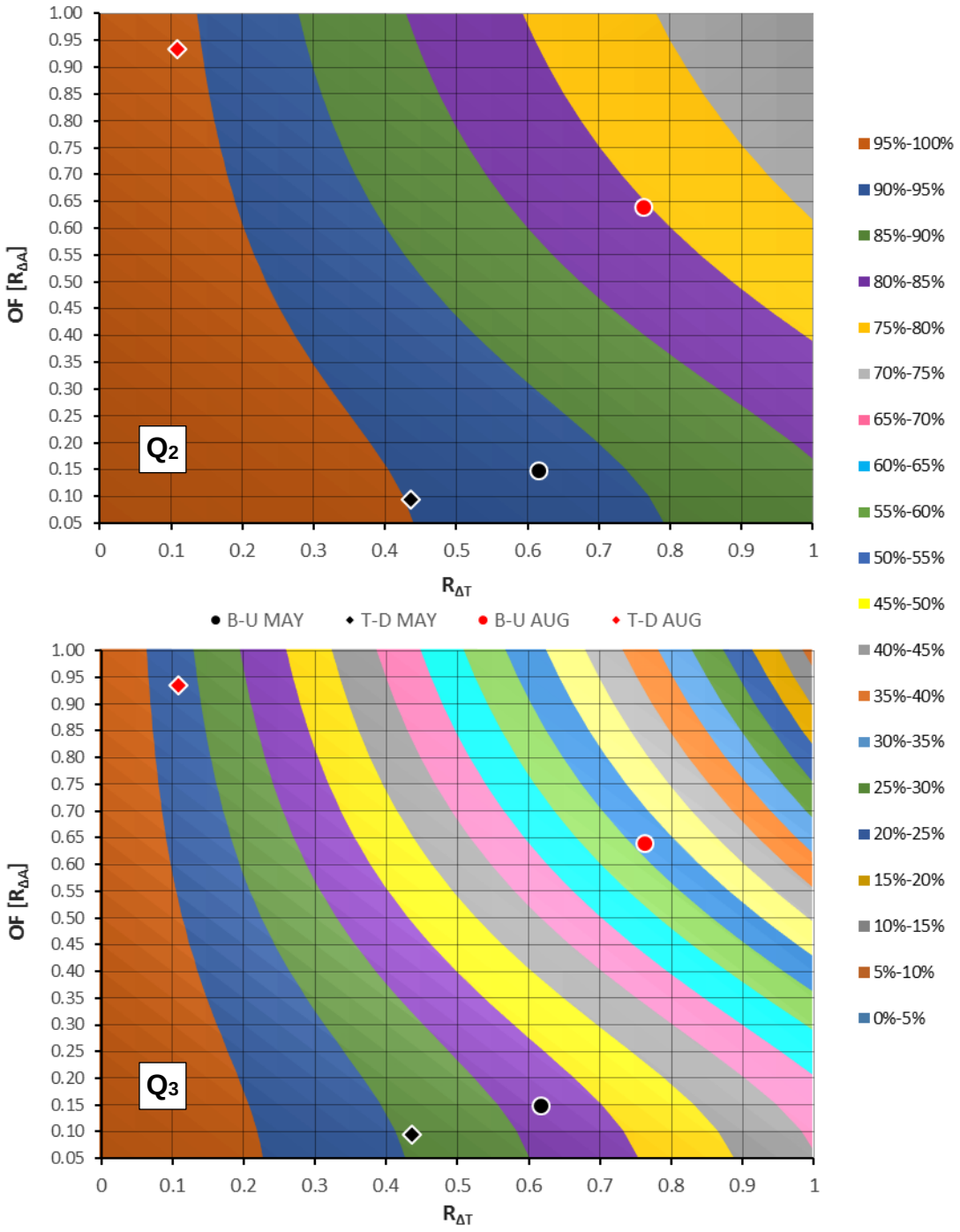

Figure 5-17 Variation of the ratio of airflow rates in the middle (Q_2) and upper (Q_3) floors of the segment to the lower floor with $R_{\Delta t}$ and R_A during the B-U and T-D flow patters

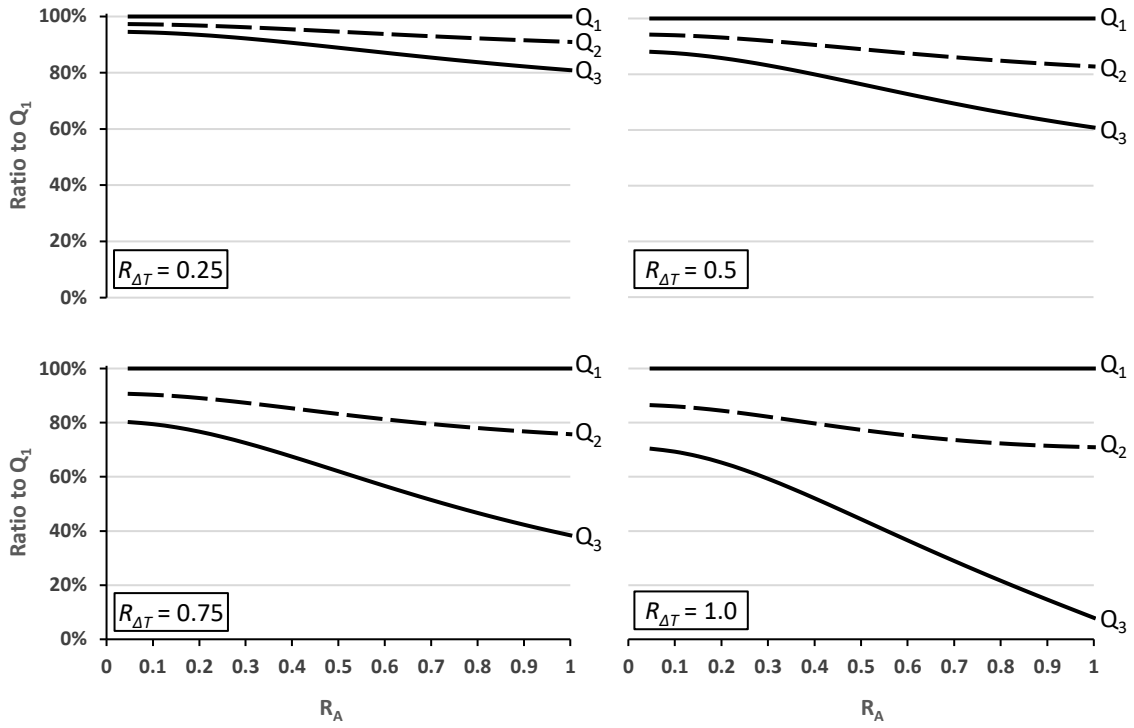

Figure 5-18 Variation of the ratio of airflow rates in the Middle (Q_2) and Upper (Q_3) floors of the segment to the airflow rate in the lower floor (Q_1) with R_A for $R_{\Delta T}$ = 0.25, 0.5, 0.75, and 1.0

As for the T-U flow pattern, the mathematical model shows that the variation in the ratio of airflow rates between floors is only affected by changes in R_A irrespective of the value of $R_{\Delta t}$. That is, for all values of $R_{\Delta t}$, the ratio remains constant for any given value of R_A and is actually equal to the ratio of airflow rates at an $R_{\Delta t}$ of 1.0 in the B-U and T-D flow patterns where the disparity is largest (Figure 5-19).

The average values of R_A during the T-U flow pattern for May (dotted line) and August (dashed line) were plotted and show that the variation in the ratio of airflow rates in the middle and upper floors to that of the lower floor between the two months is significant. Despite having a very low average value of R_A (corresponding to an average *OF* of 0.06), the ratio of the airflow rates in the

middle and upper floors to that in the lower floor during May is 87% and 70% respectively. During August, this ratio slightly drops in the middle floor to 72% but significantly falls in the upper floor to a ratio of only 21%.

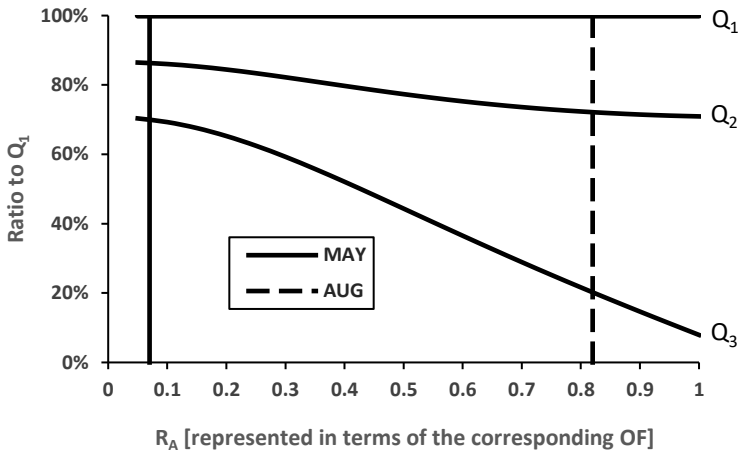

Figure 5-19 Variation of the percentage ratio of airflow rates in the middle (Q_2) and upper (Q_3) floors of the segment to the airflow rate in the lower floor (Q_1) with R_A during the T-U flow pattern

The variation of the ratio of airflow rates in the upper and middle floors to that in the lower floor with R_A as presented above only describes the flow rates in those floors in relation to the flow rate in the lower floor, i.e. the disparity in airflow rates between floors in relative terms only. To give an example, the plot could show that the ratio of the flow rate in the upper floor to that in the lower floor is decreasing with R_A whereas the flow rates in the upper floor might actually be increasing. Instead, plotting the variation of the scaled dimensionless airflow rates with R_A (Figure 5-20) as suggested by Acred and Hunt for the T-U flow pattern reveals the relation in absolute terms. The plot confirms the findings of the BCM shown in Figure 5-15b in which airflow rates in the lower and middle floor increase with R_A for all values of *OF* but that the airflow rate in the upper

floor continues to increase up to a value of R_A that corresponds to an *OF* of 0.4 at which point it starts to drop again.

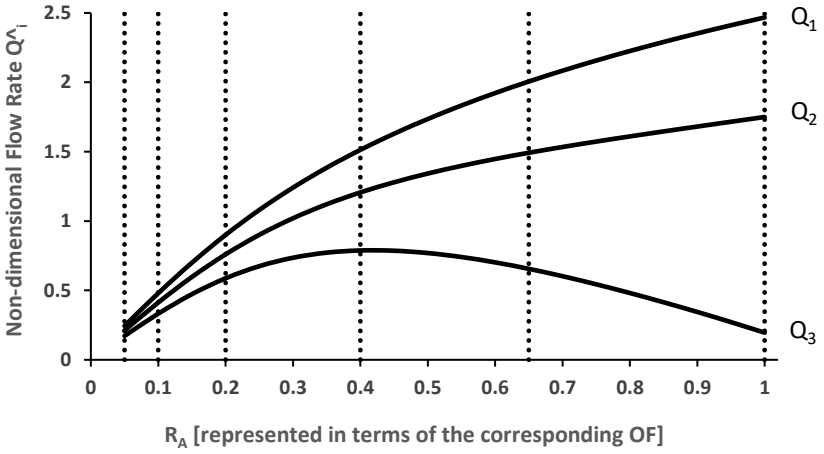

Figure 5-20 Variation of scaled dimensionless airflow rates with vent area ratio R_A

5.5 Summary

In this chapter, the thermal and airflow behaviour of the Base Case Model (BCM) of the proposed PDEC Multi-storey Office Building were presented and the associated environmental costs in terms of water and energy consumption assessed. These were modelled using EnergyPlus, a dynamic thermal simulation program with an integrated airflow network model.

A Pilot Model (PM) was first constructed to assess the preliminary validity of the proposed PDEC multi-storey office building model in EnergyPlus and accordingly allow for any necessary refinement. Results of the preliminary simulation on the PM prompted two adjustments before commencement of the full investigation on the BCM. The first involved extending the DSF beyond the upper floor of the segment and adding an upper exhaust vent to avoid restricting airflow in the segment at instances when it operates in PDEC mode and yet the

temperature of used air leaving the offices exceeds ambient temperatures and therefore flows upwards rather than downwards. The second involved modulation of airflow to prevent the large and rapid fluctuations in temperatures resulting from the alternate on and off switching of PDEC when internal temperatures approach the cooling setpoint.

For the same comfort model adopted, choice of the overheating criterion has a bearing on the way the control logic of this modulation is set up. A control logic based on a criterion wherein un upper threshold for comfort exists above and below which conditions are either uncomfortable or comfortable respectively differs from one that takes into account the magnitude and duration of departure from the comfort temperature. The former merely seeks to maintain internal conditions under that threshold whilst the latter seeks to maintain them around the comfort temperature. This has direct implications on the energy and water consumed.

If the upper boundary for the 90% acceptability range of ASHRAE's Adaptive Comfort Model (ACM) is used as the threshold above which AC is initiated and assuming that the application of the ACM is extended to PDEC buildings, then the duration in which AC is in operation is negligible and the cooling energy required is thus insignificant. However, to maintain operative temperatures as close as possible to the comfort temperature, an average of approximately 10 litres of water are daily required per occupant.

The Overheating Risk Index (ORI) is more sensitive in identifying discrepancies in comfort conditions than the Exceedance Index (EI) and thus

would be more apt for exercises that require ranking of, or comparison between, two spaces or models. Using the ORI is not straightforward though because representing it as a single value obscures the severity and/or duration of overheating because the same value of ORI could be equally arrived at by aggregating low values of *P* for long periods or high values of *P* for shorter periods. It was suggested to represent ORI as a distribution of the values of *P* in terms of their frequency of occurrence. This way the distribution of *P* could require that, for a space to be considered comfortable, *P* should not exceed a certain maximum value for more than a specified limited proportion of occupied hours for the whole year and another intermediate value for a relatively longer duration.

The disparity in thermal conditions between the floors of the segment particularly at the early hours of the occupied period, is primarily caused by differences in airflow rates across those floors due to their relative vertical position within the segment. In general, average monthly airflow rates as well as the disparity in internal conditions between floors tend to increase with external temperatures.

The interaction of two factors influence the disparity in airflow rates between floors; R_A, the ratio of the effective area of the openings at the Atrium/Office and Office/DSF interfaces to the effective area of the segment's inlet/outlet openings, and $R_{\Delta T}$, the ratio of the difference in air temperatures between the Atrium and DSF to the difference between the Atrium and external air temperature. For the B-U and T-D flow patterns, the variation in the ratio of airflow rates in the upper and middle floors to the airflow rate in the lower floor increases almost linearly

with both R_A and $R_{\Delta T}$, whereas for the T-U flow pattern, the variation only increases with R_A, and $R_{\Delta T}$ has no real effect.

Flow rates during the T-D flow pattern tend to be consistently equal across the floors for all months of the cooling season because values of $R_{\Delta T}$ tend to be small and thus negate the effects of R_A even at high values. However, for the B-U and T-U flow patterns, the difference in flow rates between the upper, middle, and lower floors tend to progressively increase with average monthly external temperature because the effect of R_A is more pronounced.

Finally, when the OF value is equal on all floors, airflow rates in the lower and middle floor continue to increase with R_A for all values of *OF* but would start to drop in the upper floor for values of *OF* above 0.4.

Chapter 6: Parametrisation and Optimisation of the BCM

6.1 Chapter Overview

In Chapter Five, the thermal and airflow behaviour of the BCM was investigated. A three-storey segment was considered as it represented the least number of floors within a segment that still captured the thermodynamic essence of the phenomenon being investigated and enabled meaningful analyses to be performed. In this chapter, parametric investigations were carried out to examine the effect of varying different input parameters on simulation outputs with the aim of optimising the PDEC strategy in the proposed generic configuration of the multi-storey office building in order to deliver acceptable internal conditions for occupants whilst minimising environmental costs.

A number of modelling assumptions were made in the BCM and among those, four key parameters were identified, namely the number of floors in the segment, the duration of PDEC operation, wind forces and orientation, and finally, the choice of comfort model and overheating criteria to be adopted. In Section 6.2, the effect of increasing the number of floors in a segment on the overall bulk airflow rates in the segment and the distribution of airflow rates across the floors is investigated together with the implications of that on internal conditions and water consumption. The effects of extending PDEC operation during unoccupied hours on reducing the mean radiant temperature the following day is discussed in Section 6.3 with the implications of that on water consumption. Section 6.4 discusses the inclusion of wind forces and their effects on airflow rates across the

floors of the segment. The effects of varying the orientation of the building segment and the subsequent change in solar gains and wind forces on the thermal and airflow behaviour of the PDEC building model is also investigated. Choice of the thermal comfort model and overheating criteria has a significant bearing on the assessment of acceptability of internal conditions for human occupancy and is therefore the subject of Section 6.4 in which the effect of adopting different comfort models and overheating criteria is examined

6.2 Segmentation

In this section, the effect of increasing the number of floors within a segment on the thermal and airflow behaviour of the PDEC model as a whole and on individual floors is investigated. In other words, the effect of segmentation, i.e. the division of a multi-storey building into smaller segments that are independent in terms of airflow with each segment comprising the same number of floors, on the performance of the PDEC model is investigated.

Current building regulations in Cairo restrict the height of new buildings to 1.5 times the width of the street that the land plot overlooks with an upper limit of 36m, roughly translated into 12 storeys. Accordingly, in addition to the BCM which is a three-storey segment (03S), a six-storey (06S) and a 12-storey (12S) segment were considered. Comparisons were then made between three models of a 12-storey building, the first made up of four three-storey segments (4 x 03S), the three-storey segment model (03SSM); the second of two six-storey segments (2 x 06S), the six-storey segment model (06SSM); and the third made up of a single 12-storey segment (1 x 12S), the 12-storey segment model (12SSM).

There are certainly other locations in Cairo that are exempt from such building height restrictions but for fire safety regulations, the maximum number of floors in a segment considered in this study was 12. For buildings with more floors, it is suggested that multiples of the segments considered here could be used.

6.2.1 Modelling assumptions

To allow for inter-comparisons between the three different models, the same modelling assumptions made for the BCM were also made for 06S and 12S (see §5.2.1). The assumptions include construction profiles, internal heat gains, occupancy schedules, and the control logic, with the latter's associated comfort model and overheating criterion also carried over. To investigate the PDEC strategy's capacity to deliver the required convective cooling, the simulations were run under a no-wind scenario, i.e. only buoyancy forces were considered. Due to the change in the number of floors served by each segment, changes had to be made to the sizing of the PDEC components (vents sizes). For this, design conditions and geometric inputs used in the EFM to calculate the initial sizes of the PDEC components of the BCM as described in Chapters Four and Five were also used to calculate the initial sizes of 06S and 12S. Table 6-1 summarizes the vent sizes of the three segments as calculated by the EFM.

For the T-D flow pattern, the calculated areas of the vents at the Atrium/Office and DSF/Office interfaces for the 12SSM were smaller than their respective areas in the 06SSM which were in turn smaller than those in the 03SSM, an expected outcome since the driving forces in a T-D flow pattern increase with the number of floors in the segment. However, for the T-U flow pattern, the calculated vent

areas at the interfaces are not dependent on the number of floors in the segment but rather on the distance between a floor's vent on one hand and the segments' Atrium and DSF top vent on the other. And since the difference in height (ΔH) between the top floor vent and the segments' Atrium and DSF top vent was kept constant at 6.6m in all three segments, the calculated vent areas in the respective floors of the three segments starting from top to bottom were also equal. For the top floors, the calculated vent area was 8.9m^2 which represents the maximum vent area required for any floor during any flow pattern. This size was therefore assumed for all floors in all three segments. So, although the areas of the vents at the Atrium/Office and DSF/Office interfaces as calculated by the EFM increase with floor level to compensate for the decreasing pressure differences, they were all assumed to be equal to 8.9 m^2 to allow for inter-comparisons between the three models.

As for the segments' inlet and outlet vents, the calculated areas varied depending on the number of floors to be served within the segment and for the same segment, on the flow pattern (design conditions) being used. Assuming an equal area for the segment's inlet and outlet vents, for the 03SSM, there was no significant difference between the calculated inlet/outlet vent area for the T-D and T-U flow patterns. However, for the 06SSM and 12SSM, the calculated vent areas for the T-U flow pattern required a 53% and 66% increase over their respective calculated vent areas for the T-D flow pattern. Accordingly, for the 06SSM and 12SSM, during T-U operation, the larger vent area sizes were used for the Atrium and top DSF vents whereas the smaller sizes were used for the Atrium and

bottom DSF vents during the B-U and T-D flow patterns to avoid excess water consumption.

Table 6-1 Vent sizes calculated by EFM

	03SSM				06SSM				12SSM			
	T-D/B-U		T-U		T-D/B-U		T-U		T-D/B-U		T-U	
	Atrium	DSF	Atrium	DSF	Atrium	DSF	Atrium	DSF	Atrium	DSF	Atrium	DSF
Top	18.8	-	18.8	18.8	27.7	-	35.6	35.6	41.6	-	69.3	69.3
Bottom	-	18.8	-	-	-	27.7	-	-	-	41.6	-	-
12									8.9	8.9	8.9	8.9
11									8.9	8.9	8.9	8.9
10									8.9	8.9	8.9	8.9
9									8.9	8.9	8.9	8.9
8									8.9	8.9	8.9	8.9
7									8.9	8.9	8.9	8.9
6					8.9	8.9	8.9	8.9	8.9	8.9	8.9	8.9
5					8.9	8.9	8.9	8.9	8.9	8.9	8.9	8.9
4					8.9	8.9	8.9	8.9	8.9	8.9	8.9	8.9
3	8.9	8.9	8.9	8.9	8.9	8.9	8.9	8.9	8.9	8.9	8.9	8.9
2	8.9	8.9	8.9	8.9	8.9	8.9	8.9	8.9	8.9	8.9	8.9	8.9
1	8.9	8.9	8.9	8.9	8.9	8.9	8.9	8.9	8.9	8.9	8.9	8.9

6.2.2 Airflow

The ultimate aim of a passive or low energy cooling strategy in a multi-storey office building is to provide internal thermal comfort conditions in all office floors with the least possible environmental costs. The primary means to achieve this in a PDEC building is by ensuring that sufficient airflow rates are equally distributed across the floors. The performance of the three models in terms of airflow is therefore discussed first.

6.2.2.1 Monthly average bulk volume airflow rates

The monthly average bulk volume airflow rates traversing the floors during occupied hours of the three models are plotted for each flow pattern independently (Figure 6-1). Note here that although the data points plotted on the

graph are discrete as they represent the monthly average flow rate at each floor level rather than along the height of the building, a line connecting the data points of each model was drawn for the sake of clarity. The months of May and August were selected as they represent the relatively temperate and warm periods of the cooling season respectively.

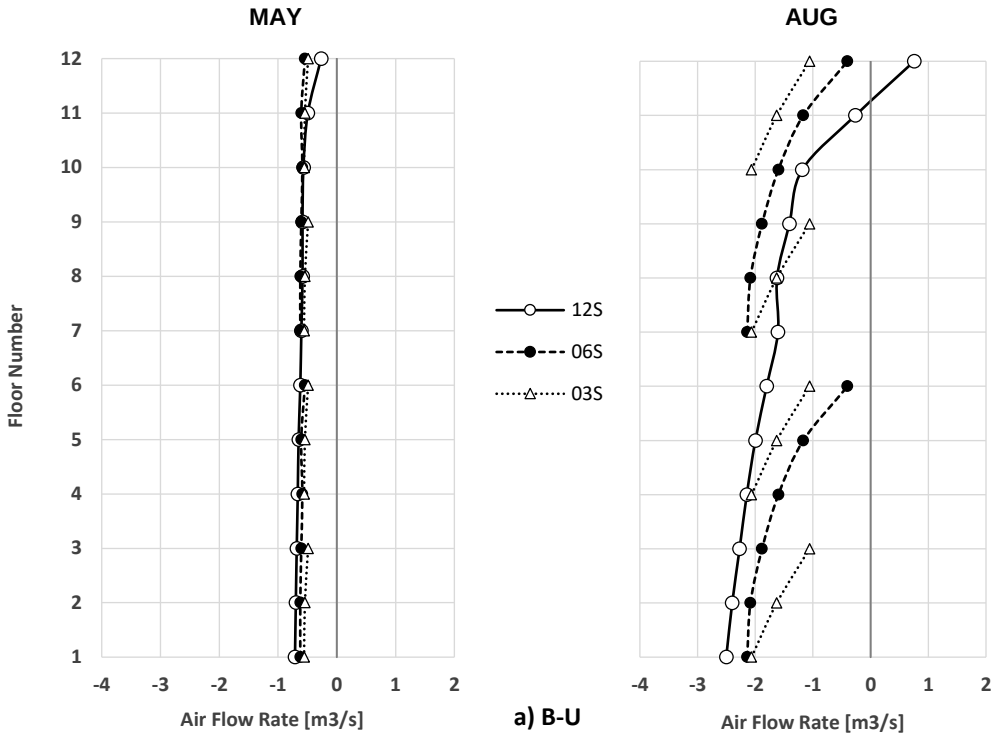

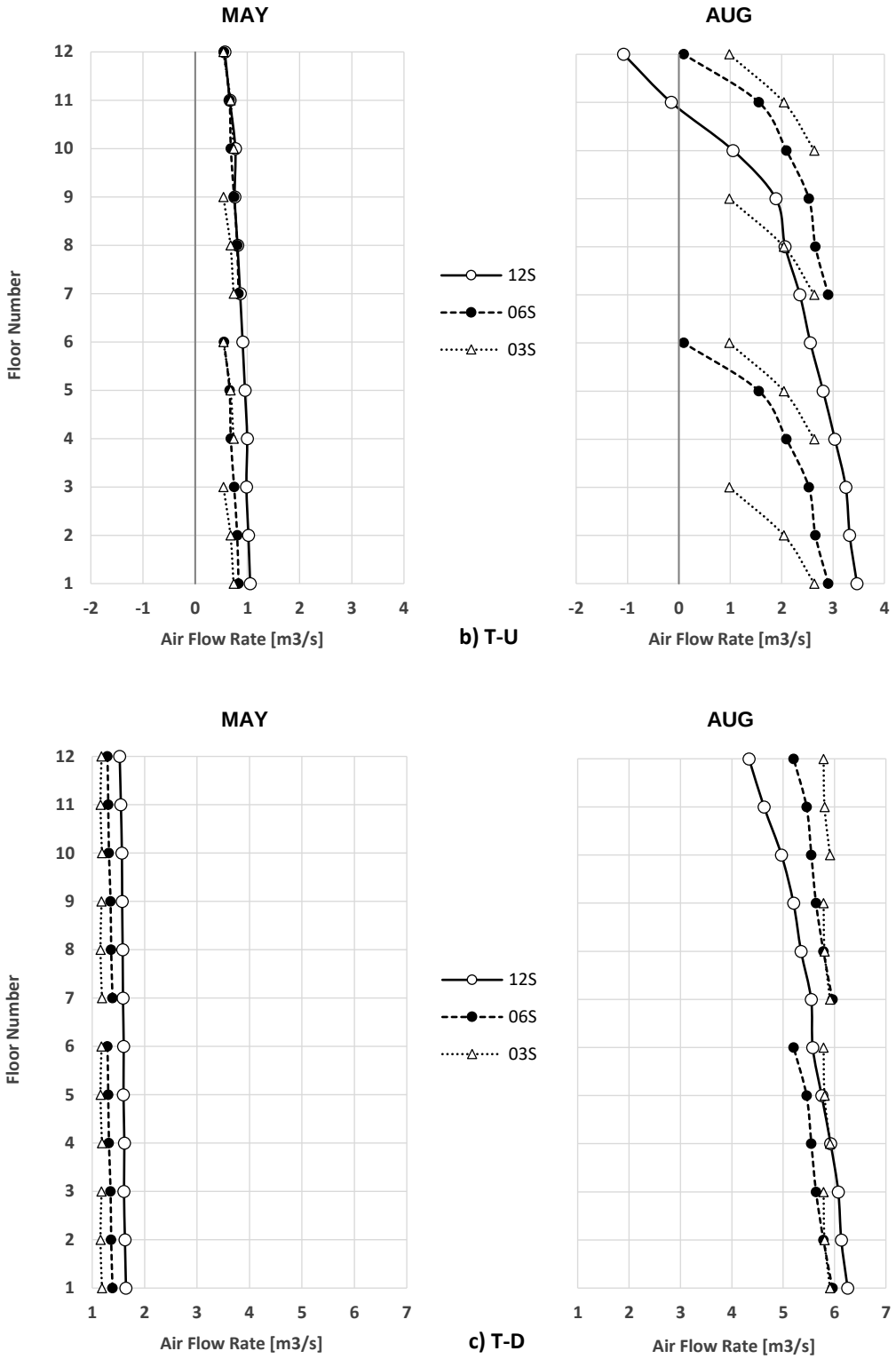

Figure 6-1 Monthly average airflow rates of the three-storey, six-storey, and 12-storey segmented 12-storey building during May and August for a) the B-U flow pattern, b) the T-U flow pattern, and c) the T-D flow pattern

The first thing to notice is that monthly average volume flow rates are generally much higher in August than they are in May which is to be expected as more convective cooling is required to offset higher heat loads. During May, volume flow rates on all floor levels in 12SSM are slightly higher than they are on their respective floors in 06SSM and 03SSM when PDEC is turned on (T-U and T-D flow patterns). However, in NV mode (B-U flow pattern), volume flow rates are only higher on floors in the bottom half of 12SSM whereas the relation is reversed for floors in the top half as flow rates are higher in 03SSM and 06SSM. The same pattern exists between 03SSM and 06SSM. In August, this reverse relation between the bottom and top half persists during B-U, T-U and T-D. For the T-D flow pattern, monthly average flow rates for August are consistently higher in 03SSM than in 06SSM and 12SSM on all but the bottom three floors of the model. It can be noticed that a point exists in all three models where the rate of reduction in flow rate with floor level increases markedly. This is more pronounced during the B-U and T-U flow patterns and occurs on the penultimate floor of each segment in 03SSM and 06SSM but drops to the 9th floor in 12SSM. Reasons for this are discussed in the following two sections.

6.2.2.2 Dispersion of airflow rates between floors

To determine the degree of dispersion during each flow pattern in May and August, the standard deviation of the monthly average volume flow rates of all floors from the overall average (mean) of the segment was calculated for each model (Figure 6-2). For all three models and flow patterns, flow rates between floors are generally more dispersed during August than they are during May and

that is more pronounced during the B-U and T-U flow patterns than it is during the T-D flow pattern.

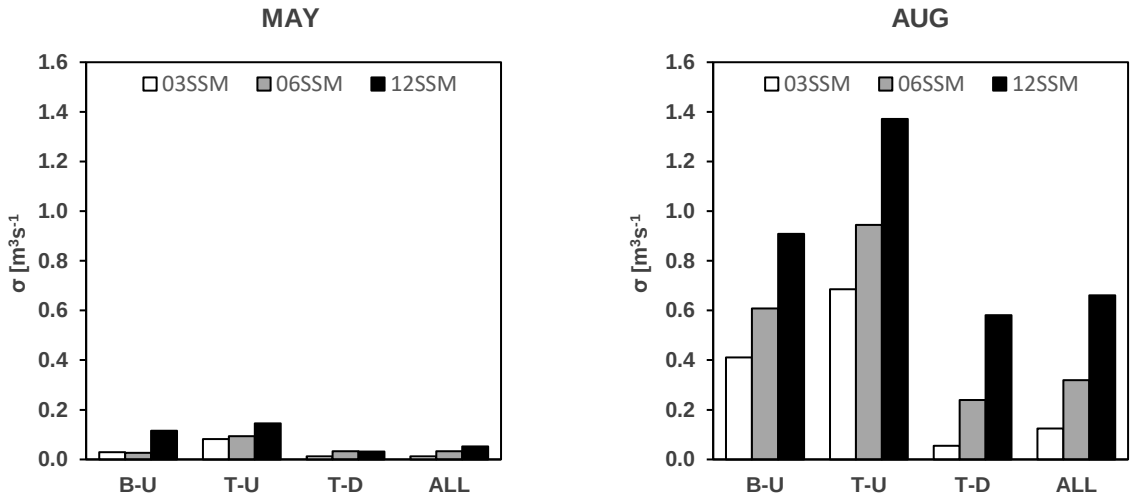

Figure 6-2 Monthly standard deviation of flow rates under different flow patterns

Between the three models, dispersion explicably increases the more floors there are in the segment due to the large variation with height in pressure differences acting on the interface vents, with the maximum dispersion occurring in 12SSM during August when the segment operates in the T-U flow pattern. Dispersion is significant to the extent that the disparity between the bottom and top floors is not only in magnitude but also in flow direction. The average airflow rate drops from 3.6m^3/s in the 1st floor to just under 0m^3/s in the 11th and to -1m^3/s in the 12th, meaning that, on average, the upper two floors experience reverse flows during that period. Similarly, during the B-U flow pattern, a reverse flow occurs on the top floor wherein the monthly average airflow rate for August is 0.8m^3/s, but remains just below zero on the 11th floor (note that a positive airflow rate value during the B-U flow pattern indicates reverse flow). Disparity in airflow

rates between floors is also evident in 06SSM. Average monthly airflow rates during the B-U flow pattern drop from -2.1m^3/s in the bottom floor to -0.3m^3/s in the top floor of each segment (85% reduction), and from 3m^3/s to 0m^3/s during the T-U flow pattern.

Discussions in Chapter Five identified two main factors, namely R_A and $R_{\Delta T}$, that explain the variation in the dispersion of monthly average airflow rates between floors from one flow pattern to the other and from one month to the other. As R_A increases, dispersion increases which explains why, for all models, it is greater in August than it is in May given that the average R_A values in the former tend to be greater than they are in the latter to compensate for the increase in heat loads. Similarly, as $R_{\Delta T}$ increases, so does dispersion. This is evident in August; although values of R_A during the B-U and T-D flow patterns are comparable, dispersion is lower during the latter because average $R_{\Delta T}$ values tend to be smaller due to the significant difference between internal and external temperatures. The temperature differential increases the buoyancy forces acting on all floors so that the airflow rate on any floor is significantly higher than the difference in airflow rates between the floors.

6.2.2.3 Flow Reversal

Analysis of the monthly average airflow rates above revealed that reverse flows consistently occur in the upper floors of 06SSM and 12SSM, particularly during the warmer months of the cooling season. Reverse flows indicate that air is flowing in a direction opposite to the one intended for the flow pattern. During flow reversal, stale air exhausted from the lower floors to either the atrium or DSF,

depending on the flow pattern, is reintroduced into the upper floors. The stale air is likely to have a negative impact not only on thermal comfort but also on indoor air quality (IAQ). It was therefore deemed useful to determine the duration and location of reverse flows in each segmentation model. The proportion of occupied time of the cooling season during which reverse flows occur on each floor of the three models is shown in Figure 6-3. Results show that reverse flows on the top floor of each segment of 06SSM occurred for 3.8% of the total occupied time of the cooling season (50hrs). That period is almost doubled for the top floor of 12SSM wherein the proportion reaches 7.2% (96hrs) but drops to 4.3% (58hrs) and 1.8% (24hrs) for the 11th and 10th floors respectively. The results also show that the proportion of time during which reverse flows occur on all floors of 03SSM and the remaining floors of 06SSM and 12SSM could be considered negligible.

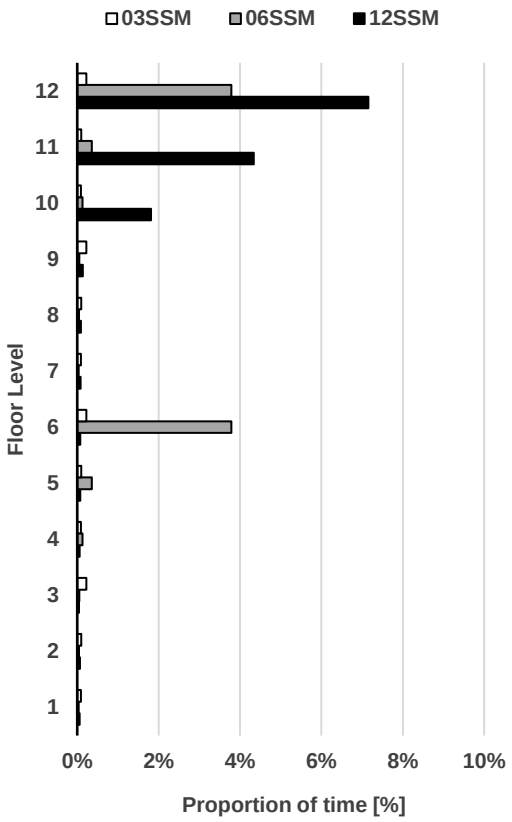

Figure 6-3 Proportion of occupied time of the cooling season during which reverse flows occur on each floor of the three models

Although analysis of the monthly airflow rates showed that reverse flows only tend to occur when the models were operating in the B-U and T-U flow patterns, breakdown of the reverse flow figures by flow pattern surprisingly revealed that in absolute terms, i.e. in terms of the total number of hours during which reverse flows occur (Figure 6-4a), reverse flows in 12SSM occurred the most during the T-D flow pattern (97hrs). This is more than the combined number of hours of reverse flows occurring during the B-U and T-U flow pattern in the same model, which were 38 and 45 respectively. The total number for each flow pattern was reached by adding the number of hours during which a reverse flow occurred on each floor. All flow patterns considered, 12SSM had by far the highest number of

hours of flow reversal (180hrs) compared to 113 hours for 06SSM and 21 hours for 03SSM.

However, results of the monthly average airflow rates can be explained if occurrence of reverse flows is presented in terms of the proportion of time in which they occur during each flow pattern. For example, reverse flows in 06SSM equally occurred during the T-D and T-U flow patterns (40hrs) as shown in Figure 6-4a but the proportion of time this represents relative to the duration of each flow pattern differs significantly (Figure 6-4b). The figure shows that reverse flows occurred for only less than 2% of the duration of the T-D flow pattern but for more than a quarter of occupied hours (27%) during the T-U flow pattern.

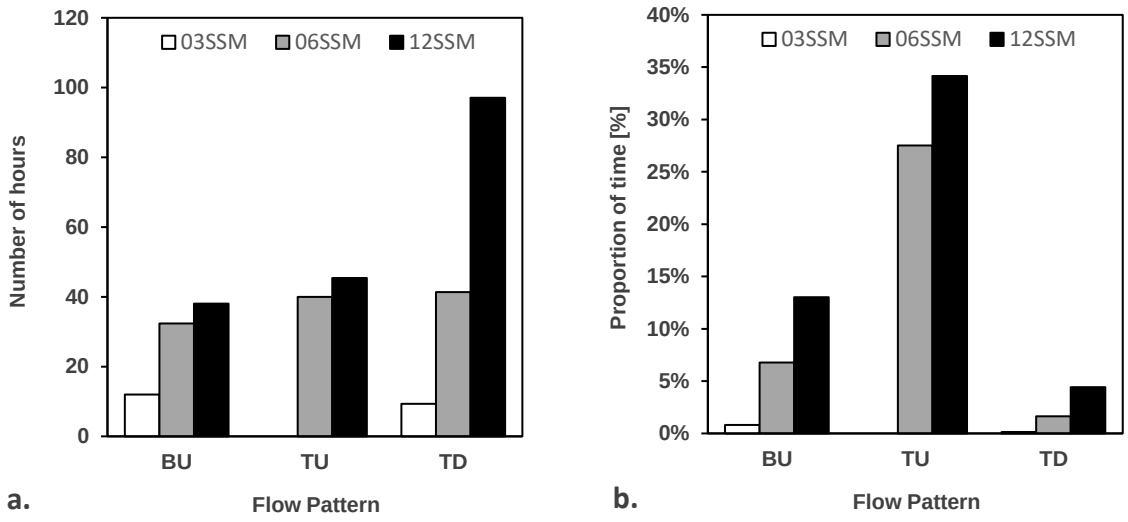

Figure 6-4 Reverse flow occurrence by flow pattern during occupied hours of the cooling season a) by total number of hours and b) as a proportion of the duration of the flow pattern

Occurrence of flow reversal during all flow patterns indicates that the neutral plane level lies somewhere between the 9th and 10th floor of the 12-storey segment and above the penultimate floor of the six-storey segment. This, and the

general dispersion in flow rates between the floors in the two variants, suggest that some of the initial sizing conditions or modelling assumptions need to be reconsidered, particularly those relating to the equal vent sizes assumed for all floors. It is likely that progressively increasing vent sizes as per the EFM calculations could yield a better distribution of flow rates across the floors. Alternatively, it would be worth investigating whether increasing the area of the vents in the floors experiencing flow reversal only could prevent flow reversal occurring on those floors whilst minimising construction costs by limiting the variation in vent sizes within the segment to two. Adding extra exhaust components to those floors could also be a viable though costlier alternative, a strategy employed in the Frederick Lanchester Library in Coventry and the SSEES building in London (Lomas, 2007). Furthermore, as flow reversal is particularly problematic during the T-U flow pattern, it is likely that raising the temperature at the segment's outlet vent at the top of the DSF (by creating a solar chimney for example) could increase the buoyancy forces in the whole segment, thus reducing dispersion. Finally, increasing the vertical distance between the upper floor and the segments outlet (ΔH) could also be considered. This strategy would potentially have two advantages; it would likely elevate the neutral plane level above the upper floor's vent and, according to EFM calculations, would require smaller vent sizes, thus reducing R_A and consequently dispersion.

6.2.3 Comfort and Overheating

To compare the overall thermal performance of the models, the cumulative frequency of the proportion of people (P) voting warm or hot on the ASHRAE seven-point scale was calculated (more details on this index can be found in

§5.4.2). Cumulative frequency analysis (Ogive more-than type curve) was adopted to facilitate the determination of the frequency of exceedance at any chosen *P* value. For each bin, the number of timesteps with *P* values lying within that bin were counted for each floor separately then summed up to give the value for each segment and then finally multiplied by the number of segments that make up the model. The final figures were then expressed in proportion to the total occupied time to give an aggregate value for each model. *P* was only counted for timesteps in which t_{op} exceeded t_{cmf_ASH}, i.e. $\Delta t_{ASH} > 0$, which is why the frequency only starts to drop after 4.5%, the value of *P* at t_{cmf_ASH}.

Figure 6-5 shows the cumulative frequency of *P* in the three models when values are aggregated over all floors and over the whole cooling season. Internal conditions in 03SSM exceeded t_{cmf_ASH} for 34.4% of occupied time during the cooling season, insignificantly more than in 06SMM (33.9%) and 12SSM (33.5%). For all values of *P* greater than 5%, the order is reversed whereby 03SSM has the least overheating followed by 06SSM and then 12SSM. The results also show that the difference in the duration of time in which internal operative temperatures exceed t_{ub_ASH} (the upper boundary of the 90% acceptability range of ASHRAE standard 55) between the three models can be considered negligible. In general, results show that internal conditions do not differ much along all incidences of *P.* This does not indicate that internal conditions on all floors are similar but that, on balance, and in considering each model as a bulk, segmentation has no significant effect on the thermal performance of the 12-storey PDEC office building model.

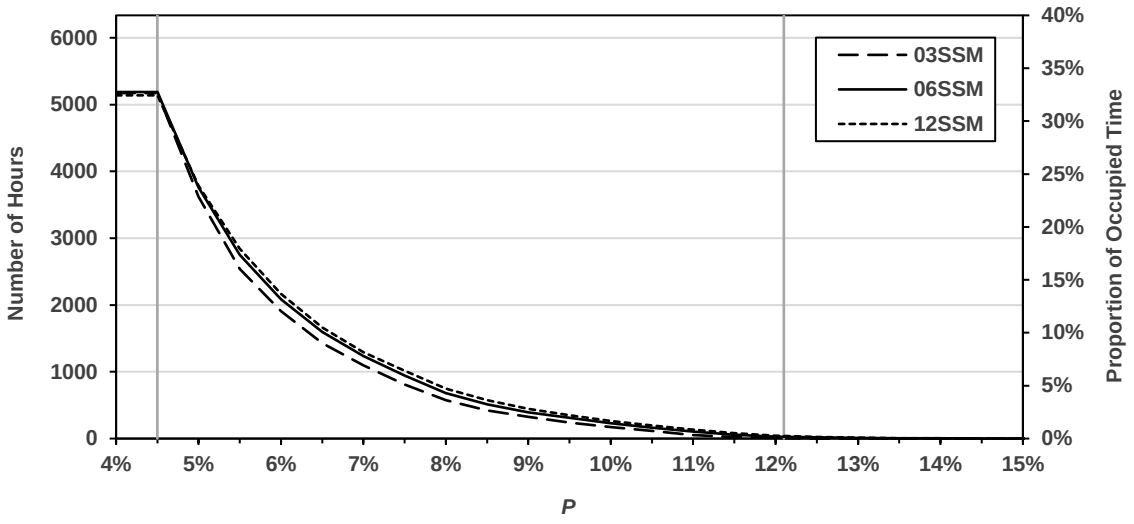

Figure 6-5 Cumulative frequency of *P* during occupied hours of the cooling season aggregated over all floors for instances when $T_{op} > T_{cmf_ASH}$ ($\Delta t_{ASH} > 0$)

However, when cumulative frequencies are aggregated over each flow pattern separately, the results show that the ranking orders of 03SSM and 12SSM in terms of thermal comfort alternate between top and bottom depending on the flow pattern whilst 06SSM maintains an intermediate position between the two. Figure 6-6 shows that during the T-U flow pattern, the sum of the number of hours on all floors in which internal operative temperatures in 12SSM exceed t_{cmf_ASH} was 511, compared to 557 and 620 hours for 06SSM and 03SSM respectively. For values of *P* above 8.5%, all curves converge, and the three models perform equally which indicates that the majority of hours in which internal conditions in 03SSM and 06SSM were warmer than they were in 12SSM during the T-U flow pattern occur at the lower range of *P* values.

However, if internal conditions are considered for floors individually, a different picture emerges because aggregating *P* values over all floors of a model could obscure the fact that some floors in that model may have higher *P* values

compared to their respective floors in the other two models but are offset by the lower *P* values in the better performing floors of the model.

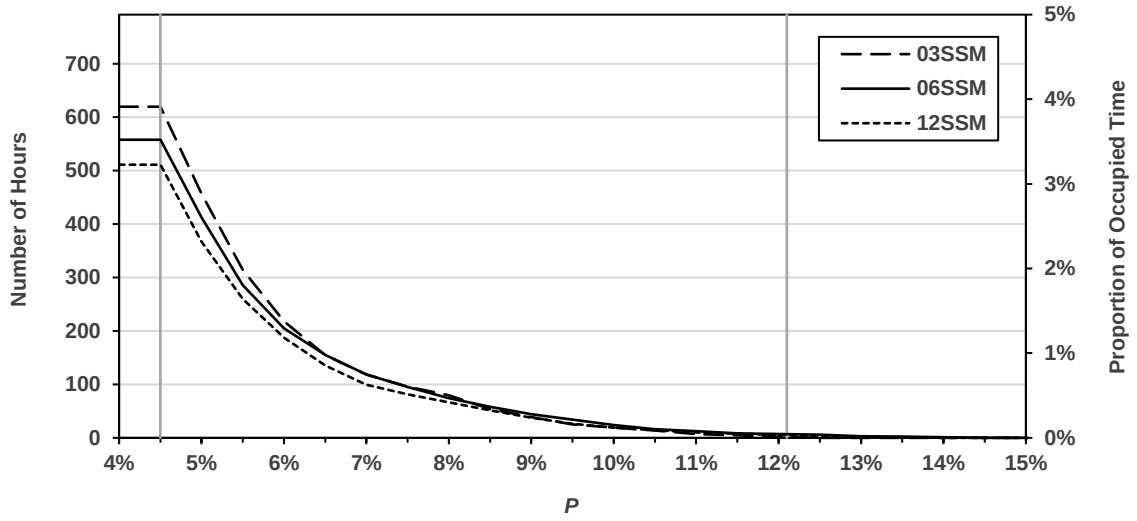

Figure 6-6 Cumulative frequency of *P* during occupied hours of the cooling season when the T-U flow pattern was in operation, aggregated over all floors for instances when $t_{op} > t_{cmf_ASH}$ ($\Delta t_{ASH} > 0$)

Analysis of the monthly average airflow rates and frequency of reverse flows suggest that conditions in the upper three floors in August during the T-U flow pattern require further consideration. Accordingly, the cumulative frequencies of *P* for levels 10, 11 and 12 were plotted for that period (Figure 6-7). Results show that the top floor of 06SSM performed the worst with an average *P* value of 8.5% and with more incidences of high *P* values than any other level. Moreover, L10 of 12SSM was found to have a comparable, though slightly lower, incidence of *P* values at the higher end (>8.5%) but with a lower overall average of 8%. L11 of 12SSM had a very similar average *P* value but frequencies were considerably lower than both the upper floor of 06SMM and L10 of 12SSM.

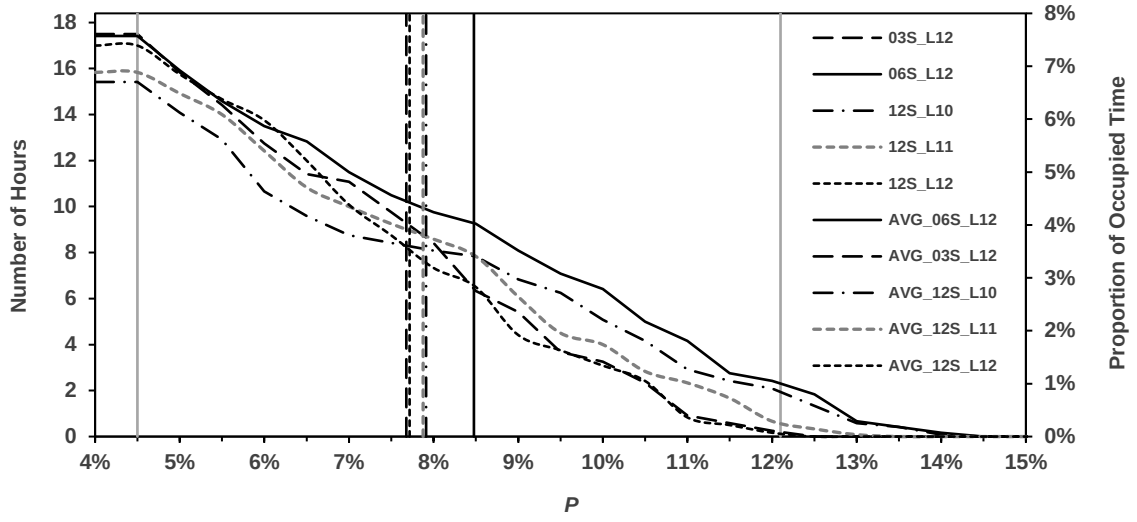

Figure 6-7 Cumulative frequency of the proportion of people voting hot or warm on the ASHRAE seven-point scale *P* during occupied hours of August

Going back to Figure 6-1b which shows the average airflow rates for August during the T-U flow pattern, it is clear that floors L12 of 06SMM and L11 of 12SSM have near-zero average airflow rates whereas L12 of 12SSM experiences higher airflow rates, although in the opposite direction as indicated by the negative value. This would explain why thermal conditions in the latter were relatively better because although air was flowing in the opposite direction, it still provided convective cooling, albeit from stale air coming from the DSF, whereas near-zero values on the other two floors indicate little or no exchange occurred between the floor and the atrium or DSF and that airflow was stalled causing heat to build up and temperatures to rise. It was less obvious though, at first glance, why internal conditions in L10 of 12SSM were warmer than in the two upper floors of the same model, particularly L12 and why, despite having the same average monthly airflow rate of 1m^3/s, L10 of 12SSM also performed worse than L12 of 03SSM. Relying on aggregate values in many cases is useful in indicating general trends

of large sets of data but in this particular case, monthly averaged airflow rates for the upper three floors of 12SSM were not accurately indicative of the actual absolute flow rates because as shown in Figure 6-4, reverse flows with negative values frequently occurred skewing the results. Alternatively, when the frequency distribution of the airflow rates for L10 and L12 of 12SSM as well as L12 of 03SSM were plotted (Figure 6-8), it became clear that the average airflow rate for L10 was misleading because the highest frequencies of occurrence revolved around a value of $0m^3/s$ while the rest were thinly dispersed across a wide range on the positive side of the axis pulling the average towards the $1m^3/s$. On the other hand, it is clear that the central tendency of airflow rates for L12 of 03SSM revolve around the $1m^3/s$ value which explains why in Figure 6-7, L10 of 12SSM has significantly higher frequencies for all *P* values above 8% than L12 of 03SSM.

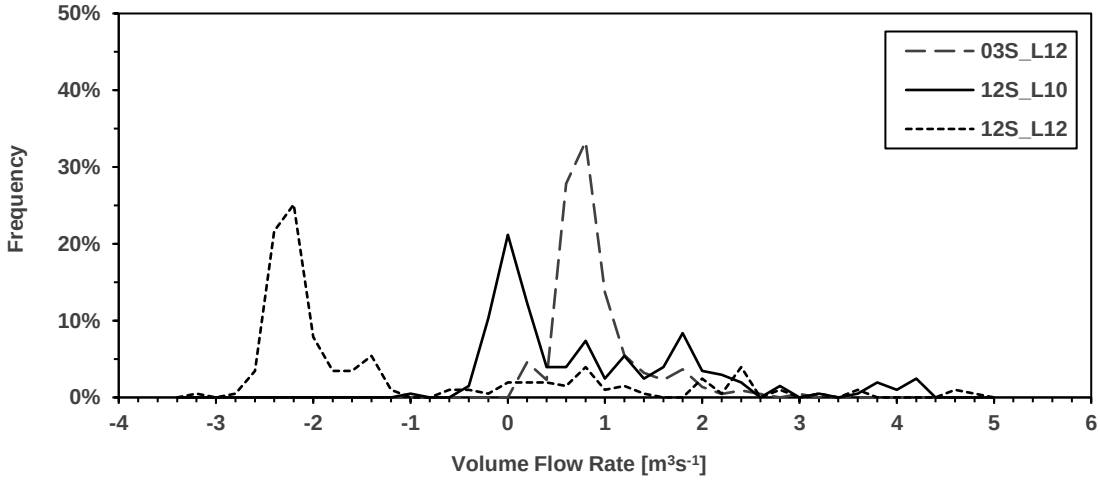

Figure 6-8 Frequency distribution of volume flow rates during occupied hours of August

To appreciate this in more detail, the operative temperature and volume flow rate profiles of the 12th floor in all three models in addition to the 10th floor of 12SSM were plotted for a 24-hour period (Figure 6-9). The 24th of August was

selected as it represents a typical example of a day in which all three flow patterns occur. The figure shows that temperature profiles correlate well with their respective volume flow rate profiles; the farther away the flow rate profile departs from zero the lower the temperature profile is irrespective of flow direction. After a great deal of fluctuation between 1:30 and 3:30am as internal temperatures approach external ones, the flow starts to stabilise when the external dry-bulb temperature further drops, and all three models operate in a B-U flow pattern. This pattern continues until the start of the working day at 8am. During that period, airflow almost stalls on the top floor of 06SSM and the 10th floor of 12SSM (indicated by near zero values) whilst the top floor of 03SSM and 12SSM have almost equal but opposite airflow rates. The flow reversal in 12SSM explains the slightly elevated operative temperature compared to that in 03SSM for the same period as air is supplied from the DSF.

At 8am, the abrupt increase in internal heat loads raises operative temperatures in all models by about 1K. At this point PDEC starts to operate but since internal temperatures are still higher than ambient, all models operate in a T-U flow pattern and flow directions on all floors are reversed accordingly. Floors that experienced flow reversal during night time ventilation continue to do so during T-U with the stalled flows on L12 of 06SSM and L10 of 12SSM causing operative temperatures to rise above t_{ul_ASH}. Operative temperature profiles of the top floors of 03SSM and 12SSM almost coincide until just after 10am when the temperature in the DSF of 03SSM drops below ambient prompting the vent at the top of the DSF to close and the model to operate in a T-D flow pattern (DSF dry-bulb temperature not shown in figure). So, although flow reversal during the

T-U flow pattern is more advantageous than near-zero flow rates in terms of internal conditions, it delays the transition to the T-D flow pattern raising operative temperatures in the process.

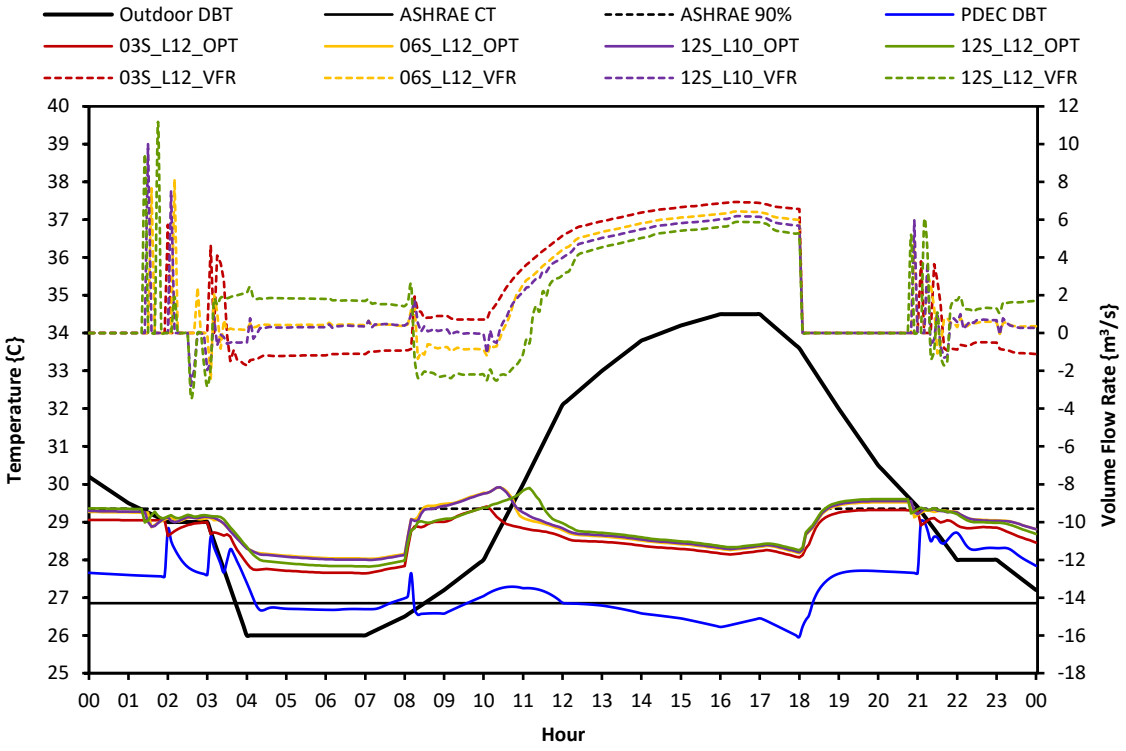

Figure 6-9 Operative temperature and Volume flow rate profiles on August 24th

6.2.4 Water Consumption

Figure 6-10 compares the quantity of water consumed by each model per unit area of spaces served by the PDEC system. Water consumption was calculated using the method described in Chapter Four. The results show that all models follow the same trend wherein water consumption increases with external monthly temperatures. During the warmer months, particularly in August, 03SSM consumed slightly more water per unit area (118) than the other two models (114 and 112 for 06SSM and 12SSM respectively) whereas during the temperate and

colder months of the year, 12SSM tended to consume more. This suggests that the effect of segmentation on the pattern of water consumption throughout the year is that the more floors there are in the segment the less water it consumes during the warmer months and the more it consumes during winter. This is likely because during the temperate and cold months of the year, the opening factor of the vents at the office/atrium and office/DSF interfaces is at its minimum when cooling is required which also means that dispersion in airflow rates between floors is at its minimum. Consequently, models with more floors in the segment benefit from the higher stack pressures acting on those vents without the drawbacks of dispersion which eventually increases the airflow rates and in turn, water consumption. Overall, all models consumed almost equal quantities of water over the course of the cooling season (420 l/m^2, 424 l/m^2, and 428 l/m^2 for 03SSM, 06SSM, and 12SSM respectively) which suggests that the effect of segmentation on water consumption is minimal.

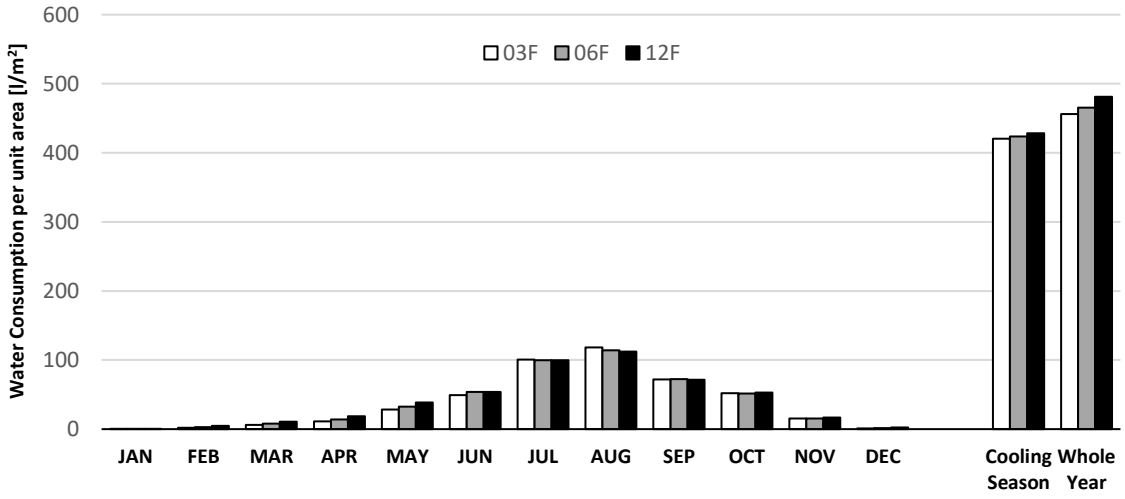

Figure 6-10 Water consumption per unit area

6.3 Duration of PDEC operation

Results of the simulation of the BCM have shown that mean radiant temperatures (t_{mr}) in offices during occupied hours are consistently higher than internal dry bulb temperatures (t_{db}). As thermal comfort corresponds to both indices, or to their combination as represented in operative temperatures (t_{op})—assumed here to be the average of the two—it was anticipated that along with nighttime-ventilative cooling (NC), allowing PDEC to operate during unoccupied hours could potentially cool down the building structure and therefore reduce t_{mr} during the following day. As always, consideration of the trade-off between comfort and environmental costs—in this case water consumption—was integral, hence this parametric exercise.

6.3.1 Modelling assumptions

Since the main aim of this exercise was to investigate the effect of extending PDEC beyond occupied hours on internal conditions, it seemed reasonable to reduce the BCM to a single floor to avoid wasting unnecessary computational time and reduce the size of the data being analysed. Accordingly, a single floor segment was modelled by removing the upper and lower floors of the BCM whilst maintaining the distance between the segment's inlet and outlet opening on one hand and the vents at the office/atrium and office/DSF interfaces on the other. EFM was again used to determine the sizes of the PDEC components for this configuration. For all variants modelled in this exercise, the size of the vents at both interfaces was 10m^2 and the size of the segment's inlet and outlet openings was 7m^2.

The BCM assumes that PDEC ceases to operate beyond occupied hours of the working day which run from 8am to 6pm. In this section, PDEC operation was allowed to begin before or extend after occupied hours in increments of one hour resulting in 27 variants (13 on either side of the working day + one variant where PDEC was allowed for the whole day) in addition to the base case (28 in total). Adjusting the control logic to accommodate this was necessary. During occupied hours of the BCM, initiation setpoints for PDEC operation were based on operative temperatures. These were kept the same but for unoccupied hours, wherein the provision of a sink for the heat stored in the structure rather than the provision of thermal comfort was the main objective, it seemed appropriate to base initiation setpoints on mean radiant temperatures. To maximise benefit from nighttime cooling, PDEC was prioritised over NC. After some trial runs, a relatively low temperature threshold for PDEC initiation was chosen and a control logic was developed as follows:

For each timestep outside occupied hours, PDEC was allowed if all the following conditions were met:

i. ($t_{mr} > t_{lb_ASH}$)

The mean radiant temperature exceeded the temperature at the lower boundary of the 90% acceptability range of the ASHRAE adaptive comfort standard.

ii. (RH < 70% or (RH < 80% when $t_x > t_{db}$))

The external relative humidity (RH) did not exceed 70%. Note here that the 80% RH threshold above which PDEC was not allowed, one which

was used in the BCM and during occupied hours in this exercise, was reduced because trial runs showed that at RH > 70%, NC would be more effective than PDEC. At such high RH values, wet-bulb temperature depressions are low and therefore any slight difference in supply air temperatures between the two modes that would potentially favour PDEC would not be sufficient to compensate for the significantly higher flow rates achieved during the NC. The only exception to this was when t_x exceeded t_{db}, in which case NC would not have been beneficial and the RH threshold above which PDEC operation ceased was allowed to extend to 80%.

iii. ($t_x > t_{lb_ASH}$) or ($t_x > t_{x_prv}$)

The external dry-bulb temperature (the supply air temperature in NC) exceeded t_{lb_ASH} or exceeded its value at the previous timestep t_{x_prv}. The latter condition was introduced so that NC would not be allowed once external temperatures had started to rise again after dropping during the night, at which point NC would not only be ineffective but would also likely increase t_{mr}.

If one or more of the previous conditions were not met, then NC was initiated provided that the internal dry-bulb temperature had exceeded the external dry-bulb temperature ($t_{db} > t_x$). Otherwise, NC and PDEC were not allowed and all vents were closed.

As noted above, t_{lb_ASH} is perhaps a relatively low threshold for PDEC initiation. Nonetheless, although investigating optimum setpoint temperatures was not

within the scope of this exercise, it was interesting to notice that during the trial runs, using higher temperature thresholds counterintuitively resulted in more water consumption.

6.3.2 Overheating and water consumption

Figure 6-11 shows water consumption per unit area and the overheating risk for the 28 variants. For each variant, *P* values at each timestep during the working hours of the cooling season were summed to give a total *P* value for that variant (*ΣP*). Values of *ΣP* are not very relevant per se, but rather provide a rapid means to rank the variants relative to each other in terms of overheating risk. For the sake of simplicity, a naming convention was used wherein the number of hours during which PDEC was allowed to operate beyond occupied hours in a variant was prefixed with a + or - sign to depict that variant. To give an example, -4 represents the variant in which PDEC was allowed to operate four hours before the start of the working day and +8 in which PDEC was allowed eight hours after occupied hours, both cases of course subject to the control logic outlined before. 00 depicts the base case where PDEC was restricted to occupied hours.

Looking at the general trend, it is clear that for the same reduction in *ΣP*, extending PDEC operation directly after occupied hours is the least efficient strategy in terms of water consumption particularly if PDEC operation was then ceased four hours or less later beyond the working day. For instance, reduction in *ΣP* resulting from extending PDEC two hours after the working day (variant +2) was almost identical to that resulting from variant -7 (*ΣP* = 680 for both) but water

consumption was significantly higher in the former at 467 l/m^2 which represents a 20% increase over that in the latter at 390 l/m^2.

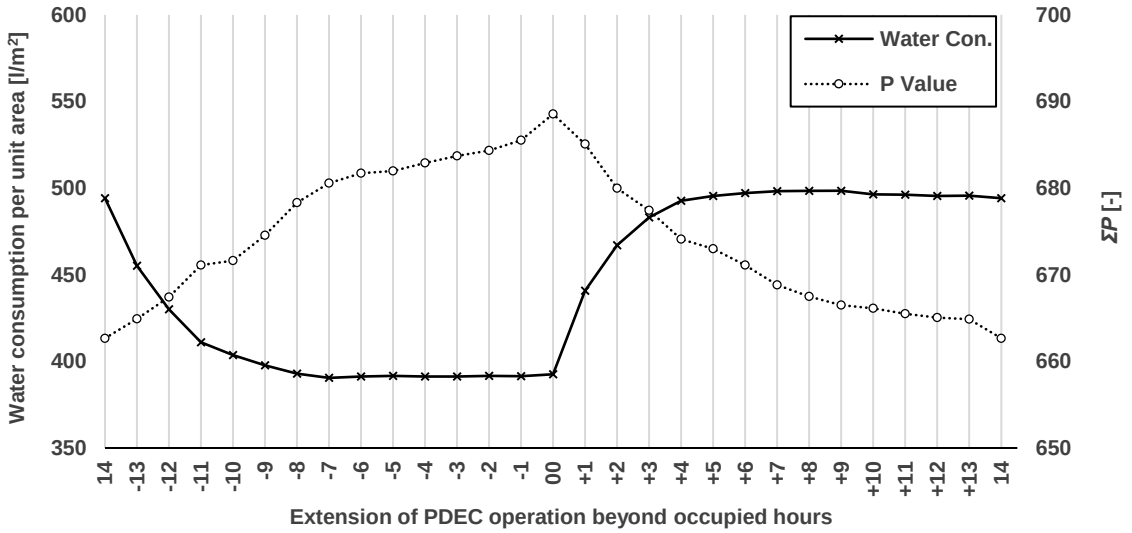

Figure 6-11 Water Consumption and Overheating Risk Index during the cooling season

Similarly, for the same consumption of water, reductions in *ΣP* can be quite disparate. For example, water consumption in variants -13 and +1 can be considered comparable at 455 l/m^2 and 441 l/m^2 respectively but a significant difference exists between their respective *ΣP* value which increased from 664 to 685. Moreover, water consumption remains constant in all variants between +4 and +14 at approximately 500 l/m^2 but *ΣP* continues to drop almost linearly from 674 to 662. The progressive increase in PDEC operation times between the first and last variant could have understandably led to the assumption that water consumption would also progressively increase. However, it is possible that the relatively prolonged operation of PDEC during unoccupied hours (leading to a cooler structure but more water consumption) had the effect of reducing PDEC

operation times during occupied hours of the following day so that on balance, the same quantity of water was consumed.

Considering the trade-off between water and comfort, for cases where water supply is an issue, allowing PDEC operation as early as eight hours before occupied hours (variant -8) evidently improves internal conditions whilst maintaining or even slightly reducing water consumption compared to the base case. For less restrictive cases, internal conditions could further be improved. To compare the performance of variants -12 and 14—representing intermediate and high levels of water consumption respectively—to that of the base case, the cumulative frequency of *P* values during occupied hours of August for the three variants were plotted (Figure 6-12).

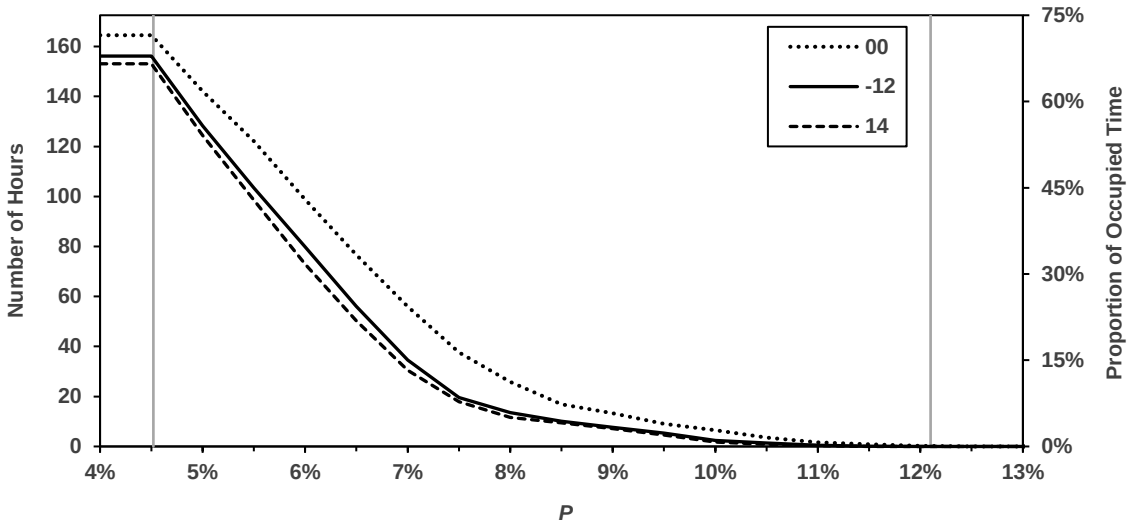

Figure 6-12 Cumulative frequency of the proportion of people voting hot or warm on the ASHRAE seven-point scale *P* during occupied hours of August

Results show that both variants perform markedly better than the base case but that the difference in internal conditions between variant -12 and 14 is not

significant. The proportion of time during which *P* exceeds 4.5% (the value of *P* at ASHRAE's adaptive comfort temperature) in variant 00 is 71% but drops to 68 and 66% in variants -12 and 14 respectively.

To appreciate the effect of the duration of PDEC operation during unoccupied hours on internal conditions during the working day in more detail, the mean radiant temperature profiles of the three variants were plotted for two consecutive days, the 23rd and 24th of August (Figure 6-13). For the 23rd of August, the average difference in mean radiant temperatures between 00 and the other two variants is approximately 1K but decreases to almost 0.5K on the 24th. Elevated humidity levels on the 24th play a major role in that, as the supply air temperature (PDEC dry-bulb temperature) is relatively higher, reducing the cooling capacity and keeping the dry-bulb and mean radiant temperature profiles relatively closer compared to the 23rd. The mean radiant temperature profiles of -12 and 14 remain very close during occupied hours on both days and only start to separate at the end of the working day when PDEC in -12 ceases to operate and the difference in t_{mr} starts to increase. t_{mr} however, recovers by the end of unoccupied hours and the profiles nearly converge again suggesting that the two-hour gap in PDEC operation had no significant effect on internal conditions but over the course of the cooling season could save as much as 64 l/m^2.

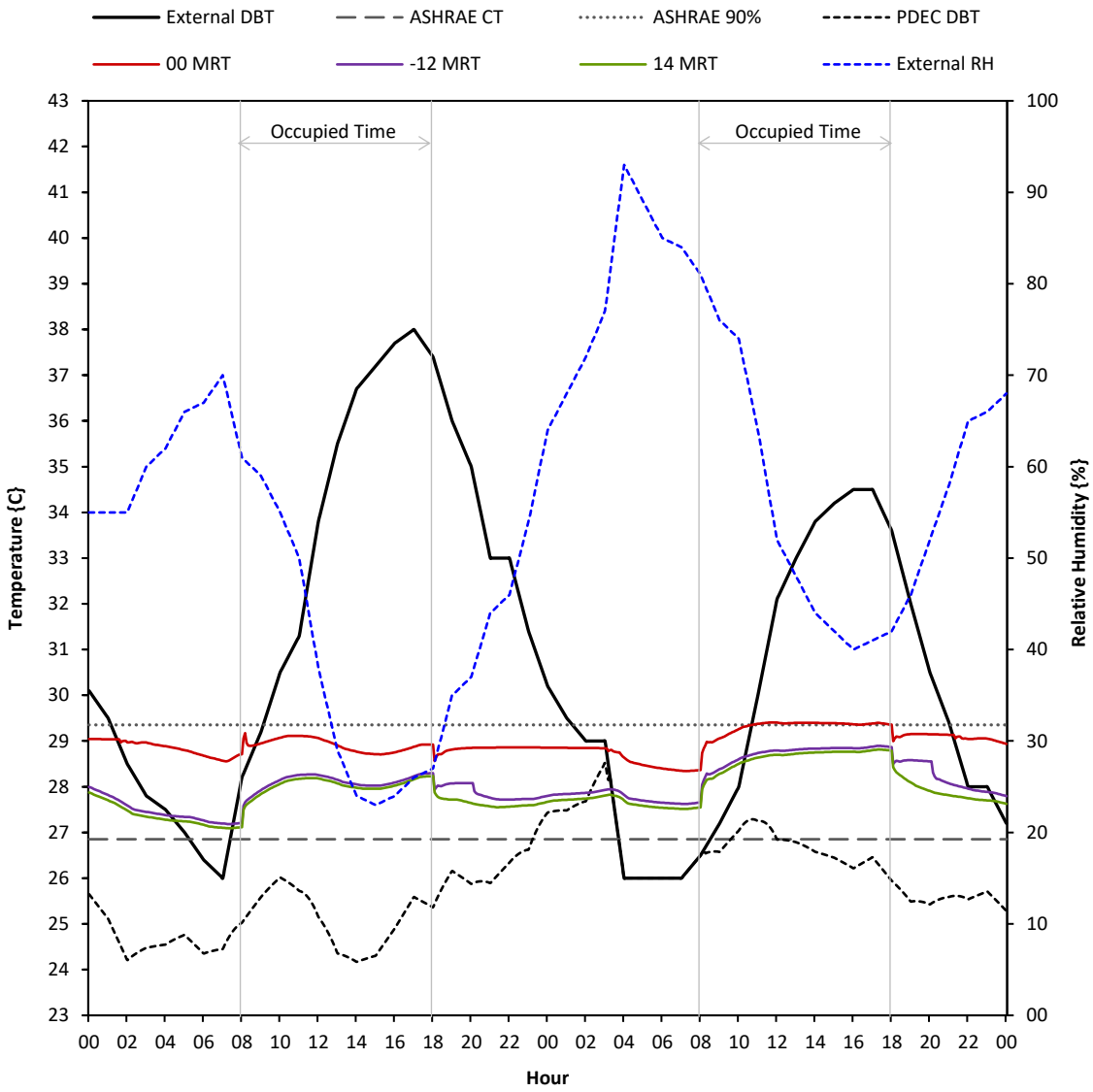

Figure 6-13 Mean radiant temperature on the 23rd and 24th of August for the base case and variants -12 and 14

6.4 Wind forces, C_p values and Orientation

The basic modelling assumption made in the BCM and all subsequent variants in the parametric investigations up to this point was the exclusion of the effect of wind forces acting on the building's envelope on airflow with the aim of investigating whether PDEC can generate sufficient airflow rates under a buoyancy only scenario, that is, with no or little assistance from wind forces, a

scenario likely to occur in urban high-density locations in the city due to the sheltering effect of surrounding buildings. In this section, the effects of wind forces on airflow rates and consequently on internal comfort conditions are reconsidered.

6.4.1 Modelling assumptions

To calculate the wind induced boundary pressure exerted on the building's envelope, it is necessary to map the free-stream wind velocity (from the weather file) onto the surface of the building as a function of both the wind's vertical velocity profile (influenced by terrain roughness) and the sheltering effect of distant and/or direct obstructions. The latter is accounted for by a dimensionless pressure coefficient (C_p) and the relationship used to express this in EnergyPlus is Bernoulli's equation, which, assuming no height change or pressure losses, can be expressed as:

$$p_w = C_p \, \rho \, \frac{U_H^2}{2} \tag{6-1}$$

where

p_w = Wind surface pressure relative to static pressure in undisturbed flow [Pa]

C_p = Wind surface pressure coefficient [dimensionless]

ρ = Air density [kg/m^3]

U_H = Reference wind speed at local height [m/s]

U_H may be expressed as (ASHRAE, 2013a):

$$U_H = U_{met} \left(\frac{\delta_{met}}{H_{met}}\right)^{\alpha_{met}} \left(\frac{H}{\delta}\right)^{\alpha} \tag{6-2}$$

where

U_{met} = wind speed in the weather file

H_{met} = height of the standard meteorological wind speed measurement

H = reference local height (building height)

α and α_{met} = Terrain-dependent exponents

δ and δ_{met} = boundary layer thickness coefficients for the given terrain type

The values of α and δ are shown in the following table:

Table 6-2 Terrain-Dependent Coefficients (ASHRAE, 2013a)

Terrain	Description	Exponent, α	Layer Thickness, δ (m)
1	Flat, open country	0.14	270
2	Rough, wooded country	0.22	370
3	Towns and cities	0.33	460
4	Ocean	0.10	210
5	Urban, industrial, forest	0.22	370

U_{met} is assumed to be measured at a meteorological station located in an open field (category 1 in Table 6-2) at a height of 10m. The values used by EnergyPlus for H_{met}, α_{met}, and δ_{met} are therefore 10, 0.14, and 270 respectively.

As for C_p values, in EnergyPlus, they can either be calculated by the program if the building is rectangular or manually inserted by the user. For the former method, EnergyPlus uses a different calculation method depending on whether the building under consideration is low-rise or high-rise.

For surfaces of a high-rise building, a two-dimensional array of surface-averaged wind pressure coefficients is generated based on wind incident angle and side ratio. The Engineering reference manual for EnergyPlus cites the wind pressure coefficients provided in ASHRAE Handbook of Fundamentals

(ASHRAE, 2013a) in the figure captioned “Surface-Averaged Wall Pressure Coefficients for Tall Buildings” (Figure 6-14). The original work was performed by Atkins, Peterka, & Cermak (1979). The incident angle has an increment of 30 degrees. The side ratio values are 0.25, 1.0, and 4.0. For a given incident angle and building aspect ratio, the program uses linear interpolation to calculate the corresponding wind pressure coefficient. If this method is selected, the user is required to enter the building’s aspect ratio and azimuth angle of the long axis of the building.

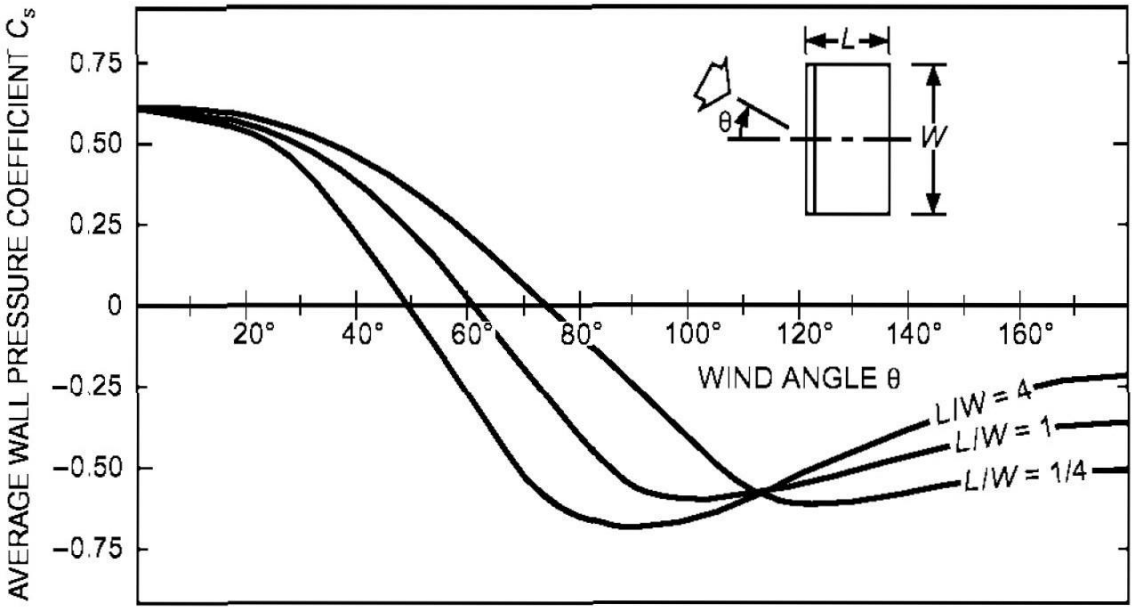

Figure 6-14 Surface-averaged Wall Pressure Coefficients for Tall Buildings (Atkins et al., 1979)

Assuming surface-averaged C_p values however, implies that for each incident wind angle (between wind direction and outward normal of surface under consideration), the same C_p value is used irrespective of the location of the opening on that surface. In this case, the only difference in p_w between one opening and the other on the same surface arises from the difference in the

calculated value of U_H when there is a height difference between the centroids of the two openings. Note here that according to ASHRAE (2013) which is cited by the EnergyPlus Engineering reference as the source of equation $U_H = U_{met}\left(\frac{\delta_{met}}{H_{met}}\right)^{\alpha_{met}}\left(\frac{H}{\delta}\right)^{\alpha}$ (6-2), U_H is the adjusted air velocity at the top of the building and therefore should remain constant for the same building, whereas in EnergyPlus, H is not calculated at the building height but at the centroid of each opening. Consequently, it can be inferred from equation $pw = C_p\,\rho\,\frac{U_H^2}{2}$ (6-1) that the ratio between p_w values at two different heights on the same surface remains constant irrespective of the wind incident angle, i.e. irrespective of whether the surface is windward, leeward or anywhere in between, an outcome that is unlikely to reflect what happens in real environments and one that renders the very idea of pressure coefficients redundant.

Alternatively, EnergyPlus offers the option of manually entering C_p values for as much as 36 wind directions (in 10° increments). Accurate determination of C_p values can only be obtained from full-scale tests, wind tunnel model tests, or CFD modelling of the specific site and building. But for the purpose of ventilation rate calculations for single, unshielded rectangular buildings, values can be reasonably estimated using existing wind tunnel data (ASHRAE, 2013a). Two sources of wind pressure coefficient data were used in this study; the data generated by Davenport & Hui (1982) for walls of a tall rectangular cross section building (high-rise) sited in urban terrain and the aerodynamic database for high-rise buildings developed by the Tokyo Polytechnic University in Japan (TPU, 2013). The database is part of the Wind Effects on Buildings and Urban

Environment project in which 22 models of high-rise buildings were tested. Contours of statistical values of local wind pressure coefficients, graphs of statistical values of area averaged wind pressure coefficients on the wall surfaces, and time series data of point wind pressure coefficients for 394 test cases are shown on the web site. The data can be used to calculate local wind pressures, area averaged wind pressure coefficients on wall surfaces, and wind induced dynamic responses of high-rise buildings. The inputs required to query results are the breadth to depth ratio, the breadth to height ratio, and the Alpha parameter for determining the exposure factor.

The BCM of the PDEC multi-storey office building was configured such that all the segment's inlet and outlet openings lie on the same surface with each opening running the whole width of that surface. Since the difference in height between the opening at the top of the atrium and the opening at the top of the DSF can be considered negligible given their proximity, it was anticipated that the main difference in p_w values would occur between the openings at the top of the atrium and bottom of the DSF. To determine the maximum extent to which wind can affect the performance of the PDEC office building model, those two openings were assumed to be at the two locations on the surface that had the largest discrepancy in p_w values.

Accordingly, C_p values were averaged over the width of the building surface at those two locations, i.e. at the levels of maximum and minimum average C_p values. This was done for each wind incident angle at an increment of 30°. The average was calculated by drawing a horizontal line across the width of the surface at the intended height. The length of the segment created between any

two contour lines was then multiplied by the average of the C_p values of those two contour lines. The products were summed and then divided by the total length of the line (i.e. the width of the surface) to obtain the average C_p value at that height. This was done for the two data sources as shown in Figure 6-15 and Figure 6-16.

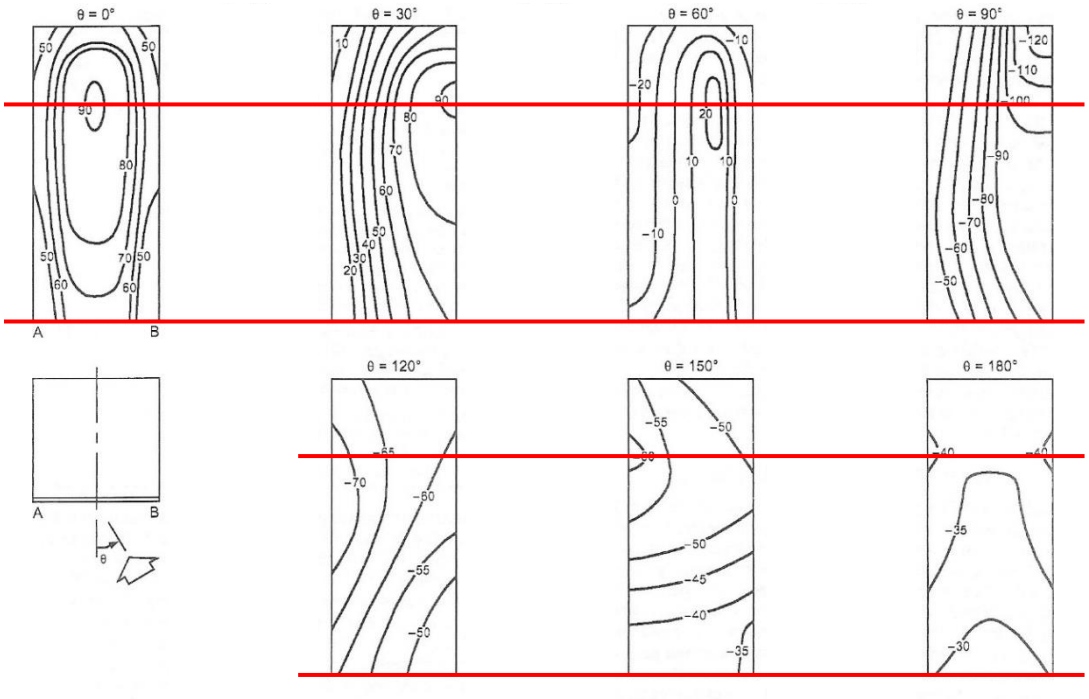

Figure 6-15 Local pressure coefficients (C_p x 100) for a tall building sited in urban terrain with wind direction varying at an increment of 30° (Davenport & Hui, 1982) with the two locations of averaged C_p values overlaid

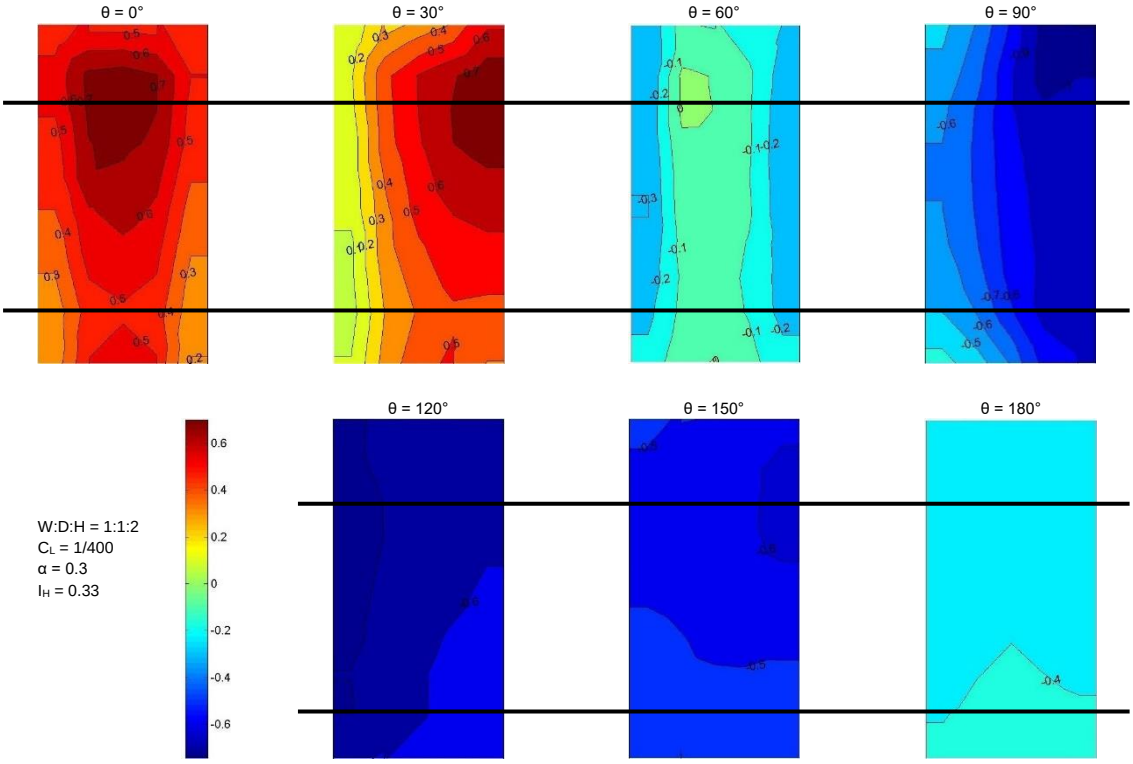

Figure 6-16 Mean wind pressure coefficients on a high-rise building with wind direction varying at an increment of 30° (TPU, 2013) with the two locations of averaged C_p values overlaid

Comparing the two sources (Table 6-3), it was found that for all wind incident angles considered, the resulting average C_p values were almost identical in terms of the difference between top and bottom locations but with the TPU dataset consistently lower by 0.1 in terms of C_p values. The comparison results give credibility to the use of either source as input. The average values calculated from Davenport and Hui where thus chosen arbitrarily.

Table 6-3 Average Cp Values at the top and bottom openings

		0°	30°	60°	90°	120°	150°	180°
Davenport and Hui	Top	0.7	0.6	0	-0.8	-0.6	-0.5	-0.4
	Bottom	0.5	0.5	0	-0.7	-0.5	-0.4	-0.3
TPU	Top	0.6	0.5	-0.1	-0.8	-0.7	-0.6	-0.5
	Bottom	0.4	0.4	-0.1	-0.8	-0.5	-0.5	-0.4

The 12-storey segment model (12SSM) seemed to be the most appropriate segmentation variant to investigate the effects of wind forces on the performance of the PDEC multi-storey office building model as it was the only variant to likely have the top and bottom openings at the two locations with the largest discrepancy in C_p values. In previous sections, the inlet and outlet openings of 12SSM were facing south. As wind effects vary greatly with orientation, 12SSM was also modelled facing the other three cardinal directions. Additionally, three other variants of 12SSM were modelled facing the three other cardinal directions only this time without wind effects (C_p values set to zero) to serve as a baseline for their respective variants with wind effects included. In total, seven variants were modelled.

6.4.2 Airflow

Figure 6-17 shows the volume airflow rates across the floors averaged over the duration of occupied hours of the cooling season for the 12-storey segment model. Each graph shows the results of the two variants that face the same cardinal direction, one with wind effects included and the other without. Generally, the results show that with wind assistance, average airflow rates across floors are slightly higher with the difference between the respective floors increasing with floor level from roughly no difference at the bottom floor to a 0.3 m^3/s increase at the top level (10% increase). The slight increase occurs equally for all cardinal directions indicating that in terms of the effect of wind on the performance of the PDEC model, changes in orientation do not play a significant role.

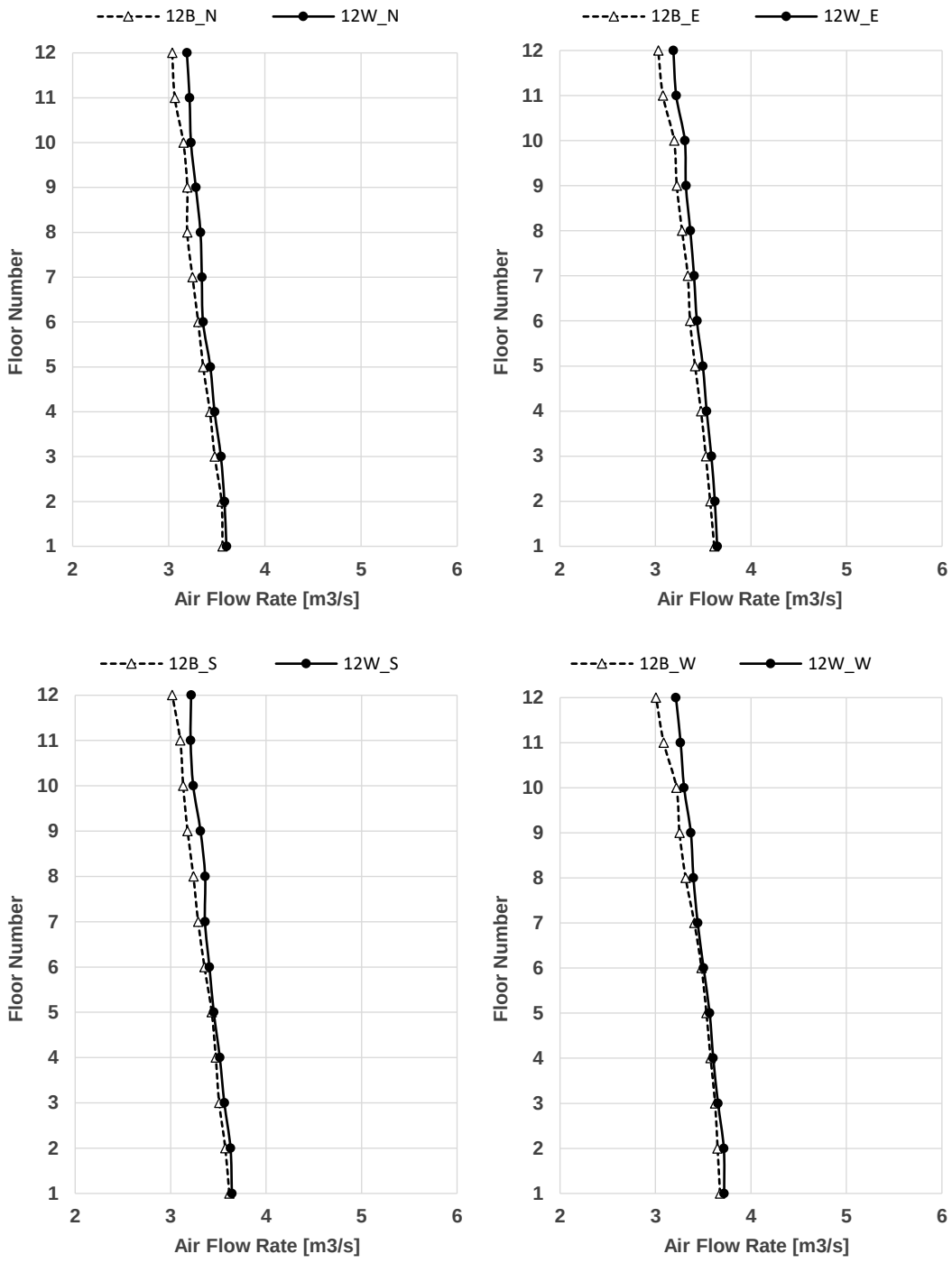

Figure 6-17 Average volume airflow rates across the floors during occupied hours of the cooling season for the 12-storey segment model at different orientations with and without wind effects

When flow patterns are considered independently, the results show that the slight increase in airflow rates in variants wherein wind effects were included

persists in all but the B-U flow pattern in which airflow rates across floors were actually reduced. The reduction is consistent for all cardinal directions as shown in Figure 6-18.

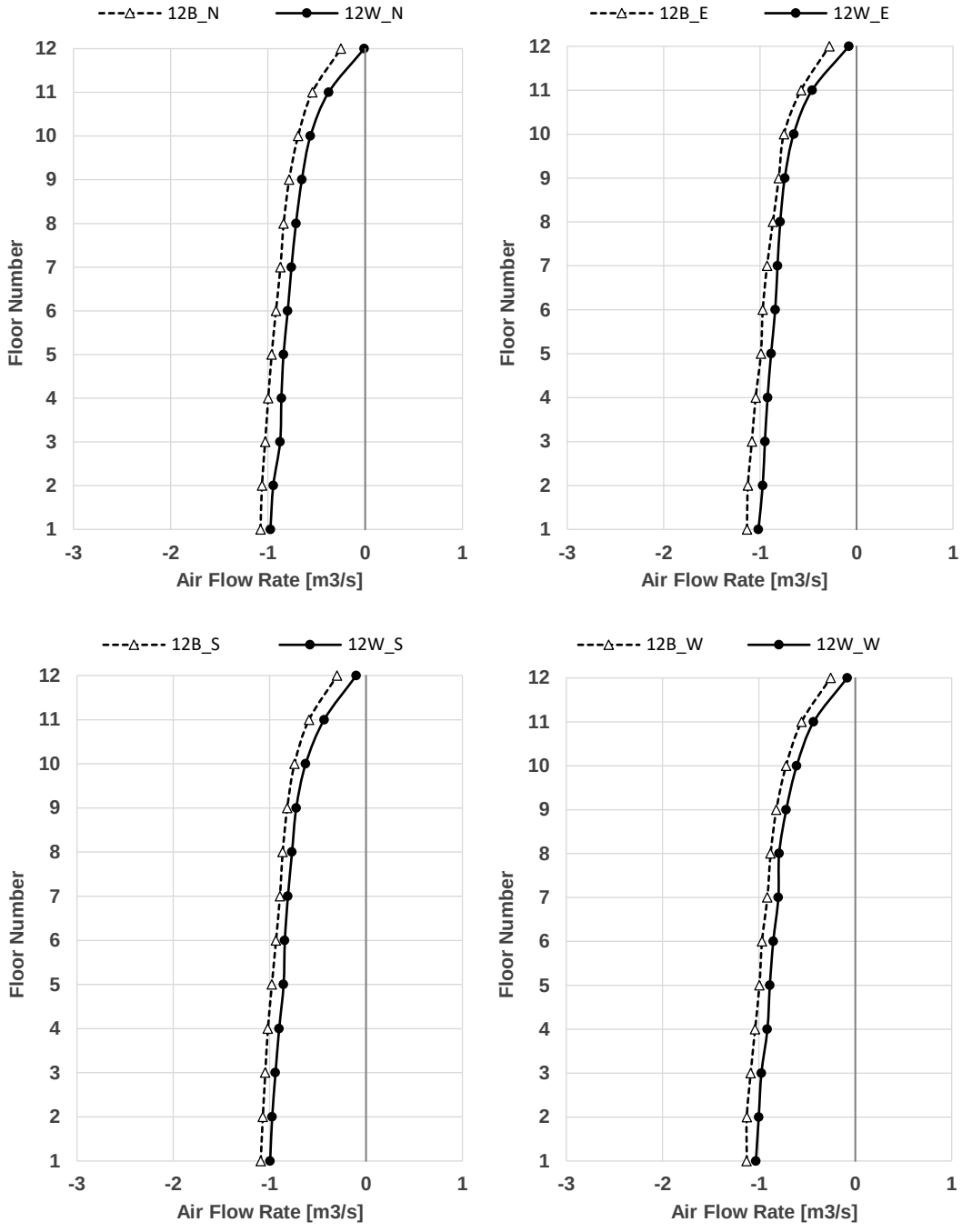

Figure 6-18 Average volume airflow rates across the floors during occupied hours of the cooling season for the 12-storey segment model in the B-U flow pattern at different orientations with and without wind effects

Reduction in airflow rates can be attributed to the fact the it is the only flow pattern in which air is drawn from the bottom opening of the DSF and is exhausted from the opening at the top of the atrium. In this case the relatively lower C_p values at the bottom opening hinders rather than enhances the flow.

6.4.1 Comfort and Water consumption

A look at the proportion of occupied time during which each flow pattern operates (Figure 6-19) shows that the flow patterns in which PDEC is in operation (T-U and T-D), occupy a slightly bigger proportion of time at the expense of the B-U flow pattern in the variants in which wind effects were included then they do in the no-wind variants.

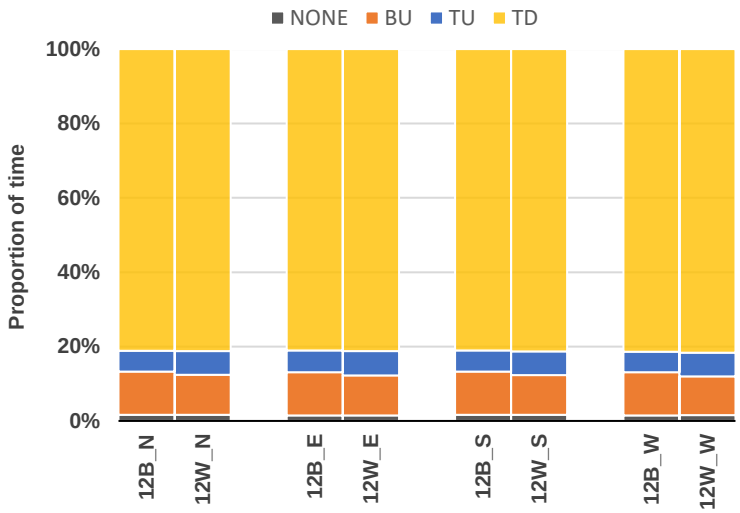

Figure 6-19 Proportion of time during which each flow pattern operates for the wind and no-wind variants of the 12-storey segment model

This is likely due to the fact that the reduction in airflow rates during the B-U flow pattern in the wind variants causes internal temperatures in the early hours of the working day to rise more rapidly prompting an earlier initiation of PDEC

and therefore a changeover to either a T-U or T-D flow pattern. It is therefore not surprising to find that for all building orientations investigated, water consumption in the wind variants was approximately 2% higher than in their respective no-wind variants as shown in Figure 6-20.

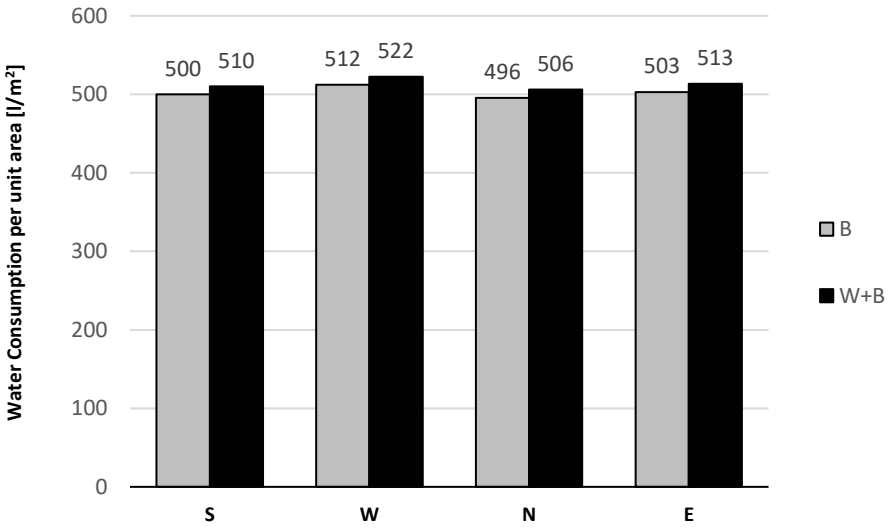

Figure 6-20 Annual water consumption per unit area for the wind and no-wind variants

The reduction in airflow rates during the B-U flow pattern in the wind variants is reflected in a slight elevation in *P* values (Figure 6-21a). Similarly, the increase in average airflow rates and in turn water consumption in the wind variants is reflected in the slight reduction in average *P* values for all cardinal directions during occupied hours of the cooling season when PDEC was operational (Figure 6-21b and c). Since the latter flow patterns are dominant during occupied hours of the cooling season, the overall effect of wind on the 12-storey segment model is the slight reduction in *P* values (Figure 6-21d).

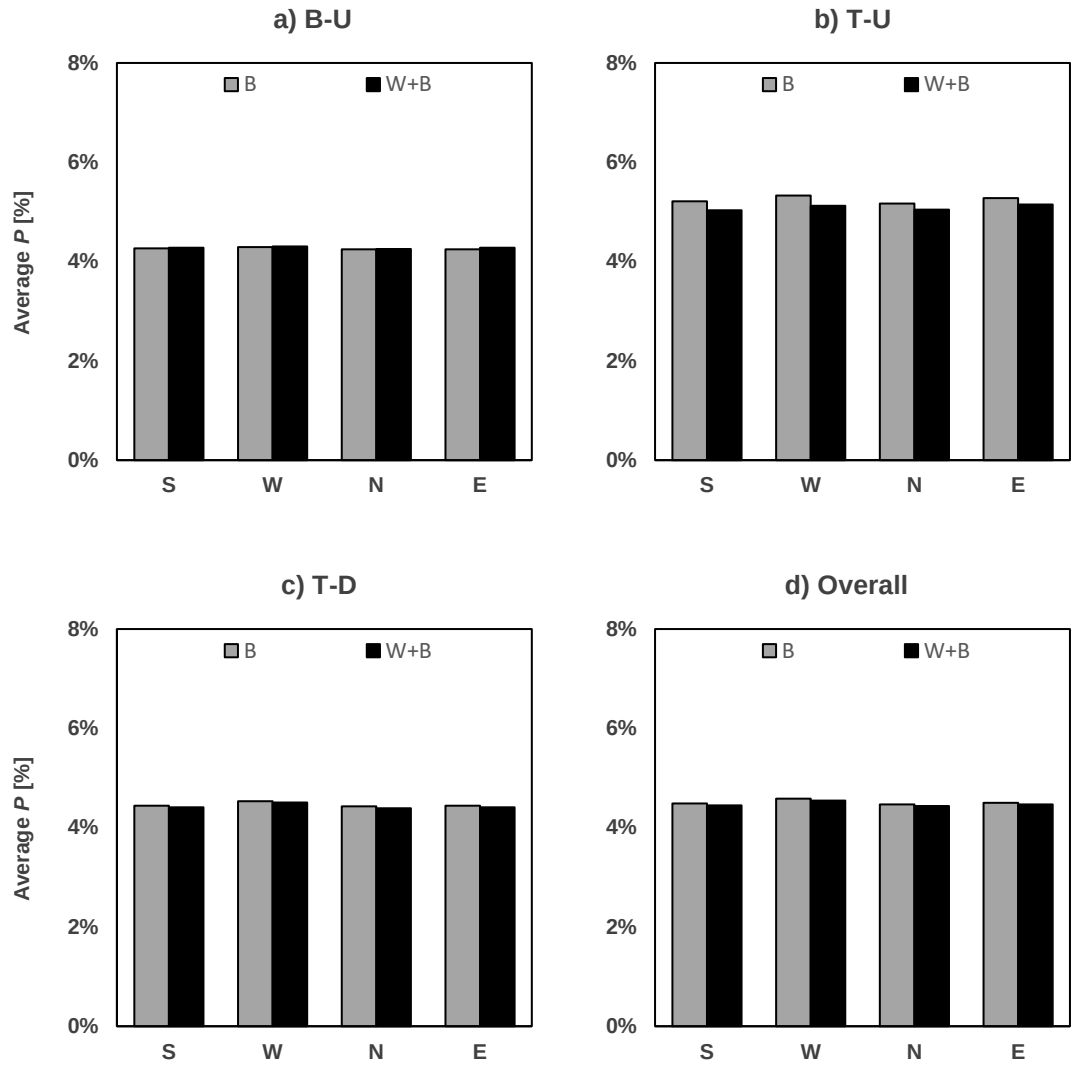

Figure 6-21 Average *P* values during occupied hours of the cooling season for the wind and no-wind variants oriented towards the four cardinal directions when a) operating in a B-U flow pattern b) in a T-U flow pattern c) in a T-D flow pattern d) overall average

6.5 Comfort model and overheating criterion

The control logic adopted in the BCM was developed to maintain internal conditions within the 90% acceptability range of adaptive comfort model as defined by ASHRAE standard 55, the assumption being that the ACM could arguably be extended to buildings with PDEC as discussed in Chapter Three. More specifically, the control logic was developed to maintain internal

temperatures as close to the neutral temperature of the ACM as possible because the overheating criterion chosen to assess the performance of the model was one wherein the magnitude and duration of departure of operative temperatures from that temperature was considered, a criterion referred to in §5.4.2 as the ASHRAE Overheating Risk Index (ORI_{ASH}). In this section, the effects of adopting different comfort models and overheating criteria on internal conditions and consequently, on water consumption are investigated.

6.5.1 Modelling assumptions

The comfort models and neutral temperatures considered here are those presented in Chapter Three, namely: The ACM as defined by ASHRAE Standard 55 (ASHRAE, 2013b) and CEN 15251 (CEN, 2008), the adaptive neutral temperatures and their associated comfort boundaries developed by Nicol & Humphreys (2007) for heated and cooled buildings in Europe and by Farghal & Wagner (2010) for free-running educational buildings in Egypt; The PMV-PPD model (ASHRAE, 2013b; Fanger, 1970; ISO, 2005); and lastly, the Fiala model (Fiala & Lomas, 2001; Fiala, Lomas, Martínez, et al., 1999; Fiala et al., 2001; Fiala, Lomas, & Stohrer, 1999; Martínez et al., 2000). Additionally, the implications of adopting the “Exceedance Index” (§5.4.2) as an overheating criterion and incorporating that in the control logic is also considered. To establish the amount of reduction in overheating resulting from the PDEC strategy, variants with no PDEC mode were also modelled to serve as a baseline. Furthermore, to establish the maximum cooling potential of the PDEC strategy, a hypothetical scenario wherein PDEC was allowed to operate at all times was also modelled.

Variants were divided into two sets according to the aim of their respective control logic based on overheating criterion adopted. For variants in which the aim of the control logic was to maintain internal temperatures as close to the neutral temperature of the ACM as possible, henceforth referred to as the Overheating Risk variants (OR variants), the same control logic of the BCM (§5.3.3.1) was used whereby the ASHRAE adaptive comfort temperature and its acceptability boundaries used in the BCM were replaced by their respective values in each variant. For variants in which the aim of the control logic was to maintain internal temperatures within the upper boundary of comfort as defined by the respective comfort model, henceforth referred to as the Exceedance variants (EX variants), two changes had to be made to the global control logic of the BCM as follows:

i. The changeover setpoint temperature t_{csp} was increased from (t_{cmf} + 1) in the BCM to (t_{cmf} + 2) allowing NV to continue to operate up to the higher end of the acceptability range.
ii. t_{s_max} was also increased from t_{lb} to t_{cmf} and for cases wherein $RH \geq 80$, it was extended from t_{cmf} to a non-fixed value whereby it would need to be at least 1K lower than the external dry-bulb temperature (t_x - 1).

Notes on the modelling assumptions

i. In this exercise, not all comfort models used to assess overheating were incorporated in the control logic before simulation. Only adaptive comfort models (those wherein neutral temperatures were derived from a relation to one or another outdoor temperature metric through linear regression of

field data) were incorporated in the control logic with the aim of reducing water consumption whereas those based on chamber studies (namely the PMV-PPD model and the Fiala model) were only used to assess comfort post processing without implications on the control logic.

ii. The ORI relates the magnitude of the departure of actual or predicted operative temperatures from the adaptive comfort temperature to the proportion of people (*P*) voting 'warm' or 'hot' on the ASHRAE comfort scale. The index was initially developed by Nicol, Hacker, Spires, & Davies (2009) for EN15251 (ORI_{EN}) and then by Carlucci (2013) for ASHRAE standard 55 (ORI_{ASH}) and was therefore only used to assess variants employing those two comfort models.

iii. When the PMV-PPD model, Fiala model, or Nicol and Humphrey's adaptive temperature for heated or cooled buildings were used to assess overheating, they were only applied to periods of occupied time during which PDEC was in operation whilst the respective adaptive comfort model was used for the remaining period.

iv. Clothing insulation and metabolic rate required as input to calculate PMV and PPD were assumed to be 0.5clo and 1.2met respectively.

v. For the ACM in EN 15251, a "Category I" environment was assumed wherein the comfort boundary extends 2K on either side of the comfort temperature.

vi. The ACM in ASHRAE standard 55 and EN 15251 is not applicable at instances when the monthly mean outdoor temperature and running mean outdoor temperature exceed 33°C and 30°C respectively. For Cairo's historic weather data, the former case does not occur whilst the

latter does on 18 occasions (18 days representing approximately 13% of the total occupied time during the cooling season) in which case the control logic was developed to initiate PDEC automatically.

6.5.2 Results

Figure 6-22 shows the cumulative frequency of *P* for the variants which have their control logic based on the ACM in ASHRAE standard 55 and EN15251 respectively. For each comfort model, three variants were developed, one with no PDEC (NV variant), another based on an Exceedance overheating criterion (EX variant), and a third on an Overheating Risk criterion (OR variant). The results show that NV alone was not sufficient to maintain internal conditions within the comfort boundaries in both comfort models (61% of occupied time for NV_{ASH} and 54% for NV_{EN} lie outside their respective comfort boundaries). On the other hand, internal conditions in variants with PDEC were kept within the comfort boundaries of their respective comfort model which, in terms of the Exceedance index (EXI), means that no overheating occurred (Figure 6-25). However, in terms of the Overheating Risk index (ORI), there was a marked difference between variants developed for that index and those developed for EXI.

For instance, operative temperatures exceed ASHRAE's adaptive neutral temperature (at P = 4.52%) for 82% of occupied time during the cooling season for EX_{ASH} but for only 29% of occupied time for OR_{ASH}. Moreover, *P* exceeds 8% for only 3% of occupied time in OR_{ASH} but exceeds this value for approximately a third of the occupied period for EX_{ASH}. Similarly, 65% of occupied hours lie above the EN15251 adaptive comfort temperature (at P = 6.87%) for EX_{EN} whereas this

figure drops to 20% for OR_{EN}. As noted previously, as far as the ACM in EN 15251 is concerned, there remains 13% of the total occupied time during which the model cannot be applied which is why the cumulative frequencies of exceedance for EX_{EN} and OR_{EN} do not fall below that value.

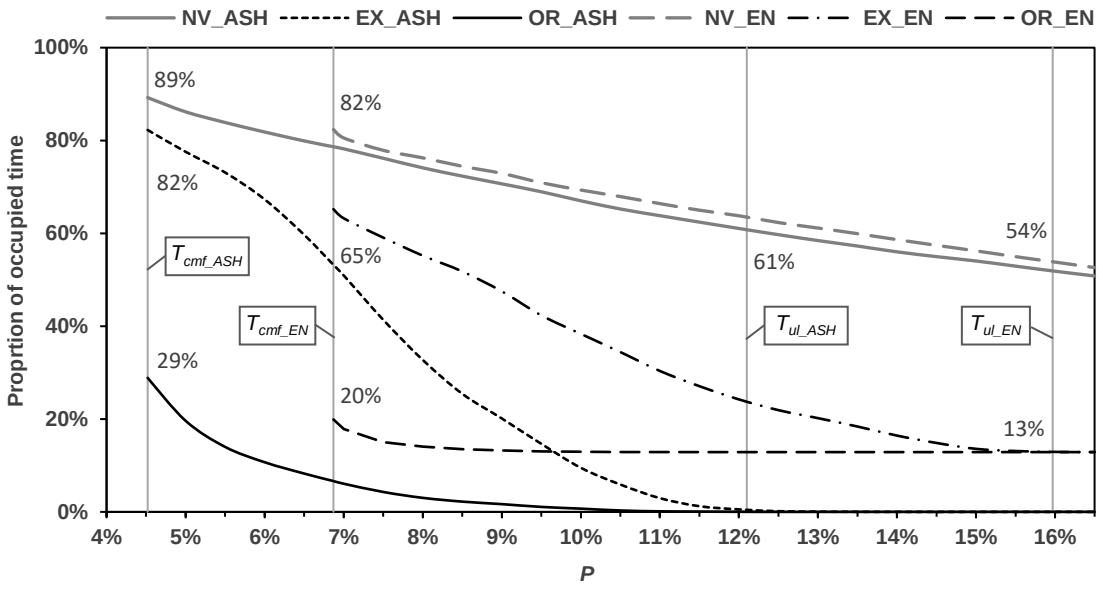

Figure 6-22 Cumulative frequency of exceedance of *P* for ORI and EXI variants

The discrepancy in internal conditions between variants developed for ORI and those for EXI is better indicated by their respective average *P* values with the average calculated assuming a *P* value of 4.52% and 6.87% for all timesteps in which $t_{op} < t_{cmf_ASH}$ and $t_{op} < t_{cmf_EN}$ respectively. Figure 6-23 shows that *P* average drops from 7.1% in EX_{ASH} to 4.9% in OR_{ASH} and from 8.9% in EX_{EN} to 6.9% in OR_{EN}. The results also show that in NV variants, average *P* rises to 20.4% and 22.8% in ASHRAE 55 and EN15251 variants respectively. Furthermore, the results show that internal conditions in the hypothetical scenario wherein PDEC is allowed to operate at all times (variant prefixed with MAX) is not significantly

better, whether assessed by ASHRAE 55 or EN 15251, than the variant with the respective comfort model and thus does not warrant the associated increase in water consumption.

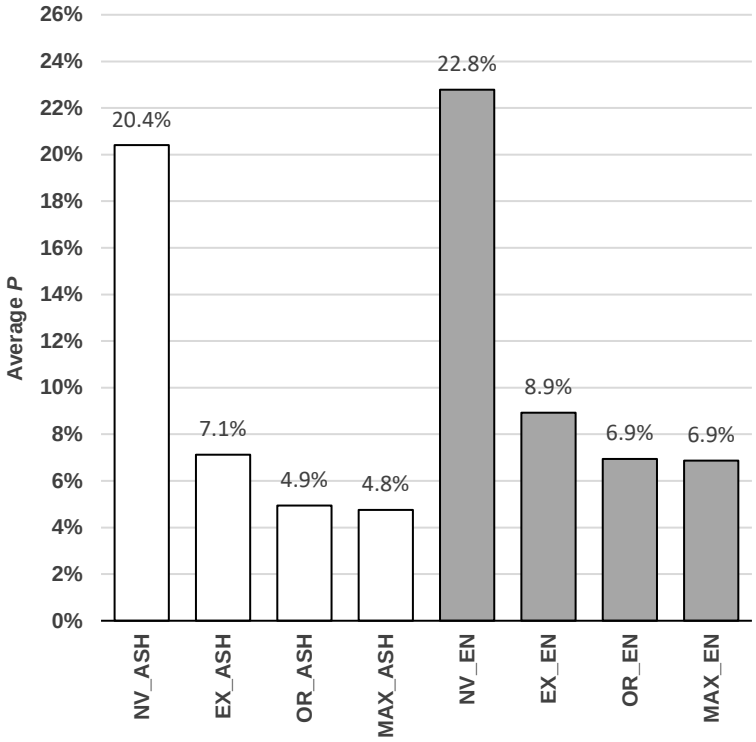

Figure 6-23 Averge *P* values of NV, EX, OR, and MAX variants

In terms of water consumption, there exists a gulf between the EX and OR variants, as shown in Figure 6-24. This was particularly evident in variants employing the ASRHAE standard 55 ACM where the annual water consumption per unit area dropped from 414 l/m^2.yr in OR_{ASH} to 149 l/m^2.yr in EX_{ASH} (a 64% reduction). A similar albeit smaller reduction occurred in the EN 15251 ACM variants as water consumption dropped from 138 l/m^2.yr in OR_{EN} to 59 l/m^2.yr in EX_{EN} (57% reduction). It would therefore seem unreasonable to maintain internal temperatures near the adaptive comfort temperature should an EXI be adopted as an indication of overheating. Reducing the daily water consumption per

occupant in the PDEC building from 9.1 to 3.3 litres would mean that the extra quantity of water required for cooling would represent an increase of only 1.3% in the average daily water consumption per capita in Egypt, currently at 211 litres per day (CAPMAS, 2015).

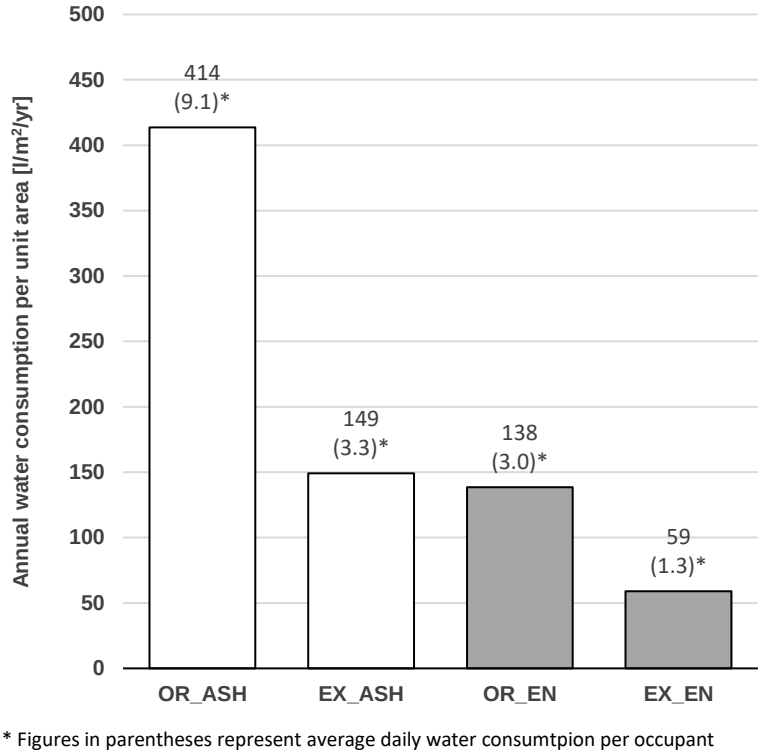

Figure 6-24 PDEC water consumption in EX and OR variants

A look at the EXI for the other ACM variants (Figure 6-25) reveals that as with the ASHRAE standard 55 variant, internal conditions in the EX variant developed to employ the Farghal & Wagner (2010) adaptive temperature were kept within the comfort boundaries for the whole occupied period. However, comfort was maintained for only 65% of occupied hours in the NV variant employing the same adaptive temperature. Finally, 80% of occupied time is considered thermally acceptable if the adaptive comfort temperature for heated

and cooled buildings (Nicol & Humphreys, 2007) is adopted and the control logic adjusted accordingly.

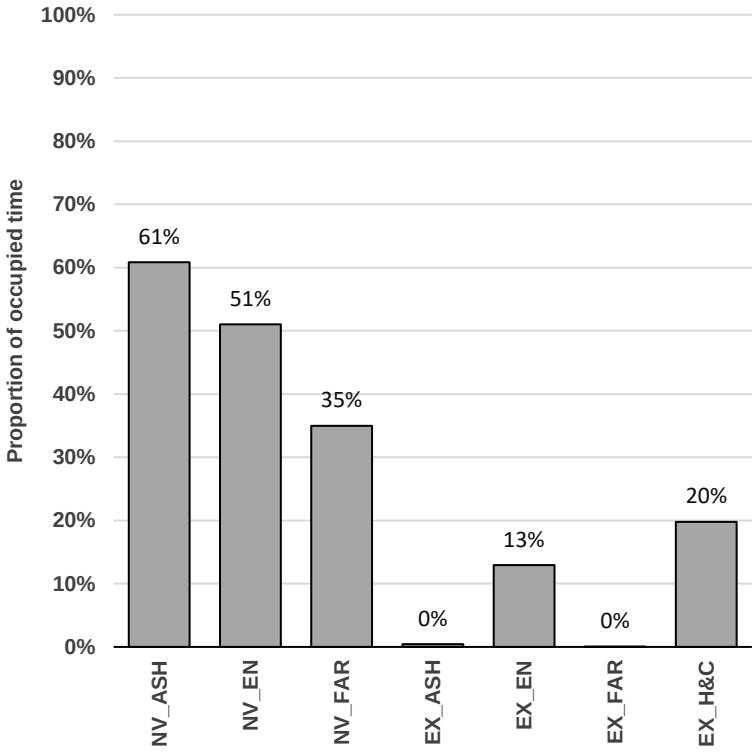

Figure 6-25 Exceedance of NV and EX variants based on their respective Adaptive comfort model

All previous results of the performance of the variants in terms of comfort and overheating were based on the premise that the application of the ACM was not limited to periods of NV operation but extends to include periods of PDEC operation as well as argued in Chapter 5. However, to determine the performance of the variants without making such an assumption, chamber based models were used to assess exceedance during periods of PDEC operation as shown in Figure 6-26. Expectedly, exceedance figures considerably increased for all variants when the PMV-PPD model as described in ASHRAE standard 55 was used

wherein internal conditions at timesteps with a PMV of 0.5 or lower were considered thermally comfortable assuming airspeeds of 0.2 m/s or lower. Exceedance rose for example from 0% to 52% for EX_{ASH} and from 11% to 46% for EX_{EN}.

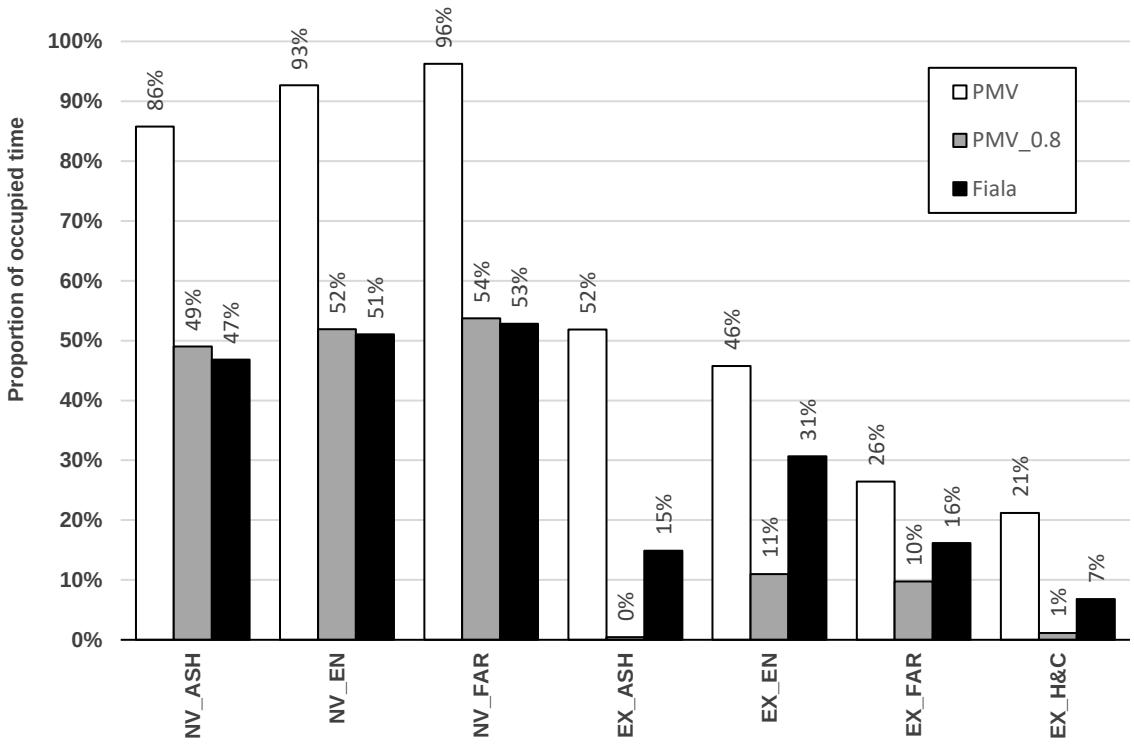

Figure 6-26 Exceedance of NV and EX variants based on the PMV-PPD model with still air conditions(PMV), the PMV-PPD model with internal airspeeds of up to 0.8m/s (PMV_0.8), and the Fiala model with air speeds of up to 0.6m/s (Fiala)

To determine the extent of reduction in exceedance due to elevated air speeds for the PMV-PPD model, the PMVs of all timesteps wherein PMV had exceeded 0.5 were recalculated using the SET model (§3.3.2) only this time the value of air speed used for input was increased in increments of 0.1m/s to a maximum of 0.8 m/s depending on the PMV value. A PMV of less than 0.6 was assigned an air speed of 0.3m/s, a PMV of less than 0.7 an airspeed of 0.4m/s

and so on until a PMV of more than 1.0 was assigned an airspeed of 0.8m/s. This measure was taken in an attempt to reflect the proportionate behaviour of occupants in response to the thermal stress of the environment through employment of fans for personal cooling. To generate the PMV values using the SET method, a spreadsheet of the environmental and personal factors of each timestep was created and uploaded to the CBE website (Tyler et al., 2017)

The results show a marked reduction in exceedance in all variants. Increasing local air speed up to 0.8 m/s eliminated overheating altogether in EX_{ASH} and reduced exceedance to 1% in $EX_{H\&C}$ indicating that even if the restrictive criteria of the PMV-PPD model is adopted, PDEC can still deliver comfort conditions for all occupied hours of the cooling season by increasing local air speed (using fans for example). This strategy is particularly effective with PDEC because as previously shown, mean radiant temperatures tend to be high and air temperatures tend to be low.

Finally, the results show that using the Fiala model to assess exceedance gives results that are comparable to the PMV-PPD model for NV variants, but underestimates and overestimates exceedance compared to the PMV-PPD model with and without elevated air speed respectively for all PDEC variants.

6.6 Summary

In this chapter parametric studies were performed to further investigate the thermal and airflow behaviour of the proposed generic configuration of the PDEC multi-storey office building under different boundary conditions and modelling assumptions. Four key parameters were identified, namely; the number of floors

in a segment being served by the same PDEC system (segmentation), the duration and timing of PDEC operation beyond occupied hours, wind forces and orientation, and choice of comfort model and overheating criterion. For each parameter, the approach for carrying out the proposed investigations was described, and the modelling assumptions outlined accordingly.

In Section 6.2, the effect of increasing the number of floors in a segment on the overall bulk airflow rates in the segment and the distribution of airflow rates across the floors was investigated together with the implications of that on internal conditions and water consumption. The effects of extending PDEC operation during unoccupied hours on reducing the mean radiant temperature the following day is discussed in Section 6.3 with the implications of that on water consumption. Section 6.4 discusses the inclusion of wind forces and their effects on airflow rates across the floors of the segment. The effects of varying the orientation of the building segment and the subsequent change in solar gains and wind forces on the thermal and airflow behaviour of the PDEC building model is also investigated. Choice of the thermal comfort model and overheating criteria has a significant bearing on the assessment of acceptability of internal conditions for human occupancy and is therefore the subject of Section 6.4 in which the effect of adopting different comfort models and overheating criteria is examined.

Segmentation

The effect of segmentation was investigated by modelling a 12-storey model of the PDEC generic building for three different segmentation cases, the first made up of four three-storey segments, the second of two six-storey segments and the third of one 12-storey segment. Only buoyancy forces were considered.

Sizes of the PDEC components were accordingly recalculated using EFM which indicated that areas for the segment's inlet and outlet openings during the T-U flow pattern needed to be significantly larger than their respective sizes during the B-U and T-D flow patterns in the six-storey and 12-storey segments.

In terms of airflow, the relative performance of the three variants varied depending on mode of operation and month within the cooling season. During the temperate period (May), it was found that during PDEC operation (T-U and T-D flow patterns), the more the number of floors there are in a segment the higher the airflow rates traversing those floors but that during NV (B-U flow pattern), floors in the smaller segments had slightly higher flow rates than their respective floor levels in the top half of the larger segments and vice versa.

For all variants, average airflow rates decrease with floor level which leads to the dispersion in flow rates between the segments' floors. As the number of floors in a segment increases, so does the dispersion. Dispersion is more pronounced in the warmer months than it is in the temperate months of the cooling season and within the same month, during the T-U and B-U flow patterns than it is during the T-D flow pattern. In the 12-storey segment, the rate of reduction in average airflow rates with floor level remains steady up until the 9th floor at which point average flow rates drop markedly. This is also observed in the six-storey segment but here the drop occurs only at the top floor.

Average airflow rates in the upper three floors of the 12-storey segment and the top floor of the six-storey segment dropped to the extent that reverse flows occurred during all flow patterns which indicated that the neutral plane level lies

somewhere between the 9th and 10th floor of the former and above the penultimate floor of the latter. Occurrence of flow reversal suggests that some of the initial sizing conditions or modelling assumptions need to be reconsidered, particularly those relating to the equal vent sizes assumed for all floors. Potential means to overcome dispersion and flow reversal were proposed.

Overall internal conditions are similar for all segmentation variants but if floors are considered individually then internal conditions in floors wherein the flow is stalled (because the pressure differences at the openings at either side of the delivery zone are equal and opposite) tend to be warmer than in floors experiencing flow reversal due to internal heat build-up. Water consumption was found to be almost equal in all segmentation cases over the course of the cooling season. However, if the whole year is considered, segmentation cases with more floors in the segment tended to consume slightly more.

PDEC duration

PDEC operation was allowed to incrementally extend (in one-hour steps) beyond occupied hours at either side of the working day. A single floor was modelled to reduce computational time and PDEC components were accordingly recalculated using EFM. 27 variants were modelled in addition to the base case. Initiation setpoints during unoccupied hours were based on mean radiant temperatures as it was the cooling of the structure rather than the thermal comfort of occupants during those hours that was of relevance.

Extending PDEC immediately after occupied hours was found to be the least efficient strategy in terms of water consumption. However, allowing PDEC to

initiate as early as eight hours before the beginning of the working day not only reduces overheating but maintains water consumption at the same level as that of the BCM. It is likely that this leads to the reduction in PDEC operation times during occupied hours of the following day so that on balance, the same quantity of water is consumed. Further reductions in overheating can be achieved but a trade-off between water and comfort needs to be considered.

Wind forces and Orientation

The effect of wind forces on airflow rates and consequently on internal comfort conditions was investigated. In the BCM, pressure coefficients were reduced to zero to nullify the effects of wind forces on airflow rates. The aim of this exercise was to establish the effect of wind forces at the other end of the spectrum wherein the difference in wind induced pressure between the segment's inlet and outlet/s is at its maximum potential value. Two sources of wind pressure coefficient data for high-rise buildings were referenced and the average C_p values at the two heights that would have the maximum disparity between them were calculated for each source. The two sources yielded very similar C_p values for the modelling conditions concerned. The values were then entered manually in EnergyPlus because the program's alternative method for automatically assigning C_p values to airflow components assumed those values to be surface-averaged, an assumption that was shown to be unrealistic. The 12-storey segment was chosen as it has the largest vertical distance between inlet and outlet. The orientation of the segment's façade and its effect on performance was also considered with and without wind effects, the latter scenario serving as a baseline to the former.

Results showed that wind forces cause a progressive increase in airflow rates with floor level starting from almost no change at the bottom floor to a 10% increase on the top floor compared to a no-wind scenario. Orientation was found to have no significant effect in terms of wind effects. An equal reduction of 0.1m^3/s in average airflow rates occurs on all floors during the B-U flow pattern. Water consumption increased by approximately 2% for all cardinal directions.

Comfort Model and overheating criterion

The effects of adopting different comfort models and overheating criteria on internal conditions and consequently, on water consumption were investigated. The comfort models considered were: the ACM as defined by ASHRAE Standard 55 and CEN 15251; the adaptive neutral temperatures and their associated comfort boundaries developed by Nicol and Humphreys for heated and cooled buildings in Europe and by Farghal and Wagner for free-running educational buildings in Egypt; the PMV-PPD model; and the Fiala model. In addition to an overheating criterion that takes into account the magnitude and duration of departure of internal conditions from the neutral temperature, an overheating criterion wherein only the number of hours during which internal conditions exceed the relevant upper threshold of comfort are considered was also included. The control logic of variants incorporating adaptive comfort models was modified accordingly to optimise water consumption. Variants with no PDEC and with PDEC operating at all times were also modelled.

NV alone could only maintain comfort conditions for 49-65% of occupied hours during the cooling season depending on the chosen comfort model. The ACM in EN 15251 was not applicable for 18 days, representing 13% of occupied

hours of the cooling season. In terms of the EXI, internal conditions in all variants were maintained within their respective comfort boundaries for approximately all occupied hours. However, in terms of the ORI, the two variants developed for this criterion (OR variants) performed considerably better for all occurrences of *P* than their counterpart EX variants with average *P* values dropping from 7.1% and 8.9% to 4.9% and 6.9% for ASHRAE 55 and EN 15251 comfort models respectively. Reduction in average *P* values for the variant in which PDEC was continuously operating was negligible compared to the OR variants. EX variants consumed approximately a third of the water consumed by their counterpart OR variants.

If the PMV-PPD and Fiala models were used to assess comfort during periods of PDEC operation, exceedance considerably increases from 0% to 52% in some variants. However, if local airspeeds were allowed to increase to 0.8 m/s, it was shown that using the Standard Effective Temperature (SET) model described in ASHRAE standard 55 to calculate PMV, no overheating occurs in the EX variant developed for the ACM of the same standard and only 1% exceedance occurs for the EX variant based on the adaptive neutral temperature developed by Nicol and Humphreys.

Results therefore indicate that even if the more restrictive criteria of the PMV-PPD model is adopted, PDEC can still deliver comfort conditions for all occupied hours of the cooling season by increasing local air speed (using fans for example). This strategy is particularly effective with PDEC because the mean radiant temperature tends to be higher than air temperature during occupied hours.

Chapter 7: Summary and Conclusions

7.1 Summary

With the increasing rates of energy consumption and associated carbon emissions resulting from excessive use of mechanical cooling in buildings and with the economic imperative for densification in urban environments, sustainable alternatives to the tightly-sealed mechanically-conditioned high-rise office building were required. In hot-dry climates, Passive Downdraught Evaporative Cooling (PDEC) is considered one such alternative but its potential in reducing overheating in medium and high-rise office buildings has never been fully exploited in research or practice as evident from the lack of literature on the subject.

The main aim of this study was to investigate the potential applicability of PDEC to medium and high-rise office buildings in the climatic context of Cairo, Egypt. The objective was to assess the relative performance of a number of design variables in terms of the generated airflow rates across the floor levels and the consequent internal thermal conditions rather than the actual performance of a specific building. Environmental costs in terms of water consumption were also investigated.

A four-stage plan was proposed to evaluate that potential. The first stage entails the development of a generic prototype of the PDEC multi-storey office building. The second stage is that of materialisation and involves giving initial sizes to all the components that make the strategy work. The third stage assesses

the performance of a base case model in terms of bulk airflow rates, airflow distribution across the floors, internal thermal conditions, and relevant environmental costs. The fourth and final stage is that of optimisation wherein the effects of varying a number of parameters on performance are established. For each stage, different tools and methods were used.

The thesis began in Chapter One by providing background on the topic, identifying the research questions, and presenting the research methodology. In Chapter Two, a literature review was presented and an overview of the driving forces, ventilation strategies, and design options involved in Natural Ventilation and PDEC was given. A method for fully describing the ventilation strategies of any building was also presented and formed the basis upon which the case study buildings that were used as precedents for the development of the generic PDEC multi-storey office buildings were selected.

The urban and climatic context in which the PDEC building is to be located was described in Chapter Three. The concept of thermal comfort in buildings was presented and issues related to the comfort requirements of occupants in PDEC buildings raised. The preliminary applicability of PDEC to Cairo's climate was investigated. The climate suitability analysis method (CSAM) was adapted to be applicable to PDEC. The pros and cons of urban densification and high-rise buildings were discussed and the case for high-rise office buildings in Cairo as a means for achieving densification argued.

A detailed analysis of precedents of naturally ventilated high-rise buildings and low-rise PDEC buildings was presented in Chapter Four. The spatial

configuration, ventilation concept, mode/s of operation, and characteristic design feature/s of each chosen building were identified. These were then used to develop a generic model of the PDEC multi-storey office building that would allow it in principle to employ three potential modes of operation/flow patterns. To predict the performance of the PDEC model, a review of existing modelling techniques and tools of NV and PDEC was performed. In light of the objectives of this study, Envelope flow models were selected for the initial sizing of the PDEC components (area of vent openings) and EnergyPlus, a Dynamic thermal simulation program with an integrated airflow network model was selected to better understand the time-varying behaviour and assess the long-term performance of the model. Description of the two methods was then given and the procedure whereby PDEC was modelled in EnergyPlus explained.

In Chapter Five, the thermal and airflow behaviour of the BCM was investigated. A three-storey segment was considered as it represented the least number of floors within a segment that still captured the thermodynamic essence of the phenomenon being investigated and enabled meaningful analyses to be performed. A pilot model was deemed necessary, the simulation results of which highlighted two critical issues; first, that another outlet vent was required at the top of the DSF, and second, that aperture modulation of the PDEC components was required to regulate internal conditions and optimise water consumption. A control logic was developed accordingly and was implemented using the Energy Management System module (EMS) in EnergyPlus, a feature that allows algorithms to be employed in the program.

In Chapter Six, parametric investigations were carried out to examine the effect of varying different input parameters on simulation outputs with the aim of optimising the PDEC strategy in the proposed generic configuration of the multi-storey office building to deliver acceptable internal conditions for occupants whilst minimising environmental costs. Four key parameters were identified, namely the number of floors in the segment, the duration of PDEC operation, wind forces and orientation, and finally, the choice of comfort model and overheating criteria to be adopted.

7.2 Conclusions

With regards to thermal comfort requirements in PDEC buildings. Due to the coupling of internal and external conditions in such buildings and to the opportunity afforded to occupants to control their thermal environment through opening and closing of windows/vents as opposed to thermostatic control of forced airflows in mechanical ventilation and cooling, it is argued that the adaptive comfort model can equally be applied to PDEC buildings and offers a more relaxed requirement.

For the same comfort model adopted, choice of the overheating criterion has a bearing on the way the control logic (building management system BMS in real buildings) is set up. A control logic based on a criterion wherein un upper threshold for comfort exists above and below which conditions are either uncomfortable or comfortable respectively differs from one that takes into account the magnitude and duration of departure from the comfort temperature. The former merely seeks to maintain internal conditions under that threshold whilst

the latter seeks to maintain them around the comfort temperature. This has direct implications on the energy and water consumed.

The Overheating Risk Index (ORI) is more sensitive in identifying discrepancies in comfort conditions than the Exceedance Index (EI) and thus would be more apt for exercises that require ranking of, or comparison between, two spaces or models. Using the ORI is not straightforward though because representing it as a single value obscures the severity and/or duration of overheating because the same value of ORI could be equally arrived at by aggregating low values of *P* for long periods or high values of *P* for shorter periods. It was suggested to represent ORI as a distribution of the values of *P* in terms of their frequency of occurrence. This way the distribution of *P* could require that, for a space to be considered comfortable, *P* should not exceed a certain maximum value for more than a specified limited proportion of occupied hours for the whole year and another intermediate value for a relatively longer duration.

Results of the climate suitability analysis method (CSAM) adapted to assess the preliminary suitability of PDEC to Cairo's climate, showed that PDEC would be able to provide comfort for 33% and 99% if the PMV-PPD model and the ACM were used respectively. Comparing this to the outcome of the thermal modelling, the CSAM was accurately able to predict suitability for the ACM but overestimated overheating when the PMV-PPD model was used. It has to be noted that the PMV-PPD model was implemented differently in the CSAM and the thermal modelling. The graphical method described in ASHRAE standard 55 was used in the former whilst detailed environmental and personal factors resulting from the simulation were used to calculate PMV in the latter.

To identify the airflow patterns, flow directions and modes of operation that are anticipated to occur in high-rise PDEC buildings; a building precedents study of both low-rise PDEC buildings and high-rise NV buildings was conducted from which it was inferred that the high-rise PDEC building should be configured to allow for two distinct airflow patterns/modes of operation; a Top-down Centre-in Edge-out flow pattern (T-D/C-E) used during PDEC operation, a Bottom-up Edge-in Centre-out flow pattern(B-U/E-C) used during daytime NV and night cooling. Preliminary simulations of a pilot model later highlighted the need for another Top-up Centre-in Edge-out flow pattern(T-U/C-E) to be used during PDEC but only when exhaust air is warmer than ambient and an upper DSF opening was introduced to accommodate this pattern.

A generic model of the high-rise PDEC office building was developed. A central atrium runs through the building's axis with floor plates on either side surrounded by a ventilated DSF. The model was vertically divided into isolated (in terms of airflow) segments each comprising the same number of floors. The atrium was extended two storeys beyond the segment's upper floor to guarantee full evaporation of water and potentially provide enough stack pressure for the top floor.

Envelope Flow Models (EFM) used for the initial sizing of the PDEC airflow components showed that the area of the openings at the atrium/office and DSF/office interfaces need to increase progressively with floor level to ensure even distribution of flow rates across floors and that different modes of operation require different areas with the largest areas required for the T-U flow pattern especially when the number of floors in the segment increases. Assuming fixed

areas on all floors to reduce initial construction costs with aperture modulation provided at the atrium/office interface resulted in some discrepancy in average flow rates particularly at larger opening sizes.

The performance of the base case model assessed using EnergyPlus indicated that PDEC alone can deliver comfort conditions for all occupied hours of the cooling season. If the upper boundary for the 90% acceptability range of ASHRAE's Adaptive Comfort Model (ACM) is used as the threshold above which AC is initiated and assuming that the application of the ACM is extended to PDEC buildings, then the duration in which AC is in operation is negligible and the cooling energy required is thus insignificant. In this case water consumption can be as low as 3.3 litres per person per day, a mere 1.5% increase on average daily water consumption in Cairo per capita. However, to maintain operative temperatures as close as possible to the comfort temperature, an average of approximately 10 litres of water are daily required per occupant. In contrast to natural ventilation, with PDEC, it was found that mean radiant temperatures were on average consistently higher than dry-bulb temperatures. This increases the potential for improving comfort conditions by increasing local air velocities.

The interaction of two factors influence the disparity in airflow rates between floors; R_A, the ratio of the effective area of the openings at the Atrium/Office and Office/DSF interfaces to the effective area of the segment's inlet/outlet openings, and $R_{\Delta T}$, the ratio of the difference in air temperatures between the Atrium and DSF to the difference between the Atrium and external air temperature. For the B-U and T-D flow patterns, the variation in the ratio of airflow rates in the upper and middle floors to the airflow rate in the lower floors increases almost linearly

with both R_A and $R_{\Delta T}$, whereas for the T-U flow pattern, the variation only increases with R_A, and $R_{\Delta T}$ has no real effect.

Parametric studies were performed to further investigate the thermal and airflow behaviour of the proposed generic configuration of the PDEC multi-storey office building under different boundary conditions and modelling assumptions. Four key parameters were identified, namely; the number of floors in a segment being served by the same PDEC system (segmentation), the duration and timing of PDEC operation beyond occupied hours, wind forces and orientation, and choice of comfort model and overheating criterion. Conclusions for each are presented below.

Segmentation

The effect of segmentation was investigated by modelling a 12-storey model of the PDEC generic building for three different segmentation cases, the first made up of four three-storey segments, the second of two six-storey segments and the third of one 12-storey segment. In terms of airflow, the relative performance of the three variants varied depending on mode of operation and month within the cooling season. During the temperate period (May), it was found that during PDEC operation (T-U and T-D flow patterns), the more the number of floors there are in a segment the higher the airflow rates traversing those floors but that during NV (B-U flow pattern), floors in the smaller segments had slightly higher flow rates than their respective floor levels in the top half of the larger segments and vice versa.

For all variants, average airflow rates decrease with floor level which leads to the dispersion in flow rates between the segments' floors. As the number of floors in a segment increases, so does the dispersion. Dispersion is more pronounced in the warmer months than it is in the temperate months of the cooling season and within the same month, during the T-U and B-U flow patterns than it is during the T-D flow pattern. In the 12-storey segment, the rate of reduction in average airflow rates with floor level remains steady up until the 9th floor at which point average flow rates drop markedly. This is also observed in the six-storey segment but here the drop occurs only at the top floor.

Average airflow rates in the upper three floors of the 12-storey segment and the top floor of the six-storey segment dropped to the extent that reverse flows occurred during all flow patterns which indicated that the neutral plane level lies somewhere between the 9th and 10th floor of the former and above the penultimate floor of the latter. Occurrence of flow reversal suggests that some of the initial sizing conditions or modelling assumptions need to be reconsidered, particularly those relating to the equal vent sizes assumed for all floors. Potential means to overcome this would be to increase the area of the vents in the floors experiencing flow reversal only thereby minimising construction costs by limiting the variation in vent sizes within the segment to two. Adding extra exhaust components to those floors could also be a viable though costlier alternative. As flow reversal is particularly problematic during the T-U flow pattern, it is likely that raising the temperature at the segment's outlet vent at the top of the DSF (by creating a solar chimney for example) could increase the buoyancy forces in the whole segment, thus reducing dispersion. Finally, increasing the vertical distance

between the upper floor and the segments outlet (ΔH) could also be considered. This strategy would potentially have two advantages; it would likely elevate the neutral plane level above the upper floor's vent and, according to EFM calculations, would require smaller vent sizes, thus reducing R_A and consequently dispersion.

Overall internal conditions are similar for all segmentation variants but if floors are considered individually then internal conditions in floors wherein the flow is stalled (because the pressure differences at the openings at either side of the delivery zone are equal and opposite) tend to be warmer than in floors experiencing flow reversal due to internal heat build-up.

Water consumption was found to be almost equal in all segmentation cases over the course of the cooling season. However, if the whole year is considered, segmentation cases with more floors in the segment tended to consume slightly more.

PDEC duration

PDEC operation was allowed to incrementally extend (in one-hour steps) beyond occupied hours at either side of the working day. Extending PDEC immediately after occupied hours was found to be the least efficient strategy in terms of water consumption. However, allowing PDEC to initiate as early as eight hours before the beginning of the working day not only reduces overheating but maintains water consumption at the same level as that of the BCM. It is likely that this leads to the reduction in PDEC operation times during occupied hours of the following day so that on balance, the same quantity of water is consumed. Further

reductions in overheating can be achieved but a trade-off between water and comfort needs to be considered.

Wind forces and Orientation

Buoyancy forces alone were shown to be sufficient in delivering the required flow rates. However, effects of wind were also investigated. Alternative sources for Cp values were referenced because the C_p values automatically generated in EnergyPlus assume those values to be surface-averaged, an assumption that has shown to be unrealistic in high-rise buildings. Results showed that wind forces cause a progressive increase in airflow rates with floor level starting from almost no change at the bottom floor to a 10% increase on the top floor compared to a no-wind scenario. Orientation was found to have no significant effect in terms of wind effects. An equal reduction of $0.1m^3/s$ in average airflow rates occurs on all floors during the B-U flow pattern. Water consumption increased by approximately 2% for all cardinal directions. The results therefore confirm the positive effects of locating the segments inlet and outlet openings on the same building façade in minimising the effects of wind forces on airflow patterns and airflow rates

Comfort Model and overheating criterion

The effects of adopting different comfort models and overheating criteria on internal conditions and consequently, on water consumption were investigated. The comfort models considered were: the ACM as defined by ASHRAE Standard 55 (ASHRAE, 2013b) and CEN 15251 (CEN, 2008); the adaptive neutral temperatures and their associated comfort boundaries developed by Nicol and Humphreys (2007) for heated and cooled buildings in Europe and by Farghal and

Wagner (2010) for free-running educational buildings in Egypt; the PMV-PPD model (ASHRAE, 2013b; Fanger, 1970; ISO, 2005); and the Fiala model (Fiala & Lomas, 2001; Fiala, Lomas, Martínez, et al., 1999; Fiala et al., 2001; Fiala, Lomas, & Stohrer, 1999; Martínez et al., 2000). In addition to an overheating criterion that takes into account the magnitude and duration of departure of internal conditions from the neutral temperature, an overheating criterion wherein only the number of hours during which internal conditions exceed the relevant upper threshold of comfort are considered was also included. The control logic of variants incorporating adaptive comfort models was modified accordingly to optimise water consumption. Variants with no PDEC and with PDEC operating at all times were also modelled.

NV alone could only maintain comfort conditions for 49-65% of occupied hours during the cooling season depending on the chosen comfort model. The ACM in EN 15251 was not applicable for 18 days, representing 13% of occupied hours of the cooling season. In terms of the Exceedance Index (EXI), internal conditions in all variants were maintained within their respective comfort boundaries for approximately all occupied hours. However, in terms of the Overheating Risk Index (ORI), the two variants developed for this criterion (OR variants) performed considerably better for all occurrences of *P* than their counterpart EX variants with average *P* values dropping from 7.1% and 8.9% to 4.9% and 6.9% for ASHRAE 55 and EN 15251 comfort models respectively. Reduction in average *P* values for the variant in which PDEC was continuously operating was negligible compared to the OR variants. EX variants consumed approximately a third of the water consumed by their counterpart OR variants.

If the PMV-PPD and Fiala models were used to assess comfort during periods of PDEC operation, exceedance considerably increases from 0% to 52% in some variants. However, if local airspeeds were allowed to increase to 0.8 m/s, it was shown that using the Standard Effective Temperature (SET) model described in ASHRAE standard 55 to calculate PMV, no overheating occurs in the EX variant developed for the ACM of the same standard and only 1% exceedance occurs for the EX variant based on the adaptive neutral temperature developed by Nicol and Humphreys.

Results therefore indicate that even if the more restrictive criteria of the PMV-PPD model is adopted, PDEC can still deliver comfort conditions for all occupied hours of the cooling season by increasing local air speed (using fans for example). This strategy is particularly effective with PDEC because the mean radiant temperature tends to be higher than air temperature during occupied hours.

7.3 Contribution to Knowledge

The originality of this work and its contribution to knowledge can be outlined in the following points:

- This study is the first to provide an understanding of how multi-storey office buildings in hot-dry climates can be designed and operated to incorporate PDEC as a viable alternative to AC. The novelty here lies not in the methodology which uses available modelling techniques albeit in a novel way, but in the detailed investigation of flow rates, flow patterns, indoor temperatures, and water consumption

- The study is the first to establish the applicability of PDEC in multi-storey office buildings within Cairo's climatic context against the backdrop of the stringent requirements of existing comfort criteria
- In this study, a detailed control logic in EnergyPlus for multi-storey PDEC buildings is developed based on internal and external conditions that could be used as a platform to investigate effects of changing setpoints on water and/or energy consumption
- The study establishes the relation between extending PDEC operation beyond occupied hours, improving internal conditions, and reducing water consumption
- The capacity of buoyancy forces alone in delivering sufficient airflow rates and consequently comfort conditions is confirmed, a vital attribute for passive strategies in high-density urban locations
- The study also shows why the dispersion in airflow rates across floors varies from one flow pattern to the other and from one month to the other
- Finally, this study proposes a building configuration of the PDEC multi-storey office building that is sufficiently generic to give designers the freedom to respond to the contingencies of programme and site

7.4 Future Work

A number of issues that warrant further investigation have not been addressed in this work either due to limitations in time, methods and tools, or scope.

- The first and most obvious is the establishment of comfort conditions in actual PDEC buildings through field surveys of occupants' responses with simultaneous environmental measurements. This would help establish climate applicability more accurately.
- Using thermal modelling integrated with airflow networks is perhaps the only way to establish the time-varying behaviour and year-long performance of buildings incorporating PDEC or similar passive cooling strategies. However, thermal modelling is limiting in its assumption of perfectly mixed room-air models. Additionally, in buildings with vertical voids spanning many floors like atria and DSFs, thermal stratification is likely to occur which would have implications on the distribution of airflow rates across the floors and in turn on internal conditions on those floors. Using small scale models and computational fluid dynamics to test those cases would be beneficial to establish local differences in temperatures and air velocities.
- Segmentation of high-rise buildings was shown to be beneficial. However, with the air inlet rising at least 6 meters above the top floor of the segment creating a gap of the same height between segments, it would be interesting to investigate the potential of using these intermediate spaces as sky-gardens not only for communal purposes but also for environmental ones. Establishing the role of vegetation in evapo-transpiration and in filtering out dust and other pollutants from incoming air would be beneficial.
- Exploring the energy savings resulting from employing active cooling systems in a downdraught strategy (perhaps in the form of cooling coils)

in lieu of misting nozzles in locations with elevated levels of humidity as an alternative to full air-conditioning.

- Mean radiant temperatures were found to be consistently higher than dry-bulb temperatures in the PDEC model. Investigating the prospect of using the evaporation of water as a heat sink for both convective and radiant cooling and the environmental costs associated in terms of water and energy in comparison to a using PDEC only could also yield interesting results.

References

Abel, C. (2003). *Sky high: Vertical Architecture*. London: Royal Academy of Arts.

Abu-Lughod, J. L. (1971). *Cairo: 1001 Years of the City Victorious*. Princeton University Press.

Acred, A., & Hunt, G. R. (2014). A simplified mathematical approach for modelling stack ventilation in multi-compartment buildings. *Building and Environment*, *71*, 121–130. http://doi.org/10.1016/j.buildenv.2013.09.004

AIJ, & IBEC. (2005). *Architecture for a sustainable future: All about the holistic approach in Japan*. (AIJ, Ed.). Tokyo: Institute for Building Environment and Energy Conservation (IBEC).

Alexander Merkel. (2014). Climate-Data.org. Retrieved October 2, 2015, from https://en.climate-data.org

Ali, M. M. (2008). The role of tall buildings in sustainable cities. *WIT Transactions on Ecology and the Environment*, *117*, 345–354. http://doi.org/10.2495/SC080331

Almaiyah, S., Elkadi, H., & Cook, M. J. (2010). Study on the Visual Performance of a Traditional Residential Neighborhood in Old Cairo. In *First International Conference on Sustainability and the Future FISC2010*. Cairo.

Anđelković, A. S., Mujan, I., & Dakić, S. (2016). Experimental validation of a EnergyPlus model: Application of a multi-storey naturally ventilated double skin façade. *Energy and Buildings*, *118*, 27–36. http://doi.org/10.1016/j.enbuild.2016.02.045

Asbridge, R., & Cohen, R. (1996). Probe 4: Queen's Building. *CIBSE Journal*, *18*(4), 35–38. Retrieved from http://www.cibse.org/getmedia/046bfc54-f25e-4018-a7b8-b1b64f1bda45/Probe-4-Queens-Building.pdf.aspx

ASHRAE. (1966). ASHRAE Standard 55-1966 Thermal Environmental Conditions for Human Occupancy. Atlanta, GA: American Society of Heating, Refrigerating and Air-Conditioning Engineers (ASHRAE).

ASHRAE. (1992). ASHRAE Standard 55-1992 Thermal Environmental Conditions for Human Occupancy. Atlanta, GA: American Society of Heating, Refrigerating and Air-Conditioning Engineers (ASHRAE).

ASHRAE. (2004a). ASHRAE Standard 55-2004 Thermal Environmental Conditions for Human Occupancy. Atlanta, GA: American Society of Heating, Refrigerating and Air-Conditioning Engineers (ASHRAE).

ASHRAE. (2004b). ASHRAE Standard 90.1-2004 Energy Standard for Buildings Except Low rise Residential Buildings. Atlanta, GA, GA: American Society of Heating, Refrigerating and Air-Conditioning Engineers (ASHRAE).

ASHRAE. (2010). ASHRAE Standard 55-2010 Thermal Environmental Conditions for Human Occupancy. Atlanta, GA: American Society of Heating, Refrigerating and Air-Conditioning Engineers (ASHRAE). http://doi.org/ISSN 1041-2336

ASHRAE. (2013a). *2013 ASHRAE handbook: fundamentals* (SI ed.). Atlanta, GA: American Society of Heating, Refrigerating and Air-Conditioning Engineers (ASHRAE).

ASHRAE. (2013b). ASHRAE Standard 55-2013 Thermal Environmental Conditions for Human Occupancy. Atlanta, GA: American Society of Heating, Refrigerating and Air-Conditioning Engineers (ASHRAE).

Atkins, R. E., Peterka, J. A., & Cermak, J. E. (1979). Average pressure coefficients for rectangular buildings. In *Wind Engineering: Proceedings of the Fifth International Conference* (pp. 369–380).

Auliciems, A. (1981). Towards a psycho-physiological model of thermal perception. *International Journal of Biometeorology*, *25*(2), 109–122. http://doi.org/10.1007/BF02184458

Auliciems, A., & Szokolay, S. V. (2007). *Thermal Comfort*. *PLEA Notes - Design Tools and Techniques*. Brisbane. http://doi.org/10.1007/s00484-010-0393-2

Awbi, H. B. (2013). *Ventilation of Buildings*. New York: Spon Press (Taylor & Francis).

Axley, J. W. (2001). *Application of natural ventilation for U.S. commercial buildings: Climate Suitability Design Strategies & Methods Modeling Studies*.

Axley, J. W., & Emmerich, S. J. (2002). A Method to Assess the Suitability of a Climate for Natural Ventilation of Commercial Buildings. In *Indoor Air 2002, 9th International Conference on Indoor Air Quality and Climate* (Vol. 2, pp. 854–859). Monterey.

Badran, A. A. (2003). Performance of cool towers under various climates in Jordan. *Energy and Buildings*, *35*(10), 1031–1035. http://doi.org/10.1016/S0378-7788(03)00067-7

Bahadori, M. N. (1994). Viability of wind towers in achieving summer comfort in the hot arid regions of the middle east. *Renewable Energy*, *5*(5–8), 879–892. http://doi.org/10.1016/0960-1481(94)90108-2

BCO. (2014). *Guide to Specification*. London: British Council for Offices.

Borgeson, S., & Brager, G. S. (2011). Comfort standards and variations in exceedance for mixed-mode buildings. *Building Research & Information*, *39*(2), 118–133. http://doi.org/10.1080/09613218.2011.556345

Bowman, N. T., Eppel, H., Lomas, K. J., Robinson, D., & Cook, M. J. (2000). Passive Downdraught Evaporative Cooling: I. Concept and precedents. *Indoor and Built Environment*, *9*(5), 284–290. http://doi.org/10.1159/000057521

Bowman, N. T., Lomas, K. J., Cook, M. J., Eppel, H., Ford, B., Hewitt, M., … Belarbi, R. (1997). Application of Passive Downdraught Evaporative Cooling (PDEC) to Non-Domestic Buildings. *Renewable Energy*, *10*(2/3), 191–196. http://doi.org/10.1016/0960-1481(96)00062-6

Bowman, N. T., Lomas, K. J., Cook, M. J., Eppel, H., Ford, B., Hewitt, M., … Belarbi, R. (1998). *The Application of passive downdraught evaporative cooling (PDEC) to non-domestic buildings*.

Brager, G. S., & de Dear, R. J. (2001). Climate, Comfort, & Natural Ventilation : A new adaptive

comfort standard for ASHRAE Standard 55. In *Moving Thermal Comfort Standards into the 21st Century*. Windsor.

Bröde, P., Krüger, E. L., Rossi, F. A., & Fiala, D. (2012). Predicting urban outdoor thermal comfort by the Universal Thermal Climate Index UTCI—a case study in Southern Brazil. *International Journal of Biometeorology*, *56*(3), 471–480. http://doi.org/10.1007/s00484-011-0452-3

Bruno, F. (2011). On-site experimental testing of a novel dew point evaporative cooler. *Energy and Buildings*, *43*(12), 3475–3483. http://doi.org/10.1016/j.enbuild.2011.09.013

Buchanan, P. (1998). Reinventing the Skyscraper. *A+U*, (No. 329 February), 30–67.

CAPMAS. (2015). *Annual Bulletin on the Statistics of Drinking Water and Sewege for the year 2013/2014 (in Arabic)*. Cairo.

CAPMAS. (2017). *General Census of Population, Housing, and Building Stock for the year 2017*. Cairo.

Carey, P. S., & Etheridge, D. W. (1999). Direct wind tunnel modelling of natural ventilation for design purposes. *Building Services Engineering Research and Technology*, *20*(3), 131–142. http://doi.org/10.1177/014362449902000305

Carlucci, S. (2013). *Thermal Comfort Assessment of Buildings*. Springer.

Castillo, P. (2001). Two Towers. In *CBTUH 6TH World Congress*. Melbourne: Council on Tall Buildings and Urban Habitat.

CEN. (2008). BS EN 15251:2007 Indoor environmental input parameters for design and assessment of energy performance of buildings addressing indoor air quality, thermal environment, lighting and acoustics. British Standards Institute.

Chen, Q., Lee, K., Mazumdar, S., Poussou, S., Wang, L., Wang, M., & Zhang, Z. (2010). Ventilation performance prediction for buildings: Model assessment. *Building and Environment*, *45*(2), 295–303. http://doi.org/10.1016/j.buildenv.2009.06.008

Chen, Z. D., Li, Y., & Mahoney, J. (2001). Experimental modelling of buoyancy-driven flows in buildings using a fine-bubble technique. *Building and Environment*, *36*(4), 447–455. http://doi.org/10.1016/S0360-1323(00)00028-7

Chikamoto, T., Kato, S., & Ikaga, T. (1999). Hybrid Air-Conditioning System at Liberty Tower of Meiji University. In *First International One day Forum on Natural and Hybrid Ventilation, HybVent Forum'99*. Sydney.

CIBSE. (2000). *Mixed mode Ventilation - CIBSE Applications Manual AM13: 2000*.

CIBSE. (2002). *CIBSE Guide J: Weather, Solar and Illuminance Data*. *Chartered Institution of Building Services Engineers*. Chartered Institution of Building Services Engineers.

CIBSE. (2006). *CIBSE Guide A: Environment Design*. *Chartered Institution of Building Services Engineers*. Chartered Institution of Building Services Engineers. http://doi.org/10.1016/B978-0-240-81224-3.00016-9

Cláudia, A., Melo, M. De, & Guedes, M. C. (2006). Passive Downdraught Evaporative Cooling

Applied on Existing Fabric: Using Traditional Chimney as Case Study in Portugal. In *Passive and Low Energy Architecture PLEA 2006 23rd Conference* (pp. 6–8). Geneva, Switzerland: PLEA.

Cody, B. (2008). Exploring the potential for natural ventilation of very tall buildings. In *29th Annual AIVC Conference* (pp. 79–84). Kyoto, Japan: AIVC.

Cook, M. J., Lomas, K. J., & Eppel, H. (1999a). Design Concept for an Innovative Naturally Ventilated Library. *CIBSE National Conference,* (3rd–5th October), 500–507.

Cook, M. J., Lomas, K. J., & Eppel, H. (1999b). Use of computer simulation in the design of a naturally ventilated library. In *Passive and Low Energy Architecture PLEA 1999 16th Conference* (pp. 597–602). Brisbane: PLEA.

Cook, M. J., Robinson, D., Lomas, K. J., Bowman, N. T., & Eppel, H. (2000). Passive Downdraught Evaporative Cooling: II. Airflow Modelling. *Indoor and Built Environment*, *9*(6), 325–334. http://doi.org/10.1177/1420326X0000900604

Crawley, D. B., Lawrie, L. K., Pedersen, C. O., & Winkelmann, F. C. (2000). EnergyPlus: Energy Simulation Program. *ASHRAE Journal*, *42*, 49–56. http://doi.org/10.1.1.122.6852

Cunningham, W. A., Mignon, G. V., & Thompson, T. L. (1987). *Establish Feasibility for Providing Passive Cooling with Solar Updraft and Evaporative Downdraft Chimneys*. Tucson AZ.

da Silva, J. J. C. (2005). Passive downdraught evaporative cooling applied to an auditorium. In *Passive and Low Energy Cooling for the Built Environment PALENC 2005 1st Conference* (pp. 555–560). Santorini: PALENC.

Daniels, K., Stoll, J., Pultz, G., & Schneider, J. (1993). *The skyscraper: naturally ventilated? Report by Top E, European Consulting Engineering Network.*

Davenport, A. G., & Hui, H. Y. L. (1982). *External and internal wind pressures on cladding of buildings, Report of the Boundary Wind Tunnel Laboratory*. London, Canada.

Davey, P. (1997). High Expectations. *Architectural Review*, *202*(1205), 27–39.

Davey, P. (2006). *Natural ventilation strategies for tall buildings*. University of Nottingham.

de Dear, R. J., & Brager, G. S. (2001). The adaptive model of thermal comfort and energy conservation in the built environment. *International Journal of Biometeorology*, *45*(2), 100–108. http://doi.org/10.1007/s004840100093

de Dear, R. J., & Brager, G. S. (2002a). Thermal comfort in naturally ventilated buildings: revision to ASHRAE standards 55,. *Journal of Energy and Buildings*, *34*, 549–561.

de Dear, R. J., & Brager, G. S. (2002b). Thermal comfort in naturally ventilated buildings: revisions to ASHRAE Standard 55. *Energy and Buildings*, *34*(6), 549–561. http://doi.org/10.1016/s0378-7788(02)00005-1

de Gids, W. F., & Jicha, M. (2010). *Hybrid Ventilation*. *Ventilation Information Paper* (Vol. 32). Retrieved from http://www.aivc.org/sites/default/files/members_area/medias/pdf/VIP/VIP 32 Hybrid Vent.pdf

Delsante, A., & Vik, T. A. (2000). *Hybrid Ventilation: state of the art review*. *International Energy Agency, Annex*. Retrieved from http://www.hybvent.civil.aau.dk/puplications/sotar.pdf

Demographia. (2017). *Demographia World Urban Areas & Population Projections: 13th Annual Edition*. *Demographia*. Retrieved from http://demographia.com/db-worldua.pdf

EEBPP. (1997). *The Queens Building, De Montfort University - New Practice Case Study*. *Energy Efficiency Best Practice Programme* (Vol. 102). Retrieved from http://www.iesd.dmu.ac.uk/msc/EEBPP_NPCS_102.pdf

El-Dessouky, H. T., Ettouney, H. M., & Bouhamra, W. (2000). A Novel Air Conditioning System Membrane Air Drying and Evaporative Cooling. *Chemical Engineering Research and Design*, *78*(7), 999–1009. http://doi.org/10.1205/026387600528111

Emmerich, S. J., Polidoro, B., & Axley, J. W. (2011). Impact of adaptive thermal comfort on climatic suitability of natural ventilation in office buildings. *Energy and Buildings*, *43*(9), 2101–2107. http://doi.org/10.1016/j.enbuild.2011.04.016

Erell, E., Pearlmutter, D., & Etzion, Y. (2008a). A multi-stage down-draft evaporative cool tower for semi-enclosed spaces: Aerodynamic performance. *Solar Energy*, *82*, 420–429. http://doi.org/10.1016/j.solener.2007.10.010

Erell, E., Pearlmutter, D., & Etzion, Y. (2008b). A multi-stage down-draft evaporative cool tower for semi-enclosed spaces: Experiments with a water spraying system. *Solar Energy*, *82*, 430–440. http://doi.org/10.1016/j.solener.2007.12.003

Ernest, R., & Ford, B. (2012). The role of multiple-courtyards in the promotion of convective cooling. *Architectural Science Review*, *55*(4), 241–249. http://doi.org/10.1080/00038628.2012.723400

Etheridge, D. W. (2002). Nondimensional methods for natural ventilation design. *Building and Environment*, *37*(11), 1057–1072. http://doi.org/10.1016/S0360-1323(01)00091-9

Etheridge, D. W. (2011a). Design Procedures. In *Natural Ventilation of Buildings* (pp. 375–413). Chichester, UK: John Wiley & Sons, Ltd. http://doi.org/10.1002/9781119951773.ch12

Etheridge, D. W. (2011b). *Natural Ventilation of Buildings: Theory, Measurement and Design*. John Wiley & Sons.

Etheridge, D. W., & Ford, B. (2008). Natural ventilation of tall buildings - options and limitations. In *CTBUH 8th World Congress*. Dubai, UAE.

Etheridge, D. W., & Sandberg, M. (1996). *Building ventilation: theory and measurement*. John Wiley & Sons.

Fanger, P. O. (1970). *Thermal comfort: Analysis and applications in environmental engineering*. Danish Technical Press.

Farghal, A. A. F., & Wagner, A. (2010). Studying the Adaptive Comfort Model a Case Study in a Hot Dry Climate. In *The Windsor Conference: Adapting to Change: New Thinking on Comfort*. Windsor: Network for Comfort and Energy Use in Buildings.

Fiala, D., Havenith, G., Bröde, P., Kampmann, B., & Jendritzky, G. (2012). UTCI-Fiala multi-node

model of human heat transfer and temperature regulation. *International Journal of Biometeorology*, *56*(3), 429–441. http://doi.org/10.1007/s00484-011-0424-7

Fiala, D., & Lomas, K. J. (2001). The Dynamic Effect of Adaptive Human Responses in the Sensation of Thermal Comfort. In *Moving Thermal Comfort Standards into the 21st Century* (pp. 147–157). Windsor.

Fiala, D., Lomas, K. J., Martínez, D. F., & Cook, M. J. (1999). Dynamic Thermal Sensation in PDEC Buildings. In *Passive and Low Energy Architecture PLEA 1999 16th Conference* (Vol. 1, pp. 243–248). Brisbane.

Fiala, D., Lomas, K. J., & Stohrer, M. (1999). A computer model of human thermoregulation for a wide range of environmental conditions: the passive system. *Journal of Applied Physiology*, *87*, 1957–1972.

Fiala, D., Lomas, K. J., & Stohrer, M. (2001). Computer prediction of human thermoregulatory and temperature responses to a wide range of environmental conditions. *International Journal of Biometeorology*, *45*(3), 143–159. http://doi.org/10.1007/s004840100099

Fiala, D., Lomas, K. J., & Stohrer, M. (2003). First Principles Modeling of Thermal Sensation Responses in Steady-State and Transient Conditions. *ASHRAE Transactions*, *109*, 179–186.

Ford, B. (2001). Passive downdraught evaporative cooling: principles and practice. *Arq: Architectural Research Quarterly*, *5*(03), 271–280. http://doi.org/doi:10.1017/S1359135501001312

Ford, B., & Diaz, C. (2003). Passive Downdraught Cooling: hybrid cooling in the Malta Stock Exchange. In *Passive and Low Energy Architecture PLEA 2003 20th Conference*. Santiago: PLEA.

Ford, B., Diaz, C., & Hewitt, M. (2000). Passive Downdraught Cooling: Architectural Integration in Seville. In *Passive and Low Energy Architecture PLEA 2000 17th Conference* (pp. 83–88). Cambridge: PLEA.

Ford, B., Patel, N., Zaveri, P., & Hewitt, M. (1998). Cooling without Air Conditioning - The Torrent Research Centre, Ahmedabad, India. *Renewable Energy*, *15*, 177–182. http://doi.org/10.1016/S0960-1481(98)00150-5

Ford, B., Schiano-Phan, R., & Francis, E. (2010). *The Architecture & Engineering of Downdraught Cooling: A Design Sourcebook*. London: PHDC Press.

Francis, E. (2000). The application of passive downdraught evaporative cooling (PDEC) to non-domestic buildings. Office building prototype design in Catania, Italy. In *Passive and Low Energy Architecture PLEA 2000 17th Conference* (pp. 88–93). Cambridge: PLEA.

Gage, S. A. (1997). Stack Ventilation and Cooling for Urban Sites: Natural ventilation with roof intake for improved air quality. In *18th Annual AIVC Conference* (pp. 87–98). Athens: AIVC.

Ghiaus, C., & Allard, F. (Eds.). (2016). *Natural Ventilation in the Urban Environment: Assessment and Design*. Routledge.

Givoni, B. (1992). Comfort, climate analysis and building design guidelines. *Energy and Buildings*, *18*(1), 11–23. http://doi.org/10.1016/0378-7788(92)90047-k

Grosso, M., & Ahmadi, M. (2016). Potential cooling energy reduction by a one-channel wind tower: case study modelling in south-Mediterranean climate. *International Journal of Ventilation*, *15*(3–4), 267–287. http://doi.org/10.1080/14733315.2016.1214397

Gu, L. (2007). Airflow network modeling in EnergyPlus. *Building Simulation 2007, 10th International IBPSA Conference*, (February), 964–971.

HBRC. (2005). ECP 306-2005 Egyptian Code for Improving the Energy Efficiency of Commercial Buildings. Cairo: Housing and Building Research Centre.

He, J., & Hoyano, A. (2010). Experimental study of cooling effects of a passive evaporative cooling wall constructed of porous ceramics with high water soaking-up ability. *Building and Environment*, *45*(2), 461–472. http://doi.org/10.1016/j.buildenv.2009.07.002

He, J., & Hoyano, A. (2011). Experimental study of practical applications of a passive evaporative cooling wall with high water soaking-up ability. *Building and Environment*, *46*(1), 98–108. http://doi.org/10.1016/j.buildenv.2010.07.004

Helmut, J., Blaser, W., Werner, S., & Matthias, S. (2003). *Post Tower: Helmut Jahn, Werner Sobek, Matthias Schuler*. Basel: Birkhauser Verlag AG.

Howell, S. A., & Potts, I. (2001). On the natural displacement ventilation flow through a full scale enclosure, driven by a source of buoyancy at floor level. In *Building Simulation 2001, 7th International IBPSA Conference* (pp. 627–634). Rio de Janeiro: IBPSA.

Humphreys, M. A. (1975). Field Studies of Thermal Comfort Compared and Applied. *Building Research Establishment Current Paper*, *75*(76).

Humphreys, M. A., & Nicol, J. F. (1996). Conflicting criteria for thermal sensation with the Fanger PMV equation. In *CIBSE/ASHRAE Joint National Conference*. Harrogate.

Ibrahim, E., Shao, L., & Riffat, S. B. (2003). Performance of porous ceramic evaporators for building cooling application. *Energy and Buildings*, *35*(9), 941–949. http://doi.org/10.1016/S0378-7788(03)00019-7

ICC. (2012). IECC - International Energy Conservation Code. *International Code Council*.

IPCC. (2008). *Climate Change 2007 Synthesis Report*.

Irving, S., Ford, B., & Etheridge, D. W. (2005). *Natural ventilation in non-domestic buildings*. *CIBSE Applications Manual AM10*. Chartered Institution of Building Services Engineers.

ISO. (2005). ISO 7730 - Ergonomics of the thermal environment - Analytical determination and interpretation of thermal comfort using calculation of the PMV and PPD indices and local thermal comfort criteria. Geneva, Switzerland: International Organization for Standardization.

Jahn, H. (2003). Post Tower in Bonn: State of the Art. *Intelligente Architektur*, (41 July/August), 1–19.

Je, H. S. (2006). Super Tall Buildings and Urban Competitive Power. In *Proceedings of the 7th international symposium of the Korea super tall building forum* (pp. 35–67). Korea: Federation of Korean industries (FKI).

Johnson, M. H., Zhai, Z. J., & Krarti, M. (2012). Performance evaluation of network airflow models for natural ventilation. *HVAC&R Research*, *18*(3), 349–365. http://doi.org/10.1080/10789669.2011.617291

Kalantar, V. (2009). Numerical simulation of cooling performance of wind tower (Baud-Geer) in hot and arid region. *Renewable Energy*, *34*, 246–254. http://doi.org/10.1016/j.renene.2008.03.007

Kampmann, B., Bröde, P., & Fiala, D. (2012). Physiological responses to temperature and humidity compared to the assessment by UTCI, WGBT and PHS. *International Journal of Biometeorology*, *56*(3), 505–513. http://doi.org/10.1007/s00484-011-0410-0

Kang, D., & Strand, R. K. (2009). Simulation of Passive Down-Draught Evaporative Cooling (PDEC) Systems in ENERGYPLUS. In *Building Simulation 2009, 11th International IBPSA Conference* (pp. 369–376).

Kang, D., & Strand, R. K. (2013). Modeling of simultaneous heat and mass transfer within passive down-draft evaporative cooling (PDEC) towers with spray in FLUENT. *Energy and Buildings*, *62*, 196–209. http://doi.org/10.1016/j.enbuild.2013.02.039

Kang, D., & Strand, R. K. (2016). Significance of parameters affecting the performance of a passive down-draft evaporative cooling (PDEC) tower with a spray system. *Applied Energy*, *178*, 269–280. http://doi.org/10.1016/j.apenergy.2016.06.055

Kant, K., Kumar, A., & Mullick, S. C. (2001). Space conditioning using evaporative cooling for summers in Delhi. *Building and Environment*, *36*(1), 15–25. http://doi.org/10.1016/S0360-1323(99)00060-8

Khalil, E. E. (2008). Efficient energy utilization in air conditioned buildings in Egypt: New directive. *2008 2nd International Conference on Thermal Issues in Emerging Technologies, ThETA 2008*, 443–448. http://doi.org/10.1109/THETA.2008.5167194

Kleiven, T. (2003). *Natural Ventilation in Buildings, architectural concepts, consequences and possibilities*. Norwegian University of Science and Technology Faculty. http://doi.org/10.1002/9781119951773

Kottek, M., Grieser, J., Beck, C., Rudolf, B., & Rubel, F. (2006). World map of the Köppen-Geiger climate classification updated. *Meteorologische Zeitschrift*, *15*(3), 259–263. http://doi.org/10.1127/0941-2948/2006/0130

Lanceta, D., Manteca, F., Martín, C., Martínez, D. F., Serna, F., & Llorente, J. (2007). Cooling of outdoor spaces by means of evaporative-cooling ceramic-pillars. In *PALENC 2007 2nd Conference and AIVC 28th Conference on Building Low Energy Cooling and Advanced Ventilation Technologies in the 21st Century* (pp. 615–620). Crete Island: PALENC.

Li, Y., & Heiselberg, P. (2003). Analysis methods for natural and hybrid ventilation: a critical literature review and recent developments. *International Journal of Ventilation*, *1*(4), 3–20.

Liddament, M. (1996). *AIVC Guide to Energy Efficienct Ventilation*.

Lomas, K. J. (2007). Architectural design of an advanced naturally ventilated building form. *Energy and Buildings*, *39*(2), 166–181. http://doi.org/10.1016/j.enbuild.2006.05.004

Lomas, K. J., & Cook, M. J. (2005). Sustainable buildings for a warmer World. In *Proceedings of the World Renewable Energy Congress* (p. 26). Aberdeen: Elsevier.

Lomas, K. J., Fiala, D., Cook, M. J., & Cropper, P. C. (2004). Building bioclimatic charts for non-domestic buildings and passive downdraught evaporative cooling. *Building and Environment*, *39*(6), 661–676. http://doi.org/10.1016/j.buildenv.2003.12.011

Lomas, K. J., Short, C. A., & Woods, A. (2004). Design strategy for low-energy ventilation and cooling within an urban heat island, *32*(3), 187–206. http://doi.org/10.1080/09613210410001679875

Long, N., Torcellini, P., Pless, S., & Judkoff, R. (2005). Evaluation of the Low-Energy Design Process and Energy Performance of the Zion National Park Visitor Center. *National Renewable Energy Laboratory of the U.S, October 2005*, (October 2005), 1–27. Retrieved from http://amet-me.mnsu.edu/userfilesshared/solarwall/Solar Passive (Trombe) Wall Documents/Technical Publications/Evaluation of the Zion National Park Visitor Center.pdf

Martínez, D. F., Fiala, D., Cook, M. J., & Lomas, K. J. (2000). Predicted Comfort Envelopes for Office Buildings With Passive Downdraught Evaporative Cooling. In *Roomvent 2000* (pp. 53–58). Reading.

McCartney, K. J., & Nicol, J. F. (2002). Developing an adaptive control algorithm for Europe. *Energy and Buildings*, *34*(6), 623–635. http://doi.org/10.1016/S0378-7788(02)00013-0

McKenzie, E. R., Pistochini, T. E., Loge, F. J., & Modera, M. P. (2013). An investigation of coupling evaporative cooling and decentralized graywater treatment in the residential sector. *Building and Environment*, *68*, 215–224. http://doi.org/10.1016/j.buildenv.2013.07.007

Merrill, K. R. (2007). *The Oil Crisis of 1973-1974: A Brief History with Documents*. Bedford/St. Martin's.

MOEE. (2016). *Egyptian Electricity Holding Company (EEHC) Annual report 2015/1016*. Cairo.

MOHUUD, & JICA. (2008). *The Strategic Urban Development Master Plan Study for Sustainable Development of The Greater Cairo Region*.

Nayak, J. K., & Prajapati, J. A. (2006). *Handbook on Energy Conscious Buildings*. *R & D project no. 3/4(03)/99-SEC between Indian Institute of Technology, Bombay and Solar Energy Centre, Ministry of Non-conventional Energy Sources*.

Nicol, J. F., Hacker, J., Spires, B., & Davies, H. (2009). Suggestion for new approach to overheating diagnostics. *Building Research & Information*, *37*(4), 348–357. http://doi.org/10.1080/09613210902904981

Nicol, J. F., & Humphreys, M. A. (2007). Maximum temperatures in European office buildings to avoid heat discomfort. *Solar Energy*, *81*(3), 295–304. http://doi.org/10.1016/j.solener.2006.07.007

Nicol, J. F., & Humphreys, M. A. (2010). Derivation of the adaptive equations for thermal comfort in free-running buildings in European standard EN15251. *Building and Environment*, *45*(1), 11–17. http://doi.org/10.1016/j.buildenv.2008.12.013

Oldfield, P., Trabucco, D., & Wood, A. (2008). Five energy generations of tall buildings: an

historical analysis of energy consumption in high-rise buildings. *The Journal of Architecture*, *14*(5), 591–613. http://doi.org/10.1080/13602360903119405

Organization for Energy Conservation and Planning. (1998). *The Architecture and Energy Guide*. Cairo: Organization for Energy Conservation and Planning.

Parsons, K. C. (2014). *Human Thermal Environments* (Third). CRC Press. http://doi.org/doi:10.1201/b16750-8

Pearlmutter, D., Erell, E., Etzion, Y., Meir, I. A., & Di, H. (1996). Refining the use of evaporation in an experimental down-draft cool tower. *Energy and Buildings*, *23*(3), 191–197. http://doi.org/10.1016/0378-7788(95)00944-2

Perini, K., Magliocco, A., & Giulini, S. (2016). Vertical greening systems evaporation measurements: does plant species influence cooling performances? *International Journal of Ventilation*, *16*(2), 152–160. http://doi.org/10.1080/14733315.2016.1214388

Phillip, T., & Lau, B. (2013). Passive downdraught evaporative cooling: an investigation of its applicability for residential space cooling in Riyadh , Saudi Arabia. In *Passive and Low Energy Architecture PLEA 2013 29th Conference*. Munich: PLEA. Retrieved from https://mediatum.ub.tum.de/doc/1169611/1169611.pdf

Prajapati, J. A. (2007). Performance of Passive Downdraft Evaporative Cooling (PDEC) system in a hot and dry climate. In *Proceedings of SOLARIS 2007, 3rd International Conference on Solar Radiation and Day Lighting*. New Delhi.

Psikuta, A., Fiala, D., Laschewski, G., Jendritzky, G., Richards, M., Blazejczyk, K., … Havenith, G. (2012). Validation of the Fiala multi-node thermophysiological model for UTCI application. *International Journal of Biometeorology*, *56*(3), 443–460. http://doi.org/10.1007/s00484-011-0450-5

Riangvilaikul, B., & Kumar, S. (2010). An experimental study of a novel dew point evaporative cooling system. *Energy and Buildings*, *42*(5), 637–644. http://doi.org/10.1016/j.enbuild.2009.10.034

Rijal, H. B., Humphreys, M. A., & Nicol, J. F. (2009). Understanding occupant behaviour: the use of controls in mixed-mode office buildings. *Building Research & Information*, *37*(4), 381–396. http://doi.org/10.1080/09613210902904221

Roaf, S., Crichton, D., & Nicol, J. F. (2009). The End of the Age of Tall Buildings. In *Adapting Buildings and Cities for Climate Change: A 21st Century Survival Guide* (pp. 237–265). Taylor & Francis.

Robinson, D., Lomas, K. J., Cook, M. J., & Eppel, H. (2004). Passive Down-Draught Evaporative Cooling: Thermal Modelling of an Office Building. *Indoor and Built Environment*, *13*(3), 205–221. http://doi.org/10.1177/1420326x04043816

Saffari, H., & Hosseinnia, S. M. (2009). Two-phase Euler-Lagrange CFD simulation of evaporative cooling in a Wind Tower. *Energy and Buildings*, *41*(9), 991–1000. http://doi.org/10.1016/j.enbuild.2009.05.006

Salib, R. (2008). *Natural Ventilation in High Rise Office Buildings*. University of Nottingham.

Santamouris, M., & Wouters, P. (2006). *Building Ventilation: The State of the Art*. London:

Routledge.

Schiano-Phan, R. (2012). Post-occupancy evaluation of non-domestic buildings using passive downdraught evaporative cooling in south-west USA. *Architectural Science Review*, *55*(4), 320–340. http://doi.org/10.1080/00038628.2012.725535

Schiano-phan, R., & Ford, B. (2008). Post Occupancy Evaluation of non-domestic buildings using downdraught cooling: Case studies in the US. In *Passive and Low Energy Architecture PLEA 2008 25th Conference*. Dublin: PLEA.

Shin, S. W. (2009). Sustainable Compact Cities and High-Rise Buildings. In E. Ng (Ed.), *Designing High-density Cities for Social and Environmental Sustainability*. Earthscan LLC.

Short, C. A., Cook, M. J., & Lomas, K. J. (2009). Delivery and performance of a low-energy ventilation and cooling strategy. *Building Research & Information*, *37*(1), 1–30. http://doi.org/10.1080/09613210802607841

Short, C. A., Cook, M. J., & Woods, A. (2009). Low energy ventilation and cooling within an urban heat island. *Renewable Energy*, *34*(9), 2022–2029. http://doi.org/10.1016/j.renene.2009.02.013

Sims, D. (2003). Urban Slums Reports: The case of Cairo, Egypt. In *Understanding slums: Case studies for the global report on human settlements 2003* (pp. 1–24). http://doi.org/10.1029/2002GL015399

Sims, D. (2012). *Understanding Cairo: The Logic of a City Out of Control*. American University in Cairo Press.

Smith, P. F. (2005). *Architecture in a Climate of Change: A Guide to Sustainable Design*. Elsevier/Architectural Press.

Sodha, M. S., Singh, S. P., & Sawhney, R. L. (1995). Evolution of design patterns for direct evaporative coolers. *Building and Environment*, *30*(2), 287–291. http://doi.org/10.1016/0360-1323(94)00034-P

Spentzou, E., Cook, M. J., & Emmitt, S. (2017). Modelling natural ventilation for summer thermal comfort in Mediterranean dwellings. *International Journal of Ventilation*, 1–18. http://doi.org/10.1080/14733315.2017.1302658

Steemers, K., Chenvidyakarn, T., & Woods, A. (2002). Visualising ventilation - Salt bath modelling from research to practice. In *Passive and Low Energy Architecture PLEA 2002 19th Conference*. Toulouse.

The Usable Buildings Trust. (2006). Building Use Studies (BUS). Retrieved June 1, 2011, from www.usable buildings.co.uk

TPU. (2013). TPU Aerodynamic Database of High-rise Buildings. Retrieved March 20, 2001, from http://www.wind.arch.t-kougei.ac.jp/info_center/windpressure/highrise/Homepage/homepageHDF.htm

Tyler, H., Stefano, S., Alberto, P., Toby, C., Dustin, M., & Kyle, S. (2017). CBE Thermal Comfort Tool. Center for the Built Environment, University of California Berkeley. Retrieved from http://comfort.cbe.berkeley.edu/

United Nations. (2015). *World Urbanization Prospects: The 2014 Revision*.

van Heemst, L. V. (2001). *Hybrid Ventilation: An Integral Solution for Ventilation, Health and Energy*. *IEA Annex 35: Hybrid ventilation in new and retrofitted office buildings*. Retrieved from http://hybvent.civil.auc.dk/puplications/paper met kaft-scherm.pdf

Walton, G. N. (1989). *A Computer Program for Building Airflow Network Modeling*. NIST.

Walton, G. N., & Dols, W. S. (2003). CONTAM 2.1 Supplemental User Guide and Program Documentation. National Institute of Standards and Technology.

Wells, M. (2005). *Skyscrapers: Structure and Design*. Laurence King Publishing.

Wilson, S., & Hedge, A. (1987). *The Office Environment Survey: A Study of Building Sickness*. London: Building Use Studies Ltd. Retrieved from https://books.google.co.uk/books?id=EN69tgAACAAJ

Wood, A. (2007). Integrity of Place. *Urban Land (Publication of the Urban Land Institute)*, *66*(11/12), 71–75.

Wood, A., & Salib, R. (2013a). *Guide to Natural Ventilation in High Rise Office Buildings*.

Wood, A., & Salib, R. (2013b). *Natural ventilation in high-rise office buildings*. (R. Salib & C. on T. B. and U. Habitat, Eds.). Abingdon: Routledge.

Woods, A., Chenvidyakarn, T., & Short, C. A. (2003). Reversing flow in a naturally ventilated building with multiple stacks. In *Passive and Low Energy Architecture PLEA 2003 20th Conference* (pp. 2022–2029). Santiago: PLEA.

Yeang, K. (2002). *Reinventing the Skyscraper: A Vertical Theory of Urban Design*. London: Wiley Academy.

Zhai, Z., Johnson, M. H., & Krarti, M. (2011). Assessment of natural and hybrid ventilation models in whole-building energy simulations. *Energy and Buildings*, *43*(9), 2251–2261. http://doi.org/10.1016/j.enbuild.2011.06.026

Appendix A

In this appendix, a review of the available design and analysis tools of NV and PDEC mentioned in Chapter 4 is presented in more detail, stating their relative advantages and limitations together with some examples of their application in the design of NV and PDEC buildings.

A.1 Simple Analytical and Empirical models

Analytical models can provide global information with little computational effort. Most analytical solutions are based on a conventional macroscopic approach that utilises the Bernoulli Equation. This equation, which is based on the conservation of energy, is used to calculate air velocities through openings. The Law of Mass Conservation is then applied to balance the mass flow rate of air into and out of the space (i.e. mass flow in is equal to mass flow out) (Li & Heiselberg, 2003). A brief description of two analytical models follows;

A.1.1 Envelope Flow Models EFM:

Envelope flow models are used for the initial sizing of openings at the chosen design conditions in the early stages of design. For example, the summer design condition may determine the maximum sizes of the openings such as windows, whereas the winter design condition may determine the minimum sizes of openings such as trickle ventilators. Envelope flow models solve the equations that govern the flow of air through openings in the envelope of a building. They rely on assumptions about the internal density (temperature) distribution. More

detailed descriptions of EFM can be found in (Etheridge, 2011b; Etheridge & Sandberg, 1996; Irving et al., 2005)

A.1.2 Non-dimensional Graphs:

Models developed not only from theoretical calculations, but also from data of experimental measurements or advanced computer simulations are called empirical models. When represented by graphs in non-dimensional form, they can have much wider application.

Wind tunnel data are often presented in this form, because a small number of tests at one condition can then be applied to many other conditions. One example of this is the use of the pressure coefficient, which can be used for any wind speed (Irving et al., 2005). Similarly, graphs generated from envelope flow models allow quick calculations to be made and may be useful at any stage of a design to give a quick estimate of proposed changes. Examples of graphs are given in (Etheridge, 2002) which cover conventional design conditions and, perhaps more importantly, off-design conditions. The off-design conditions include effects which would normally require a great deal of effort to calculate for a particular building e.g. the effects of adventitious leakage and wind turbulence. With the graphs described, a designer can obtain a quick indication of whether such effects are important.

Advantages and Limitations

Both analytical and empirical models are very simple to use and provide quick results. They are the only models that can be used at the early design

stages as they require very little input data. However, the results they yield are very approximate.

A.2 Small-scale Physical Models

Small scale models can provide more practical temporal and spatial resolutions than full-scale models. Scaled models can also incorporate complex flows, geometries, and thermal conditions, unlike analytical and empirical models. Furthermore, small scale models have an advantage over numerical ones in that they are visual. Their impact on design is more immediately communicated, bringing not only numerical data but also greater understanding of the processes.

In order to represent correctly the ventilation flow in an actual room or building, small-scale models should be designed following similarity analysis, in which the relevant dimensionless flow parameters are almost identical between small and full-scale models (e.g. Reynolds, Grashof, Prandtl, and Archimedes numbers) (Q. Chen et al., 2010).

A.2.1 Salt-Bath Technique:

Salt-bath also called brine-water modelling is a technique which can be used to visualise the ventilation flow. The technique uses a scale model of a building and water as the working fluid to simulate the ventilation flow. The buoyancy forces driving the ventilation flow are reproduced by the density contrast between the fresh water and salt solution. A detailed description of this technique together with benefits and limitations are reported in (Steemers, Chenvidyakarn, & Woods, 2002). Only a brief description is given here.

A typical experiment involves an abstract model of the building of scale between 1:10 to 1:100 constructed from acrylic sheets and submerged into a large tank of water. The degree of salinity of this water depends on the phenomenon to be simulated. In most cases fresh water is used to represent the ambient fluid (air) while a salt solution is continuously introduced into the model to represent inputs of heat or cold.

In order to visualise the flow, the shadow graph technique (which shows density differences in the flow) and dyes to colour the fluids are used. Quantitative estimates of the specific temperature distribution can be made by measuring the solution concentration using a conductivity probe whilst digital image data processing can give quantitative measurements of the flow parameters such as velocity and density (Steemers et al., 2002).

This technique has been widely accepted for modelling ventilation flows in buildings and has been used to study the following natural ventilation scenarios:

- Ventilation flow driven by buoyancy forces (displacement and mixing ventilation)
- The neutral level (i.e. when there is a vertical stratification of the interior air)
- Ventilation flow driven by combined wind and buoyancy forces (wind-assisted and wind opposed)
- Stack-driven ventilation without internal sources of buoyancy
- Stack-driven ventilation with internal sources of buoyancy (single source, multiple sources, distributed line sources, area sources)

- Other forms of stack-driven ventilation (solar chimney ventilation, heat recovery, ventilation through a single-sided opening, ventilation through a doorway)

It has also yielded considerable insights to the area of natural ventilation design and application in real building projects. For example, salt-bath modelling was used in the SSEES to reveal critical design flaws. It was found that the larger stacks at the rear of the building could draw air into the top of the double facade at the front and across the floor plates, thus turning the double facade into an inlet rather than an outlet which would generate very cold draughts, especially in winter, when the condition was most likely to occur (Lomas, 2007). Furthermore, salt-bath modelling was used to investigate how the pre-cooling designed for this building might overcome the danger of stalling the air flow in periods of high external temperatures (Short, Cook, & Woods, 2009). A series of simplified hydrostatic pressure profiles which may develop in the atrium and the outflow stacks, were also investigated so that the different possible flow regimes might be identified.

The experiments were conducted in a small-scale Perspex model of the building which included the stacks on various floors and the central atrium supplying (pre-cooled or pre-heated) air to the building. The models were immersed in a reservoir of 5% saline water and fresh water was added to different floors in the model building to simulate the generation of heat associated with the occupants. The summer cooling of air entering the top of the light well was modelled by the injection of 10% saline fluid at this point. By dying the input fluids,

the flow patterns in the floor space and stacks could be visualized (Woods, Chenvidyakarn, & Short, 2003).

Advantages

There are number of valuable opportunities that salt bath modelling offers, either as an independent technique for research and demonstration, or as part of a combination of analysis tools for design projects.

- The ability to cope relatively easily with complex geometries (Steemers et al., 2002)
- The model is inexpensive and can be easily constructed as well as easily adapted to respond to changes in the design.
- With the aid of shadowgraph imagery and dyes, this technique produces real, 3-D, time-dependent flows, providing effective means of transferring knowledge to the design team.
- Complex ventilation flows can be simulated straightforwardly with acceptable quantitative accuracy and good dynamic similarity. For example, there are no real problems in achieving high Reynolds numbers with Archimedes numbers (Carey & Etheridge, 1999). This means that the information obtained from small-scale models, can be extrapolated to full-sized buildings.
- The effects of external wind pressures and heat transfer can also be incorporated to make the modelling more realistic. The effects of winds are simulated by suspending the model in a large tank containing fresh water, in which flumes of controllable speed are generated. The effects of heat

transfer are simulated by fitting a heating (or cooling) device (such as a heating plate) to the model.

Limitations

However, there are several disadvantages in the salt-bath modelling system. A concern in ventilation design using the salt-bath technique is the realistic quality of the modelling. In general, every modelling technique contains some simplifications. For the salt-bath modelling, limitations and simplifications include, for example:

- Adiabatic room envelopes: Heat transfer boundary conditions at surfaces are not completely simulated and therefore local effects, such as solar patching on the floor of an atrium, cannot be dealt with (Irving et al., 2005)
- Mechanisms of heat transport: It has been reported in Howell & Potts, (2001) that a difference in temperature profile occurs between salt-bath technique results and experimental data established within a full-scale enclosure in modelling the temperature stratification for the natural displacement ventilation flow driven by a source of buoyancy at floor level within the space. This is due to the fact that salt-bath techniques neglect the mechanisms of thermal radiation and diffusion present within the test-room. This is because, whilst the kinematic viscosity of water is only about one-tenth that of air, the diffusivity of salt in water is less than one ten-thousandth that of heat in air. The salt-bath technique is, therefore, only suitable for modelling flows where diffusion of heat is insignificant, since salt diffuses too slowly in water to represent the diffusion of heat in air

- Simplified heat sources: In reality, heating systems are designed to achieve a constant temperature difference, rather than a constant heat input which is the case with this type of modelling. This can result in large variations with time of the heat input to the space and hence large variations in the buoyancy source, at least in winter conditions. Furthermore, although the technique attempts to model the internal flow such that the internal pressure distribution reflects temperature stratification arising from buoyancy sources, this approach may be no better than that of imposing a uniform temperature. This is because it assumes that the internal temperature distribution is adequately modelled despite the complexity of buoyancy sources (positive and negative) in rooms (Carey & Etheridge, 1999)

A.2.2 Fine-bubble modelling

A novel method was developed in which an electrolytically generated fine hydrogen bubble plume in water is used to simulate the buoyancy effect induced by temperature differences in buildings. The main idea of the new modelling technique is using fine bubble-generated buoyancy plumes in water to simulate the thermal buoyancy-driven flows in buildings (Z. D. Chen, Li, & Mahoney, 2001).

Advantages

- Natural ventilation and stratification phenomenon in a single-zone building induced by a point or a line source can be successfully simulated by the fine hydrogen-bubble technique.

- Since no heating elements are involved in the system, the set-up and operation for the fine-bubble method are simple.
- In contrast to the salt-bath technique, the fine-bubble system does not require a big liquid reservoir because the properties of the bulk liquid will not change throughout the experiments since the bubbles leave the free water surface during the experimental process. Consequently, a compact modelling system can be easily constructed.

Limitations

It should be noted that there are several limitations for the fine-bubble technique;

- Constant temperature boundary conditions on the wall other than constant heat flux boundary conditions (including adiabatic) are difficult to be simulated using the fine-bubble technique.
- When the top opening is lower than the ceiling level, bubbles will accumulate on the top of the building, which gives rise to unrealistic flow fields.
- The slip velocity between the bubbles and the liquid may influence the ventilation process at the large top opening size.
- Consequently, the application of the fine-bubble technique is limited to the modelling of natural ventilation due to buoyancy in single-cell buildings only.

A.2.3 Wind Tunnels

Wind tunnels are mostly used to determine pressure coefficients from which ventilation rates can be obtained indirectly either by means of an analytical model

or by providing boundary conditions at openings in numerical models such as computational fluid dynamics.

Alternatively, wind tunnels can also be used for measuring directly the ventilation rate of a building. This technique enables models of buildings and their surroundings to be subjected to varying and controlled wind speeds and directions. Pressure measurements taken over the building facade help to inform parameters of the design such as position of openings and likely air change rates. Flow visualisation is possible using smoke injection. The potential advantage offered by the direct approach is that wind effects are more accurately accounted for than they are by the indirect approach.

Wind tunnel testing can also be used to optimise the performance of specific ventilation openings, such as chimneys or wind towers. They have been used extensively to optimise the termination design of exhaust stacks in many recent advanced naturally ventilated buildings ANV. This may take the form of simply measuring wind pressures at the outlet of the openings to ensure that they are negative or can be used to test a specific termination design such as wind baffles.

Advantages

One advantage of using direct wind tunnel testing is the possibility of determining ventilation rates under the effect of wind or buoyancy, or the combined effect of the two. Simple scaling laws are applied to calculate the full-scale ventilation rate.

Another advantage of direct wind tunnel testing is that it offers relatively high accuracy in the determination of ventilation rates due to wind. This is primarily because the effects of wind turbulence are inherent in the measurements and

that purpose-provided openings have flow characteristics that are not sensitive to Reynolds number.

Limitations

There are some limitations on the size of the building and the openings in wind tunnel testing. For example, the envelope volume of the model scale of a building at say 1/100 has to be large enough to allow a tracer gas measurement to be taken. Similarly, the full-scale openings need to be large enough for them to be accurately modelled. For example, an open window can be adequately modelled at 1/100 scale, but a domestic air vent may not be (due to dependence on Reynolds number causing errors in applying the results to full-scale) (Irving et al., 2005).

A.3 Thermal Models (DTM) and Airflow Network Models (AFN)

For predicting ventilation performance in large or moderately-sized buildings, only numerical modelling by a multi-zone airflow network model could give the required information at a reasonable cost. The analytical and empirical models would not produce useful information for ventilation performance analysis. The experimental measurements with small-scale models are not realistic in terms of their costs. Moreover, a CFD model would need days of computing time for such a building (Q. Chen et al., 2010).

AFN enable a building to be divided into several discrete zones connected by flow paths to form a flow network and assume that the air temperature in each zone is uniformly constant. A zone may be used to represent a room or corridor while flow paths might represent open doors, windows and cracks (infiltration).

There are two main types of multi-zone methods, the node continuity approach and the loop pressure equation-based approach.

Loop approaches have been used extensively in the duct networks analysis. They provide an ‘exact’ analytical approach to size components of natural and hybrid ventilation systems and offer a number of advantages when compared to the node continuity approach (Santamouris & Wouters, 2006).

The PHDC Air Flow software (Ford et al., 2010) implements a multi-zone loop approach to perform the following tasks:

- Generate the individual pressure loop equations for specific loops in a building airflow system.
- Generate the whole-building system equations based on this specific loop equation.
- Solve the whole-building system equations providing the air flow through each floor.
- Generate a correlation that gives the air flow in each floor as a function of temperatures, relative humidities and outdoor wind velocity.

It is important to remember that natural ventilation is driven by wind and indoor/outdoor and interzonal temperature difference. These parameters are introduced to zonal models via the boundary conditions. However, the ventilation flow itself will often alter the thermal boundary condition (e.g. incoming air heating or cooling the space). For this reason, there is often a strong need to integrate ventilation models with thermal models so that the temperature and hence ventilation condition can be solved simultaneously (Li & Heiselberg, 2003). Ideally the two models would be completely integrated such that the governing equations

are solved simultaneously. A simpler strategy is to solve the two models separately, with some form of link between their solutions.

Application to Building Design

A dynamic thermal model was used to investigate the likely frequency of overheating in the SSEES building, both with and without the mechanical cooling. A 24-node airflow network was included to model the passive ventilation strategy. The simulations confirmed the need for mechanical cooling, a way of controlling the amount of air delivered to each floor in response to differing heat gains, and a stack design that would preclude back flow from the lower to the upper floors (Lomas, Short, et al., 2004).

Advantages

A multi-zone network model seems to be the only acceptable model for analysing ventilation performance for large and moderately -sized buildings. The multi-zone model can quickly obtain ventilation performance results. Furthermore, multi-zone integrated air flow and thermal models can be used to provide boundary conditions for CFD applications.

Limitations

However, due to the assumption that the air temperature in each zone is uniformly constant, these models are limited to the predictions of the average characteristics of airflows and contaminant distributions and are unable to predict local air velocities, temperatures and humidities. The assumptions include the uniform air temperature and contaminant distributions in a zone and the neglect of momentum effects amongst others.

A.4 Computational Fluid Dynamics (CFD)

This technique is used primarily for calculating velocities, temperatures, and pressures at all points of a specified space in a geometric domain to give a detailed picture of the complete flow field. The geometric domain under analysis is subdivided into a large number of small cells to create a two or three-dimensional mesh. The conservation equations of mass, momentum, energy, and species concentrations are then discretised and solved in each cell using the values for velocity, pressure and enthalpy in the adjacent cells as boundary conditions.

Most commercial CFD software packages contain three parts (Irving et al., 2005):

A Pre-processor: Where the values of boundary conditions for the solution are input, including the creation of a grid and the number of cells.

A Solver: Where the numerical solution is carried out. This is an iterative procedure, which continues until convergence is obtained. Solution times can vary from a few hours to several days, depending on the complexity of the boundary conditions, the number of cells and the capacity of the computer.

A Post-processor: Where the results are presented in a suitable form. Since the solution generates vast amounts of data it is important to be able to present it in a meaningful way. One common form of output is the contour plot where parameters such as velocity and temperature that lie in certain ranges are identified by different coloured areas.

A turbulence model has to be incorporated in CFD to accurately describe the flow field. These vary from simple time averaged eddy-viscosity models and Reynolds stress models to more time dependent and expansive models in terms of computer power requirement like large eddy simulation (LES).

Advantages

CFD models are potentially very accurate. They are able to predict spatial information giving values for variables throughout the entire flow domain. Furthermore, it is relatively easy to investigate changes in geometry and operating conditions. Another key point is the relative ease with which other physical models such as radiation models and contaminant dispersion can be added. Additionally, they can cope with wind and buoyancy-driven flows, radiant exchanges between surfaces, convective exchange between the air and thermally massive surfaces, and the two phases associated with water droplet evaporation, thus they can consider all the thermo-physical phenomena which are involved in PHDC buildings

Limitations

Although CFD solve fundamental equations, they still rely on assumptions and approximations. The main ones relate to the properties of turbulence and to heat transfer, particularly close to surfaces.

The use of CFD requires a high level of expertise in terms of data input, assumptions and interpretation.

Running CFD is very computationally intensive prohibiting detailed simulations of the entire building over long periods and is therefore more suited to generate a snap-shot scenario.

Appendix B

This appendix shows the various control logic algorithms written for the Energy Management System (EMS) module in EnergyPlus. The EMS module is intended to emulate the types of controls possible with the building management systems (BMS) used in real buildings. Here, it was used for aperture modulation and operation mode selection in the BCM. An EMS is able to access a wide variety of “sensor” data and use this data to direct various types of control actions using “actuators”. For example, a sensor could be set as the dry-bulb temperature of a zone which then controls an actuator such as the opening factor of a vent. The algorithms were written in the EnergyPlus Runtime Language as described in the “Application Guide for EMS” document.

```
EnergyManagementSystem:Program,
Control_Logic,           !- Name
RUN Variable_Calculator, !- Program Line 1
IF CurrentTime>=8 && CurrentTime<=18 && DayOfWeek<6,  !- Program
Line 2
RUN OM_Indicator_01,     !- A4
RUN OM_Indicator_02,     !- A5
RUN OM_Indicator_03,     !- A6
RUN OM_Indicator,        !- A7
SET GMp012 = (GM==GMp1 && GMp1==GMp2),  !- A8
IF GM==2,                !- A9
SET EC_MFRa = NULL,      !- A10
SET A_V_OFa = 1.0,       !- A11
SET DSF_V1_OFa = Tdsf<Tdb,  !- A12
SET DSF_V2_OFa = Tdsf>Tdb,  !- A13
ELSEIF GM==1,            !- A14
SET EC_MFRa = 0.0,       !- A15
SET A_V_OFa = 1.0,       !- A16
SET DSF_V1_OFa = 1.0,    !- A17
SET DSF_V2_OFa = 0.0,    !- A18
ELSE,                    !- A19
SET EC_MFRa = 0.0,       !- A20
SET A_V_OFa = 0.0,       !- A21
SET DSF_V1_OFa = 0.0,    !- A22
SET DSF_V2_OFa = 0.0,    !- A23
ENDIF,                   !- A24
SET L01_DSF_V_OFa = LM01>=1,  !- A25
```

```
SET OF01mx = (LM01>=1 && ((GM==1 && GMp1==2 && OF01s>0) ||
(OF01mxp==1 && GM==GMp1))),  !- A26
IF LM01>=1,                  !- A27
IF (GMp012==1 && To01>Tcsp) || OF01mx==1,  !- A28
SET OF01a = 1.0,             !- A29
ELSEIF To01<=Tll || LM01p==0 || (GM==2 && OF01s>0 && GMp1<2 &&
DT>2),  !- A30
SET OF01a = 0.05,            !- A31
ELSEIF GM==2 && OF01s>0 && To01<=(Tisp-1) && To01<=To01p,  !- A32
RUN L01_Previous_Opening_Factor_Indicator_Minus,  !- A33
ELSEIF To01<=To01p || To01<=Tisp || (GM==2 && OF01s>0 && (GMp1<2 ||
GMp2<2)),  !- A34
SET OF01a = OF01s,           !- A35
ELSE,                        !- A36
RUN L01_Previous_Opening_Factor_Indicator_Plus,  !- A37
ENDIF,                       !- A38
ELSE,                        !- A39
SET OF01a = 0.0,             !- A40
ENDIF,                       !- A41
SET L02_DSF_V_OFa = LM02>=1,  !- A42
SET OF02mx = (LM02>=1 && ((GM==1 && GMp1==2 && OF02s>0) ||
(OF02mxp==1 && GM==GMp1))),  !- A43
IF LM02>=1,                  !- A44
IF (GMp012==1 && To02>Tcsp) || OF02mx==1,  !- A45
SET OF02a = 1.0,             !- A46
ELSEIF To02<=Tll || LM02p==0 || (GM==2 && OF02s>0 && GMp1<2 &&
DT>2),  !- A47
SET OF02a = 0.05,            !- A48
ELSEIF GM==2 && OF02s>0 && To02<=(Tisp-1) && To02<=To02p,  !- A49
RUN L02_Previous_Opening_Factor_Indicator_Minus,  !- A50
ELSEIF To02<=To02p || To02<=Tisp || (GM==2 && OF02s>0 && (GMp1<2 ||
GMp2<2)),  !- A51
SET OF02a = OF02s,           !- A52
ELSE,                        !- A53
RUN L02_Previous_Opening_Factor_Indicator_Plus,  !- A54
ENDIF,                       !- A55
ELSE,                        !- A56
SET OF02a = 0.0,             !- A57
ENDIF,                       !- A58
SET L03_DSF_V_OFa = LM03>=1,  !- A59
SET OF03mx = (LM03>=1 && ((GM==1 && GMp1==2 && OF03s>0) ||
(OF03mxp==1 && GM==GMp1))),  !- A60
IF LM03>=1,                  !- A61
IF (GMp012==1 && To03>Tcsp) || OF03mx==1,  !- A62
SET OF03a = 1.0,             !- A63
ELSEIF To03<=Tll || LM03p==0 || (GM==2 && OF03s>0 && GMp1<2 &&
DT>2),  !- A64
SET OF03a = 0.05,            !- A65
ELSEIF GM==2 && OF03s>0 && To03<=(Tisp-1) && To03<=To03p,  !- A66
RUN L03_Previous_Opening_Factor_Indicator_Minus,  !- A67
ELSEIF To03<=To03p || To03<=Tisp || (GM==2 && OF03s>0 && (GMp1<2 ||
GMp2<2)),  !- A68
SET OF03a = OF03s,           !- A69
ELSE,                        !- A70
RUN L03_Previous_Opening_Factor_Indicator_Plus,  !- A71
ENDIF,                       !- A72
ELSE,                        !- A73
```

```
SET OF03a = 0.0,          !- A74
ENDIF,                    !- A75
ELSE,                     !- A76
SET EC_MFRa = 0.0,        !- A77
SET DSF_V2_OFa = 0.0,     !- A78
SET OF01mx = 0.0,         !- A79
SET OF02mx = 0.0,         !- A80
SET OF03mx = 0.0,         !- A81
SET GMp012 = 0.0,         !- A82
SET L01_DSF_V_OFa = (T01>Tdb && T01>Tll),  !- A83
IF T01>Tdb && T01>Tll,    !- A84
SET LM01 = -1.0,          !- A85
IF (T01-Tdb)>3.0,         !- A86
SET OF01a = 0.05,         !- A87
ELSE,                     !- A88
SET OF01a = 1.0,          !- A89
ENDIF,                    !- A90
ELSE,                     !- A91
SET LM01 = 0.0,           !- A92
SET OF01a = 0.0,          !- A93
ENDIF,                    !- A94
SET L02_DSF_V_OFa = (T02>Tdb && T02>Tll),  !- A95
IF T02>Tdb && T02>Tll,    !- A96
SET LM02 = -1.0,          !- A97
IF (T02-Tdb)>3.0,         !- A98
SET OF02a = 0.05,         !- A99
ELSE,                     !- A100
SET OF02a = 1.0,          !- A101
ENDIF,                    !- A102
ELSE,                     !- A103
SET LM02 = 0.0,           !- A104
SET OF02a = 0.0,          !- A105
ENDIF,                    !- A106
SET L03_DSF_V_OFa = (T03>Tdb && T03>Tll),  !- A107
IF T03>Tdb && T03>Tll,    !- A108
SET LM03 = -1.0,          !- A109
IF (T03-Tdb)>3.0,         !- A110
SET OF03a = 0.05,         !- A111
ELSE,                     !- A112
SET OF03a = 1.0,          !- A113
ENDIF,                    !- A114
ELSE,                     !- A115
SET LM03 = 0.0,           !- A116
SET OF03a = 0.0,          !- A117
ENDIF,                    !- A118
SET A_V_OFa = ((LM01 + LM02 + LM03) < 0.0),  !- A119
SET DSF_V1_OFa = ((LM01 + LM02 + LM03) < 0.0),  !- A120
IF (LM01 + LM02 + LM03) < 0.0,  !- A121
SET GM = -1.0,            !- A122
ELSE,                     !- A123
SET GM = 0.0,             !- A124
ENDIF,                    !- A125
ENDIF;                    !- A126

EnergyManagementSystem:Subroutine,
Variable_Calculator,      !- Name
SET M = Minute,           !- Program Line 1
```

```
SET Epr = @TrendValue E_trend 12,  !- Program Line 2
IF RH>=80,                !- A4
SET Emod = 0.0,           !- A5
ELSE,                     !- A6
SET Emod = Epr+((M*(Ecur-Epr))/60),  !- A7
ENDIF,                    !- A8
SET ECspa = Tdb-(Emod*(Tdb-Twb)),  !- A9
SET ECsp = Tdb-(Emod*(Tdb-Twb)),  !- A10
SET Tll = Tcm - 2.5,      !- A11
SET Tul = Tcm + 2.5,      !- A12
SET Tisp = Tcm,           !- A13
SET Tcsp = Tcm + 1.0,     !- A14
SET DT = Tdb-ECsp,        !- A15
SET To01p = @TrendValue To01_trend 2,  !- A16
SET To02p = @TrendValue To02_trend 2,  !- A17
SET To03p = @TrendValue To03_trend 2,  !- A18
SET Tdbp = @TrendValue Tdb_trend 2,  !- A19
SET GMp1 = @TrendValue GM_trend 1,  !- A20
SET GMp2 = @TrendValue GM_trend 2,  !- A21
SET LM01p = @TrendValue LM01_trend 1,  !- A22
SET LM02p = @TrendValue LM02_trend 1,  !- A23
SET LM03p = @TrendValue LM03_trend 1,  !- A24
SET OF01sp = @TrendValue OF01s_trend 2,  !- A25
SET OF02sp = @TrendValue OF02s_trend 2,  !- A26
SET OF03sp = @TrendValue OF03s_trend 2,  !- A27
SET OF01mxp = @TrendValue OF01mx_trend 1,  !- A28
SET OF02mxp = @TrendValue OF02mx_trend 1,  !- A29
SET OF03mxp = @TrendValue OF03mx_trend 1;  !- A30

EnergyManagementSystem:Subroutine,
OM_Indicator_01,          !- Name
IF LM01p<=0,              !- Program Line 1
IF To01>Tisp && T01>Tdb && (Tdb<=Tll || (RH>=80 && Tdb<=Tisp)),  !-
Program Line 2
SET LM01 = 1.0,           !- A4
ELSEIF To01>Tisp && T01>ECsp && RH<80,  !- A5
SET LM01 = 2.0,           !- A6
ELSE,                     !- A7
SET LM01 = 0.0,           !- A8
ENDIF,                    !- A9
ELSEIF GMp1==1,           !- A10
IF To01<=Tisp || (To01<Tcsp && (OF01sp<1 || To01<=To01p)) ||
(RH>=80 && Tdb<=T01),  !- A11
SET LM01 = 1.0,           !- A12
ELSEIF RH<80,             !- A13
SET LM01 = 2.0,           !- A14
ELSE,                     !- A15
SET LM01 = 0.0,           !- A16
ENDIF,                    !- A17
ELSEIF GMp1==2,           !- A18
IF To01<=Tisp && (RH>=80 || Tdb<Tll || (Tdb<=(Tisp-1) &&
Tdbp>(Tisp-1))),  !- A19
SET LM01 = 1.0,           !- A20
ELSEIF RH<80,             !- A21
SET LM01 = 2.0,           !- A22
ELSE,                     !- A23
SET LM01 = 0.0,           !- A24
```

```
ENDIF,                   !- A25
ENDIF;                   !- A26

EnergyManagementSystem:Subroutine,
OM_Indicator_02,         !- Name
IF LM02p<=0,             !- Program Line 1
IF To02>Tisp && T02>Tdb && (Tdb<=Tll || (RH>=80 && Tdb<=Tisp)),  !-
Program Line 2
SET LM02 = 1.0,          !- A4
ELSEIF To02>Tisp && T02>ECsp && RH<80,  !- A5
SET LM02 = 2.0,          !- A6
ELSE,                    !- A7
SET LM02 = 0.0,          !- A8
ENDIF,                   !- A9
ELSEIF GMp1==1,          !- A10
IF To02<=Tisp || (To02<Tcsp && (OF02sp<1 || To02<=To02p)) ||
(RH>=80 && Tdb<=T02),  !- A11
SET LM02 = 1.0,          !- A12
ELSEIF RH<80,            !- A13
SET LM02 = 2.0,          !- A14
ELSE,                    !- A15
SET LM02 = 0.0,          !- A16
ENDIF,                   !- A17
ELSEIF GMp1==2,          !- A18
IF To02<=Tisp && (RH>=80 || Tdb<Tll || (Tdb<=(Tisp-1) &&
Tdbp>(Tisp-1))),  !- A19
SET LM02 = 1.0,          !- A20
ELSEIF RH<80,            !- A21
SET LM02 = 2.0,          !- A22
ELSE,                    !- A23
SET LM02 = 0.0,          !- A24
ENDIF,                   !- A25
ENDIF;                   !- A26

EnergyManagementSystem:Subroutine,
OM_Indicator_03,         !- Name
IF LM03p<=0,             !- Program Line 1
IF To03>Tisp && T03>Tdb && (Tdb<=Tll || (RH>=80 && Tdb<=Tisp)),  !-
Program Line 2
SET LM03 = 1.0,          !- A4
ELSEIF To03>Tisp && T03>ECsp && RH<80,  !- A5
SET LM03 = 2.0,          !- A6
ELSE,                    !- A7
SET LM03 = 0.0,          !- A8
ENDIF,                   !- A9
ELSEIF GMp1==1,          !- A10
IF To03<=Tisp || (To03<Tcsp && (OF03sp<1 || To03<=To03p)) ||
(RH>=80 && Tdb<=T03),  !- A11
SET LM03 = 1.0,          !- A12
ELSEIF RH<80,            !- A13
SET LM03 = 2.0,          !- A14
ELSE,                    !- A15
SET LM03 = 0.0,          !- A16
ENDIF,                   !- A17
ELSEIF GMp1==2,          !- A18
IF To03<=Tisp && (RH>=80 || Tdb<Tll || (Tdb<=(Tisp-1) &&
Tdbp>(Tisp-1))),  !- A19
```

```
SET LM03 = 1.0,           !- A20
ELSEIF RH<80,             !- A21
SET LM03 = 2.0,           !- A22
ELSE,                     !- A23
SET LM03 = 0.0,           !- A24
ENDIF,                    !- A25
ENDIF;                    !- A26

EnergyManagementSystem:Subroutine,
OM_Indicator,             !- Name
IF LM01==2 || LM02==2 || LM03==2,  !- Program Line 1
SET GM = 2.0,             !- Program Line 2
ELSEIF LM01==1 || LM02==1 || LM03==1,  !- A4
SET GM = 1.0,             !- A5
ELSE,                     !- A6
SET GM = 0.0,             !- A7
ENDIF;                    !- A8

EnergyManagementSystem:Subroutine,
L01_Previous_Opening_Factor_Indicator_Plus,  !- Name
IF OF01s == 1.00,         !- Program Line 1
SET OF01a = 1.00,         !- Program Line 2
ELSEIF OF01s == 0.65,     !- A4
SET OF01a = 1.00,         !- A5
ELSEIF OF01s == 0.40,     !- A6
SET OF01a = 0.65,         !- A7
ELSEIF OF01s == 0.20,     !- A8
SET OF01a = 0.40,         !- A9
ELSEIF OF01s == 0.10,     !- A10
SET OF01a = 0.20,         !- A11
ELSEIF OF01s == 0.05,     !- A12
SET OF01a = 0.10,         !- A13
ENDIF;                    !- A14

EnergyManagementSystem:Subroutine,
L01_Previous_Opening_Factor_Indicator_Minus,  !- Name
IF OF01s == 0.05,         !- Program Line 1
SET OF01a = 0.05,         !- Program Line 2
ELSEIF OF01s == 0.10,     !- A4
SET OF01a = 0.05,         !- A5
ELSEIF OF01s == 0.20,     !- A6
SET OF01a = 0.10,         !- A7
ELSEIF OF01s == 0.40,     !- A8
SET OF01a = 0.20,         !- A9
ELSEIF OF01s == 0.65,     !- A10
SET OF01a = 0.40,         !- A11
ELSEIF OF01s == 1.00,     !- A12
SET OF01a = 0.65,         !- A13
ENDIF;                    !- A14

EnergyManagementSystem:Subroutine,
L02_Previous_Opening_Factor_Indicator_Plus,  !- Name
IF OF02s == 1.00,         !- Program Line 1
SET OF02a = 1.00,         !- Program Line 2
ELSEIF OF02s == 0.65,     !- A4
SET OF02a = 1.00,         !- A5
ELSEIF OF02s == 0.40,     !- A6
```

```
SET OF02a = 0.65,         !- A7
ELSEIF OF02s == 0.20,     !- A8
SET OF02a = 0.40,         !- A9
ELSEIF OF02s == 0.10,     !- A10
SET OF02a = 0.20,         !- A11
ELSEIF OF02s == 0.05,     !- A12
SET OF02a = 0.10,         !- A13
ENDIF;                    !- A14

EnergyManagementSystem:Subroutine,
L02_Previous_Opening_Factor_Indicator_Minus,  !- Name
IF OF02s == 0.05,         !- Program Line 1
SET OF02a = 0.05,         !- Program Line 2
ELSEIF OF02s == 0.10,     !- A4
SET OF02a = 0.05,         !- A5
ELSEIF OF02s == 0.20,     !- A6
SET OF02a = 0.10,         !- A7
ELSEIF OF02s == 0.40,     !- A8
SET OF02a = 0.20,         !- A9
ELSEIF OF02s == 0.65,     !- A10
SET OF02a = 0.40,         !- A11
ELSEIF OF02s == 1.00,     !- A12
SET OF02a = 0.65,         !- A13
ENDIF;                    !- A14

EnergyManagementSystem:Subroutine,
L03_Previous_Opening_Factor_Indicator_Plus,  !- Name
IF OF03s == 1.00,         !- Program Line 1
SET OF03a = 1.00,         !- Program Line 2
ELSEIF OF03s == 0.65,     !- A4
SET OF03a = 1.00,         !- A5
ELSEIF OF03s == 0.40,     !- A6
SET OF03a = 0.65,         !- A7
ELSEIF OF03s == 0.20,     !- A8
SET OF03a = 0.40,         !- A9
ELSEIF OF03s == 0.10,     !- A10
SET OF03a = 0.20,         !- A11
ELSEIF OF03s == 0.05,     !- A12
SET OF03a = 0.10,         !- A13
ENDIF;                    !- A14

EnergyManagementSystem:Subroutine,
L03_Previous_Opening_Factor_Indicator_Minus,  !- Name
IF OF03s == 0.05,         !- Program Line 1
SET OF03a = 0.05,         !- Program Line 2
ELSEIF OF03s == 0.10,     !- A4
SET OF03a = 0.05,         !- A5
ELSEIF OF03s == 0.20,     !- A6
SET OF03a = 0.10,         !- A7
ELSEIF OF03s == 0.40,     !- A8
SET OF03a = 0.20,         !- A9
ELSEIF OF03s == 0.65,     !- A10
SET OF03a = 0.40,         !- A11
ELSEIF OF03s == 1.00,     !- A12
SET OF03a = 0.65,         !- A13
ENDIF;                    !- A14
```

```
EnergyManagementSystem:Program,
Calculated_Variables,     !- Name
SET Dw = @RhoH2O Twb,     !- Program Line 1
SET A_VFR = A_V_VFR_2_1 - A_V_VFR_1_2,  !- Program Line 2
SET A_MFR = A_V_MFR_2_1 - A_V_MFR_1_2,  !- A4
SET L01_VFR = A_L01_V_VFR_1_2 - A_L01_V_VFR_2_1,  !- A5
SET L02_VFR = A_L02_V_VFR_1_2 - A_L02_V_VFR_2_1,  !- A6
SET L03_VFR = A_L03_V_VFR_1_2 - A_L03_V_VFR_2_1,  !- A7
SET DSF_V1_VFR = DSF_V1_VFR_2_1 - DSF_V1_VFR_1_2,  !- A8
SET DSF_V2_VFR = DSF_V2_VFR_2_1 - DSF_V2_VFR_1_2,  !- A9
SET DSF_VFR = DSF_V1_VFR + DSF_V2_VFR,  !- A10
IF EC_MFRs>0.0,           !- A11
SET Wec_calc = @WFnTdbTwbPb ECsp Twb P,  !- A12
SET RHec_calc = (@RhFnTdbWPb ECsp Wec_calc P) * 100,  !- A13
SET WatCon = @ABS(A_MFR) * (Wec_calc - W) * 5 * 60 * 1000 / Dw,  !-
A14
ELSE,                     !- A15
SET Wec_calc = Wec,       !- A16
SET RHec_calc = RHec,     !- A17
SET WatCon = 0.0,         !- A18
ENDIF,                    !- A19
IF LM01==2,               !- A20
SET W01_calc = Wec_calc + (W01 - Wec),  !- A21
ELSE,                     !- A22
SET W01_calc = W01,       !- A23
ENDIF,                    !- A24
IF LM02==2,               !- A25
SET W02_calc = Wec_calc + (W02 - Wec),  !- A26
ELSE,                     !- A27
SET W02_calc = W02,       !- A28
ENDIF,                    !- A29
IF LM03==2,               !- A30
SET W03_calc = Wec_calc + (W03 - Wec),  !- A31
ELSE,                     !- A32
SET W03_calc = W03,       !- A33
ENDIF,                    !- A34
SET RH01_calc = (@RhFnTdbWPb T01 W01_calc P) * 100,  !- A35
SET RH02_calc = (@RhFnTdbWPb T02 W02_calc P) * 100,  !- A36
SET RH03_calc = (@RhFnTdbWPb T03 W03_calc P) * 100;  !- A37
```